Model Predictive Control for Helicopter Flight Control

Evaluating Linear and Nonlinear Model Predictive Control for Reducing Cross-coupling Effects in Helicopter Flight

Lotte Wellens
March 25, 2021

TU Delft
Delft
University of
Technology

Challenge the future

Model Predictive Control for Helicopter Flight Control

Evaluating Linear and Nonlinear Model Predictive Control for Reducing Cross-coupling Effects in Helicopter Flight

by

Lotte Wellens

in partial fulfillment of the requirements for the degree of

Master of Science
in Aerospace Engineering

at the Delft University of Technology,
to be defended publicly on Monday April 12, 2021 at 2:00 PM.

Supervisors:	Prof. dr. ir. M. D. Pavel,	TU Delft
	Dr. ir. A. Jamshidnejad,	TU Delft
Thesis committee:	Prof. dr. ir. M. D. Pavel,	TU Delft
	Dr. ir. A. Jamshidnejad,	TU Delft
	Dr. ir. O. A. Sharpanskykh,	TU Delft

An electronic version of this thesis is available at `http://repository.tudelft.nl/`.

TU Delft

Delft
University of
Technology

Preface

This is the final thesis report of my master thesis in the Control & Simulation track of the Aerospace Engineering Faculty at Delft University of Technology over the course of 2019 till 2021 on model predictive control for helicopter flight control. Being able to research and work on the subject of helicopters and model predictive control, which were both completely new topics for me, was a very interesting, challenging and enriching experience.

I would like to express my gratitude towards my daily supervisor Marilena for her guidance and support throughout the thesis. During our weekly conversations you were able to guide me through the process of performing academic research and taught me all I needed to know about helicopters. I would also like to thank my supervisor Anahita who was always there when I had questions about model predictive control or when I needed advise on how to proceed further. It was truly an honor to be able to work with two smart and ambitious women at the Faculty of Aerospace Engineering.

Furthermore, I would like to thank my friends and housemates from DS4 who stood by me during these times of hard work but also gave me a good amount of necessary distraction, keeping me motivated in life and on track with my thesis even during the difficult times of corona.

Finally, my family deserves a big thank you for bearing with me and supporting me over the past years of my study. Thank you for giving me this chance of studying abroad and for encouraging me to discover myself and to do what I love.

Lotte Wellens
Delft, April 2021

Contents

List of Figures

List of Tables

List of Abbreviations

ADS Aeronautical Design Standard

CARIMA Controlled Auto-Regressive and Integrated Moving Average

DMC Dynamic Matrix Control

DOF Degree of Freedom

DVE Degraded Visual Environment

GAS Global Asymptotic Stability

GPC Generalized Predictive Control

GVE Good Visual Environment

LAS Local Asymptotic Stability

LMPC Linear Model Predictive Control

LQR Linear Quadratic Regulator

MPC Model Predictive Control

MTE Mission Task Element

NLMPC Nonlinear Model Predictive Control

PID Proportional Integral and Differential

RHC Receding Horizon Control

TA & T Target Acquisition and Tracking

TT Tracking Task

UAV Unmanned Aerial Vehicle

List of Symbols

α_1, α_2 $\mathcal{K}_\infty$-function

α_3 positive definite function

β flapping angle of the blade, sideslip angle

δ perturbation

Δt control sampling time

ℓ stage cost

ϵ prediction model error, slack variable system, model mismatch compensation term

γ lock number

Λ non-dimensionalization factor

λ_0 non-dimensional uniform inflow velocity

λ_c non-dimensional inflow velocity of the control plane

λ_i eigenvalue

$\lambda_{0_{tr}}$ non-dimensional tail rotor uniform inflow velocity

$\mathbb{R}^n$ real-valued n-vectors

$\mathbb{X}$ region of attraction

$\mathcal{K}_\infty$ infinity $\mathcal{K}$-function: a continuous, positive, strictly increasing function with the origin in zero and the limit to infinity equal to infinity

μ tip speed ratio

Ω rotor angular velocity

ϕ fuselage roll angle

ψ fuselage yaw angle, azimuth angle

σ standard deviation of ε

τ time constant

θ fuselage pitch angle

θ_0 collective pitch angle

θ_{1c} lateral cyclic pitch angle

θ_{1s} longitudinal cyclic pitch angle

ε simulation model uncertainty or disturbance

A state matrix

a_0 coning angle

a_1 longitudinal flapping angle

B input matrix

b_1 lateral flapping angle

C_T thrust coefficient

D_{MPC} estimated derivative used in the prediction model

D_{actual} actual helicopter derivative

e tracking error, upper and lower input bound vector

$\bar{e}$ tracking error vector along the prediction horizon

f upper and lower output bound vector

$\bar{F}$ total external force vector

h altitude

i prediction horizon time step

I_x moment of inertia around the X-axis

I_y moment of inertia around the Y-axis

I_z moment of inertia around the Z-axis

J_{xz} product of inertia

K feedback gain

k control time step

L total external rolling moment

M total external pitching moment

$\bar{M}$ total external moment vector

n number of states

N total external yawing moment, prediction horizon

N_u control horizon

n_z normal acceleration

p roll rate

P_f terminal weight matrix

Q tracking error weight matrix

q pitch rate

R control action weight matrix

r yaw rate, reference state vector

$\bar{r}$ reference state vector along the prediction horizon

t time

T period

u velocity along the helicopter body X-axis, input vector

$\bar{u}$	optimal control input vector along the prediction horizon
v	velocity along the helicopter body Y-axis
V_f	terminal cost
V_N	objective function
V_x	ground velocity in x-direction
V_y	ground velocity in y-direction
V_z	ground velocity in z-direction
w	velocity along the helicopter body Z-axis
w_i	eigenvector corresponding to eigenvalue λ_i
x	x-coordinate, state vector
$\bar{x}$	predicted state vector along the prediction horizon
X	sum of external forces acting along the X-axis
x_y	non-dimensional stability derivative of X with respect to y (see Appendix A)
$X_y = \dfrac{\partial X}{\partial y}$	dimensional stability derivative of X with respect to y
y	y-coordinate
Z	total of external forces acting along the Z-axis
z	z-coordinate

subscript 0 trim condition

subscript mr main rotor

subscript tr tail rotor

subscript fus fuselage

subscript ht horizontal tail

subscript vt vertical tail

subscript pk peak

subscript min minimum

subscript max maximum

subscript ref reference

superscript BEM according to blade element theory

superscript Gl according to the Glauert theory

1

Introduction

This report is the results of a master thesis on the application of Model Predictive Control (MPC) to helicopters at the Aerospace Faculty of the Technical University of Delft. The purpose of the report is on one hand to evaluate the possibilities of and previous research on applying MPC to helicopters by means of a literature review. On the other hand, more specific research was performed to evaluate linear and nonlinear model predictive control for reducing cross-couplings in helicopters to improve its handling qualities.

1.1. Background

Compared to fixed-wing aircraft, helicopters are highly versatile vehicles that can be used to execute a diverse range of commercial and military missions mainly due to its extreme maneuverability in low- and high-speed flight, vertical take-off and landing capabilities and the ability to hover. However, these great capabilities come with the fact that they are very difficult to control: they have fast, complex dynamics, are inherently unstable and its motion is highly coupled. Not only does this increase the workload of the pilot tremendously, it is also the cause of many fatal accidents [3]. With the introduction of flight control systems and fly-by-wire in helicopters in the 90's-00's, the flying characteristics of the helicopter could be adjusted to the pilot's needs to make the helicopter easier and safer to fly [4, 5]. Furthermore, handling quality requirements were set up in order to serve as a guideline for desired flight characteristics to improve the ease of controlling an aircraft [6]. However, to this day helicopters remain hard to fly and not accessible to the general public. Therefore, designing flight control systems in order to improve the helicopter handling qualities and safety is an important but challenging task.

At the same time Model Predictive Control (MPC) is emerging as a promising model-based optimal control technique with the powerful capabilities of including constraints on inputs and outputs, and including an objective function directly in the control algorithm. Furthermore, MPC has the advantage of being able to take into account future information of the system and the environment. This allows MPC to deal efficiently with time delays, non-minimum phase behaviour and to anticipate on future events [7]. Therefore, MPC offers an easy way to directly incorporate technical specifications, safety limits and performance bounds into the helicopter flight control design and to calculate the optimal control input based on a customized objective function and future information of the flight dynamics and flight condition. On the other hand the optimization process in MPC brings along a big computational burden. Even though optimization methods and computer power are rapidly improving, the real time application of MPC to fast dynamic systems such as helicopters is still in development. Furthermore, when the theoretical and unpractical Lyapunov stability modifications are not implemented to the MPC problem, the MPC problem has to be stabilized by means of tuning. This can be time consuming and requires expertise as no structured tuning approach exists. Especially for nonlinear MPC, the computational burden and stability matter can become critical [8]. MPC was originally used in the 80's for industrial processes in areas as refining, petrochemicals and pulp and paper but is now making its way into other applications such as electronics, medicine, energy and environment and the automotive and aerospace industry [9–11]. Hence, with the rising popularity of MPC, new possibilities for improving helicopter flight are emerging [12].

1

1.2. Objective

The first objective of this report is to investigate the previous research and possibilities of the online application of MPC to helicopters. In order to do this, first it will be investigated what makes helicopters so hard to control by looking at the fundamentals of helicopter dynamics and stability. Moreover, research will be performed into the handling qualities of helicopters, more specifically into how they are defined and how they are affected. Secondly, the concept of model predictive control and its capabilities and drawbacks will be investigated. Finally, the possibilities of applying MPC to helicopters will be investigated by finding the advantages and disadvantages specific to MPC applied to helicopters and analyzing the previous research performed on it.

From this literature study, a more specific research objective with research questions arose which defines the objective of the thesis work and hence the second objective of this report. The thesis work objective is to investigate whether linear and nonlinear MPC are suitable to apply to helicopters to reduce cross-coupling effects by evaluating its performance on the cross-coupling handling quality requirements of the ADS-33 document. On one hand, it will be investigated how well linear and nonlinear MPC are able to reduce cross-coupling effects on the handling quality rating scale and compared to an uncontrolled and PID controlled helicopter. On the other hand, it will be investigated how sensitive the MPC controllers are to prediction model errors when reducing cross-coupling effects. Furthermore, the similarities and differences between linear and nonlinear MPC will be analyzed.

1.3. Outline

This thesis report is divided in four parts: the scientific article, the literature review, the thesis work and the appendices. In Part I, a scientific article about the conducted thesis work can be found. Part II covers the literature review on the application of MPC to helicopters. Here, Chapter 2 describes the helicopter dynamics and stability together with an introduction to helicopter handling qualities. An introduction to MPC and its possibilities and drawbacks can be found in Chapter 3. Chapter 4 describes the advantages and disadvantages of MPC applied to helicopters accompanied by a thorough investigation of the previous research conducted on MPC applied to helicopters. Finally, Chapter 5 presents a conclusion of the performed literature study.

Next, Part III presents the thesis work on the ability of linear and nonlinear MPC to reduce cross-couplings in helicopters in order to improve its handling qualities. In Chapter 6, the thesis objective and research questions that come forward of the research gap will be described followed by the research approach which will be followed. After this, Chapter 7 will describe the set-up of the cross-coupling simulations and sensitivity analysis simulations that will be performed for the thesis work. Next, the cross-coupling requirement results will be presented in Chapter 8. Then, Chapter 9 will describe the results of the sensitivity analysis to prediction model errors when reducing cross-couplings. Finally, Chapter 10 and 11 present respectively the conclusion of the thesis work and recommendations for future work that follow from the conclusion.

Part IV contains the appendices of this report. In Appendix A, the non-dimensionalization and a comparison of the helicopter stability derivatives can be found. Appendix B shows the 8 degrees of freedom linearized model of the helicopter for hover and forward flight. Next, some additional cross-coupling requirement simulations are presented in Appendix C. Finally, Appendix D shows the individual analyses of the important derivatives of the sensitivity analysis.

Part I

Scientific Article

Evaluating Linear and Nonlinear Model Predictive Control for Reducing Cross-coupling Effects in Helicopter Flight

Lotte Wellens

Abstract—**Model predictive control is an optimal, model-based control method that has the powerful capability of directly including input and output constraints. Next to this, it is known that helicopters are hard to fly with its complex, unstable and highly coupled dynamics. With the introduction of the concept of handling qualities, guidelines for helicopter and flight control system design were set in the ADS-33 document to improve the ease of controlling rotorcraft. In order to improve helicopter handling qualities, this paper investigates whether linear and nonlinear MPC are suitable for online application to helicopters to reduce cross-coupling effects. This was investigated by evaluating its performance on the cross-coupling requirements of the ADS-33 handling quality document. It was found that both linear and nonlinear MPC are very effective to reduce cross-coupling effects even when disturbances or prediction model errors are present. The model predictive controller could reduce the off-axis coupling response by around 99% compared to the uncontrolled helicopter. Furthermore, it performed 90% to 99% better than a PID controller in most coupling cases.**

Index Terms—**cross-coupling effects, flight control, handling qualities, helicopters, model predictive control.**

NOMENCLATURE

ADS	Aeronautical Design Standard
DOF	Degree of Freedom
LMPC	Linear Model Predictive Control
MPC	Model Predictive Control
NLMPC	Nonlinear Model Predictive Control
PID	Proportional Integral Derivative
TA&T	Target Acquisition and Tracking

β	sideslip angle
$\delta_{lon}, \delta_{lat}$	longitudinal and lateral stick displacement
Δt_s	simulation sampling time
ϵ	error in the derivatives of the prediction model
λ_0	non-dimensional uniform inflow velocity
$\lambda_{0_{tr}}$	tail rotor non-dimensional uniform inflow velocity
σ	standard deviation of ε
$\theta_0, \theta_{1s}, \theta_{1c}, \theta_{0_{tr}}$	helicopter control inputs: collective pitch angle, longitudinal cyclic pitch angle, lateral cyclic pitch angle and tail rotor collective pitch angle
ϕ, θ, ψ	fuselage Euler angles
ε	simulation model uncertainty or disturbance
D_{MPC}	estimated derivative used in the prediction model
D_{actual}	actual helicopter derivative

L. Wellens was a MSc student in Control and Simulation at the Faculty of Aerospace Engineering, Delft University of Technology, The Netherlands. E-mail: wellenslotte@hotmail.com

e	tracking error
$\bar{e}$	tracking error vector along the prediction horizon
h	altitude
i	prediction horizon time step
K	feedback gain
k	control time step
N	prediction horizon
N_u	control horizon
n_z	normal acceleration
p, q, r	helicopter body angular rates
pk	subscript peak
Q	tracking error weight matrix
$\bar{r}$	reference state vector along the prediction horizon
ref	subscript reference
t	time
$trim$	subscript value at trim
u	control input vector
u, v, w	helicopter velocity along the body axes
$\bar{u}$	control input vector along the prediction horizon
x	state vector
x, y, z	helicopter coordinates in the Earth reference frame
$\bar{x}$	predicted state vector along the prediction horizon

I. INTRODUCTION

COMPARED to fixed-wing aircraft, helicopters are highly versatile vehicles that can be used to execute a diverse range of commercial and military missions mainly due to its extreme maneuverability in low- and high-speed flight, vertical take-off and landing capabilities and the ability to hover. However, these great capabilities come with the fact that they are very difficult to control: they have fast, complex dynamics, are inherently unstable and its motion is highly coupled. Not only does this increase the workload of the pilot tremendously, it is also the cause of many fatal accidents [1]. With the introduction of flight control systems and fly-by-wire in helicopters in the 90's-00's, the flying characteristics of the helicopter could be adjusted to the pilot's needs to make the helicopter easier and safer to fly [2], [3]. Furthermore, handling quality requirements were set up in order to serve as a guideline for desired flight characteristics to improve the ease of controlling an aircraft [4]. However, to this day helicopters remain hard to fly and not accessible to the general public. Therefore, designing flight control systems in order to improve the helicopter handling qualities and safety is an important but challenging task.

At the same time Model Predictive Control (MPC) is emerging as a promising model-based optimal control technique with the powerful capabilities of including constraints on inputs and outputs, and including an objective function directly in the control algorithm. Furthermore, MPC has the advantage of being able to take into account future information of the system and the environment. This allows MPC to deal efficiently with time delays, non-minimum phase behaviour and to anticipate on future events [5]. Therefore, MPC offers an easy way to directly incorporate technical specifications, safety limits and performance bounds into the helicopter flight control design and to calculate the optimal control input based on a customized objective function and future information of the flight dynamics and flight condition.

On the other hand the optimization process in MPC brings along a big computational burden. Even though optimization methods and computer power are rapidly improving, the real time application of MPC to fast dynamic systems such as helicopters is still in development. Furthermore, when the theoretical and unpractical Lyapunov stability modifications are not implemented to the MPC problem, the MPC problem has to be stabilized by means of tuning. This can be time consuming and requires expertise as no structured tuning approach exists. Especially for nonlinear MPC, the computational burden and stability matter can become critical [6].

MPC was originally used in the 80's for industrial processes in areas as refining, petrochemicals and pulp and paper but is now making its way into other applications such as electronics, medicine, energy and environment and the automotive and aerospace industry [7]–[9]. With the rising popularity of MPC new possibilities for improving helicopter flight are emerging [10]. Research has been performed on MPC applied to helicopters from the 00's onwards where mainly tracking tasks but also other tasks were investigated such as formation flying [11], object avoidance [12], [13], flying in autorotation [14] and for defining control limits corresponding to flight envelope limits [15], [16] or load limits [17]. It has been demonstrated by Liu et al. (2012) that MPC has excellent tracking performance for flying a pirouette maneuver showing that the controller can handle the extremely coupled lateral and longitudinal dynamics [18]. Furthermore, the square maneuver performed by Liu et al. (2010) tests the MPC controlled helicopter's ability to fly forwards, backwards and sideways [19]. Here, flying the square trajectory was performed within 10 cm of the reference trajectory in a small-scaled flight test. It was also shown that by using robust MPC, the controller can deal with bounded external disturbances [20] and with constant wind gusts [18]. However, most previous research on MPC applied to helicopters focused on application in simulation. Only few research tested the controller experimentally in a mechanical set-up with limited Degrees of Freedom (DOF) [21]–[23] or in a small-scaled flight test with an unmanned aerial vehicle [18], [24]–[26].

In short, it can be seen that there is a clear need for helicopters to achieve good handling qualities such that helicopters will be easier to fly and maneuver. One of the biggest reasons it is so hard to fly a helicopter is because of the many cross-coupling effects in its dynamics. Therefore, this is also a big

aspect in the handling quality requirements specified in the "ADS-33 Aeronautical design standard performance specification: handling qualities requirements for military rotorcraft" [27]. With MPC having numerous advantages and making its way into the aerospace industry, it is being applied to helicopters in multiple researches. In this research, it will be investigated how MPC can be used for helicopter flight control to reduce cross-coupling effects and achieve better handling qualities. Therefore, the objective of this research is:

to investigate whether linear and nonlinear MPC are suitable for online application to helicopters to reduce cross-coupling effects by evaluating its performance on the cross-coupling handling quality requirements of the ADS-33 document.

On one hand, it will be investigated how well Linear Model Predictive Control (LMPC) and Nonlinear Model Predictive Control (NLMPC) are able to reduce cross-couplings on the handling quality rating scale, compared to an uncontrolled helicopter and compared to a Proportional Integral Derivative (PID) controlled helicopter. On the other hand, it will be investigated how sensitive the MPC controllers are to prediction model errors when reducing cross-coupling effects. Furthermore, the similarities and differences between linear and nonlinear MPC will be analyzed.

This paper will first clarify the methodology used to fulfill the research objective in Section II. Section III shows the model predictive control design that will be analyzed. Next, Section IV presents the results of the cross-coupling requirement simulations after which the results of the sensitivity analysis will be presented in Section V. Finally, the findings of this paper and recommendations for future work will be stated in Section VI.

II. METHODOLOGY

In this section the method used for answering the research objective will be described. First the cross-coupling requirements that will be investigated will be explained. After this, the simulation set-up of the cross-coupling requirement simulations and the sensitivity analysis will be stated. Then, the uncertainty implemented in the simulation model for the cross-coupling requirement simulations will be introduced. Furthermore, the error implemented in the prediction model for the sensitivity analysis will be presented. Next, the nonlinear and linear helicopter model used for the simulations will be introduced. Finally, the PID controller used to compare the MPC controller to will be presented.

A. Cross-coupling Requirements

First, some background information on cross-coupling effects and the requirements defined by the Aeronautical Design Standard (ADS) will be given. After this, the cross-coupling test cases used for the simulations will be presented.

1) Background: When for example a step input is given in the collective stick of the helicopter, a change in height is the helicopter's primary dynamic response. However, due to the helicopter's complex dynamics many secondary, off-axis responses arise as well: because of the change in collective

TABLE I
PRIMARY AND SECONDARY RESPONSES FOR EACH INPUT AXIS [28].

Input \ Response	Pitch θ	Roll ϕ	Heave w	Yaw ψ
Longitudinal cyclic θ_{1s}	primary response	due to lateral flapping	desired in forward flight	negligible
Lateral cyclic θ_{1c}	due to longitudinal flapping	primary response	descent with roll angle	undesired
Collective input θ_0	due to longitudinal flapping	due to lateral flapping and sideslip	primary response	due to change in torque requires tail rotor thrust
Tail rotor collective θ_{0tr}	negligible	due to tail rotor thrust and sideslip	undesired	primary response

TABLE II
CROSS-COUPLING REQUIREMENTS SPECIFIED BY THE ADS-33 FOR OFF-AXIS DYNAMIC RESPONSES [29].
* NO CURRENT REQUIREMENTS.

Input \ Response	Pitch θ	Roll ϕ	Heave w	Yaw ψ
Pitch θ (Longitudinal cyclic θ_{1s})	X	$\Delta\phi_{pk}/\Delta\theta_4$ hover and fwd flight	flight path response not objectionable in forward flight	* yaw response due to rotor torque changes in aggressive pitch manoeuvres
Roll ϕ (Lateral cyclic θ_{1c})	$\Delta\theta_{pk}/\Delta\phi_4$ hover and fwd flight	X	* thrust/torque spikes in rapid roll reversals	$\Delta\beta/\Delta\phi$ ratios in fwd flight
Heave w (Collective input θ_0)	$\Delta\theta_{pk}/\Delta n_{z_{pk}}$ in fwd flight	* $\Delta\phi_{pk}/\Delta n_{z_{pk}}$	X	$r/\left|\dot{h}\right|$ ratios in hover
Yaw ψ (Tail rotor collective θ_{0tr})	* pitching moments due to sideslip in fwd flight	dihedral effect on roll control power	not objectionable in hover	X

input, there is a change in torque of the main rotor which will cause the helicopter to yaw. In order to counter this yaw motion, the pedal needs to be used to generate a counter-acting moment coming from the tail thrust. Similarly, when an input is given to one of the other control inputs, the helicopter responds with a primary on-axis response and some secondary responses in the off-axis degrees of freedom. An overview of the primary and secondary responses of each control input is given in Table I where it can be seen that many cross-coupling effects are caused by lateral or longitudinal flapping of the rotor blades or by changes in the rotor torque. These off-axis responses are often referred to as inter-axis coupling, input-output coupling or cross-coupling effects. They are mostly undesired as they increase the workload of the pilot immensely even for straightforward tasks such as maintaining hover.

Therefore, requirements on the amount of cross-coupling effects in helicopter flight are widely described in the ADS-33 handling qualities document [27]. Here, the ADS-33 puts requirements on the amount of off-axis response present such that the helicopter has good handling qualities. In this way, the ADS-33 provides a way to objectively measure cross-coupling effects and handling qualities and serves as a guidance for the design of the helicopter and its flight control systems. Here, handling qualities are defined as *"those qualities or characteristics of an aircraft that govern the ease and precision with which a pilot is able to perform the tasks required in support of an aircraft role"* by Cooper and Harper (1969) [30]. For most cross-coupling effects, the document has defined a certain parameter indicating the amount of

off-axis response compared to the amount of on-axis input given. Hence, when flying the helicopter and giving a step input in one of the controls, this parameter that resembles the amount of off-axis response should remain within the required limits in order to have a certain level of handling qualities. In order to specify these limits, level 1, 2 and 3 handling quality boundaries for these parameters were defined based on Cooper-Harper ratings of flight tests. This rating scale subjectively measures the ease of controlling an aircraft by letting the pilot answer a series of questions about flying the maneuver to then categorize the maneuver in a level of handling quality [30]. Here, level 1 is the best level with excellent to fair handling qualities requiring no to minimal pilot workload to perform the maneuver. Level 2 captures the maneuvers with aircraft characteristics with minor to very objectionable but tolerable deficiencies. Level 3 indicates the worst level of handling qualities where major deficiencies are present in the aircraft characteristics and an extensive workload is required to fly the maneuver. These boundaries can then be used as design requirements or just as indicative guidelines. The cross-coupling requirements specified in the ADS-33 document for off-axis responses are summarized in Table II with its respective parameter representing the amount of cross-coupling.

2) Test Cases: There are 10 cross-coupling requirements that will be tested which are formulated in the ADS-33 in Section 3.3.9 page 12 on interaxis coupling for hover and low speed flight and 3.4.5 page 17 on interaxis coupling for forward flight. The hover and low speed flight requirements

will be performed at 0 knots flight speed and the forward flight requirements will be simulated at 80 knots or 41 m/s flight speed. For all these requirements, an excitation in one of the control inputs is given after which the off-axis response will be measured by means of a predefined cross-coupling parameter that scales with the off-axis response. The cross-coupling criteria for hover and low speed flight and for forward flight that will be tested are presented below and will be explained more thoroughly in Section IV.

For hover and low speed flight:

1) yaw due to collective for aggressive agility
2) pitch due to roll coupling for aggressive agility
3) roll due to pitch coupling for aggressive agility
4) pitch due to roll coupling for target acquisition & tracking
5) roll due to pitch coupling for target acquisition & tracking

For forward flight:

6) pitch attitude due to collective control
   a) small collective inputs
   b) large collective inputs
7) pitch due to roll coupling for aggressive agility
8) roll due to pitch coupling for aggressive agility
9) pitch due to roll coupling for target acquisition & tracking
10) roll due to pitch coupling for target acquisition & tracking

Both time (for aggressive agility) and frequency (for target acquisition and tracking) requirements are set out in the ADS-33 for pitch and roll coupling as coupling handling qualities are not only task but also frequency dependent. "A pilot may be less tolerant of large amounts of coupling at high frequency for an aggressive-precision task but may find the same amount acceptable for a non-aggressive low precision task." as discussed by Blanken et al. (1997) [31]. Therefore, the frequency domain criteria is needed in order to also capture the short-term coupling response that corresponds to high precision, agile tracking tasks.

For the time domain requirements, the control input that will be given in order to excite the on-axis response will mostly be a step input of plus or minus 10% of the control input range given one second after the simulation started. This usually leads to a significant and fast change in the on-axis attitude. In some simulation cases, which will be mentioned, the step input is smaller than the 10% change because of helicopter limits. The control input that will be given for the frequency domain requirements will be explained in Section IV-E.

B. Simulation Set-up

This section will discuss the control and model set-ups used for the cross-coupling requirement simulations and the sensitivity analysis. An overview of the models used as simulation and prediction model for the cross-coupling simulations and the sensitivity analysis can be found in Figure 1.

1) Cross-coupling Requirement Simulations: The effectiveness of MPC to reduce cross-coupling effects during helicopter flight will be evaluated by investigating its performance on the 10 cross-coupling requirements set out by the ADS-33 document for hover and forward flight. The performance of reducing cross-coupling effects will be measured by means
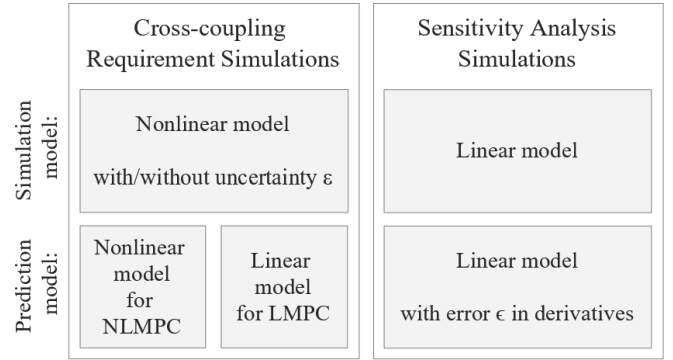
Fig. 1. Overview of simulation and prediction model set-up for the cross-coupling requirement and sensitivity analysis simulations.

of the cross-coupling parameter defined in the ADS-33 and the handling quality level it corresponds to. This will be done in a simulation of the BO-105 helicopter where each of the cross-coupling cases will be tested for the helicopter with nonlinear MPC applied to it, with linear MPC applied to it, the helicopter without controller and the PID controlled helicopter. In this way, the performance of the MPC controllers can be compared to the uncontrolled helicopter and to a conventional control technique. Furthermore, the linear and nonlinear MPC controller can be compared to each other. In this simulation the objective of the controllers will be to minimize the off-axis attitude responses when simulating both a positive and negative step in the on-axis control input. The position of the helicopter and the on-axis response will be uncontrolled. In the uncontrolled simulations, the on-axis and relevant off-axis attitude will be uncontrolled. The off-axis attitude that is not part of the cross-coupling case will be controlled to remain constant using the simple PID controller from Section II-F e.g. yaw attitude in the pitch due to roll coupling case.

The simulation will use the nonlinear, 8 DOF helicopter model ran at 100 Hz as simulation model which has to represent the actual helicopter dynamics. Furthermore, the MPC controllers also use a helicopter model in order to predict the future states of the helicopter. The same nonlinear 8 DOF model is used as prediction model for the nonlinear MPC controller whereas the linear MPC controller will use the linearized 8 DOF model. Both models will be explained further in Section II-E. In order to be able to compare the performance of NLMPC with LMPC without the bias of NLMPC having a perfect future state prediction, an uncertainty is added to the simulation model. Hence, the 4 control configurations will be tested in a simulation with and without uncertainty added to the simulation model. In this way, not only an unbiased comparison can take place but also a more realistic behaviour of the helicopter can be simulated as the uncertainty will be implemented as a disturbance in the main rotor thrust. More on this uncertainty that is added to the simulation model can be found in Section II-C.

2) Sensitivity Analysis Simulations: The robustness or sensitivity of MPC to prediction model errors will be investigated by evaluating the decoupling performance of the MPC controllers when a mismatch or error is present in the prediction

model. In order to be able to systematically implement an error in the prediction model, the linear prediction model will be used. In this way the error can be applied to one of the relevant derivatives in the state and input matrix. To reduce the model mismatch between the simulation and prediction model, the linear model is also used for the simulation. The implementation of the fixed error in the prediction model will be explained in Section II-D

The aim of the sensitivity analysis is twofold. First of all, for each cross-coupling case the important derivatives will be identified by means of implementing a fixed error in every prediction model derivative relevant to the cross-coupling case, one at a time. Then, cross-coupling requirement simulations are performed and the cross-coupling parameters are measured. Based on the change in cross-coupling parameter and if the controller still has level 1 handling qualities the derivatives which alter the handling qualities of the MPC controlled helicopter the most can be found. This information is important as to known which prediction model derivative needs to be of high accuracy in order to still have level 1 handling qualities. Secondly, once the important derivatives have been identified they will be investigated further by varying the error that is implemented and measuring how this affects the cross-coupling parameter. This information gives understanding to how sensitive these derivatives are to errors and what kind of errors are most performance degrading (over/underestimating, changing sign, etc.). It must be noted that in this research only the influence of one error at a time will be investigated as to pinpoint the important derivatives. The robustness to multiple errors at the same time is beyond the scope of this research.

C. Introducing the Uncertainty

An uncertainty will be implemented in the nonlinear simulation model for the cross-coupling simulations for two reasons. Firstly and most importantly, the error is introduced in order to remove the positive bias of the nonlinear MPC controller. Secondly, the addition of the uncertainty into the helicopter model adds more realistic dynamics as the uncertainty that is added acts as a disturbance to the main rotor thrust. Without the uncertainty, the nonlinear MPC would have a perfect prediction model which is unrealistic and yields an unfair comparison of the nonlinear MPC with the linear MPC. Furthermore, it was decided to introduce the uncertainty in the simulation model instead of in the prediction model in order to have a consistent implementation for both the linear and nonlinear MPC, maintaining comparability. This entails that there is also a disturbance introduced in the helicopter dynamics which will be noticeable in the behavior of the helicopter but not unwanted.

The uncertainty ε is introduced as a time-varying random variable with normal distribution $\varepsilon \sim \mathcal{N}(\sigma, 0)$ with a standard deviation of σ and zero mean [32]. It is applied to the main rotor thrust coefficient as the thrust force is the main aerodynamic force acting on the helicopter, affecting the motion in all degrees of freedom, and is also very hard to predict. Hence, adding an uncertainty in the thrust coefficient in the model is realistic. It is applied according to Equation 1 so
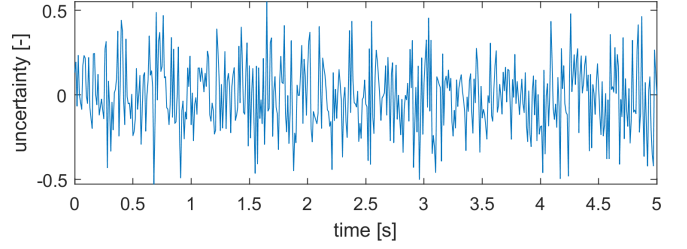
Fig. 2. A 5 second trial of the uncertainty ε with $\sigma = 0.2$ over time.

that C_T is being decreased or enlarged with ε multiplied with the original thrust coefficient. As can be seen, the uncertainty varies with time: each simulation time step Δt the uncertainty ε changes. As the uncertainty is randomly generated each time step, every simulation is different. Therefore, a series of 6 simulations, called trials, are ran where the cross-coupling results are linearly averaged.

$$C_T = C_T \cdot (1 + \varepsilon(\Delta t)) \tag{1}$$

For the simulations, a standard deviation of $\sigma = 0.2$ is chosen which means that 68% of the generated uncertainties will be within $[-0.2, 0.2]$ and 95% will be within $[-0.4, 0.4]$. In Figure 2, one can see a trial of this randomly generated uncertainty over 5 seconds.

D. Introducing the Sensitivity Analysis Error

The error will be implemented in the prediction model of the MPC controller in the elements of the state matrix A and input matrix B of the linear helicopter model. More specifically, it will be implemented in the relevant elements only e.g. for yaw due to collective coupling the error will be implemented in the derivatives of the yaw acceleration so $\frac{\partial \dot{r}}{\partial u}, \frac{\partial \dot{r}}{\partial v}, ...$ in the A matrix and $\frac{\partial \dot{r}}{\partial \theta_0}, \frac{\partial \dot{r}}{\partial \theta_{1s}}, ...$ in the B matrix. Here, a simplified notation will be used such that for example the derivative $\frac{\partial \dot{r}}{\partial u}$ will be noted as $\dot{r}_u$.

The error ϵ will be implemented to the actual derivative in a dimensionless manner as can be seen in Equation 2. Here, the estimated derivative D_{MPC}, so the derivative with error used by the MPC controller, will be equal to the actual derivative D_{actual} plus a fraction ϵ of the actual derivative. An overview of how the error value influences the proportions between the actual and the MPC derivative can be found in Equation 3.

$$D_{MPC} = D_{actual}(1 + \epsilon) \tag{2}$$

$$
\begin{aligned}
\epsilon < -1 : \quad & \mathrm{sgn}(D_{MPC}) = -\mathrm{sgn}(D_{actual}) \\
\epsilon = -1 : \quad & D_{MPC} = 0 \\
-1 < \epsilon < 0 : \quad & |D_{MPC}| < |D_{actual}| \\
\epsilon = 0 : \quad & D_{MPC} = D_{actual} \\
\epsilon > 0 : \quad & |D_{MPC}| > |D_{actual}|
\end{aligned} \tag{3}
$$

In order to find out how large such an error realistically could be when modeling a helicopter, data from Pavel (1996), considered as estimated derivatives, was compared to data from the NASA model of Heffley et. al (1979), considered as actual derivatives [33], [34]. Here, it could be seen that most

errors are within -1 and 0, hence underestimating the actual derivative in absolute value. It is only for a few cases that a greater positive or negative error occurs but still around an absolute value of 1. Furthermore, some outliers were spotted with errors of ± 30. However, these only occur when the actual derivative is almost zero. As will be clear later from the results of the sensitivity analysis, the accuracy of these derivatives barely influence the MPC performance at all.

Based on an error analysis of the data from Pavel (1996) and Heffley et. al (1979), it was chosen to first find the important derivatives by applying an error of 10 and -10 to all of the relevant derivatives one by one and measuring the cross-coupling parameters [33], [34]. After this a range of errors from -10 to 10, so $\epsilon = -10, -9, -8, -7, -6, -5, -4, -3, -2, -1, 0, 1, 2, 3, 4, 5, 6, 7, 8, 9, 10$, will be applied to the most important derivatives in order to have an individual analysis.

E. Helicopter Model

The 8 DOF nonlinear model of the BO-105 helicopter used for the simulations in this research was developed at the TU Delft and consists out of 6 helicopter body DOFs and 2 rotor inflow DOFs, one for the main rotor and one for the tail rotor [33], [35]. The rotor inflow dynamics is added because the hingeless rotor system of the BO-105 causes the rotor and body dynamics to be highly coupled [36]. Furthermore, the body dynamics takes into account the forces and moments from the main rotor, tail rotor, fuselage, horizontal tail and vertical tail. The helicopter's motion will be described by a total of 14 states and will be controlled by 4 control inputs namely the main rotor collective, the longitudinal cyclic, the lateral cyclic and the tail rotor collective as seen in Equation 4 and 5 respectively.

$$x = [u\ v\ w\ p\ q\ r\ \psi\ \theta\ \phi\ x\ y\ z\ \lambda_0\ \lambda_{0_{tr}}]' \quad (4)$$

$$u = [\theta_0\ \theta_{1s}\ \theta_{1c}\ \theta_{0_{tr}}]' \quad (5)$$

The linear 8 DOF model of the system is obtained by linearizing the nonlinear model around a certain trim condition (x_{trim}, u_{trim}) using perturbation linearization [37][p. 563]. The linear model then approximates the nonlinear model at and around this trim condition. The more the helicopter state deviates from the trim condition or the more nonlinear the helicopter behaves at this trim condition, the worse the linear approximation will be.

Furthermore, some physical boundaries are imposed on the control inputs because of actuator limits. Firstly, the control inputs are bounded by upper and lower limits. The data for these limits of the BO-105 helicopter is retrieved from Prouty (2002) [37]. Secondly, the rate of change in each control input is limited. No rate limits were found for the BO-105 so the rate data for the Bell 412 helicopter from Voskuijl et al. (2010) was used [38]. The input ranges and input rate limits of the BO-105 helicopter model can be found in Table III.

F. PID Controller Design

In order to be able to compare the performance of the MPC controller with a controlled helicopter, a simple Proportional

TABLE III
INPUT RANGE AND RATE LIMITS.

Limit	Value [deg]	Limit	Value [deg]	Limit	Value [deg·s]
$\theta_{0_{min}}$	-0.2	$\theta_{0_{max}}$	15.0	$\Delta\theta_{0_{max}}$	$16.0 \cdot \Delta t$
$\theta_{1s_{min}}$	-6.0	$\theta_{1s_{max}}$	11.0	$\Delta\theta_{1s_{max}}$	$28.8 \cdot \Delta t$
$\theta_{1c_{min}}$	-5.7	$\theta_{1c_{max}}$	4.2	$\Delta\theta_{1c_{max}}$	$16.0 \cdot \Delta t$
$\theta_{0_{tr_{min}}}$	-8.0	$\theta_{0_{tr_{max}}}$	20.0	$\Delta\theta_{0_{tr_{max}}}$	$32.0 \cdot \Delta t$

TABLE IV
PID CONTROLLER GAINS FOR THE SIMULATIONS.

Gain	Value [-]	Gain	Value [-]	Gain	Value [-]
K_{θ_1}	3	K_{ϕ_1}	0.55	K_{ψ_1}	16
K_{θ_2}	11.2	K_{ϕ_2}	40	K_{ψ_2}	170
K_q	0.8	K_p	-0.35	K_r	1.9

Integral Derivative controller will be implemented. This PID controller uses control rules based on the error between the reference state and the actual state, the integral of this error and the gradient of this error. For the cross-coupling simulations, only the attitude of the helicopter will be controlled. Therefore, the PID rules, which can be seen in Equation 6-8, are implemented to θ_{1s_0}, θ_{1c} and $\theta_{0_{tr_0}}$ only [36]. Here, the $K_{...}$'s are the gains that were tuned using the Ziegler-Nichols method and fine-tuned using trial and error. The final values of the gains can be seen in Table IV. Furthermore, the integral term in these PID rules is taken in discrete time over an interval of $t - 5\Delta t$ to t where t is the current time and Δt_s is the simulation time step. As can be seen, the inputs are solely dependent on the on-axis tracking error e.g. θ_{1s} depends on $\theta - \theta_{ref}$ only.

$$\theta_{1s} = \theta_{1s_{trim}} + K_{\theta_1}(\theta - \theta_{ref}) + K_q q \quad (6)$$
$$+ K_{\theta_2} \sum_{t-5\Delta t_s}^{t} (\theta - \theta_{ref})\Delta t$$

$$\theta_{1c} = \theta_{1c_{trim}} + K_{\phi_1}(\phi_{ref} - \phi) + K_p p \quad (7)$$
$$+ K_{\phi_2} \sum_{t-5\Delta t_s}^{t} (\phi_{ref} - \phi)\Delta t$$

$$\theta_{0_{tr}} = \theta_{0_{tr_{trim}}} + K_{\psi_1}(\psi - \psi_{ref}) + K_r r \quad (8)$$
$$+ K_{\psi_2} \sum_{t-5\Delta t_s}^{t} (\psi - \psi_{ref})\Delta t$$

Similar to the MPC controller, only the relevant DOFs will be tracked in a simulation. The inputs for the uncontrolled DOFs are then set to the trim value instead of applying the PID rule. Furthermore, the inputs calculated by the PID controller are limited to their respective maximum or minimum boundary value as there are physical constraints on the control inputs.

III. MODEL PREDICTIVE CONTROL

This section will first introduce the concept of linear and nonlinear model predictive control for reference tracking after
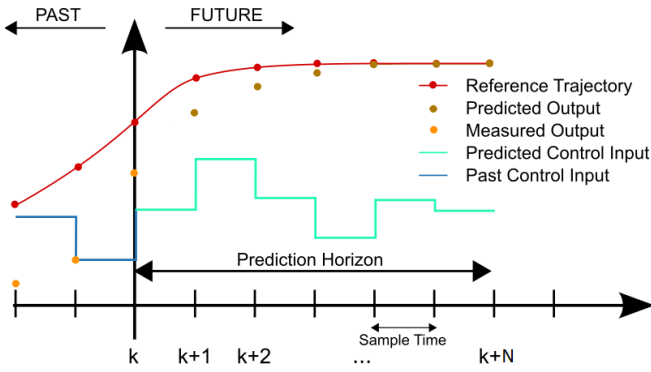
Fig. 3. The concept of MPC in discrete time for reference tracking [39].

which the MPC controller design used for the simulations will be presented.

A. Introduction to MPC

MPC is a type of model-based, optimal control where at each time step, k, an optimal control input sequence $\bar{u}_k = [u_k, \ u_{k+1}, \ \ldots, \ u_{k+N-1}]$ is computed online over a future time horizon, the prediction horizon N, by solving an open-loop optimization problem that has knowledge of the system model [5]. The optimization uses the current state of the system as initial state and a model of the system to compute the future states along the prediction horizon in order to optimize a desired objective function. Then, only the first control input in this optimal control input sequence u_k is applied to the system. At the next time step, the prediction horizon of the optimization problem shifts one step forward, to $k + 1$, and the next optimal control sequence $\bar{u}_{k+1} = [u_{k+1}, \ u_{k+2}, \ \ldots, \ u_{k+N}]$ is computed.

In Figure 3, one can see the concept of MPC explained in discrete time for a reference tracking problem. In a reference tracking problem, the objective function of the optimization is to minimize the error $\bar{e} = [e_{k+1}, \ \ldots, \ e_{k+N}]$ between the reference trajectory $\bar{r} = [r_{k+1}, \ \ldots, \ r_{k+N}]$ and the predicted output trajectory $\bar{x} = [x_{k+1}, \ \ldots, \ x_{k+N}]$. Then, the optimization problem consists of computing the optimal control input over the prediction horizon such that the tracking error is minimized and the constraints are met.

A distinction can be made between linear and nonlinear model predictive control. The difference lies in the use of a linear or nonlinear objective function, constraints and prediction model. If one these elements is nonlinear, the controller is considered a nonlinear MPC controller [5]. Nonlinearity often comes with non-convexity which can cause the optimization problem to have multiple local optima and which also increases the complexity of solving the optimization problem. Therefore, NLMPC usually has an increased computation time and can cause the optimization solution to become suboptimal. However, also the fidelity of the model plays a big roll in the closed-loop performance as the algorithm optimizes the error between the predicted state and the reference state over the prediction horizon. When MPC with a linear prediction model is applied to a highly nonlinear system, the prediction

model might not be of sufficient fidelity. A discussion on how this influences the results of the cross-coupling requirement simulations is held in Section IV-F4. Furthermore it must be noted that in this report use is made of a quadratic objective function with positive definite weight and of a constraint with an absolute value function which are nonlinear but convex functions. Nevertheless, when the linear prediction model is used the controller will still be considered a linear MPC controller as the objective function, constraints and prediction model are still convex.

B. Controller Design

The MPC design used for the simulations will be presented in this section including its objective function, constraints, the prediction models and tuning parameters.

1) Objective Function: The goal of the controller in the cross-coupling requirement simulations is to reduce the off-axis response when an on-axis input is given. In order to achieve this, the MPC controller is going to track a constant trim reference signal for the off-axis responses only. Then, the objective of the MPC controller in the cross-coupling requirement simulations is to minimize the error between the state and the reference signal for the off-axis states. A quadratic objective function will be used to minimize the tracking error with weight Q and reference trajectory r as can be seen in Equation 9.

$$\underset{\bar{u}_k, \ \bar{x}_k}{\text{minimize}} \quad \sum_{i=0}^{N} \left\{ \left(x_{k+i} - r_{k+1} \right)' Q \left(x_{k+i} - r_{k+1} \right) \right\} \qquad (9)$$

Here, the weight Q changes depending on the cross-coupling case. For example, if the requirement for pitch due to roll cross-coupling is being simulated, the pitch and yaw angle will be tracked whereas the roll angle won't be controlled. For this case Q will be equal to $\text{diag}(0, 0, 0, 0, 0, 0, 1, 0, 1, 0, 0, 0, 0, 0)$. The reference trajectory of the pitch and yaw angle will be the trim value of the respective angle. It must be noted that only the attitudes (ψ, θ, ϕ) will be controlled and not the angular rates (p, q, r) or angular accelerations $(\dot{p}, \dot{q}, \dot{r})$. This would yield steady-state offsets if no integral term would be added. Furthermore, it is only the attitude that is the direct state that needs to be controlled.

2) Constraints: One of the big advantages of model predictive control is that it can incorporate soft and hard constraints on inputs and states directly in the controller. Hence, some physical boundaries on the input range and input rates are imposed because of actuator limits. Firstly, the input range is limited for each control input by $u_{min} = [\theta_{0_{min}} \quad \theta_{1s_{min}} \quad \theta_{1c_{min}} \quad \theta_{0_{tr_{min}}}]'$ and $u_{max} = [\theta_{0_{max}} \quad \theta_{1s_{max}} \quad \theta_{1c_{max}} \quad \theta_{0_{tr_{max}}}]'$. Secondly, the rate of change in each control input is limited by $\Delta u_{max} = [\Delta\theta_{0_{max}} \quad \Delta\theta_{1s_{max}} \quad \Delta\theta_{1c_{max}} \quad \Delta\theta_{0_{tr_{max}}}]'$. The values of the limits used in the simulations can be seen in Table III. These limits are implemented according to Equation 10 and 11 and hold over the entire prediction horizon and for all control

inputs. The state variables are not bounded by upper and lower limits but are constraint by the dynamics of the helicopter.

$$u_{min} < u_{k+i} < u_{max} \qquad \text{for } i = 1, 2, \ldots, N \qquad (10)$$

$$|u_{k+i} - u_{k+i-1}| < \Delta u_{max} \qquad \text{for } i = 1, 2, 3, \ldots, N \quad (11)$$

3) Prediction Model: The 8 DOF BO-105 helicopter model described in Section II-E will be used as prediction model in the MPC controller. Depending on whether linear or nonlinear MPC will be implemented, the linear or nonlinear 8 DOF model will be used as prediction model. It must be noted that by using the nonlinear model as prediction model, the optimization of the MPC controller becomes non-convex. More on the differences between NLMPC and LMPC can be found in IV-F4.

4) Tuning Parameters: First of all, the controller will have a sampling time of 0.03 s. With a simulation sampling time of 0.01 s this means the controller calculates a new control input every 3 simulation time steps. In the remaining steps, the control input is kept the same as the previously calculated input. Next, a constant prediction horizon N of 5 control time steps (0.15 s) is used. In order to reduce the computation time, a control horizon N_u of 3 control steps (0.09 s) was selected. Hence, after 3 control time steps the control input of the last step is fixed for the remaining steps in the prediction horizon.

5) Complete MPC Formulation: To summarize the MPC controller design that is used in the cross-coupling simulations and the sensitivity analysis simulations, the complete MPC optimization problem is presented in Equation 12. The optimization problem will be solved in Matlab 2020b with the fmincon-function using sequential quadratic programming as optimization algorithm which is a smooth nonlinear optimization method. Here, the trim control inputs are used as initial value. It must be noted that for each simulation individual components can change such as the model when using LMPC or NLMPC or implementing the error from the sensitivity analysis, or the weight Q when a different cross-coupling case is tested.

$$\underset{\bar{u}_k, \, \bar{x}_k}{\text{minimize}} \quad \sum_{i=1}^{N} \left\{ \left(x_{k+i} - r_{k+1} \right)' Q \left(x_{k+i} - r_{k+1} \right) \right\}$$

$$\text{subject to: } x_{k+i} = f(x_{k+i-1}, u_{k+i-1}) \quad \text{for } i = 1, 2, ..., N$$
$$u_{min} < u_{k+i} < u_{max} \qquad \text{for } i = 0, 1, ..., N-1$$
$$|u_{k+i} - u_{k+i-1}| < \Delta u_{max} \quad \text{for } i = 0, 1, ..., N-1$$
$$\text{with: } \quad x = [u \, v \, w \, p \, q \, r \, \psi \, \theta \, \phi \, x \, y \, z \, \lambda_0 \, \lambda_{0_{tr}}]'$$
$$u = [\theta_0 \, \theta_{1s} \, \theta_{1c} \, \theta_{0_{tr}}]'$$
$$(12)$$

IV. CROSS-COUPLING REQUIREMENT SIMULATIONS

This section will present the results and analysis of the cross-coupling requirement simulations for all 10 cross-coupling cases. For each coupling case the cross-coupling parameter results for one simulation setting will be shown. In general, the results of the other settings are comparable and will therefore be discussed briefly in the overview tables in Section IV-F. Furthermore, a demonstration of how to calculate the cross-coupling parameter will be presented for

Fig. 4. Pitch due to roll requirement simulation of the uncontrolled helicopter for 80 knots for a positive (right) lateral cyclic step input.
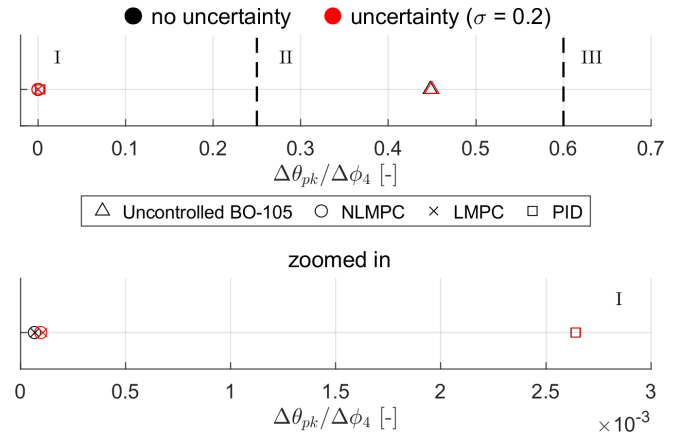
Fig. 5. Pitch due to roll requirement results for 80 knots for a positive (right) lateral cyclic step input.

pitch due to roll for both the time and frequency domain requirement. Moreover, an off-axis rate response analysis will be performed for pitch due roll coupling as an example in order to analyze and compare the coupling reduction performance of the PID and MPC controller.

A. Pitch due to Roll Coupling

For both pitch due to roll and roll due to pitch coupling the ADS33 states that "*The ratio of peak off-axis attitude response from trim within 4 seconds to the desired (on-axis) attitude response from trim at 4 seconds, $\Delta\theta_{pk}/\Delta\phi_4$ ($\Delta\phi_{pk}/\Delta\theta_4$), following an abrupt lateral (longitudinal) cockpit control step input, shall not exceed $\pm$ 0.25 for Level 1 or $\pm$ 0.60 for Level 2. Heading shall be maintained essentially constant.*" [27]. Therefore, a step input of $\pm$10% the control range is given in the lateral cyclic at $t = 1$ s as can be seen in Figure 4. In this Figure a demonstration is given on how to calculate the cross-coupling parameter of the uncontrolled helicopter using Equation 13. A $\Delta\theta_{pk}/\Delta\phi_4$ of 0.45 was obtained.

$$\text{if a step input is given at } t = 0 \text{ s}$$
$$\Delta\theta_{pk} = (\text{max } |\theta| \text{ before } t = 4 \text{ s}) - \theta_{trim} \qquad (13)$$
$$\Delta\phi_4 = \phi(t = 4 \text{ s}) - \phi_{trim}$$
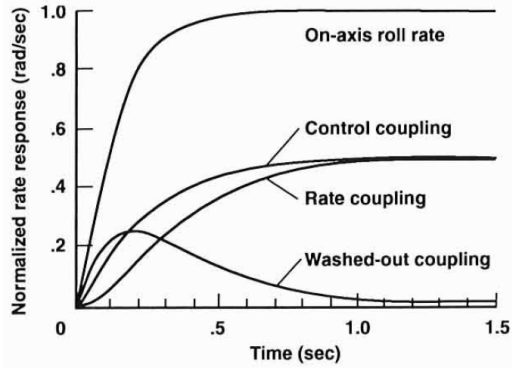
Fig. 6. On- and off-axis rate responses to a lateral cyclic input [31].
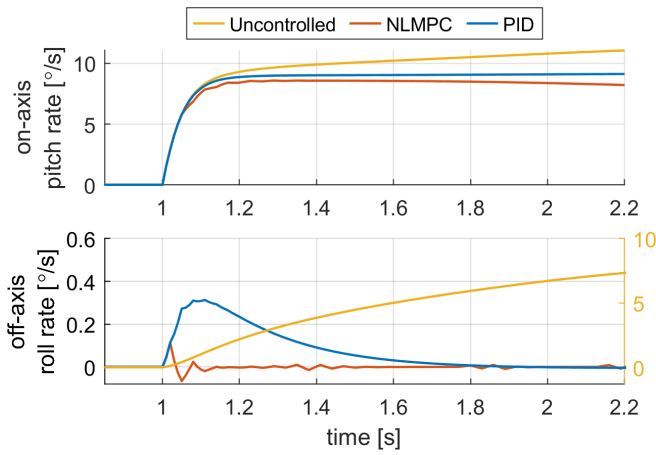
Fig. 7. Pitch due to roll coupling on/off-axis response analysis for 80 knots for a positive (right) lateral cyclic step input.

The cross-coupling parameter results for all control configurations for 80 knots flight with a positive lateral cyclic step input can be seen in Figure 5. It can be seen that the cross-coupling parameter is reduced significantly when the helicopter is being controlled, going from level 2 to level 1 with plenty of margin. When zooming in to 10^{-3} one can see that NLMPC reduces the off-axis response the most with shortly after that the LMPC controller. The PID controller also performs great but cannot surpass the MPC performance. Moreover, it can be seen that the uncertainty doesn't seem to have much of effect to the coupling reduction performance for all control set-ups.

As to investigate the off-axis rate response of the different control set-ups and to indicate the difference between the PID and MPC coupling reduction behaviour, the pitch and roll rate responses for a step input in the lateral cyclic at $t = 1$ s are investigated. The different types of off-axis rate responses defined by Blanken et al. (1997) can be seen in Figure 6. Here, the ideal off-axis rate response is the response with no coupling so with a rate staying as close to zero as possible. In Figure 7 it can be seen that the uncontrolled helicopter shows an off-axis rate response with control coupling. When the controllers are introduced, the off-axis response reduces significantly, eliminating most cross-coupling effects. The PID
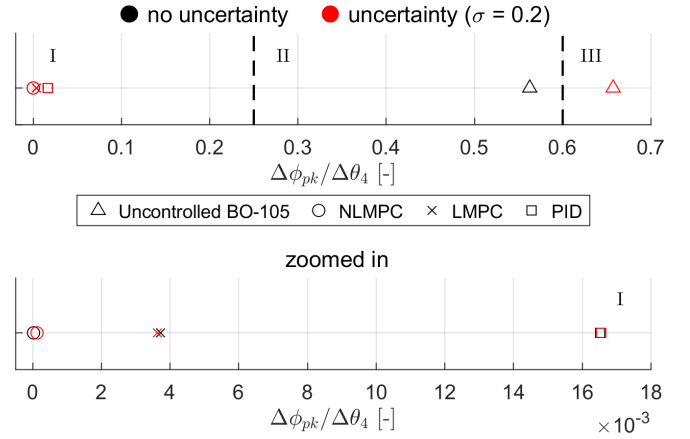
Fig. 8. Roll due to pitch requirement results for 80 knots for a positive (up) longitudinal cyclic step input.

controller shows a small and quick washed-out coupling response whereas the MPC controller reduces the off-axis rate even more and faster, showing a response with quasi no coupling.

B. Roll due to Pitch Coupling

The requirement for roll due to pitch coupling is very similar to the pitch due to roll coupling requirement and is therefore already explained in Section IV-A. The computation of the cross-coupling parameter can be seen in Equation 14.

if a step input is given at $t = 0$ s
$$\Delta\phi_{pk} = (\max |\phi| \text{ before } t = 4 \text{ s}) - \phi_{trim} \quad (14)$$
$$\Delta\theta_4 = \theta(t = 4 \text{ s}) - \theta_{trim}$$

In Figure 8 one can see that again the controllers reduce the handling qualities from level 3 or 2 to level 1. When zooming in to 10^{-3} it can be seen that NLMPC performs best at minimizing the roll angle, almost completely eliminating the cross-coupling effects. Close after NLMPC comes LMPC and then the PID controller. Again, the uncertainty barely has an effect on the cross-coupling parameter results with controller. Without controller, the uncertainty degrades the handling qualities to level 3.

C. Yaw due to Collective Coupling

The ADS-33 states that "*The yaw rate response to abrupt step collective control inputs with the directional controller fixed shall not exceed the boundaries specified in Figure 11. The directional controller may be free if the rotorcraft is equipped with a heading hold function. Pitch and roll attitudes shall be maintained essentially constant. ... Oscillations involving yaw rates greater than 5 deg/sec shall be deemed objectionable.*" [27]. The yaw rate boundaries that are referred to can be seen in Figure 9. Here, r_1 is defined as the largest peak of yaw rate by magnitude between the start of the step input and 3 seconds after the step input. Furthermore, $\dot{h}(3)$ is the value of $\dot{h}$ at 3 seconds after the step input. Finally, r_3 is equal to $r(3) - r_1$ for $r_1 > 0$ and to $r_1 - r(3)$ for $r_1 < 0$
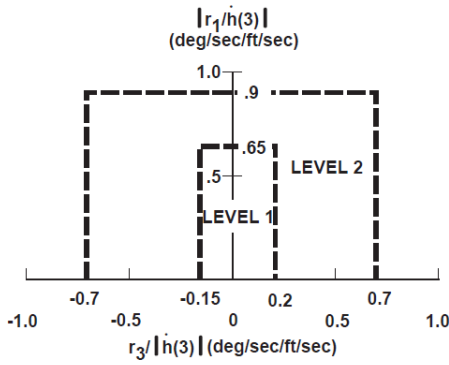
Fig. 9. Yaw due to collective coupling requirement [27]
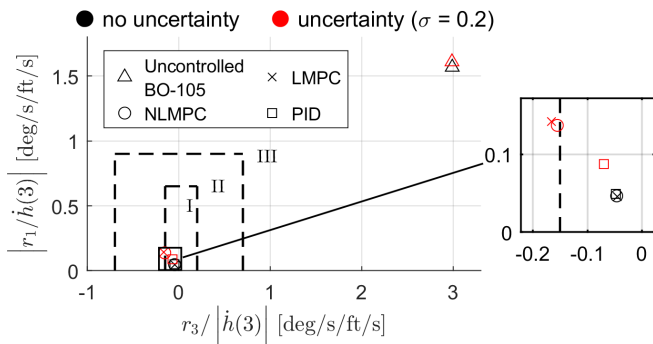
Fig. 10. Yaw due to collective requirement results for hover for a positive (up) collective step input.

where $r(3)$ is the yaw rate at 3 seconds after the step input. The complete computation of the cross-coupling parameters can be seen in Equation 15.

$$\text{if a step input is given at } t = 0 \text{ s}$$
$$\dot{h}(3) = \dot{h}(t = 3 \text{ s})$$
$$r_1 = \max |r| \text{ before } t = 3 \text{ s} \qquad (15)$$
$$\text{if } r_1 > 0 : r_3 = r(t = 3 \text{ s}) - r_1$$
$$\text{if } r_1 < 0 : r_3 = r_1 - r(t = 3 \text{ s})$$

The results of the yaw due to collective requirement simulations for hover for a positive input can be seen in Figure 10. Here, again the handling qualities are improved from level 3 to level 1 when a controller is introduced. However, when the uncertainty is present the results of the linear and nonlinear MPC controllers are both located just over the border of the level 1 boundary. Nevertheless, the result of the PID controller with uncertainty remains in level 1.

This rather large performance difference can be explained by the fact that the MPC uses the prediction model of the helicopter which now has a mismatch with the disturbed simulation model. Furthermore, this coupling case is significantly more vulnerable to the mismatch as the uncertainty is applied to the thrust coefficient which is directly related to the collective input. Moreover, when the positive input is given the thrust of the helicopter increases, as opposed to the negative input, causing the disturbance in the thrust coefficient to have more effect. As can be seen in Table V, the MPC controllers
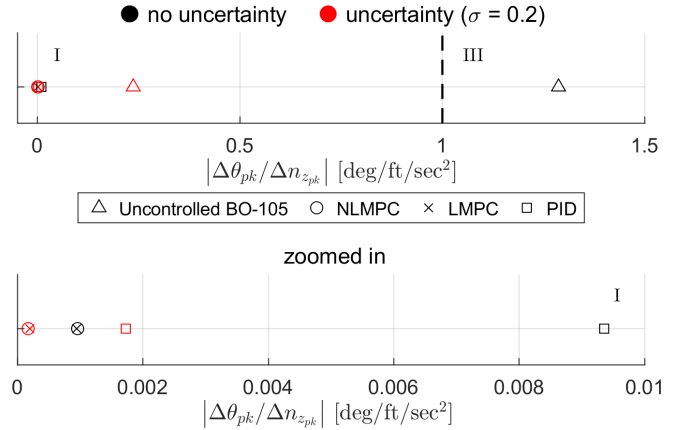
Fig. 11. Pitch due to collective requirement results for 80 knots for a small, positive (up) collective cyclic step input.

are still in the level 1 zone for the negative input case. Hence, it can be concluded that for yaw due to collective coupling the MPC controllers are sensitive to this uncertainty in the main rotor thrust. However, one could improve the robustness of the MPC controller to this kind of model mismatches by implementing robust MPC.

D. Pitch due to Collective Coupling

The requirement for pitch due to collective coupling is split in a requirement for small collective inputs ($<20\%$ rotor torque change) and large collective input ($>20\%$ rotor torque change). For small collective inputs the ADS-33 says that *"the peak change in pitch attitude from trim, $\Delta\theta_{pk}$, occurring within the first 3 seconds following a step change in collective causing less than 20% torque change, shall be such that the ratio $\left|\Delta\theta_{pk}/\Delta n_{z_{pk}}\right|$ is no greater than 1.0 deg/ft/sec^2, where $\Delta n_{z_{pk}}$ is the peak incremental normal acceleration from 1 g flight."* [27]. For large collective inputs, the ratio $\left|\Delta\theta_{pk}/\Delta n_{z_{pk}}\right|$ should be no greater than 0.5 deg/ft/sec^2 for a positive collective input and no greater than 0.25 deg/ft/sec^2 for negative collective inputs. The computation of the cross-coupling parameter can be seen in Equation 16.

$$\text{if a step input is given at } t = 0 \text{ s}$$
$$\Delta\theta_{pk} = (\max |\theta| \text{ before } t = 3 \text{ s}) - \theta_{trim} \qquad (16)$$
$$\Delta n_{z_{pk}} = (\max |\dot{w}| \text{ before } t = 3 \text{ s}) - \dot{w}_{trim}$$

The cross-coupling results for pitch due to small collective inputs can be seen in Figure 11. Here, it is clear that again the handling qualities are improved from level 3 or 2 to level 1 when a controller is applied. When zooming in to 10^{-3} it can be seen that both NLMPC and LMPC have a very small cross-coupling parameter, almost completely eliminating the off-axis response. The PID controller also improves the handling qualities a lot but still has a larger cross-coupling parameter than the MPC controllers.

What is remarkable about these simulations is that the simulation with uncertainty has, for all control set-ups, significantly better coupling reduction performance. This can be explained by the random behaviour of the uncertainty that is
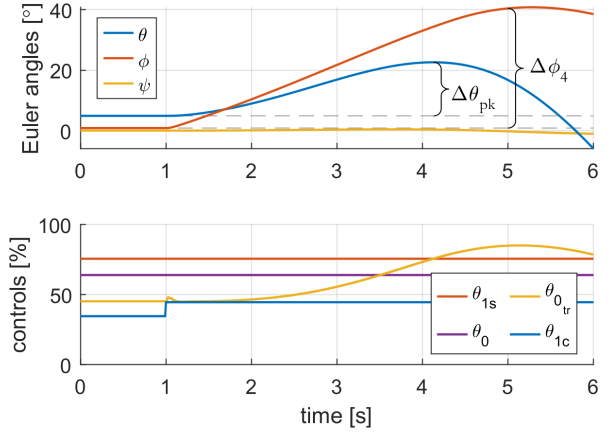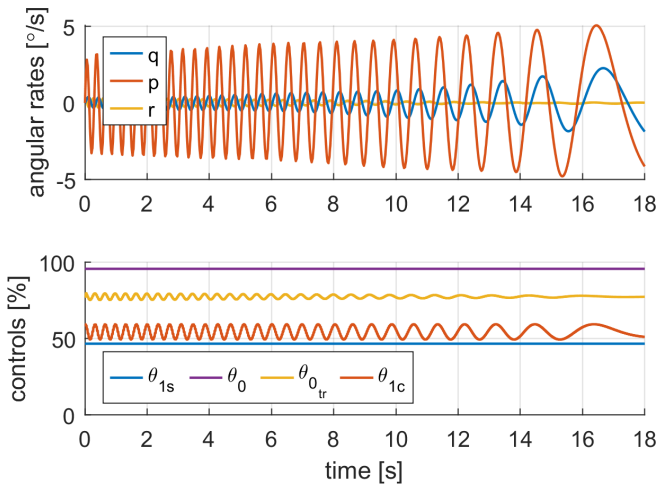
Fig. 12. Pitch due to roll frequency requirement simulation of the uncontrolled helicopter for 80 knots for a positive (right) lateral cyclic step input.
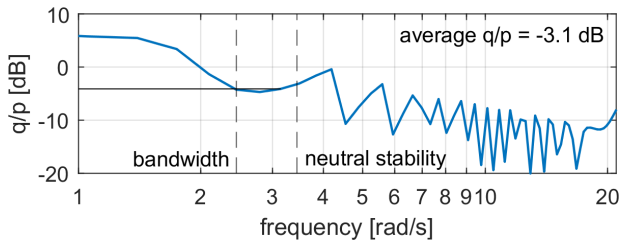

Fig. 13. q/p frequency response of the uncontrolled helicopter for 80 knots for a positive (right) lateral cyclic step input (corresponding to Figure 12).

implemented in the thrust coefficient and that changes each simulation time step. This causes $\dot{w}$ and hence $n_{z_{pk}}$ to change each time step as well, yielding a very large $\Delta n_{z_{pk}}$. Therefore, in this coupling case the cross-coupling parameter does not give a proper indication of the off-axis response compared to on-axis input. That is, the cases with uncertainty cannot be compared to the undisturbed cases. Still, the same performance proportions are found for the uncontrolled, NLMPC, LMPC and PID controlled helicopter with uncertainty as compared to the results without uncertainty.

E. Pitch due to Roll and Roll due to Pitch Coupling for Target Acquisition and Tracking

The ADS-33 states that the pitch due to roll (q/p) and roll due to pitch (p/q) coupling parameters should not exceed the boundaries indicated in Figure 14 where *"the average q/p and average p/q are derived from ratios of pitch and roll frequency responses. Specifically, average q/p is defined as the magnitude of pitch-due-to-roll control input (q/δ_{lat}) divided by roll-due-to-roll control input (p/δ_{lat}) averaged between the bandwidth and neutral-stability (phase = -180 deg) frequencies of the pitch-due-to-pitch control inputs (θ/δ_{lon}). Similarly, average p/q is defined as the magnitude (p/δ_{lon}) divided by (q/δ_{lon}) between the roll-axis (ϕ/δ_{lat}) bandwidth and neutral stability frequencies."* [27]. Here, the bandwidth is defined as the lesser of the phase bandwidth, which is the frequency corresponding to -135° phase, and gain bandwidth,
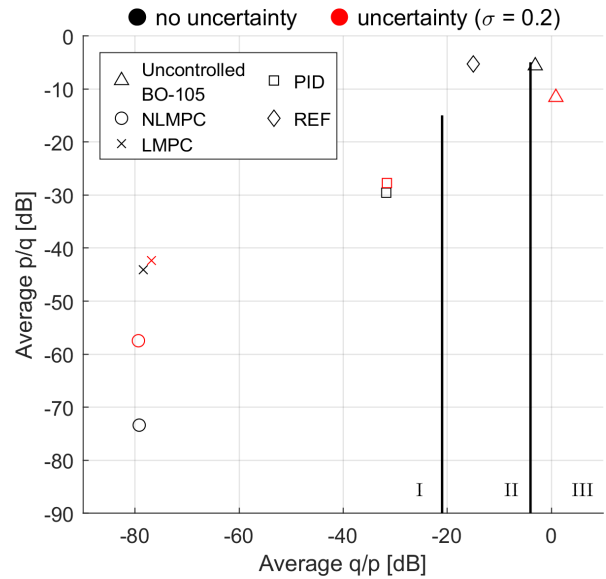
Fig. 14. Average p/q over average q/p for 80 knots [31].

which is the frequency corresponding to the magnitude at neutral stability with a margin of 6 dB added to it. For the calculation of the pitch and roll bandwidth it was assumed that δ_{lon} and δ_{lat} are equivalent to θ_{1s} and θ_{1c} respectively. As the limits set by the ADS-33 are not perfectly clear, the limits for q/p will be set to -21 dB for level 1/2 and -4 dB for level 2/3 and for p/q to -10 dB for level 1/2 and -5 dB for level 2/3.

As a demonstration for the frequency parameter calculations, the simulation of the pitch due to roll frequency requirement for the uncontrolled helicopter in 80 knots flight is shown in Figure 12. Here, a frequency sweep was given in the lateral cyclic input from 20 rad/s to 0.5 rad/s for 18 s. The longitudinal cyclic and collective were kept constant whereas the tail rotor collective was controlled by a PID controller in order to maintain a constant yaw angle. As can be seen, the on-axis roll rate is oscillating with the lateral input, inducing the off-axis pitch rate to oscillate as well but with a slightly smaller amplitude. By calculating the frequency response of the pitch rate divided by the roll rate using the fast Fourier transform algorithm, the q/p gain can be obtained. Here, the gain of q/p gives an accurate indication of the amount of off-axis pitch rate response compared to on-axis roll rate. As can be seen in Figure 13, the average q/p gain between the pitch bandwidth and neutral stability frequency was found to be -3.1 dB. This means that for a roll rate amplitude of 10°/s the pitch rate amplitude would be 7°/s on average for frequencies between 2.4 and 3.4 rad/s.

The average p/q over average q/p for 80 knots results for the different control set-ups can be seen in Figure 14. Here, the uncontrolled helicopter has level 3, at the border of level 2, handling qualities. When the controllers are introduced the handling qualities go to level 1. The PID controller brings the amount of cross-coupling back to around -30 dB for both pitch due to roll and roll due to pitch coupling, with and without uncertainty. This indicates that for a roll (pitch) rate amplitude of 10°/s the pitch (roll) rate amplitude would be 3°/s

TABLE V
OVERVIEW OF THE CROSS-COUPLING HANDLING QUALITY LEVEL RESULTS.

Cross-coupling case	Condition	BO-105		NLMPC		LMPC		PID	
		$\sigma = 0$	$\sigma = 0.2$	$\sigma = 0$	$\sigma = 0.2$	$\sigma = 0$	$\sigma = 0.2$	$\sigma = 0$	$\sigma = 0.2$
Pitch d.t. roll	0 kn, +ve input	III	III	I	I	I	I	I	I
	0 kn, -ve input	II	II	I	I	I	I	I	I
	80 kn, +ve input	II	II	I	I	I	I	I	I
	80 kn, -ve input	III	III	I	I	I	I	I	I
Roll d.t. pitch	0 kn, +ve input	III	III	I	I	I	I	I	I
	0 kn, -ve input	III	III	I	I	I	I	I	I
	80 kn, +ve input	II	III	I	I	I	I	I	I
	80 kn, -ve input	II	II	I	I	I	I	I	I
Yaw d.t. collective	+ve input	III	III	I	II	I	II	I	I
	-ve input	III	III	I	I	I	I	I	I
Pitch d.t. collective	small, +ve input	III	I	I	I	I	I	I	I
	small, -ve input	III	I	I	I	I	I	I	I
	large, +ve input	III	III	I	I	I	I	I	I
	large, -ve input	III	III	I	I	I	I	I	I
Pitch d.t. roll for TA&T	0 kn	II	II	I	I	I	I	I	I
	80 kn	III	III	I	I	I	I	I	I
Roll d.t. pitch for TA&T	0 kn	II	II	I	I	I	I	I	I
	80 kn	II	I	I	I	I	I	I	I

on average. The MPC controllers go even further to about -80 dB for q/p indicating a pitch rate amplitude of only 0.002°/s for a roll rate amplitude input of 10°/s. For p/q NLMPC goes to -75 dB without and -57 dB with uncertainty whereas LMPC goes to about -45 dB for both with and without uncertainty.

F. Overview of the Cross-coupling Results

This section will first present an overview of the handling quality levels of each cross-coupling case. Next, a comparison of the cross-coupling parameter of NLMPC with the uncontrolled helicopter and of NLMPC and LMPC with the PID controller will be made for both the simulations with and without uncertainty. Lastly, a comparison of the performance of linear and nonlinear MPC will be presented.

1) Overview of Handling Quality Levels: An overview of the cross-coupling handling quality level results can be seen in Table V. Here, the uncontrolled helicopter mostly has level 3 or 2 handling qualities. Once a controller is introduced, the handling qualities are improved to level 1. This indicates that all controllers succeed very well at reducing the cross-coupling effects in order to have good handling qualities. Even with uncertainty added to the simulation model, the controllers are able to obtain level 1 handling qualities. The only exception is the NLMPC controller for the yaw due to collective case for a positive collective input which obtained level 2 handling qualities with the uncertainty. This exception will be further explained when looking at Table VII.

2) Comparison of the Cross-coupling Parameter ($\sigma = 0$): In Table VI a comparison of the cross-coupling parameters in percentage increase can be seen for the simulations without uncertainty. First of all, the NLMPC results are compared to the uncontrolled helicopter results where a negative percentage indicates a reduction of cross-couplings. Next, the NLMPC

and LMPC are compared to the PID controller by indicating how much percent the MPC cross-coupling parameter is increased with respect to the PID cross-coupling parameter. Here, the positive values are indicated in red and indicate the PID controller is better at reducing couplings than MPC. It must be noted that for the yaw due to collective case, the $r_3 / \left| \hat{h}(3) \right|$ parameter is used for the percentages as this was the limiting parameter for most cases.

First of all, it can be seen that the NLMPC reduces coupling by about 99.9% for almost all cross-coupling cases which is remarkably high. It indicates that the off-axis response can be almost entirely eliminated by introducing the MPC controller. Furthermore, when comparing the MPC to the PID controller almost all cases have much better cross-coupling reduction than the PID controller. Percentages of about 90% and 99% better than the PID controller are achieved for NLMPC whereas the LMPC has slightly lower percentages especially for roll due to pitch.

The roll due to pitch case for hover and a positive input even has the PID controller performing better than LMPC. This degradation of the LMPC performance happens because of the mismatch between the linear prediction model and nonlinear simulation model. It was found that at some point in the simulation the linear model estimates the roll and pitch rate to be of opposite sign as the actual nonlinear model causing the controls to change drastically, decreasing the coupling reduction performance. Nevertheless, the handling qualities of LMPC still remain far within the level 1 zone.

Next to this, the yaw due to collective case with a negative input seems to have a better cross-coupling parameter with PID controller. Furthermore, for a positive input the cross-coupling parameter for MPC is only 3 to 5 percent better than the PID controller which is much lower than in the other

TABLE VI
COMPARISON OF THE CROSS-COUPLING PARAMETER RESULTS IN PERCENTAGE INCREASE FOR THE SIMULATIONS WITHOUT UNCERTAINTY.

Cross-coupling case	Condition	NLMPC compared to BO105 [%]	NLMPC compared to PID [%]	LMPC compared to PID [%]
Pitch d.t. roll	0 kn, +ve input	-99.99	-97.71	-56.74
	0 kn, -ve input	-99.98	-98.35	-92.57
	80 kn, +ve input	-99.99	-97.47	-97.39
	80 kn, -ve input	-99.99	-98.95	-98.97
Roll d.t. pitch	0 kn, +ve input	-99.99	-98.99	58.20
	0 kn, -ve input	-100.00	-99.54	-92.70
	80 kn, +ve input	-100.00	-99.86	-77.47
	80 kn, -ve input	-99.96	-97.66	-73.36
Yaw d.t. collective	+ve input	-98.44	-3.13	-5.42
	-ve input	-98.13	4.40	6.25
Pitch d.t. collective	small, +ve input	-99.93	-89.73	-89.89
	small, -ve input	-99.93	-90.13	-89.98
	large, +ve input	-99.92	-89.37	-89.90
	large, -ve input	-99.94	-90.59	-90.11
Pitch d.t. roll for TA&T	0 kn	-99.95	-99.29	-99.45
	80 kn	-99.98	-99.58	-99.54
Roll d.t. pitch for TA&T	0 kn	-99.96	-99.53	-99.53
	80 kn	-99.96	-99.36	-81.21

TABLE VII
COMPARISON OF THE CROSS-COUPLING PARAMETER RESULTS IN PERCENTAGE INCREASE FOR THE SIMULATIONS WITH AN UNCERTAINTY OF $\sigma = 0.2$.

Cross-coupling case	Condition	NLMPC compared to BO105 [%]	NLMPC compared to PID [%]	LMPC compared to PID [%]
Pitch d.t. roll	0 kn, +ve input	-99.97	-95.01	-69.54
	0 kn, -ve input	-99.90	-90.89	-87.17
	80 kn, +ve input	-99.98	-96.35	-95.98
	80 kn, -ve input	-99.97	-96.46	-96.09
Roll d.t. pitch	0 kn, +ve input	-99.98	-98.82	60.42
	0 kn, -ve input	-99.98	-98.10	-90.39
	80 kn, +ve input	-99.98	-99.25	-78.07
	80 kn, -ve input	-99.82	-90.62	-64.22
Yaw d.t. collective	+ve input	-94.81	121.77	137.05
	-ve input	-97.26	5.85	13.72
Pitch d.t. collective	small, +ve input	-99.93	-90.12	-88.52
	small, -ve input	-99.93	-89.57	-88.49
	large, +ve input	-99.91	-88.59	-89.74
	large, -ve input	-99.96	-89.57	-89.24
Pitch d.t. roll for TA&T	0 kn	-99.76	-97.07	-95.61
	80 kn	-99.99	-99.59	-99.45
Roll d.t. pitch for TA&T	0 kn	-99.83	-98.04	-98.23
	80 kn	-99.49	-96.73	-81.39

cases. This can be explained by the fact that this parameter relies on the yaw rate response instead of the yaw angle. It is the only cross-coupling parameter depending on the angular rate instead of attitude. Since the MPC controller is focusing solely on minimizing the attitude error, aggressive yaw rate motions are induced causing the cross-coupling parameter to take up higher values. The PID controller is not that aggressive because of the differential term. The results for this case could be improved by adding a term to the objective function that directly minimizes the yaw rate.

3) Comparison of the Cross-coupling Parameter ($\sigma = 0.2$): In Table VII one can see the comparison of cross-coupling parameters in percentage increase for the simulations with uncertainty applied to the thrust coefficient. In general, it can be seen that the absolute percentages are only slightly lower than the absolute percentages of the simulations without uncertainty. This indicates that the MPC controllers are robust to this disturbance, preserving the coupling reduction performance.

Here, the yaw due to collective coupling case seems to be the exception. With uncertainty, the handling qualities for the
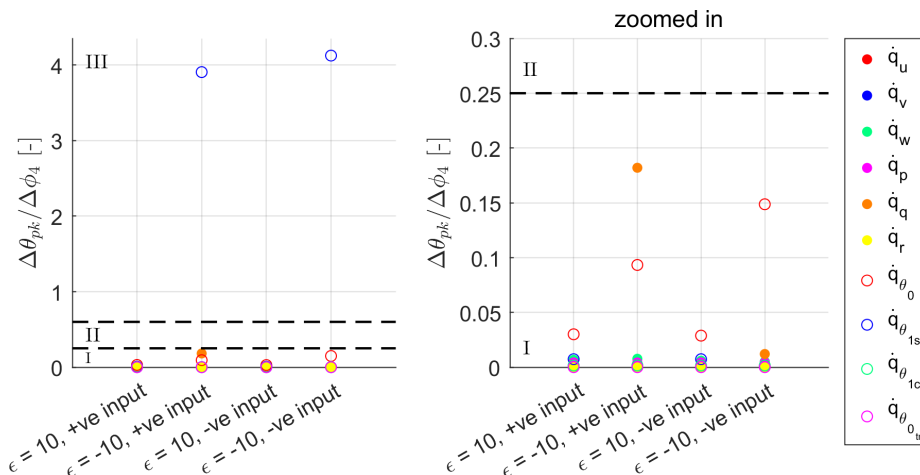
Fig. 15. Pitch due to roll requirement sensitivity analysis for 80 knots for a positive (right) and negative (left) lateral cyclic and for a positive and negative error implemented in one of the derivatives.
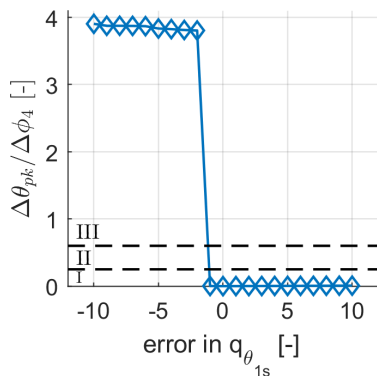
Fig. 16. Analysis of error in $\dot{q}_{\theta_{1s}}$-derivative for pitch due to roll coupling at 80 knots for a positive input.

positive input are even decreased to level 2 as said before. As the uncertainty is implemented in the thrust coefficient, which greatly influences the rotor torque, the yaw coupling is directly influenced. With this poorly estimated main rotor torque in the MPC prediction model, the MPC controller is unable to reduce the couplings in the yaw axis sufficiently. Also when comparing the MPC controllers to the PID controller, which does not rely on a prediction model, it is clear that the PID controller performs much better. A solution to this deteriorated performance of the MPC due to the highly influential disturbance could be to implement robust model predictive control. This will improve the performance of MPC to unmeasured disturbances but at the cost of decreased overall performance.

Next to this, the yaw due to collective coupling case seems to be the case with the least reduction of cross-couplings compared to the uncontrolled helicopter. This was also seen for the results without uncertainty as the yaw rate instead of angle is measured in the parameter.

4) Comparison of Linear and Nonlinear MPC: As discussed before in Section III-A, the difference between linear and nonlinear MPC in this report lies in the use of the nonlinear or linear prediction model in the MPC algorithm.

On one hand, the nonlinearity in the optimization scheme comes with non-convexity and hence multiple local optima and a heavier computational burden. On the other hand, also the fidelity of the prediction model plays a roll in the closed-loop performance. Here, the linear prediction model might fall short as the linearization of the nonlinear system around a trim point only approximates the system at and around this trim point. The more the helicopter state deviates from the trim condition, the worse the linear approximation will be. Also, the more nonlinear the helicopter behaves at this trim condition, the worse the linear approximation will be.

In the cross-coupling results in this chapter it can be seen that both linear and nonlinear MPC perform very well at reducing couplings, even with an uncertainty applied in the simulation model. The performance difference between linear and nonlinear MPC for these simulations is very small. In most cases the nonlinear controller performs slightly better than the linear controller or has almost similar performance as the linear controller. This is an indication that the fidelity of the linear model is sufficient for the cross-coupling simulations to be used as prediction model. This can be explained by means of two reasons based on properties specific to the cross-coupling simulations. First of all, the model mismatch stays small because of the use of a very short prediction horizon which prevents the accumulation of error along the horizon. Secondly, as the reference trajectory that is tracked is the trim condition around which is linearized, the state stays relatively close to the linearization point which also limits the linear model mismatch.

There is one case, the roll due to pitch coupling case for hover with a positive input, where the linear controller performs worse than the PID controller. This was due to a linear model mismatch where the linear model predicted that $\dot{p}, \dot{q} > 0$ whereas the actual, nonlinear model states that $\dot{p}, \dot{q} < 0$, resulting in a sudden change of controls which is not present in the NLMPC and PID simulations. Nevertheless, the fidelity is still good enough to have level 1 handling qualities.

Overall it can be concluded that the differences in cross-

coupling reduction performance between LMPC and NLMPC are so small they do not noticeably deteriorate the handling qualities and can be assumed to be non existent. As linear MPC has the advantage of having a shorter computation time and no suboptimal solutions, linear MPC is preferred over nonlinear MPC in order to reduce cross-coupling effects.

V. SENSITIVITY ANALYSIS

This section will present the results of the sensitivity analysis simulations for all 10 cross-coupling cases. First, the sensitivity analysis of the pitch due to roll coupling case will be worked out as an example. Next, the final results of all coupling cases will be introduced in an overview table.

A. Pitch due to Roll Coupling

The sensitivity analysis for pitch due to roll coupling for 80 knots can be seen in Figure 15. Here, each dot represents the value of the cross-coupling parameter when the error of 10 or -10 is implemented in the corresponding derivative as indicated in the legend. It can be seen that the only derivative that gets the handling qualities out of the level 1 zone when an error, namely a negative error, is applied is the change in pitch acceleration due to longitudinal cyclic derivative $\dot{q}_{\theta_{1s}}$. When zooming in to the level 1 zone, it can be seen that also negative errors in $\dot{q}_q$ and $\dot{q}_{\theta_0}$ increase the cross-coupling parameter. Nevertheless, the handling qualities for these derivatives stay within level 1. It is notable that these three derivatives are also the ones with largest absolute value in the A and B matrix as can be seen in the pitch acceleration derivatives in Equation 17. This is also highly logical as the elements with the largest absolute value influence the dynamics of that degree of freedom the most.

From implementing this large error, it was found that $\dot{q}_{\theta_{1s}}$ is the important derivative for this coupling case, bringing the handling qualities from level 1 to level 3. Therefore, a more elaborate individual analysis is performed varying the error implemented in $\dot{q}_{\theta_{1s}}$. This individual analysis can be seen in Figure 16 and shows that once the error gets smaller than -1, so when the estimated derivative changes sign, the handling qualities jump from level 1 to level 3. Physically this is logical because if the change in pitch acceleration due to longitudinal cyclic input is estimated to be of opposite sign, then pulling the cyclic stick up would be causing the helicopter to pitch down. Hence, when the MPC prediction model has this physically incorrect and influential derivative, the resulting optimal control input cannot reduce the cross-coupling effects sufficiently in closed-loop. Nevertheless, positive errors seem to barely have an effect on the handling qualities when implemented to $\dot{q}_{\theta_{1s}}$.

B. Overview of the Sensitivity Analysis

An overview of the important derivatives for each cross-coupling case can be seen in Table VIII together with some characteristics of how the error influences the cross-coupling parameters. For example, when it says $\epsilon < -1$, it means that the handling qualities are degraded to level 2 or 3 only for errors

smaller than -1. Furthermore, 'symmetrical' means the error in the derivative influences the handling qualities in a symmetric way: when the absolute value of the error increases the cross-coupling parameter increases and hence the handling qualities decrease. When 0 or 80 knots is stated in the characteristics this means the handling qualities are only affected negatively for this flight speed. Furthermore, the actual values of the derivatives at 80 knots can be seen in Equation 17.

$$
\begin{bmatrix} \dot{p}_u & \dot{p}_v & \dot{p}_w & \dot{p}_p & \dot{p}_q & \dot{p}_r \\ \dot{q}_u & \dot{q}_v & \dot{q}_w & \dot{q}_p & \dot{q}_q & \dot{q}_r \\ \dot{r}_u & \dot{r}_v & \dot{r}_w & \dot{r}_p & \dot{r}_q & \dot{r}_r \end{bmatrix} =
$$

$$
= \begin{bmatrix} 0.1 & -0.1 & -0.2 & -17.4 & 4.5 & 0.4 \\ 0.1 & 0.0 & 0.2 & 1.5 & -4.0 & 0.0 \\ 0.0 & 0.3 & -0.2 & -2.8 & 1.5 & -1.4 \end{bmatrix}
$$

$$
\begin{bmatrix} \dot{p}_{\theta_0} & \dot{p}_{\theta_{1s}} & \dot{p}_{\theta_{1c}} & \dot{p}_{\theta_{0tr}} \\ \dot{q}_{\theta_0} & \dot{q}_{\theta_{1s}} & \dot{q}_{\theta_{1c}} & \dot{q}_{\theta_{0tr}} \\ \dot{r}_{\theta_0} & \dot{r}_{\theta_{1s}} & \dot{r}_{\theta_{1c}} & \dot{r}_{\theta_{0tr}} \end{bmatrix} =
$$

$$
= \begin{bmatrix} 4.3 & -8.7 & 159.6 & 9.0 \\ 23.5 & -49.8 & 4.6 & 0.0 \\ 4.6 & 8.4 & 21.8 & -22.5 \end{bmatrix}
$$

$$(17)$$

Similar to the pitch due to roll coupling analysis, it is in general noticeable that the important derivatives are the derivatives that either have a relatively large value in the state-space matrix (Equation 17) or that experience a large change from trim throughout the cross-coupling simulations. Again, this is quite logical as the product of the derivative and the deviation of the state from trim determines the acceleration of that degree of freedom. Hence, when an error is present in the derivative with a large value, the mismatch between the estimated and actual motion increases. Being able to deduct which derivatives are important from the state-space matrices enables to extend the results of this BO-105 sensitivity analysis to other helicopters as well.

It can also be seen in this overview that the important derivatives are mostly control derivatives from matrix B. Furthermore, mostly negative errors, at least smaller than -1, degrade the handling qualities to level 2 or 3 whereas the positive errors barely change the cross-coupling effects in most cases. For the control derivatives this is highly logical because the error smaller than -1 indicates the derivative changes sign, meaning that the controls would be working in the opposite direction. For example, if the $\dot{r}_{\theta_{0tr}}$ derivative is of opposite sign, the tail rotor force would be pointing the opposite direction. For the pitch damping derivative $\dot{q}_q$, the opposite sign is degrading the handling qualities because this is an important stability derivative for the phugoid Eigenmotion. When the sign is estimated incorrectly, the Eigenmotion of the helicopter is majorly affected.

Besides the control derivatives and the pitch damping derivative that degrade when negative errors are implemented, there are the $\dot{p}_p$ and $\dot{p}_u$ derivatives which are important for the roll due to pitch coupling for both positive and negative errors. Here, the roll damping derivative $\dot{p}_p$ is characteristic for the roll subsidence Eigenmotion and is therefore also important to be accurate regardless of the sign. Furthermore,

TABLE VIII
OVERVIEW AND CHARACTERISTICS OF THE IMPORTANT DERIVATIVES FOR EACH CROSS-COUPLING CASE.

Cross-coupling case	Important derivatives	Characteristics	Cross-coupling case	Important derivatives	Characteristics
Pitch d.t. roll	$\dot{q}_{\theta_{1s}}$	$\epsilon <$-1	Pitch d.t. roll for TA&T	$\dot{q}_q$	$\epsilon \leq$-8
				$\dot{q}_{\theta_0}$	$\epsilon \leq$-4, 80 kn
				$\dot{q}_{\theta_{1s}}$	$\epsilon \leq$-1
Roll d.t. pitch	$\dot{p}_u$	symmetrical, 0 kn	Roll d.t. pitch for TA&T	$\dot{p}_p$	$\sim$ symmetrical
	$\dot{p}_p$			$\dot{p}_{\theta_{1c}}$	$\epsilon \leq$-1
	$\dot{p}_{\theta_{1c}}$	$\epsilon \leq$-1		$\dot{p}_{\theta_{0tr}}$	$\epsilon \leq$-6, 80 kn
Yaw d.t. collective	$\dot{r}_{\theta_0}$	symmetrical			
	$\dot{r}_{\theta_{1c}}$	$\epsilon \leq$-3			
	$\dot{r}_{\theta_{0tr}}$	$\epsilon \leq$-1			
Pitch d.t. collective	$\dot{q}_{\theta_{1s}}$	$\epsilon \leq$-1			

the $\dot{p}_u$ derivative is a coupling derivative which couples the lateral and longitudinal motion when the rotor is tilting and a forward velocity change occurs. Hence, the tilting forward during the roll due to pitch maneuver creates this large change in forward velocity u, giving this derivative more importance in the helicopter dynamics.

As the error in the derivative was found to mostly stay within -1 and 1 in Section II-D, it can be concluded that the MPC controller is robust to these model errors and keeps having level 1 handling qualities. However, when the absolute error increases and specially when the errors gets smaller than -1, the performance of the MPC controller deteriorates to level 2 or 3 handling qualities. This could be solved by implementing robust MPC which improves the performance when an unmeasured error or disturbance is present.

VI. CONCLUSION AND RECOMMENDATIONS

This work investigated whether linear and nonlinear model predictive control are suitable for online application to helicopters to reduce cross-coupling effects by evaluating its performance on the cross-coupling handling quality requirements of the ADS-33 document. The cross-coupling requirements were tested in simulation by implementing a step in one control input and measuring the cross-coupling parameter which represents the amount of off-axis response.

It was found that both linear and nonlinear MPC are able to reduce the off-axis response of the tested cross-coupling cases by around 99% compared to the uncontrolled helicopter bringing all handling quality levels from level 2 or 3 to level 1. Here, handling qualities of level 1 indicate having minimal pilot workload and desired aircraft characteristics. Also the PID controller is able to bring the handling qualities from level 2 or 3 to level 1. However, when comparing the MPC to the PID controller almost all MPC cases have 90% to 99% better cross-coupling reduction than the PID controller which can be explained by the optimal and model-based behaviour of the MPC controllers. Where the PID controller shows a washed-out coupling off-axis rate response, the MPC controllers almost eliminate all coupling showing a quasi decoupled off-axis rate response.

When a disturbance is introduced in the simulation model, the cross-coupling reduction performance is only slightly less, keeping level 1 handling qualities for most coupling cases. This indicates that MPC is robust to this disturbance. Only the yaw due to collective coupling case with uncertainty for a positive collective input gives level 2 handling qualities for the MPC controllers. However, this can be explained by the poorly estimated yaw coupling in the prediction model because of the unknown disturbance in rotor thrust and by the cross-coupling parameter that is based on the yaw rate instead of yaw angle which is optimized for. This could be solved by implementing a robust MPC controller or adapting the objective function to also minimize the yaw rate.

Furthermore, the differences in performance between linear and nonlinear MPC for the cross-coupling simulations are so small they do not noticeably degrade the handling qualities and can be assumed to be non-existent. As linear MPC has the advantage of having a shorter computation time and no suboptimal solutions, linear MPC is preferred over nonlinear MPC in order to reduce cross-coupling effects.

In addition, it was examined how sensitive MPC is to prediction model errors when reducing cross-coupling effects by implementing a fixed error in the relevant derivatives of the linear prediction model and measuring the performance change. It was found that the derivatives sensitive to errors are the derivatives that either have a relatively large value in the state-space matrix or that experience a large change from trim throughout the simulation. These derivatives were mainly control derivatives. After individual analysis of the important derivatives it was found that mostly negative errors smaller than -1 degrade the handling qualities to level 2 or 3 whereas the positive errors barely change the cross-coupling effects in most cases. For the control derivatives this is highly logical because the error smaller than -1 indicates the derivative changes sign, meaning that the controls would be working in the opposite direction according to the prediction model. As the error in the derivative was found to mostly stay within -1 and 1, it can be concluded that the MPC controller is robust to these model errors and keeps having level 1 handling qualities. Nevertheless, when the absolute error increases and

specially when the errors gets smaller than -1, the degradation in performance could be solved by implementing robust MPC which improves the performance when an unmeasured error or disturbance is present.

As a recommendation for future work it is suggested to test the established controller more elaborately by extending the test cases with more flight speeds and by evaluating the performance to a disturbance implemented in other parts in the model. Besides this, robust MPC could be implemented in order to improve the robustness to both model errors and disturbances in the simulation model. By implementing robust MPC, one increases the robustness going at the cost of the overall performance. Therefore, this trade-off between robustness and performance should be investigated.

REFERENCES

[1] H. S. A. T. of IHSTI-CIS, "Helicopter accidents: Statistics, trends and causes," International Helicopter Safety Team - Commonwealth of Independent States, Louisville, Kentucky, USA, Tech. Rep., 03 2016.

[2] H. Huber and P. Hamel, "Helicopter flight control: State of the art and future directions," in *Nineteenth European Rotorcraft Forum*. Cernobbio (Como), Italy: European Rotorcraft Forum, 09 1993.

[3] G. Padfield, "Helicopter handling qualities and control: is the helicopter community prepared for change?" in *Royal Aeronautical Society Conference on Helicopter Handling Qualities and Control*, Royal Aerospace Establishment. London: Controller HMSO London, 11 1988.

[4] D. G. Mitchell, D. B. Doman, D. L. Key, D. H. Klyde, D. B. Leggett, D. J. Moorhouse, D. H. Mason, D. L. Raney, and D. K. Schmidt, "Evolution, revolution, and challenges of handling qualities," *Journal of Guidance, Control, and Dynamics*, vol. 27, no. 1, pp. 12–28, 2004.

[5] J. Rawlings, D. Mayne, and M. Diehl, *Model Predictive Control: Theory, Computation, and Design*, 2nd ed. Santa Barbara, California: Nob Hill Publishing, 11 2017.

[6] Y.-G. Xi, D. Li, and S. Lin, "Model predictive control — status and challenges," *Acta Automatica Sinica*, vol. 39, p. 222–236, 03 2013.

[7] S. Qin and T. A. Badgwell, "A survey of industrial model predictive control technology," *Control Engineering Practice*, vol. 11, no. 7, pp. 733–764, 07 2003.

[8] D. Hrovat, S. Di Cairano, H. E. Tseng, and I. V. Kolmanovsky, "The development of model predictive control in automotive industry: A survey," in *2012 IEEE International Conference on Control Applications*, 11 2012, pp. 295–302.

[9] S. Vazquez, J. Leon, L. Franquelo, J. Rodriguez, H. Young, A. Marquez, and P. Zanchetta, "Model predictive control: A review of its applications in power electronics," *Industrial Electronics Magazine, IEEE*, vol. 8, pp. 16–31, 03 2014.

[10] U. Eren, A. Prach, B. B. Koçer, S. V. Rakovic, E. Kayacan, and B. Acikmese, "Model predictive control in aerospace systems: Current state and opportunities," *Journal of Guidance, Control, and Dynamics*, vol. 40, no. 7, pp. 1541–1566, 2017.

[11] H. Chung and S. Sastry, "Autonomous helicopter formation using model predictive control," in *Collection of Technical Papers - AIAA Guidance, Navigation, and Control Conference*, vol. 1, Keystone, CO, USA, 12 2006, pp. 459–473.

[12] B. J. N. Guerreiro, C. Silvestre, and R. Cunha, "Terrain avoidance nonlinear model predictive control for autonomous rotorcraft," *Journal of Intelligent and Robotic Systems: Theory and Applications*, vol. 68, no. 1, pp. 69–85, 2012.

[13] S. Salmah, S. Sutrisno, E. Joelianto, A. Budiyono, I. E. Wijayanti, and N. Y. Megawati, "Model predictive control for obstacle avoidance as hybrid systems of small scale helicopter," in *Proceedings of 2013 3rd International Conference on Instrumentation, Control and Automation, ICA 2013*, 2013, pp. 127–132.

[14] K. Dalamagkidis, K. P. Valavanis, and L. A. Piegl, "Nonlinear model predictive control with neural network optimization for autonomous autorotation of small unmanned helicopters," *IEEE Transactions on Control Systems Technology*, vol. 19, no. 4, pp. 818–831, 2011.

[15] C. Bottasso Luigi and P. Montinari, "Rotorcraft flight envelope protection by model predictive control," *Journal of the American Helicopter Society*, vol. 60, 04 2015.

[16] W. Greer and C. Sultan, "Helicopter ship landing envelope for model predictive control," in *75th Annual Vertical Flight Society Forum and Technology Display*, vol. 4, Pennsylvania, USA, 05 2019, pp. 2670–2678.

[17] C. E. Mballo and J. V. R. Prasad, "Helicopter maneuver performance with active load limiting," in *the 45th European Rotorcraft Forum*, Warsaw, Poland, 09 2019.

[18] C. Liu, W. Chen, and J. Andrews, "Tracking control of small-scale helicopters using explicit nonlinear mpc augmented with disturbance observers," *Control Engineering Practice*, vol. 20, no. 3, pp. 258–268, 2012.

[19] C. Liu, W. Chen, and J. Andrews, "Model predictive control for autonomous helicopters with computational delay," in *UKACC International Conference on Control 2010*. Coventry, UK: IET, 09 2010, pp. 1–6.

[20] M. H. Maia and R. K. H. Galvao, "Robust constrained predictive control of a 3dof helicopter model with external disturbances," *ABCM Symposium Series in Mechatronics*, vol. 3, pp. 19–26, 2008.

[21] A. Dutka, A. Ordys, and M. Grimble, "Non-linear predictive control of 2 dof helicopter model," in *the 42nd IEEE Conference on Decision and Control*, vol. 4, Hawaii, USA, 12 2003, pp. 3954 – 3959.

[22] M. Gulan, P. Minarcik, and M. Lizuch, "Real-time stabilizing mpc of a 2dof helicopter," in *Proceedings of the 22nd International Conference on Process Control, PC 2019*, 2019, pp. 215–221.

[23] M. Mehndiratta and E. Kayacan, "Receding horizon control of a 3 dof helicopter using online estimation of aerodynamic parameters," *Proceedings of the Institution of Mechanical Engineers, Part G: Journal of Aerospace Engineering*, vol. 232, no. 8, pp. 1442–1453, 2018.

[24] M. T. Frye, Chunjiang Qian, and R. D. Colgren, "Receding horizon control of a 6-dof model of the raptor 50 helicopter: robustness to changing flight conditions," in *Proceedings of 2005 IEEE Conference on Control Applications, 2005. CCA 2005.*, 08 2005, pp. 185–190.

[25] J. Du, Y. Zhang, and T. Lü, "Unmanned helicopter flight controller design by use of model predictive control," *WSEAS Transactions on Systems*, vol. 7, no. 2, pp. 81–87, 2008.

[26] K. Kunz, S. M. Huck, and T. H. Summers, "Fast model predictive control of miniature helicopters," in *2013 European Control Conference, ECC 2013*, 2013, pp. 1377–1382.

[27] M. Höfinger, "Ads-33e-prf - aeronautical design standard, performance specification, handling qualities requirements for military rotorcraft," 11 2005.

[28] S. Taamalllah, "Small-scale helicopter automatic autorotation," Ph.D. dissertation, Delft University of Technology, 2015.

[29] G. D. Padfield, *Helicopter Flight Dynamics*, 2nd ed. Blackwell Publishing, 01 2007.

[30] G. E. Cooper and R. P. J. Harper, "The use of pilot rating in the evaluation of aircraft handling qualities," NASA TN-D5153, Tech. Rep., 4 1969.

[31] C. L. Blanken, C. J. Ockier, H.-J. Pausder, and R. C. Simmons, "Rotorcraft pitch-roll decoupling requirements from a roll tracking maneuver," in *50th American Helicopter Society Annual Forum 1994*. Washington, DC: the American Helicopter Society. Inc., 07 1997.

[32] D. P. Loucks and E. van Beek, *Modeling Uncertainty*. Cham: Springer International Publishing, 2017, pp. 301–330.

[33] M. Pavel, *Six Degrees of Freedom Linear Model for Helicopter Trim and Stability Calculation*, ser. Memorandum. Delft University of Technology, Faculty of Aerospace Engineering, 12 1996.

[34] R. K. Heffley, W. F. Jewell, J. M. Lehman, and R. A. Vanwinkle, "A compilation and analysis of helicopter handling qualities data. volume 1: Data compilation," NASA, Tech. Rep. NASA-CR-3144, 08 1979.

[35] J. Van Der Vorst, "Advanced pilot model for helicopter manoeuvres," Master's thesis, Delft University of Technology, 1998.

[36] M. Pavel, "On the necessary degrees of freedom for helicopter and wind turbine low-frequency mode modelling," Ph.D. dissertation, Delft University of Technology, 2001.

[37] R. W. Prouty, *Helicopter performance, stability, and control*. Krieger Publishing, 10 2002.

[38] M. Voskuijl, G. Padfield, D. Walker, B. Manimala, and A. Gubbels, "Simulation of automatic helicopter deck landings using nature inspired flight control," *The Aeronautical Journal*, vol. 114, no. 1151, pp. 25–34, 2010.

[39] M. Behrendt, https://creativecommons.org/licenses/by-sa/3.0), accessed: 2020-01.

Part II

Literature Review

<div style="text-align: right; font-size: 3em;">2</div>

Helicopter Dynamics

This chapter will introduce elaborate on helicopter flight dynamics and rotor dynamics with the four-bladed, light-utility, hingeless BO-105C helicopter as example helicopter. First, the flight controls used in the helicopter and the helicopter cross-couplings will be explained. Second, the Equations of Motion of an 8 DOF helicopter model will be presented. Furthermore, the flapping dynamics of the rotor blades will be described. Then, dynamic and static stability during flight of the helicopter will be discussed. Finally, the concept op helicopter handling qualities will be explained.

2.1. Flight Controls

In this section a look will be taken at how the pilot can control the helicopter by changing the pitch of the helicopter blades by means of a swashplate mechanism. Furthermore, the cross-coupling effects arising when controlling the helicopter will be discussed [13].

2.1.1. Control Inputs

The helicopter is being controlled by means of a swashplate: a mechanical device that translates the control inputs into pitching of the rotor blades. By changing the pitch of the blades of the main and tail rotor, the lift produced by each blade is changed. This enables the ability to steer the helicopter in all six Degrees of Freedom (DOF).

The swashplate, as can be seen in Figure 2.1 (a), consists out of a stationary ring and a rotating ring. The stationary ring, able to move vertically and tilt in all directions, is connected to the flight controls via control rods. The rotating ring, rotating along with the rotor mast, is connected to the pitch bearings of the rotor blades via pitch links. The rotating ring is also connected to the stationary ring by means of a bearing such that both rings can move vertically and tilt as one system.

The pilot gives control inputs through four different helicopter controls which can be seen in Figure 2.1 (b): the collective stick for vertical motion, the cyclic stick for longitudinal and lateral motion and the pedal for directional control. These controls are connected to the stationary ring of the swashplate such that when the pilot gives an input, the swashplate moves and the pitch of the blades changes.

First of all, when the pilot gives a positive collective stick input, the swashplate moves up in order to increase the blade pitch via the pitch links to get more lift and climb up. Secondly, when a cyclic stick input is given, the swashplate tilts such that along one side of the rotor disc the blade pitch is increased and along the other side of the rotor disc the blade pitch is decreased. In this way, a roll or pitch maneuver can be executed. For example, when the longitudinal cyclic stick is pushed forward, the plate tilts causing the advancing blade to have a lower pitch and the retreating blade to have a higher pitch. Because of gyroscopic effects, the lift force will act 90 degrees azimuth later. This lift difference between the front and the back of the rotor disc will cause the helicopter to have a pitch-down motion. As a consequence, the thrust force of the rotor is directed forward which results in forward motion. Similarly, an input to the lateral cyclic will cause the aft and forward blade pitch to change in order to roll. Finally, when the pedals are pushed, the pitch of the tail rotor blades is changed, giving a yaw moment to the helicopter.

(a) Swashplate [14].

(b) Flight controls [15].
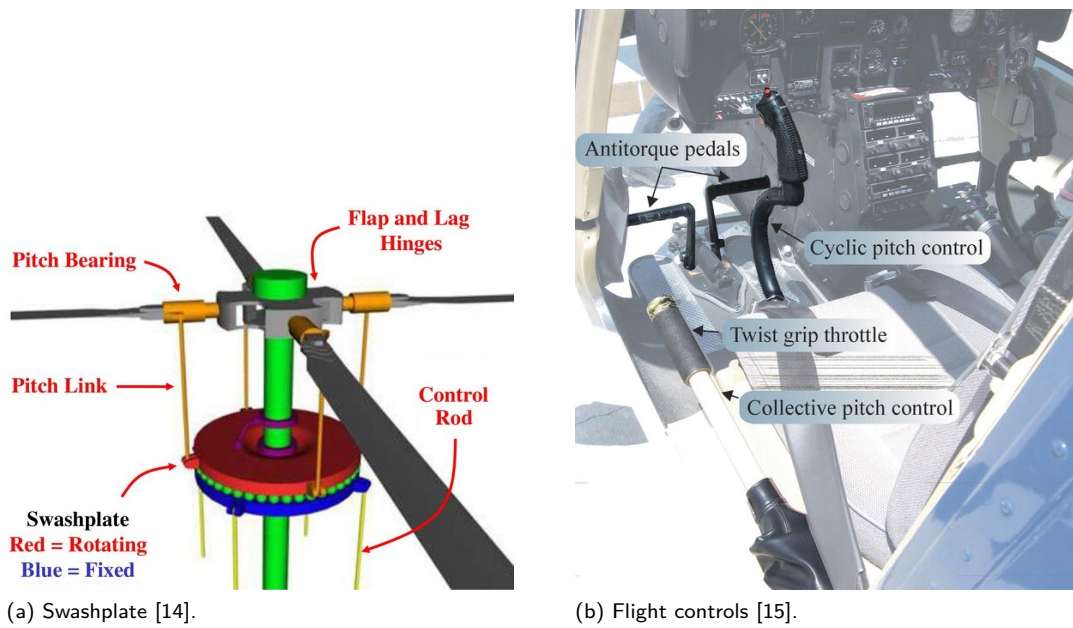
Figure 2.1: Helicopter control system.

2.1.2. Cross-coupling Effects

When controlling the helicopter in one axis, many secondary responses in the other axes arise as well. These secondary responses are often referred to as inter-axis coupling, input-output coupling or cross-coupling effects. The presence of many cross-coupling effects is one of the reasons why a helicopter is very difficult to control. An overview of the primary and secondary responses of each control input is given in Table 2.1.

The main cross-coupling effects that occur are yaw due to collective coupling, collective due to lateral coupling and lateral due to longitudinal coupling. Furthermore, lateral flapping of the rotor cone due to a pitching moment induces a rolling moment and vice versa which causes the pitch-axis and roll-axis to be coupled as well. More on the cross-coupling behaviour due to flapping will be explained in Section 2.3.

Table 2.1: Primary and secondary responses of each input axis [16].

Input axis \ Response	Pitch θ	Roll ϕ	Heave w	Yaw ψ
Longitudinal cyclic θ_{1s}	Primary response	Due to lateral flapping	Desired in forward flight	Negligible
Lateral cyclic θ_{1c}	Due to longitudinal flapping	Primary response	Descent with roll angle	Undesired
Collective input θ_0	Due to longitudinal flapping	Due to lateral flapping and sideslip	Primary response	Due to change in torque Requires TR thrust
Tail rotor collective $\theta_{0_{tr}}$	Negligible	Due to TR thrust and sideslip	Undesired	Primary response

First of all, the yaw due to collective coupling arises from the reaction torque of the main rotor. When the helicopter is in equilibrium and a collective input is given, there is a change in torque of the main rotor which will cause the helicopter to yaw. In order to counter this yaw motion, the pedal needs to be used to generate a counter-acting moment coming from the tail thrust.

Next, the collective due to lateral coupling originates from the horizontal component of the rotor thrust force when a lateral cyclic input is given. This horizontal force has to be countered by applying pedal. Hence, the helicopter starts yawing which requires more collective.

Finally, the lateral due to longitudinal coupling, also called swashplate mixing, happens for example when a maneuver from hover to forward flight is flown. In order to move forward, the cyclic stick is pushed forward causing the helicopter to pitch-down and increase the forward component of the thrust force. This will also decrease the vertical component of the thrust force which requires a collective block in put to maintain height. This collective input will change the torque of the main rotor which in turn requires a pedal input to counter the yawing motion. Since the tail rotor thrust is now changed, the horizontal force balance is disrupted. Therefore, a lateral cyclic input is needed to maintain horizontal force balance. Hence, the cyclic stick is moved forward and to the left at the same time which requires control mixing in the swashplate mechanism.

2.2. 8 DOF Nonlinear Helicopter Model

The 8 DOF nonlinear model of the BO-105 helicopter used to demonstrate the dynamics of the helicopter and for the simulations in this research was developed at the TU Delft and consists out of 6 helicopter body DOFs and 2 rotor inflow DOFs, one for the main rotor and one for the tail rotor [1, 17]. Hence, the helicopters motion will be described by a total of 14 states namely $x = [u\ v\ w\ p\ q\ r\ \psi\ \theta\ \phi\ x\ y\ z\ \lambda_0\ \lambda_{0_{tr}}]'$ and will be controlled by 4 control inputs namely the main rotor collective, longitudinal cyclic, lateral cyclic and the tail rotor collective $u = [\theta_0\ \theta_{1s}\ \theta_{1c}\ \theta_{0_{tr}}]'$. The axis systems used to express the helicopter states in will be described in Section 2.2.1. Next, the 6 DOF equations of motion of the helicopter will be stated in Section 2.2.2 along with its kinematics equations. Then, Section 2.2.3 will describe the 2 DOF inflow dynamics equations. Finally, the trim conditions of this 8 DOF model will be computed in Section 2.2.4.

2.2.1. Axis Systems

Use will be made of three different axis systems when describing the dynamics and state of the helicopter. First of all, a body axis system is used to express the linear and angular velocity in. As can be seen in Figure 2.2, the axes of the system are fixed with the body and the system has its origin in the center of gravity. The X-axis is pointing towards the front, the Y-axis towards the right and the Z-axis to the ground in a right-handed, orthogonal manner.
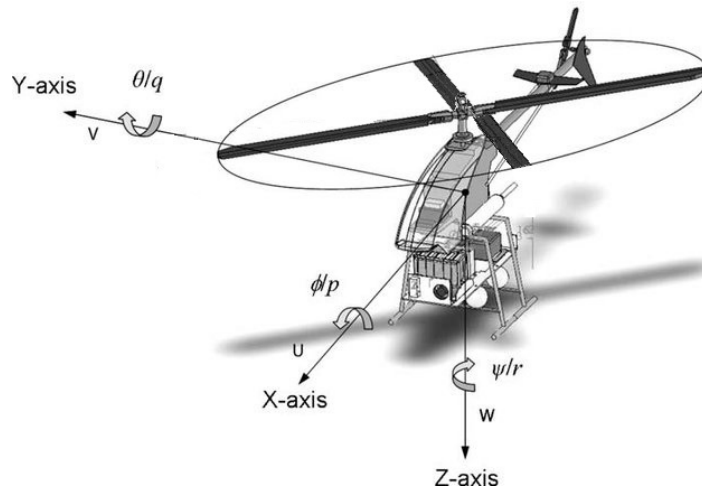
Figure 2.2: The helicopter body axis system [18].

Furthermore, the coordinates of the helicopter are expressed in the world axis system which has its origin in the initial position of the helicopter in the simulation or test, its X-axis and Y-axis parallel to the surface of the earth and in the direction of, respectively, the body system X-axis and Y-axis at the initial position and its Z-axis orthogonal to the surface pointing downwards. This axis system is fixed with the world such that the coordinates of the helicopter can be expressed with respect to the initial position of the helicopter.

Finally, the blade flapping dynamics will be expressed in the non-rotating disc plane, the plane described by the path followed by the tip of the blades, with respect to the control plane, the plane containing the swashplate. As can be seen in Figure 2.3, the coning angle a_0 is the angle between the disc axis and the blade, the longitudinal and lateral flapping angles, a_1 and b_1, are the angles between the disc axis and the

control axis at 0/180° and 90/270° azimuth respectively. The longitudinal flapping angle is positive when the rotor disc is tilting backwards. The lateral flapping angle is positive when the rotor disc is tilting to the right.
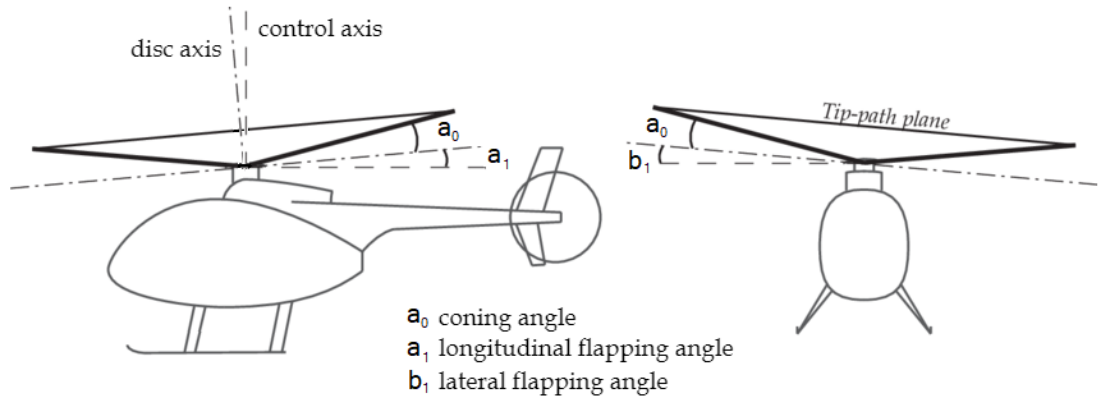
Figure 2.3: The helicopter flapping angle axis system [19].

2.2.2. 6 DOF Equations of Motion

The 6 DOF dynamics of the helicopter body can be described by the fundamental nonlinear equations of motion of a rigid body in the body axis system. The helicopter's motion is then described by its linear velocity $[u \; v \; w]$ and angular velocity $[p \; q \; r]$. Furthermore, rotational and translational kinematics of the body are added to the helicopter model in order to express the helicopters attitude and position in the world axis system by means of Euler angles $[\phi \; \theta \; \psi]$ and position coordinates $[x \; y \; z]$.

The linear velocity can be computed by applying the nonlinear equations of motion for translational dynamics as can be seen in Equation 2.1. Furthermore, the angular velocity can similarly be computed in Equation 2.2 by applying the nonlinear equations of motion for rotational dynamics. Here, X, Y and Z and L, M and N are respectively the external forces and moments acting on the helicopter in x- y- and z-direction according to the body axis-system. Each of them are constructed by superposition of the force and moment contributions of all helicopter subsystems. The subsystems taken into account for the model used in the simulations of this research are: the main rotor, tail rotor, fuselage, horizontal tail and vertical tail. Hence, the total external force $\bar{F} = [X \; Y \; Z]'$ and moment $\bar{M} = [LMN]'$ are computed by $\bar{F} = F_{mr} + F_{tr} + F_{fus} + F_{ht} + F_{vt}$ and $\bar{M} = M_{mr} + M_{tr} + M_{fus} + M_{ht} + M_{vt}$. The calculations for the individual contributions to the force and moment vector can be found in Simplicio (2011) [20].

$$
\begin{aligned}
\dot{u} &= \frac{X}{m} - g \sin \theta - qw + rv \\
\dot{v} &= \frac{Y}{m} + g \sin \phi \cos \theta - ru + pw \\
\dot{w} &= \frac{Z}{m} + g \cos \theta \cos \theta - pv + qu
\end{aligned}
\tag{2.1}
$$

$$
\begin{aligned}
\dot{p} &= \frac{1}{I_x}\Big(L - (I_z - I_y)qr + J_{xz}(\dot{r} + pq)\Big) \\
\dot{q} &= \frac{1}{I_y}\Big(M - (I_x - I_z)rp - J_{xz}(p^2 - r^2)\Big) \\
\dot{r} &= \frac{1}{I_z}\Big(N - (I_y - I_x)pq + J_{xz}(\dot{p} - rq)\Big)
\end{aligned}
\tag{2.2}
$$

Furthermore, the helicopter's position and attitude with respect to the world axis system can be obtained by applying the rotational and translational kinematics as can be seen in Equation 2.3 and 2.4. These equations are obtained from transforming the angular velocity [p q r] and [u v w] from the body axis system to the world axis system using transformation matrices.

$$\dot{\phi} = p + q \sin\phi \tan\theta + r \cos\phi \tan\theta$$
$$\dot{\theta} = q \cos\phi - r \sin\phi \tag{2.3}$$
$$\dot{\psi} = q \frac{\sin\phi}{\cos\theta} + r \frac{\cos\phi}{\sin\theta}$$

$$\dot{x} = u \cos\psi \cos\theta + v(\cos\psi \sin\theta \sin\phi - \sin\psi \cos\phi) + w(\cos\psi \sin\theta \cos\phi + \sin\psi \sin\phi)$$
$$\dot{y} = u \sin\psi \cos\theta + v(\sin\psi \sin\theta \sin\phi + \cos\psi \cos\phi) + w(\sin\psi \sin\theta \cos\phi - \cos\psi \sin\phi) \tag{2.4}$$
$$\dot{z} = -u \sin\theta + v \cos\theta \sin\phi + w \cos\theta \cos\phi$$

2.2.3. Inflow Dynamics

The BO-105 helicopter is a hingeless helicopter meaning the rotor system doesn't contain hinges, instead the blades are connected to the rotor head by means of a solid titanium block. In order to still allow movement in the blades, the blades are made from a reinforced-plastic glass-fiber composite material which gives great flexibility [21]. Because of this hingeless rotor system, the rotor dynamics and body dynamics of the helicopter are highly coupled. Hence it is important to take the rotor inflow dynamics is into account when modelling hingeless helicopters [22]. Therefore, the 6 DOF nonlinear rigid body model is extended by adding two quasi-dynamic rotor inflow equations as can be seen in Equation 2.5. Here, the induced velocity is calculated using a time constant based on the quasi-dynamic inflow.

$$\dot{\lambda}_0 = \frac{1}{\tau_{mr}} \left(C_T^{BEM} - C_T^{Gl} \right)$$
$$\dot{\lambda}_{0_{tr}} = \frac{1}{\tau_{tr}} \left(C_{T_{tr}}^{BEM} - C_{T_{tr}}^{Gl} \right) \tag{2.5}$$

2.2.4. Trim Condition

The trim condition is defined as the equilibrium condition in forces and moments such that straight level flight with constant velocity is obtained. Hence, in trim the sum of the forces and moments along each axis as well as the total linear and angular accelerations are equal to zero as can be seen in Equation 2.6. The simulations performed for this research always start from a trim condition, usually at hover (0 knots) or in forward flight (80 knots). For the BO-105 helicopter, the trim states and controls are computed numerically and can be seen in the Appendix in Equation B.1 for 0 knots and Equation B.2 for 80 knots.

$$\dot{u}, \dot{v}, \dot{w}, \dot{p}, \dot{q}, \dot{r} = 0 \tag{2.6}$$

Trim values from flight test data of the BO-105 helicopter can be seen in Table 2.2 and are used to compare the trim values of the nonlinear 8 DOF model with. It can be seen that the pitch and roll angle and longitudinal cyclic are overestimated compared to the flight test trim values. Furthermore, the main rotor collective shows a similar trim value at 0 knots but is underestimating at 80 knots. Then again, the tail rotor collective is very well approximated at 80 knots but is slightly overestimated at 0 knots. Finally, the lateral cyclic trim values of the model are quite similar to the flight test trim value for both 0 and 80 knots.

Table 2.2: Trim values of the 8 DOF model compared with flight test data from [1].

	Trim value at 0 knots in [deg]		Trim value at 80 knots in [deg]	
	8 DOF	Flight test	8 DOF	Flight test
θ_0	9.24	2.5	4.88	-2.5
ϕ_0	-1.35	-3.0	0.85	-2.5
θ_{0_0}	14.36	14.0	9.53	12.5
θ_{1s_0}	1.93	-0.5	6.86	2.5
θ_{1c_0}	-0.31	-1.0	-2.28	-1.5
θ_{0tr_0}	13.69	10.0	4.67	4.0

2.3. Flapping Motion

In a fully articulated rotor system, the blades of the helicopter are connected to the hub by means of hinges in order to allow the blades to move independently of each other. Flapping, lagging and feather hinges allow the blades to respectively move up and down, forward and backward and to change the pitch of the blades. The flap and lag hinges and the pitch bearing for feathering motion can be seen in Figure 2.1 (a). As the rotor and the helicopter are connected through the rotor hub, much of these rotor movements are translated to the helicopter body. Especially the flapping motion of the helicopter contributes much towards the longitudinal-lateral cross-coupling behaviour. Hence, for the 8 DOF model used in the simulations, the steady-state flapping angles are taken into account in order to be able to model the pitch and roll cross-couplings due to flapping. The lagging motion and flapping dynamics of the blades is neglected in this research for simplicity.

The flapping angle of the blade β is defined as the angle between the control axis and the blade and represents the out-of-plane motion of the blades in function of the blade azimuth angle. It can be modelled using different approximations in the analytical expression. During manoeuvring flight, effects of non-uniform induced velocity distribution along the rotor disc, effects of unsteady flow along the rotor blade and effects of higher order coupling terms can occur. Hence, correction factors for dynamic inflow and sweep or including higher order terms can improve the model of the flapping angles depending on the type of maneuver [23]. In this study, the classical formulation with a correction factor to account for the non-uniformity of the induced velocity is used with no higher order terms. In order to compute the flapping angle, it is assumed that the aerodynamics of the blade is linear, which can be assumed for angles of attack lower than the stall angle of attack, rigid blades and for small flap and induced inflow angles [24].

$$a_0 = \frac{\gamma}{8}\theta_0\left(1 + \mu^2\right) - \frac{\gamma}{6}\left(\lambda_c + \lambda_0\right) + \frac{\gamma}{12}\frac{p}{\Omega}\mu$$

$$a_1 = \frac{\frac{8}{3}\mu\theta_0 - 2\mu\left(\lambda_c + \lambda_0\right) - \frac{16}{\gamma}\frac{q}{\Omega} + \frac{p}{\Omega}}{1 - \frac{1}{2}\mu^2}$$

$$b_1 = \frac{\frac{4}{3}\mu a_0 + \frac{q}{\Omega} - \frac{16}{\gamma}\frac{p}{\Omega}}{1 + \frac{1}{2}\mu^2} + K'$$

$$\text{with: } K' = \frac{1.33\frac{\mu}{|(\lambda_c + \lambda_0)|}}{1.2 + \frac{\mu}{|(\lambda_c + \lambda_0)|}}$$

(2.7)

When the flapping motion of the blade would be plotted over azimuth, one could see that the motion is periodic with a period of exactly one blade revolution. Expressing the flapping angle in the stationary disc plane as opposed to the rotating blade frame, the blade disc position can be described by a longitudinal and lateral flap angle, a_1 and b_1, and a coning angle a_0. In Equation (2.7), the stationary flapping angles used in the simulations of this research can be found which apply to a translating, pitching and rolling helicopter [23]. It must be noted that the correction factor K' is used for the lateral disc tilt in order to account for the non-uniformity of the induced velocity [1].

Hence, when a positive pitching moment (upward) is applied in hover, the rotor cone longitudinally tilts forward damping and stabilizing the fuselage motion, and laterally tilts to the left causing an off-axis moment in roll. This lateral tilt is the main reason for the roll due to pitch coupling motion in helicopter. However, in forward flight when pitching up, the rotor cone tends to pitch backwards. This means that flapping is now destabilizing the pitching motion. When rolling to the right in hover the rotor cone tilts to the left damping and stabilizing the rolling motion and tilts backward causing an off-axis moment in pitch. Again, this explains the undesired pitch due to roll cross-coupling [25].

2.4. Stability

There are two kinds of stability in a helicopter: static and dynamic stability. On one hand, static stability refers to the tendency of the helicopter in trim to go back to the trimmed state after a disturbance is applied. On the other hand, dynamic stability focuses on the motion of the helicopter in time after the disturbance, which can be oscillatory or non-oscillatory, and whether the helicopter is diverging or converging to the trim state in the end. Hence, if a helicopter is dynamically stable, and it returns towards the trim state after a

period of time, it is also statically stable. However, when a helicopter experiences a disturbance and it starts oscillating around the trim point but diverges in time, the helicopter is statically stable but dynamically unstable. Having a dynamically stable helicopter design makes controlling the helicopter easier but it is compromised with maneuverability and agility during flight.

In this section, the static and dynamic stability of the helicopter in general will be evaluated, after which a stability analysis of the BO-105 will be performed.

2.4.1. Static Stability Derivatives

The static stability of a system is analysed using the linearized system around a trim state. As the linearized system around trim changes with airspeed, the stability of the system changes with airspeed as well. This linear system, of the form that can be seen in Equation (2.8), can be obtained by applying perturbation linearization around the desired trim point [26][p. 563] as explained in Section 7.1.2. In perturbation linearization, the nonlinear model is perturbed by a small change in a state or input variable which induces a change in the states. The change of each state with respect to a perturbation in each state individually, divided by the perturbation, is taken to obtain the elements of the state matrix and the change of each state with respect to a perturbation in an input, divided by the perturbation, is taken to obtain the elements of the input matrix.

The linearized 6 DOF system has the form that can be seen in Equation (2.9). The elements of the A and B matrix represent the stability derivatives. Each derivative varies with helicopter configuration and flight condition and tells something about the static stability of the helicopter. They can be interpreted as the amount of change in variable X as a result of the perturbation of the other variable y for $X_y = \frac{\partial X}{\partial y}$ [1].

Often, stability derivatives are non-dimensionalized to be able to compare derivatives of different helicopters with each other. Non-dimensionalization and a comparison of the derivatives of the 8 DOF model with the NASA model of Heffley et. al. (1979) can be found in Appendix A [2].

$$\delta \dot{x} = A\delta x + B\delta u$$
$$\text{with: } \delta x = x - x_0, \; \delta \dot{x} = \dot{x} - \dot{x}_0 \text{ and } \delta u = u - u_0 \tag{2.8}$$

$$
\begin{bmatrix} \dot{u} \\ \dot{v} \\ \dot{w} \\ \dot{p} \\ \dot{q} \\ \dot{r} \end{bmatrix} =
\begin{bmatrix}
\frac{X_u}{m} & \frac{X_v}{m} & \frac{X_w}{m} & \frac{X_p}{m} & \frac{X_q}{m} - w_0 & \frac{X_r}{m} + v_0 \\
\frac{Y_u}{m} & \frac{Y_v}{m} & \frac{Y_w}{m} & \frac{Y_p}{m} + w_0 & \frac{Y_q}{m} & \frac{Y_r}{m} - u_0 \\
\frac{Z_u}{m} & \frac{Z_v}{m} & \frac{Z_w}{m} & \frac{Z_p}{m} - v_0 & \frac{Z_q}{m} + u_0 & \frac{Z_r}{m} \\
\frac{L_u}{I_x} & \frac{L_v}{I_x} & \frac{L_w}{I_x} & \frac{L_p}{I_x} & \frac{L_q}{I_x} & \frac{L_r}{I_x} \\
\frac{M_u}{I_y} & \frac{M_v}{I_y} & \frac{M_w}{I_y} & \frac{M_p}{I_y} & \frac{M_q}{I_y} & \frac{M_r}{I_y} \\
\frac{N_u}{I_z} & \frac{N_v}{I_z} & \frac{N_w}{I_z} & \frac{N_p}{I_z} & \frac{N_q}{I_z} & \frac{N_r}{I_z}
\end{bmatrix}
\begin{bmatrix} u \\ v \\ w \\ p \\ q \\ r \end{bmatrix} +
\begin{bmatrix}
X_{\theta_0} & X_{\theta_{1s}} & X_{\theta_{1c}} & X_{\theta_{0tr}} \\
Y_{\theta_0} & Y_{\theta_{1s}} & Y_{\theta_{1c}} & Y_{\theta_{0tr}} \\
Z_{\theta_0} & Z_{\theta_{1s}} & Z_{\theta_{1c}} & Z_{\theta_{0tr}} \\
L_{\theta_0} & L_{\theta_{1s}} & L_{\theta_{1c}} & L_{\theta_{0tr}} \\
M_{\theta_0} & M_{\theta_{1s}} & M_{\theta_{1c}} & M_{\theta_{0tr}} \\
N_{\theta_0} & N_{\theta_{1s}} & N_{\theta_{1c}} & N_{\theta_{0tr}}
\end{bmatrix}
\begin{bmatrix} \theta_0 \\ \theta_{1s} \\ \theta_{1c} \\ \theta_{0tr} \end{bmatrix} \tag{2.9}
$$

Two important derivatives with respect to longitudinal static stability are the speed stability derivative M_u, which is the change in pitching moment as a result of an increase in horizontal velocity, and the angle-of-attack stability derivative M_w, which is the change in pitching moment as a result of an increase in vertical velocity.

A helicopter is said to have positive speed stability when, after an increase in horizontal speed, the helicopter pitches up directing the thrust vector backward with as result a deceleration of the horizontal speed. If the speed stability derivative $M_u > 0$ is greater than zero, the helicopter has speed stability. Furthermore, positive speed stability enhance the ease of controlling the helicopter.

Angle-of-attack instability or incidence instability is initiated by an upward (negative) perturbation in vertical velocity w which causes an increase in lift of the blades where the lift on the advancing side of the disc is greater than the lift produced by the retreating side of the disc. This causes the disc to flap back resulting in a destabilizing nose-up pitching moment. In order to have positive angle-of-attack stability, the derivative $M_w > 0$ should be greater than zero. Stabilizing the angle-of-attack stability results in an oscillatory mode in forward flight namely the phugoid which will be discussed in the next section.

2.4.2. Dynamic Stability Modes

The dynamic stability of the helicopter is evaluated by computing the Eigenvalues of the input matrix A of the system. Each Eigenvalue corresponds to a natural dynamic mode of the helicopter which has a certain

damping and frequency, is either stable or unstable and can be oscillatory or neutral depending on the real and imaginary part of the Eigenvalue.

The free motion of the helicopter in time can be entirely described by the linear combination of these dynamic modes as can be seen in Equation (2.10). Here, each mode is characterized by the exponent of its Eigenvalue, distributed along the states by means of the corresponding Eigenvector, multiplied by a constant depending on the initial condition x_0. The Eigenvalues and Eigenvectors of the helicopter can be computed by solving Equation (2.11).

$$x(t) = \sum_i^n c_i(x_0) \cdot w_i \cdot e^{\lambda_i t}, \qquad \text{n = number of states} \tag{2.10}$$

$$\det\left[\lambda I - A\right] = 0$$
$$A \cdot w_i = \lambda_i \cdot w_i \tag{2.11}$$

Similar characteristics can be recognized in the natural modes of different types of helicopters which enables to categorise them based on their Eigenvalue and Eigenvector. The typical modes of a helicopter are: the phugoid or long period, the short period, the dutch roll, the spiral mode and the roll subsidence. However there is still a big difference in the characteristics of the modes per helicopter depending on e.g. the type of rotor configuration, the horizontal and vertical stabilizers, the position of the center of gravity, etc. as can be seen in literature [27], [28], [29], [30], [31][p. 239-249]. Also, the characteristics of the modes can change drastically over the flight speed range. In general, the modes are to be divided in longitudinal and lateral/directional modes and will be discussed next [31][p.236-251], [26][p. 616-635].

Longitudinal Modes   The longitudinal modes of a helicopter consist of the phugoid or long period and the short period. In some cases, the short period is non-oscillatory and is replaced by a pitch and heave subsidence.

First of all, the phugoid mode is characterized by an interchange between forward speed and altitude at a nearly constant angle of attack initiated by a vertical gust or collective control input. It is a very slow and unstable mode. The unstable phugoid can still be controlled by the pilot in visual flight as long as the period is very long (T>20s). However, the stability of the phugoid is being influenced negatively during turns or pull-ups as the load factor increases which makes the free motion less controllable for the pilot. When separating the phugoid equations of motion using reduced order modelling, it is found that the ratio of speed stability M_u over pitch rate damping M_q greatly influences the frequency and damping of the phugoid.

Secondly, the short period, observed in the beginning of the phugoid, is a very rapid angle-of-attack adjustment with little change in forward speed. The mode depends mainly on the angle-of-attack stability derivative M_w. When M_w increases, the frequency of the short period also increases. When the short period is non-oscillatory, the mode consists of a pitch and heave subsidence. This usually happens at low speeds. The eigenvalues of the pitch and heave subsidence are directly related to the pitch damping derivative M_q and heave damping derivative Z_w respectively. At higher speeds, pitch and heave can become coupled because of the angle-of-attack stability resulting in a short period.

Lateral Modes   The lateral modes of a helicopter consist of a dutch roll, sometimes called lateral directional oscillation or lateral phugoid, a spiral mode and an aperiodic roll subsidence [32].

The periodic dutch roll is usually a damped mode which combines yaw, roll and side-slip motion when perturbed by a lateral gust. The mode depends mainly on the yaw due to roll derivative N_p, which should be negative in order to have a stable dutch roll. The vertical stabilizer contribution increases the derivative making it possible to size the stabilizer for stable dutch roll. The dutch roll motion is known to highly affect the pilot workload. Therefore, a well damped dutch roll mode is desired by the pilot. The short roll subsidence mode is an aperiodic, damped mode initiated by a lateral cyclic input causing the helicopter to have a roll rate response with a time constant. The behaviour of the mode depends mainly on the roll damping derivative L_p. The spiral mode is an aperiodic motion in yaw and side-slip and is either unstable or weakly damped.

2.4.3. Stability Analysis of BO-105

In order to analyse static and dynamic stability of the 6 DOF helicopter model used in this research, the model was linearized for different flight speeds as explained in Section 7.1.2. From the state and control

matrix, the static stability derivatives and Eigenvalues were derived.

First of all, the static stability derivatives for hover and forward flight (80 knots) of the BO-105 model used in this research can be seen in Section 7.1.2. The derivatives are non-dimensionalized in Appendix A and compared with the non-dimensional derivatives of the NASA model of Heffley et. al (1979) [2]. Here, it can be seen that the signs of the derivatives of the NASA model and the BO-105 model of this research are mostly similar, with some exceptions such as z_u, z_w and l_r and some control derivatives. Furthermore, most state derivatives have the same order of magnitude. The control derivatives of the 6 DOF model are very small in magnitude whereas the NASA model derivatives have much greater magnitude. From these derivatives, it can be seen that indeed M_u and M_w are positive which indicates respectively positive speed and angle-of-attack stability.

Table 2.3: Eigenvalues of the 6 DOF BO-105 model for hover.

Eigenmode	Eigenvalue [rad/s]	Natural frequency [rad/s]	Damping ratio [-]
Phugoid	$0.081 \pm 0.724i$	0.728	-0.111
Short period	-3.800 (pitch subsidence)	3.800	1.000
	-0.914 (heave subsidence)	0.914	1.000
Spiral	0.311	0.311	-1.000
Dutch roll	$-0.657 \pm 0.363i$	0.751	0.875
Aperiodic roll	-16.600	16.600	1.000

For the dynamic stability analysis the Eigenvalues of the 6 DOF state matrix were calculated at different speeds using Equation 2.11. The Eigenvalues for hover can be seen in Table 2.3 whereas the Eigenvalues over a flight speed range from 0 to 70 m/s can be seen in Figure 2.4 (a). In hover, the helicopter Eigenmotions consist of a slightly unstable and oscillatory phugoid mode, a stable pitch and heave subsidence, an unstable spiral mode, a stable aperiodic roll subsidence and a stable dutch roll motion. As can be seen in Figure 2.4 (a), the phugoid motion develops into two aperiodic Eigenmodes characterized by u and w at higher flight speeds (> 57 m/s). Furthermore, the stable roll and pitch subsidence and unstable spiral mode become more damped when flight speed increases in contrast to the heave subsidence becoming less damped and almost unstable. The dutch roll Eigenmode remains stable and oscillatory over the full flight speed range but increases its natural frequency with increasing flight speed. Generally, the Eigenmodes of the 6 DOF model resemble the Eigenmodes of the higher fidelity Helisim model in Figure 2.4 (b) with the exception of the phugoid mode splitting up in two aperiodic motions and the spiral being unstable in the 6 DOF model.

2.5. Handling Qualities

This section will explain the concept of flying qualities and more specifically handling qualities. Furthermore, it will present the established subjective and objective criteria for measuring aircraft handling qualities. Finally, a closer look will be taken into the helicopter cross-coupling requirements specified in the ADS-33E-PRF document.

2.5.1. Definition

The concept of flight performance or flight quality is difficult to objectively define or measure. Therefore, throughout history two concepts of flying performance were defined: flying qualities and handling qualities. The concept of flying qualities was first defined by Philips (1949) who described it as *"the stability and control characteristics that have an important bearing on the safety of flight and on the pilots' impressions of the ease of flying an airplane in steady flight and in manoeuvers"* [33]. The handling qualities of an aircraft however were first described by Cooper and Harper (1969) as *"Those qualities or characteristics of an aircraft that govern the ease and precision with which a pilot is able to perform the tasks required in support of an aircraft role"* [34] and depend not only on the aircraft but also on the maneuver that has to be flown, the visibility, the pilot's personal opinion and expertise and any human-machine interfaces present as can be seen in Figure 2.5. The handling qualities can thus be seen as a part of the flying qualities of an aircraft [6]. As it is generally known that helicopters are hard to fly, having good handling qualities is an important requirement when designing a helicopter. In order to facilitate the design of helicopters and its flight control systems, a subjective and objective assessment of handling qualities was established which
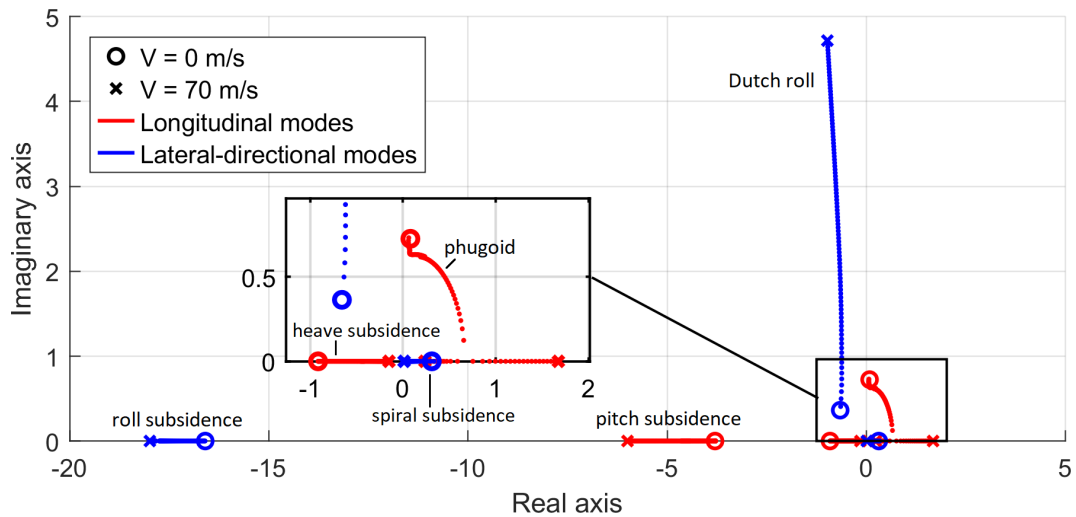
(a) 6 DOF model.
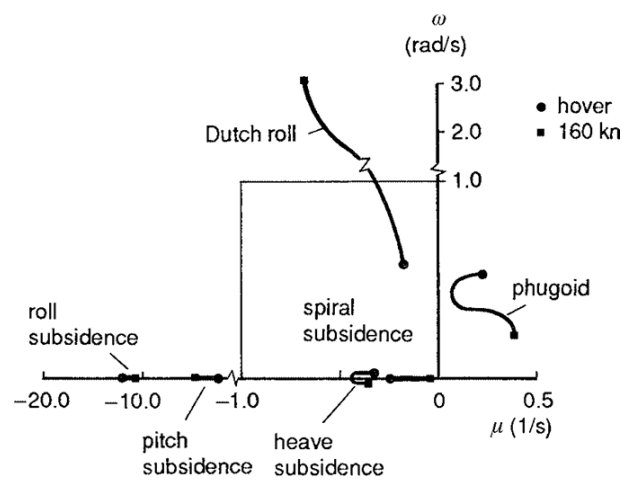
(b) Helisim model (coupled dynamics) [31]

Figure 2.4: Dynamic stability analysis of the 6 DOF model and the Helisim model of the BO-105 showing the Eigenvalues in the complex plane.

could be used as a guideline for desired flight behavior.

2.5.2. Handling Quality Rating

In 1969 Cooper and Harper invented a way to subjectively measure the ease of controlling an aircraft by means of the Cooper-Harper Handling Qualities Rating Scale [34]. This rating scale is to this date used and recognized as a reference for measuring handling qualities. It is based on a series of questions the pilot has to answer about flying a specific maneuver after which a certain level of handling quality is obtained as can be seen in Figure 2.6. The scale has three levels of handling quality. Level 1 is the best level with excellent to fair handling qualities requiring no to minimal pilot workload to perform the maneuver. Level 2 captures the maneuvers with aircraft characteristics with minor to very objectionable but tolerable deficiencies. Level 3 indicates the worst level of handling qualities where major deficiencies are present in the aircraft characteristics and an extensive workload is required to fly the maneuver. This rating scale is entirely based on the pilot's subjective opinion. Hence, there was still a need for an objective rating system for helicopter handling qualities which could contribute to setting up helicopter and flight control system design guidelines.

In 1985 a mission-oriented way of objectively measuring handling qualities for military rotorcraft was established by the US Army Aviation and Missile Command in the "ADS-33 Aeronautical design standard performance specification: handling qualities requirements for military rotorcraft" based on the Cooper-

Figure 2.5: Handling qualities influencing factors [35].

Harper rating [36]. This document specifies handling quality requirements for predefined Mission Task Elements (MTE) in order to provide a sound guidance for the design of the helicopter and flight control systems. Depending on the type of helicopter (scout/attack or cargo/utility), the visual environment (Degraded Visual Environment (DVE) or Good Visual Environment (GVE)) and the MTEs (e.g. hover, slalom, pullup), control and maneuverability requirements were set. Besides the requirements for the MTEs, stability requirements were made and new handling quality parameters were defined in order to specify the required responses to control and disturbance inputs, to specify the required quickness for certain attitude changes and to specify the allowable amount of interaxis coupling [6].

2.5.3. Cross-coupling Requirements

As mentioned before in Section 2.1.2, helicopters have many and mostly undesirable cross-couplings which make controlling a helicopter very difficult. Therefore, cross-couplings or interaxis couplings are also widely described in the ADS-33 document for both hover and low speed flight, and forward flight. For most cross-couplings, the document has defined a certain parameter indicating the amount of off-axis response compared to the on-axis input. Hence, when flying or simulating the helicopter and giving a step input in one of the controls, this parameter that resembles the amount of off-axis response should remain within the required limits. In order to specify these limits, level 1, 2 and 3 handling quality boundaries for these parameters were defined based on Cooper-Harper ratings of flight tests. These boundaries could then be used as design requirements or just as indicative guidelines. The cross-coupling requirements specified in the ADS-33 document for off-axis dynamic responses are summarized in Table 2.4 with its respective parameter representing the amount of cross-coupling. More on these individual cross-coupling requirements can be found in Chapter 8.
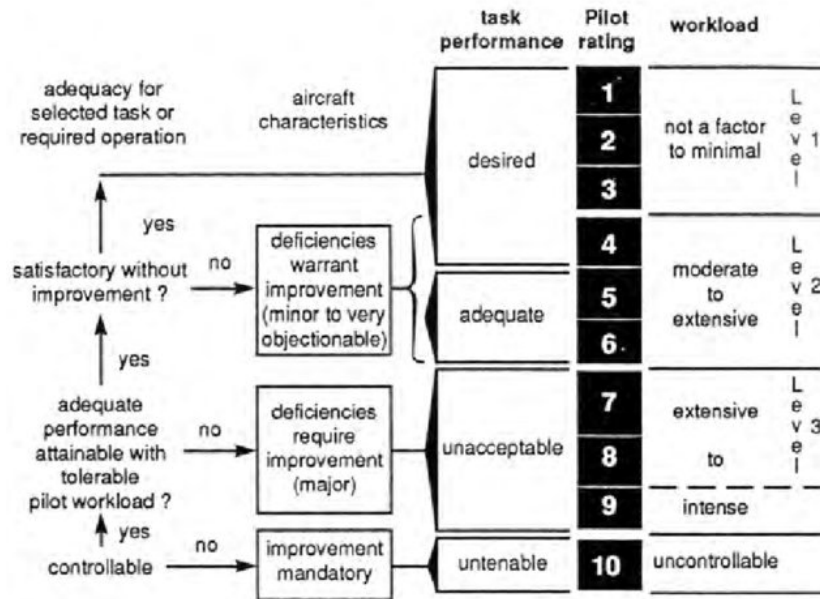
Figure 2.6: Summarized Cooper – Harper handling qualities rating scale [31].

Table 2.4: Cross-coupling requirements specified by the ADS-33 for off-axis dynamic responses [31].
* no current requirements.

Input \ Response	Pitch θ	Roll ϕ	Heave w	Yaw ψ
Pitch θ	X	$\Delta\phi_{pk}/\Delta\theta_4$ hover and fwd flight	flight path response not objectionable in forward flight	* yaw response due to rotor torque changes in aggressive pitch manoeuvres
Roll ϕ	$\Delta\theta_{pk}/\Delta\phi_4$ hover and fwd flight	X	* thrust/torque spikes in rapid roll reversals	$\Delta\beta/\Delta\phi$ ratios in fwd flight
Heave w	$\Delta\theta_{pk}/\Delta n_{z_{pk}}$ in fwd flight	* $\Delta\phi_{pk}/\Delta n_{z_{pk}}$	X	$r/|\dot{h}|$ ratios in hover
Yaw ψ	* pitching moments due to sideslip in fwd flight	dihedral effect on roll control power	not objectionable in hover	X

<div align="right">

3

</div>

Model Predictive Control

This chapter will elaborate on Model Predictive Control (MPC), the control theory. First, an introduction on the concept, different types of MPC, history and current research will be given. Next, each component of MPC will be discussed separately after which the stability of the MPC algorithm will be discussed.

3.1. Concept

First of all, it should be noted that MPC will be explained and implemented in its discrete-time version where the discrete control sampling time is indicated by k. MPC is a type of model-based, optimal control where at each time step, k, an optimal control input sequence $\bar{u}_k = [u_k, u_{k+1}, \ldots, u_{k+N-1}]$ is computed online over a future time horizon, the prediction horizon N, by solving an open-loop optimization problem that has knowledge of the system model [7]. The optimization uses the current state of the system as initial state and a model of the system to compute the future states along the prediction horizon in order to optimize a desired objective function. Then, only the first control input in this optimal control input sequence u_k is applied to the system. At the next time step, the prediction horizon of the optimization problem shifts one step forward, to $k + 1$, and the next optimal control sequence $\bar{u}_{k+1} = [u_{k+1}, u_{k+2}, \ldots, u_{k+N}]$ is computed.
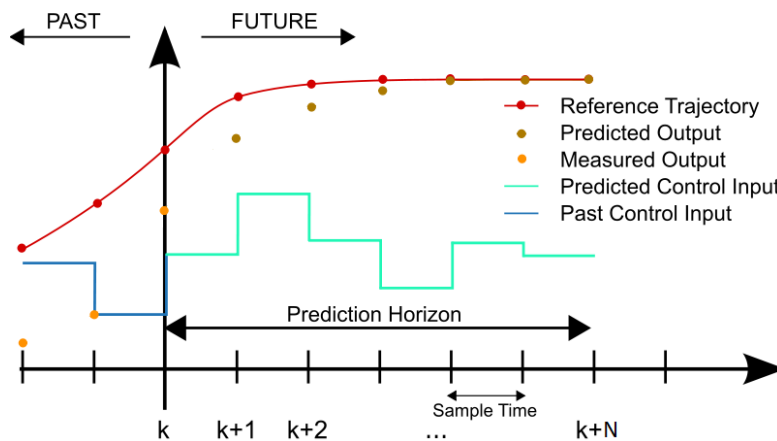
Figure 3.1: The concept of MPC in discrete time [37].

In Figure 3.1, one can see the concept of MPC explained in discrete time for a reference tracking problem. The closed-loop block diagram of the MPC concept can be seen in Figure 3.2 where the case of a reference tracking problem is taken for illustration. In a reference tracking problem, the objective function of the optimization is to minimize the error, $\bar{e} = [e_{k+1}, \ldots, e_{k+N}]$, between the reference trajectory, $\bar{r} = [r_{k+1}, \ldots, r_{k+N}]$, and the predicted output trajectory $\bar{x} = [x_{k+1}, \ldots, x_{k+N}]$. Then, the optimization problem consists of computing the optimal control input over the prediction horizon such that the tracking error is minimized and the constraints are met. The optimizer has knowledge of the systems future behaviour by means of the current state feedback, x_k, and the system model. This means the future states and control

inputs are calculated in the open-loop MPC algorithm. Once the sequence of control inputs is optimized for the objective function, only the first control input, u_k, is applied to the system. In this way, the feedback loop is closed going from receiving the measured state to computing the optimal control input sequence over a prediction horizon to applying the first control input to the system, all in one time step. Finally, the prediction horizon shifts one time step forward, the new state measurements are fed to the optimizer and the process repeats itself [7].
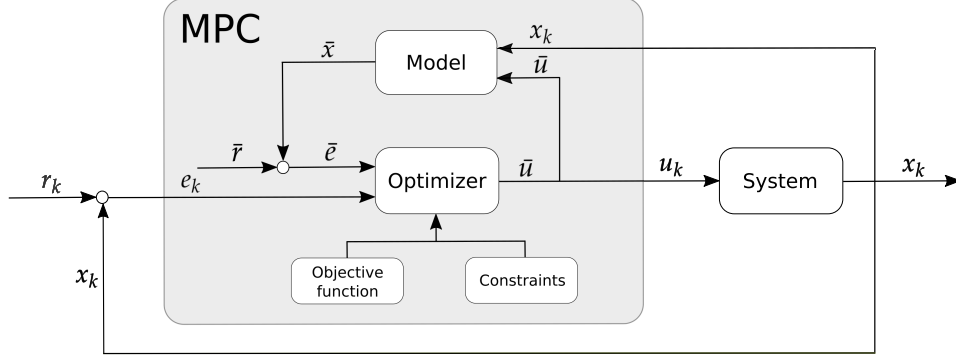
Figure 3.2: Block diagram of MPC applied to a system for reference tracking [38].

The optimization problem for MPC in general is formulated in Equation (3.1), where k is the current time step, x_k is the current measured state, $\bar{x} = [x_{k+1}, \ldots, x_{k+N}]$ is the vector containing the predicted state along the prediction horizon N, V_N is the objective function and $\mathbb{X}_f$ is the terminal region. Since MPC is entirely based on an optimization problem, input and output constraints are very easily incorporated in the controller design. The objective function, as can be seen in Equation (3.2), usually consists of a stage cost ℓ and a terminal cost V_f. The terminal constraint and terminal cost are in some cases needed because of stability reasons which will be explained further in Section 3.6.

$$
\begin{aligned}
\underset{\bar{u},\,\bar{x}}{\text{minimize}} \quad & V_N(x_k, \bar{u}) \\
\text{subject to:} \quad & \text{system dynamics} \\
& \text{input/output constraints} \\
& \text{terminal constraint: } x_{k+N} \in \mathbb{X}_f
\end{aligned}
\tag{3.1}
$$

$$
V_N(x_k, \bar{u}) = \sum_{i=0}^{N-1} \{\ell(x_{k+i}, u_{k+i})\} + V_f(x_{k+N})
\tag{3.2}
$$

In Equation (3.3), a standard, unconstrained, linear quadratic example for a reference tracking problem can be seen where $e_{k+i} = x_{k+i} - r_{k+i}$. The objective function is written as the sum of a quadratic tracking error term weighted with the matrix Q, a quadratic control action term weighted with matrix R and a terminal quadratic tracking term weighted with matrix P_f. Here, the control action term penalizes having large control actions. The linear system dynamics used to predict the states is expressed using a discretized, linear state-space model.

$$
\begin{aligned}
\underset{\bar{u},\,\bar{x}}{\text{minimize}} \quad & V_N(x_k, \bar{u}) = \sum_{i=0}^{N-1} \left\{ e'_{k+i}\, Q\, e_{k+i} + u'_{k+i}\, R\, u_{k+i} \right\} + e'_{k+N} P_f e_{k+N} \\
\text{subject to:} \quad & x_{k+i} = A\, x_{k+i-1} + B\, u_{k+i-1} \quad \text{for } i = 1, 2, \ldots, N
\end{aligned}
\tag{3.3}
$$

3.2. Types of MPC

Different types of MPC can be differentiated based on the optimization algorithm, computation method or model used. Some of these types will be discussed in this section.

Linear and Nonlinear MPC   The most general types of MPC are Linear and Nonlinear MPC (LMPC and NLMPC). The difference lies in the use of a linear or nonlinear objective function, constraints and prediction model. If one these elements is nonlinear, the controller is considered a nonlinear MPC controller [7]. Despite many processes in industry being nonlinear, linear MPC is mainly applied as it is easier to identify a linear model from test data which could be still representative for the nonlinear process. Also optimal and faster convex optimization can take place if a linear model is used. However, when the process is highly nonlinear or large deviations from the linear trim point are achieved, the linear model is not a good approximation of the real process anymore. Therefore, nonlinear MPC was introduced where a nonlinear model is used in the optimization. This causes the optimization to become non-convex and thus multiple local optima could exist. Hence, nonlinear MPC comes with suboptimality meaning it is not guaranteed to reach the global optimum, the optimal control input. Multiple initial values can be tried each step in an attempt to still reach the global optimum. Again, this goes at the cost of longer computation time [39]. More on convex and non-convex optimization can be found in Section 3.5.4.

Explicit MPC   Explicit MPC was introduced in the early 2000s in order to reduce the computation time of the optimization. It uses an explicit optimization formulation specific to each application calculated offline which severely speeds up the optimization process. The explicit solution is calculated offline using parametric programming techniques such that the optimization problem is a parametric function of the state. However, for systems with a large number of variables the offline calculation of the explicit solution can take up a lot of memory. Explicit MPC is often used for systems which require small sampling times such that it is possible for these systems to use MPC in real-time [40].

Robust MPC   For uncertain systems and systems subject to noise, an MPC control law with robustness is needed such that, for a certain amount of noise or model variation, the stability of the system and required performance is maintained. However, the addition of robustness to the MPC controller comes with the drawback of having less optimal results. Different methods of robust MPC are defined such as min-max MPC, constraint tightening MPC, tube MPC and multi-stage MPC [41].

Hybrid MPC   Finally, a distinction in MPC techniques can be made for MPC applied to hybrid system, called hybrid MPC. These systems have a dynamical model which can integrate discrete and continuous components, logic conditions, switching, etc. as more and more applications have to deal with hybrid systems. In order to formulate this hybrid problem in a solvable way, the system is rewritten as a mixed-integer quadratic or linear program to which solution techniques are available [42].

3.3. Historical Background and Applications

The idea of MPC was first introduced in the 1960s however the technology was only used in industry from the 1980s [43]. The MPC concept was first applied in industrial processes under many different names: Dynamic Matrix Control (DMC), Generalized Predictive Control (GPC), Model Algorithm Control whose software is called IDCOM, etc. Each of these control theories apply the same model-based, receding horizon concept but in a different manner. For example, in DMC the system dynamics is represented as a linear step response model and can only be applied to linear open-loop stable systems whereas in GPC the system dynamics is formulated using a CARIMA model, the control technique takes into account disturbances and can handle open-loop unstable systems [44], [45]. DMC, developed by Shell Oil, GPC and other variations of MPC were widely used in chemical and petrochemical industries, refineries, air and gas industry and food processing [9]. It is only 10 to 20 years after MPC was first being applied that the theoretical proofs for stability, feasibility and optimality of MPC were being researched and nonlinear, explicit and even hybrid MPC was developed.

Nowadays, this control technique is known as MPC or Receding Horizon Control (RHC) and is considered a promising model-based technique to control constrained multivariable systems. Furthermore, MPC has immensely grown in popularity and has application over a much wider variety of industries including automotive, aerospace, electronics, metallurgy, medicine, energy, environment etc. [10], [11]. The applications of MPC are no longer limited to industrial processes, which brings along new challenges.

3.4. Challenges and Current Research

Until now, MPC theory and application is well established for linear industrial processes which are slow, small-scale and don't have many constraints. However, as applications are extending to large scale, fast dynamic, low cost and nonlinear systems and as society puts more and more requirements and constraints on safety, energy, economics, etc. MPC is facing new challenges.

Some of these challenges and research areas related to these challenges are addressed by Xi (2013) [8]. The paper categorizes four existing challenges or problems for the current MPC theory and application: effectiveness, nonlinearity, usability and scientificness and elaborated on how these challenges are tackled currently in the research field. Besides deficiencies in the control algorithm, the applicability and performance of MPC is also often limited by difficulties in state estimation, modeling, sensing, diagnosis and fault detection [46]. In this way, MPC points out new needs in other technologies or fields as well. Firstly, the challenges that MPC is facing will be explained after which an update on the current research to handle these challenges is given with prospects to the future.

Upcoming Challenges   First of all, current MPC theory has low effectiveness when a small sampling time is required meaning that the MPC optimization is slow and has a heavy online computation burden. Currently, MPC can only be applied in real-time to relatively slow systems, because fast systems require a small sampling time, or applications with high performance computers.

Furthermore, MPC theory is less practical for nonlinear systems as nonlinear optimization for large systems is slow, the optimum can be local and stability guarantees are difficult to obtain. Stability proofs and feasibility are well established for linear MPC whereas the theoretical research for NLMPC and nonlinear optimization still lacks understanding of the reliability and efficiency. Nonlinear MPC has been an active research topic for several years. However, in industry NLMPC is still at an early stage.

Next, MPC needs to become easier to work with. Applying and tuning MPC relies heavily on experience as no direct relationship between the design parameter and the system performance exist because no explicit solution exist for constrained problems. This makes applying and maintaining MPC costly.

Finally, there is a big gap between the practical application of MPC in industry and the theoretical research on MPC theory. There is a lack of scientificness in MPC applications. For example, theoretical terminal penalty terms or constraints, which are needed to guarantee stability according to the Lyapunov stability theory, have an unclear physical meaning in the optimization formulation. Therefore, these results of MPC research are rarely applied in the implementation of commercial MPC. Hence, there is a need for an MPC theory and design that takes into account the physical intuition and computation time while guaranteeing control performance.

Current Research   Research already has been performed to tackle these challenges. Although many problems still need more investigation and solutions in order to be able to apply MPC to large scale, fast dynamic, low cost and nonlinear systems. Many studies are performed regarding the effectiveness challenge trying to improve the structure, strategy and algorithm of MPC to reduce the computation time. On structural level, hierarchical control and distributed control for large scale systems such as transportation systems and power systems are being researched and developed. On strategic level, explicit MPC is still elaborated upon to make it possible to find an explicit solution for large, nonlinear and hybrid systems. On algorithmic level, optimization methods for linear and nonlinear problems are being improved or approximated in order to reduce the optimization time.

Research is also being performed on the practical implementation of MPC enhancing its usability. Toolboxes, such as the Matlab MPC Toolbox, are being developed to enhance MPC prototyping, aiding the MPC setup, tuning and validation [47]. Hybrid MPC was introduced to practically implement MPC to hybrid system, as many nonlinear systems are hybrid system. However, solutions to the complicated mixed integer programming problem are existent but still need more investigation. Furthermore, practical implementations for stochastic and nonlinear systems are being investigated. Studies on NLMPC performance guarantees attempt to find more applicable algorithms while maintaining the real-time optimization and decreasing the complexity of the design. Aside from stability and robustness studies, nonlinear MPC research is extended to output feedback, state estimation and tracking problems with explicit and numerical algorithms [48].

Finally, researchers are working on extending the application areas to more fields such as automotive industry, ship systems, energy systems, aerospace systems and power electronics. MPC can even be used

for purposes other than control: calculating extremal control inputs corresponding to load limits or flight envelope limits, etc. [49], [50].

Conclusion   In conclusion it can be said that the rising challenges coming along with new application areas and more constraints are already being researched to some extent. However, great effort is still needed in order to make MPC effective, usable, scientific and applicable to nonlinear systems by creating high-efficiency, user-friendly algorithms with both theoretical guarantee of stability and real-time application.

3.5. Components

The three main components of MPC are the prediction model, the optimization problem consisting of an objective function and constraints, and the receding horizon policy. In this section, the model used for the predictions, the objective function, the constraints, the optimization and the tuning parameters in MPC will be discussed.

3.5.1. Model

In MPC the basic concept is to use a dynamic model to predict the systems behaviour in the future in order to optimize the prediction to obtain the optimal control inputs. This model can be represented in many different ways each having its upsides and downsides. The general discrete formulation for the dynamics of a system is given by Equation (3.4) which can be shortly written as $x^+ = f(x, u)$.

$$x_{k+i+1} = f(x_{k+i}, u_{k+i}) \text{ for } i = 1, 2, \ldots, N-1 \tag{3.4}$$

From the 1980s onwards, the finite step response model and finite impulse response model are mainly used for MPC in industry [51]. These models use a finite superposition of, respectively, step and impulse response functions consisting of a gain and a time to represent the output. The downside of these models is that they require a lot of memory to store the response functions. Furthermore, transfer functions or input-output models can be used to represent the system dynamics if only little is known about the system's internal structure by only giving the relation between the output and the input. Besides that, GPC makes use of a Controlled Auto-Regressive and Integrated Moving Average (CARIMA) model which has the advantage that it can include disturbances in the model. However, in academic research the state-space representation which can be seen in Equation 2.8 is mainly used for linear models [52].

Apart from these different types of models, the models can also be divided in categories. As most systems have nonlinear dynamics, the model used by the MPC algorithm can be nonlinear or can also be a linearized version of the nonlinear dynamical model. Hence, two major categories can be distinguished: the linear and nonlinear models. Mostly, the linear model is preferred as it has the characteristic of being convex which majorly simplifies the optimization process and guarantees to have a global optimum. However, for highly nonlinear processes this linear representation is not always an accurate fit. Therefore, NLMPC was introduced which uses a nonlinear model in a non-convex optimization algorithm. The difficulty of nonlinear models in MPC theory is that a proof or guarantee for stability and optimality is difficult to obtain [39].

Furthermore, models can be divided in time-varying or time-invariant models, referring to the fact that the state-space matrices are depending on time or not, and in deterministic or stochastic models, referring to the inclusion of noise or disturbances in the model [7][p. 1-11].

Finally, the fidelity of the model is of great importance for the MPC application as it should provide a balance between the accuracy and resemblance of the important dynamics of the system and the computational time and complexity. Especially for fast dynamical systems such as helicopters, the computational complexity of the model and its computation time is significant in this trade-off.

3.5.2. Objective Function

The objective function is the most defining, and meaningful component for the final optimal output in the MPC algorithm. Based on the objective function, the output is determined. Hence, it is very important to choose the objective function such that every term is of significance and that the objective function of the MPC corresponds to the objective of the physical system to control.

The objective function typically consists of a stage cost and an end cost as can be seen in Equation 3.2. This end cost or terminal penalty is usually needed because of stability reasons. Now, it will be assumed that no specific terminal penalty is required. This objective function can then be described by a sum of linear,

quadratic or nonlinear terms. Each term is scaled by a weight such that more importance can be given to one objective than the other. These weights can then be tuned in order to get the desired closed-loop behavior. When the terms are linear or quadratic and the model is linear, the optimization problem can be easily solved numerically or explicitly using quadratic programming.

As seen in the example in Section 3.1, the objective of the MPC can be a tracking task. However, the objective function shouldn't be limited to following a reference trajectory. For example, one can use this powerful tool to optimize for minimum fuel consumption, structural or vibrational loads [49], emissions [53], flying in formation [54], passenger comfort, travel time, handling qualities, etc. The MPC algorithm can then find the optimal path and control actions to maximise this performance objective.

3.5.3. Constraints

One of the great advantages of MPC is that it can easily incorporate input and output constraints simultaneously. Constraints on the control inputs are typically physical boundaries whereas constraints on outputs are usually operability, product quality or safety limits. Next to this, also 'artificial' constraints can be put on the outputs such as the terminal set constraint for stability. The mathematical formulation of an input and output constraint can be seen in, respectively, Equation 3.5 and 3.6.

$$E \cdot u_{k+i} \leq e \quad \text{for } i = 1, 2, \dots, N \tag{3.5}$$

$$F \cdot x_{k+i} \leq f \tag{3.6}$$

with:
$$E = F = \begin{bmatrix} I \\ -I \end{bmatrix}$$

$$e = \begin{bmatrix} u_{max} \\ -u_{min} \end{bmatrix}, \ f = \begin{bmatrix} x_{max} \\ -x_{min} \end{bmatrix}$$

such that:
$$u_{min} \leq u_{k+i} \leq u_{max}$$
$$x_{min} \leq x_{k+i} \leq x_{max}$$

As more and more constraints are put on the optimization problem, the feasible region of possible control inputs gets smaller and smaller. It is convenient to model input constraints as hard constraints since they are usually physical limits. However, the output constraints are considered more desirables than limits. Therefore, in order to prevent the problem from becoming infeasible, the hard output constraints can be replaced by soft constraints when the problem becomes infeasible. In this way, the soft constraint is relaxed such that a solution can still be found. Once the optimization problem is feasible again, the soft constraint reverts back to a hard constraint. This is done by adding a slack variable ϵ to the constraint as can be seen in Equation 3.7. This slack variable is considered a decision variable and is added as a weighted term to the objective function. Furthermore, the slack variable has to be greater than or equal to zero which is guaranteed by including this as a constraints.

$$F \cdot x_{k+i} \leq f + \epsilon_{k+i}$$
$$\epsilon_{k+i} \geq 0 \tag{3.7}$$

3.5.4. Optimization

The optimization problem and algorithm in MPC is a key component as it is the means to finding the optimal control input. However, solving the optimization problem is very time consuming. Even though fast methods and better computation power are making their advance, its computation time is a substantial drawback for systems with fast dynamics. Many different analytical and numerical methods to solve the optimization problem exist. Next, a distinction will be made between convex and non-convex optimization.

An optimization problem is convex if the objective function is convex, the inequality constraint functions are convex and the equality constraint functions are affine. When the system model is nonlinear, the optimization becomes non-convex. The advantage of convex optimization is that there are no local optima and the optimization problem can be solved rather quickly and easily. A convex optimization problem can be solved using linear or quadratic programming. Different methods exist such as Newton's method, interior-point methods, gradient-based methods, etc. In convex optimization without constraints, an explicit

solution can be found by means of dynamic programming such that the optimal control input can be directly computed as a function of the initial state. This severely speeds up the computation process.

If the optimization problem is non-convex, multiple local optima exist. Therefore, finding the global optimum becomes a complex and time consuming task. However, optimality is not required by MPC, only feasibility [55]. Even if the outcome of the optimization problem is not the global optimum but a local one, called suboptimality, the controller can still be stable provided that minor modifications are made to the optimization problem.

In order to speed up the optimization process, many tricks, algorithms and tuning can be implemented [56]. For example, neural networks can be used that mimic the behaviour of the MPC optimization [57], explicit solutions to the optimization problem can be found, the sampling time and prediction horizon can be tuned, the model can be reduced such that there are less variables to compute in the optimization, faster optimization algorithms such as using Pontryagin's Minimum Principle can be implemented [58], etc. Furthermore, a control horizon N_u is often implemented which is smaller than the prediction horizon. The optimizer will only compute the control input sequence up to time step $k + N_u$. After this time step, the control input for the remaining prediction horizon is assumed to be equal to u_{k+N_u-1}. In this way, the amount of measurable variables in the optimization are reduced, reducing the computation time.

3.5.5. Tuning Parameters

The MPC algorithm contains several design parameters that require tuning specific to each application and task. Those parameters are the sampling time Δt, the prediction and control horizon N and N_u, and the weights specific to the objective function. The tuning parameters and the closed-loop performance are related to each other in a complex matter, especially when the system model is not very accurate to the real system dynamics. In general, no structured tuning method is available for MPC. It requires engineering expertise and insight to evaluate the closed-loop performance as parameters and scenarios are changed until satisfactory results are obtained. This makes tuning of the MPC rather difficult. When the MPC algorithm is modified such that stability is guaranteed, not much tuning is needed to obtain good performance. However, when stability is not guaranteed, the MPC has to be tuned by trial and error in order to have a stable controller and obtain the desired performance. Nevertheless, some general guidelines and best practices to tune each parameter exist.

It is common to first select a proper sampling time and keep it constant throughout tuning. A proper sampling time can be found by trial and error and should be small enough to capture the system dynamics, but large enough to enable real-time control.

The prediction and control horizon selection is as well a trade-off between performance and computation time since large horizons increase the amount of variables to optimize. A large prediction horizon is in general good for stability but bad when a lot of inaccuracies between the MPC model and the real system dynamics exist since the error accumulates over time. Furthermore, a small prediction horizon might be good for the computation time, it also limits the future information available about the system. When the prediction horizon is too small, it might be possible that delays or non-minimum phase behaviour of the system cannot be captured. Hence, the controller needs a prediction horizon large enough to be able to anticipate on future events such as constraint violations, delays and non-minimum phase behaviour sufficiently early to allow for a corrective control action.

The control horizon is usually taken lower than the prediction horizon in order to decrease the amount of variables in the optimization problem and improve the computation time in a way such that performance is not affected.

The weights of each term in the objective function are the tuning parameters that are very important with respect to the objective of the entire controller. They represent how much each term is valued. In the unconstrained linear quadratic example for reference tracking in Equation 3.3, Q, R and P_f are the weighting matrices for respectively the tracking term, the control action term and the terminal tracking term. They are diagonal matrices with the elements on the diagonal being the weights corresponding to the importance of their respective variables. When the weights of the R matrix are large with respect to the Q matrix, the system will have very small control actions with a slower response. Whereas, when the Q matrix has larger weights than the R matrix, the system will behave faster and more aggressive at the cost of large control actions. The terminal tracking weight term can be different from the stage tracking weight Q for stability reasons. Furthermore, it is important to note that the weight of each variable should scale with its units.

For example, one meter deviation from the reference trajectory cannot be compared to one degree deviation from the reference angle.

3.6. Stability Theory

In this chapter, the stability theory for MPC problems will be summarized. Stability of the MPC problem is beneficial as only then the controller will guaranteed make the system converge to a certain equilibrium state. However, it is not needed in order to have a functioning MPC controller. With proper tuning and a sufficiently long prediction horizon, the system can also converge to the equilibrium state. Therefore, in this research this MPC stability theory will not be applied. Nevertheless, some words will be held on the definition of stability, how to proof stability and how to enforce stability in an MPC problem.

3.6.1. Asymptotic Stability

An equilibrium point or trim point of a system x_0 is the state of the system at which it will remain if the system starts from that point and no disturbances or inputs are given. This trim point can be unstable, locally stable, Locally Asymptotically Stable (LAS) or Globally Asymptotically Stable (GAS) depending on if the state, starting from any point (for global stability) or a point near the trim point (for local stability), diverges or converges over time towards the trim point (asymptotically) or to a state near the trim point (non-asymptotically) when a disturbance is given [7][p. 112 - 131].

In MPC, the closed-loop stability will mostly be non-global due to the presence of input and state constraints or due to nonlinearity and hence non-convexity of the system. Furthermore, if the MPC problem is said to be asymptotically stable, the closed-loop problem is by definition stable independent from the tuning parameters or the open-loop stability.

3.6.2. Lyapunov Stability Theorem

Stability of the controlled system is required in order to have convergent system behaviour. However, optimality does not ensure stability which implies that even though an optimal input is applied to the system, the closed-loop system is not necessarily stable. Hence, stability still has to be ensured for the MPC problem. This can be done by finding a Lyapunov function which proves guaranteed stability, or by tuning the controller and evaluating its closed-loop behaviour until the state converges.

A Lyapunov Function of a system is a generalized energy function of that system which enables to make conclusions about the trajectory of a system without explicitly finding the trajectories. The Lyapunov stability theorem holds that if there exists a Lyapunov function in a positive invariant set $\mathbb{X}$ for which $x_{k+i} \in \mathbb{X} \subseteq \mathbb{R}^n$, then the equilibrium point $x_0 \in \mathbb{X}$ is LAS for $x^+ = f(x, u)$. If the positive invariant set is equal to $\mathbb{R}^n$, then the equilibrium point is GAS for $x^+ = f(x, u)$. Here, a Lyapunov function can be defined as a function $V(x)$ which is lower and upper bounded by the $\mathcal{K}_\infty$-functions α_1 and α_2 and where $V(f(x)) - V(x) \leq -\alpha_3$ holds for the positive definite function α_3, indicating a Lyapunov decrease of the state as the state progresses.

In MPC, the objective function is often found to be a Lyapunov function. Hence, if the objective function and possibly constraints in an MPC problem can be written as a Lyapunov function, then the closed-loop system is asymptotically stable for all tuning parameters. This makes the Lyapunov stability theorem a way to proof that the MPC problem is stable.

3.6.3. Enforcing Stability

It is now clear that having a stable MPC controller and being able to proof this is very beneficial. However, it is still needed to know under what conditions the MPC problem is proven to be stable and what can be done to design a stable MPC controller. In order to understand this first a look needs to be taken at the infinite horizon MPC problem. After this, it will be explained how modifications to the MPC problem can be used to enforce stability.

Infinite Horizon Problem   An unconstrained MPC problem for a stable linear system and most importantly, with an infinite prediction horizon, always has guaranteed closed-loop asymptotic stability if it has a quadratic cost function with positive definite, symmetric weighting matrices [7][p. 19-20]. Let's say now the linear system is unstable, the system $\{A, B\}$ has to be stabilizable in order to guarantee stability for the closed-loop infinite horizon problem [59]. Hence, under these conditions, an MPC controller with an infinite horizon can always bring the state to the equilibrium point in a finite number of steps. Proof for this theorem is

constructed based on the backward Riccati iteration which is a backward dynamic programming technique used for solving linear quadratic control problems which exploits the recursive or multistage property of the objective function. However, when the MPC problem does not have an infinite prediction horizon the closed-loop system can become unstable. The smaller the prediction horizon the sooner the closed-loop system goes unstable. This is the reason why, when designing the MPC controller enlarging the prediction horizon stabilizes the controller.

Stabilizing Modifications   As finite horizons are highly desirable for computational reasons, a stability proof for finite horizons needs to be found. Similarly, if constraints are added to the infinite horizon problem or if the prediction model is nonlinear, the stability proof does not hold anymore resulting in a possibly unstable closed-loop problem. Therefore, ways have been found to enforce the MPC problem to still have asymptotically stability. Namely, if for a certain MPC problem the objective function is not a Lyapunov function then, by bringing modifications to the objective function or constraints, a Lyapunov function can be created.

The modifications and assumptions to the MPC problem that are required for stability are specific to the type of problem: infinite or finite horizon, linear or nonlinear model, stable or unstable model, type of terms in the objective function, constrained or unconstrained problem, etc [46]. The most important examples of stabilizing modifications are adding a terminal penalty term in the objective function or adding an 'artificial' terminal state constraint in order to force the objective function to decrease over the prediction horizon. The terminal penalty serves to penalize the error at the end of the prediction horizon more than the stage error whereas the terminal constraint ensures that the final state, at N, is in the given terminal set $\mathbb{X}_f$. Many research has been performed on stability proofs for various types of MPC problems. For linear MPC the stability proofs are well established [60] [59]. Whereas for nonlinear MPC the theoretical proofs are commonly too complex to implement in practice [61] [62].

In practice, these stability proofs are not often implemented. Instead, use is made of proper tuning of the prediction horizon, weights and other tuning parameters. In this way, the controller is not proven to be guaranteed to stabilize the state for all initial points but it is still stable for the conditions that are tuned for.

4

Model Predictive Control for Helicopters

This chapter will elaborate on the application of MPC to helicopters by firstly specifying the advantages and disadvantages of applying MPC specifically to helicopters. Then, previous research on MPC applied to helicopters will be discussed with the focus on differences and similarities in the objective of the MPC, the application to a helicopter in simulation or to an Unmanned Aerial Vehicle (UAV) in simulation and/or in test, the use of linear or nonlinear MPC, the model fidelity used for the prediction model, the algorithm used for calculating the optimal control input and the application of stability proofs.

4.1. Advantages and Disadvantages

Conventional controllers such as Proportional Integral and Differential (PID) and Linear Quadratic Regulator (LQR) control are in general not suitable for helicopter control as the dynamics of the system is highly nonlinear and many cross-couplings between the states exist. In order to make clear that MPC is an excellent technique for controlling a helicopter, that is able to deal with the complications PID and LQR control cannot deal with, the advantages and disadvantages of applying MPC to a system such as a helicopter are listed.

Advantages   The MPC controller is capable of:

- Enabling multivariate control with similar complexity as single variable control.

- Directly dealing with technical specification in the control algorithm through hard and soft constraints on inputs, states and outputs such as actuator limits, safety boundaries, performance bounds etc.

- Having optimized open-loop performance as specified by the customized objective function.

- Explicit specification of the objective function corresponding to the actual objective of the mission. This enables the ability to combine the guidance step and flight control step in controlling a helicopter by optimizing for the guidance objective computing directly the control inputs while taking into account input and output constraints which is not possible when separating the two steps.

- Taking advantage of future information of the system and trajectory enabling to deal with time delays and non-minimum phase behaviour present in rotor and inflow dynamics and anticipate on future events such as obstacles, turns, approaching a state constraint etc.

- Handling measured and unmeasured disturbances and modelling uncertainties such as wind gusts and parameter variances by means of recalculating the open-loop optimization problem every control step based on the new state feedback and by implementing robust and stochastic MPC.

- Enabling simple reconfigurability of tuning parameters, model type, model parameters, objective function etc.

- Allowing for flexible control architectures such as distributed, decentralized and hierarchical control for large scale systems e.g. formation flight. Similarly, the MPC can be used in an architecture in combination with another controller for instance a low-level conventional controller and a high-level MPC controller or for instance having the MPC computing input limits that are then fed to the actual flight control block.

Disadvantages The MPC controller comes with:

- A heavy computational burden due to the time consuming optimization process.

- No integral control directly included as integral action is not necessarily optimal but sometimes needed to eliminate a steady state offset that might occur in disturbance rejection.

- Complex artificial end constraints or end penalties which are needed in order to guarantee stability regardless of the tuning parameters.

- No systematic tuning method for tuning for stability.

As the helicopter is a multivariate, highly nonlinear system with time delays subjected to disturbances and restricted by physical and safety limits, the MPC control technique is highly suitable to implement [12]. Furthermore, as microprocessors technology and optimization algorithms are constantly advancing, the computational burden that comes with MPC can eventually be mitigated.

4.2. Previous Research

As can be seen from all the advantages of MPC in the previous section, applying MPC to helicopters can be very fortunate. Therefore, research has been performed on applying MPC to helicopters or small-scaled helicopters in the last 20 years and is still being researched. However, no examples of MPC operating on a helicopter in flight could be found. To get an overview of the research performed on the application of MPC to helicopters a chronological list of 34 papers and its characteristics is made in Table 4.1. Here, a distinction is made between papers using nonlinear MPC or linear MPC and papers applying MPC to a helicopter model or to a model of a small-scaled unmanned helicopter also referred to as UAV. Furthermore, it is checked whether the paper tested the controller not only in simulation but also experimentally. Lastly, the objective or task of the controller is noted where TT stands for Tracking Task. The characteristics of these papers mentioned in the table and the content of some interesting papers will be discussed in this section.

4.2.1. Objective

The amount of papers performing a tracking task is remarkable. No less than 72% of the papers investigated used MPC to track a reference trajectory. On one hand, this is logical as MPC is a very suitable control technique for reference tracking. On the other hand, it is a pity to only utilize MPC for this straightforward task as MPC is capable of fulfilling and optimizing much more advanced objectives. As some reference tracking papers command the helicopter or UAV to fly a certain maneuver such as a turn, landing or fly a square pattern while maintaining heading, other papers give step or sine inputs to certain states such as the velocity or position. Next, some trajectory tracking papers and some papers with more diverse objectives will be discussed.

Tracking Task Objectives From the tracking task papers in Table 4.1 two types of tracking tasks can be distinguished: tracking a maneuver and tracking a signal. The papers tracking a maneuver aim at testing the MPC for a specific mission or for a specific acrobatic movement with many cross couplings. Types of maneuvers tested are for example helical turns, pull-up/pull-overs, following a square in x- and y-position maintaining the same heading, flying a pirouette, flying an eight shape, etc. For example, the pirouette maneuver performed by Liu et al. (2012), where the helicopter flies a straight line while continuously changing its heading at 120°/s, aims to test the MPC to dynamics subject to the lateral-longitudinal coupling [63]. The MPC controller was able to track this complex maneuver with high quality. Furthermore, the square maneuver performed by Liu et al. (2010) tests the helicopters ability to fly forward/backward and sideways [64]. Here, flying the square trajectory was performed within 10 cm of the reference trajectory.

Other maneuvers tested in these papers included some of the ADS-33 Mission-Task-Elements such as hovering to ensure the MPC can keep the helicopter stable or pull-up/pull-over maneuvers to simulate avoiding and obstacle on ground [65], [50]. Sultan and Oktay (2012) even tracked a discontinuous maneuver [66]. A helical and banked turn were performed by tracking a roll angle of -0.1 rad in the beginning, a discontinuity of $\pm$ 2 seconds and then a roll angle of 0.1 rad, starting at an initial condition of 0 rad roll angle. Meanwhile, the pitch and yaw angle of the helicopter needed to remain constant. It could be seen from simulations that even though the trajectory was discontinuous, very good tracking was achieved.

Several papers did not track a certain maneuver but tracked a certain signal in one degree of freedom and kept the other state parameters constant in order to test the controller. Dutka et al. (2003) tracked a step in pitch angle from 0.25 rad to 0.4 rad and 0.7 rad while maintaining constant heading [67]. With nonlinear MPC the tracking performance was very accurate and fast. Gulan et al. (2019) tracked a trajectory of multiple set points in pitch and in yaw while maintaining constant attitude [68]. They compared the response of the MPC controller to linear quadratic control and concluded that overall MPC has good tracking performance and a lower tracking error than the linear quadratic regulator. Mehndiratta et al. (2018) tracked a square-like signal of 0.03 Hz and a sinusoidal signal of 0.05 Hz in order to test the MPC controller [69]. For both signals, the tracking error was very small as well.

When evaluating the tracking performance of MPC, not only the tracking error can be evaluated but also its performance when subjected to disturbances, model and process noise or model uncertainties. By means of using robust MPC [70], adding a Kalman filters [69], implementing a disturbance observer [63], etc. the MPC can cope with these disturbances.

Other Objectives   The few papers that did use MPC for other purposes than reference tracking had as objective for example to autonomously fly in autorotation mode and to avoid objects during a certain trajectory or to limit vibrational loads in the pitch link. Hereby, these papers are exploiting the power of the objective function of this optimal control technique. It can be noticed that some of these papers used MPC as main controller and therefore combined the guidance task and flight control task. However, other papers used MPC only for the guidance task and fed that information to another flight control system. Firstly, the papers using MPC as main controller will be discussed.

Chung and Sastry (2006) for example designed a distributed MPC controller in order to autonomously fly a team of helicopters in formation [54]. Here, distributed MPC is a form of MPC that can be applied to several or different system that have interacting dynamics. In this case, the interaction of one helicopter in the formation to the others expresses itself in the relative position to each other that needs to be maintained. First, they designed an MPC for an individual helicopter, gaining stability by adding a terminal cost. Next, inter-vehicle coupling terms were added to the objective function consisting of gap errors between the helicopter in question and the other helicopters in the formation. Minimization of these gap errors is performed by means of a constant gap or varying gap strategy. This method was then applied in a decentralized manner meaning that each helicopter has a local MPC controller which communicates with the other helicopters by sending its spatial positions. When testing the designed controller in simulation for 8 helicopters in echelon formation, the controller was able to successfully damp out the applied external disturbances.

Dalamagkidis et al. (2011) controlled the collective pitch angle with an MPC controller in order to autonomously autorotate and safely land [71]. To be clear, autorotation is a state in helicopter flight when a steady rate of descent is maintained by using the air flow through the rotor disk to rotate the main rotor as opposed to driving the main rotor. Autorotation is mainly used in emergency situations such as engine failures. Dalamagkidis et al. used a simplified vertical autorotation model in order to predict the helicopter sink rate. As they applied the controller to a small scaled unmanned helicopter, the primary goal of the autorotation controller was to minimize the kinetic energy near ground such that impact with possible bystanders won't cause fatalities. Therefore, a smart objective function was defined penalizing sink rates with a weight depending on the height of the helicopter. At the final stage of descent a penalty is given when the sink rate is higher than 125% of the altitude. This objective function ensures that the kinetic energy in the last 2.5 m of descent remains below 15 J for a helicopter of 3 kg. When implementing this optimization scheme, the optimal collective input can be computed in order to protect bystanders and safely land. Again, this is an example of utilizing the power of the objective function in order to combine the guidance and flight control task.

Three of the investigated papers didn't use MPC as the main controller but applied it to perform only

a guidance task. Then, it was implemented as a part of the control architecture where the MPC calculates control input limits that will then be fed to the actual flight control system or pilot. Hence, the MPC only calculates certain control input boundaries whereas the actual control inputs are provided by a pilot or a different controller.

For example, Mballo and Prasad (2019) used MPC to calculate the control input boundaries such that a previously determined limit load of the pitch link is not exceeded. The MPC algorithm then uses a structural model in order to predict the loads in the pitch link. The input boundaries calculated with the MPC algorithm were then used as an input to a Dynamic Inversion control block designed to perform manoeuvres [49]. Through attitude command and rate command simulations, the ability to limit the pitch link load and the direct effect on the maneuver performance was evaluated. An 80% reduction in limit exceedance was achieved when implementing the load limiting control. However, it could be seen that the actual pitch link load exceeds the limit load slightly at some points which can be explained by the mismatch between the prediction model used in the MPC algorithm and the actual loads in simulation. Furthermore it was seen that constraining the control inputs to the computed input boundaries limits the maneuver aggressiveness. Hence, the desired attitude was reached with a delay of about 7 seconds compared to the simulation without load limits for both the rate and attitude command tasks.

Similarly, Bottasso and Montinari (2015) calculated the control input limits corresponding to the flight envelope boundary [50]. They were calculated online by minimizing the difference between the actual state and the state at the flight envelope boundary. These control input boundaries were then fed to the pilot and flight control system. The limit parameter to optimize for was chosen to be the hub moment resultant. Hence, the critical control input corresponding to a maximum hub moment resultant was calculated at each instant in the simulation. This algorithm was tested for a pull-up/pull-over, a terrain avoidance and an acceleration/deceleration maneuver. Results showed that, when no mismatch between the MPC model and simulation model is present, the actual hub moment never exceeds the maximum hub moment.

Furthermore, Greer and Sultan (2019) created a landing envelope for landing on the deck of a ship accounting for average velocity of the helicopter and landing time [72]. The MPC used models for the helicopter dynamics, the ship motion and the ship induced air wake. The envelope was created by minimizing a landing tracking error for varying average approach velocity and varying set time to land. The closed-loop tracking errors found for these settings were than mapped onto the landing envelope. By determining a maximum tracking error, the maximum average velocity for a certain landing time can be determined. This landing envelope could then be forwarded to a pilot or to the flight control system.

4.2.2. Helicopter or UAV

It can be noticed from Table 4.1 that the MPC is either being applied to a helicopter or to a small-scaled unmanned helicopter. In some cases such as [68], [67] and [69], the system was a setup of a mechanical device with rotors with limited degrees of freedom in order to reduce the complexity of the system and controller. This setup was also indicated as UAV in the table despite it not being a flying vehicle. For example, Dutka et al. (2003) and Mehndiratta et al. (2018) used a 2 Degrees of Freedom experimental set up with rotors with angular freedom in pitch and yaw [67], [69]. Using this set-up, they could test if MPC was able to stabilize this unstable, helicopter-like system. In both cases, the tracking performance of the MPC controller was good and the controller was able to stabilize the system when a tracking set point in pitch or yaw was commanded.

Using a small-scaled helicopter as system has the big advantage of enabling flight testing of the developed controller. Out of the papers using a UAV as system, 60% was experimentally tested in a flight test of which all of them showed the desired performance. Frye et al. (2005) tested MPC using a Thunder Tiger Raptor 50 V2 remote controlled helicopter [65]. They subjected the small-scaled helicopter of less than 5 kg to out-of-trim flight conditions and used MPC to return to a stable trim condition. The UAV was able to transition from forward flight ($u = 20$, $w = 0$, $q = 0$, and $\theta = 0$) to hover within 1.25 sec and from vertical flight ($u = 0$, w =-50, $q = -3$, and $\theta = 0$) to hover within 1.70 seconds. The lateral dynamics was tested by going from state $v = 10$, $p = 4$, $\phi = 0$, and $r = 10$ to the trim which was done within 2.09 sec.

Liu et al. (2012) performed a climb, hovering and perturbation test using a Trex-250 miniature helicopter [63]. The MPC algorithm augmented with a disturbance observer was able to take-off, climb 0.5 meter hover and then hover with a frontal wind gust of 3 m/s with only minimal deviation in position and attitude. A second flight test was performed, flying the extremely challenging pirouette maneuver as discussed in Section 4.2.1. Again the MPC controller tracked the trajectory very well.

Unfortunately, the papers applying MPC to a helicopter were not able to experimentally verify their

simulation results. In fact, no papers could be found testing MPC applied to helicopter in a flight test.

4.2.3. Linear or Nonlinear MPC

Nonlinear and linear MPC are used an almost equal amount of times in the investigated literature (60% linear, 40% nonlinear). Linear MPC is mainly used for flight scenarios which can be approximated well by a linear model whereas nonlinear MPC is used when the maneuver includes large deviations from the linearized model. However, it is unclear how large these deviations are allowed to go in order to still have a well performing MPC. The deviations are mainly large when highly nonlinear behaviour is present and/or when the flight conditions differ significantly from the linearization point.
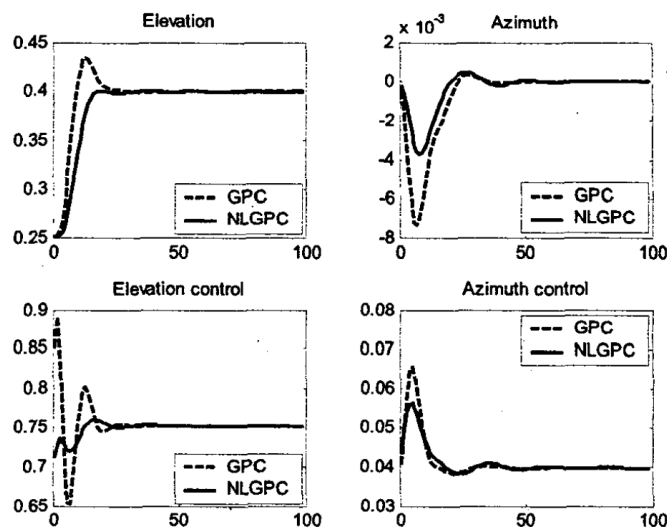

Figure 4.1: Comparison between GPC (LMPC) and NLMPC for a set-point of 0.4 rad in elevation [67].

Dutka et al. (2003) illustrated that last point in a 2 DOF helicopter simulation in pitch and yaw [67]. While remaining a constant yaw angle, the MPC controller was set to track a step in pitch first from 0.25 rad to 0.4 rad and then from 0.25 rad to 0.7 rad. For comparison, both a nonlinear and linear MPC controller was used to track this trajectory. Here, the linear MPC controller uses a linearized model around the set point trim conditions (so around 0.4 rad for the first case and around 0.7 rad for the second case). The tracking performance of the nonlinear MPC in the first case was remarkably better than the linear MPC as can be seen in Figure 4.1. The linear MPC was not only slower but also had a big overshoot. Furthermore, a steady state offset was present in the simulation with the linear MPC. This offset is present due to the mismatch between the linear model and nonlinear dynamics. In the second simulation with a step in pitch to 0.7 rad, the mismatch between linear model and nonlinear dynamics became too big in order to still have a stable controller. Hence, no tracking of the step trajectory could be achieved using the linear MPC controller. The nonlinear MPC however did track the step to 0.7 rad in pitch with no overshoot and while maintaining a constant yaw angle. Hence, when the mismatch between nonlinear and linear model is too large because of a large deviation in flight condition or because of highly nonlinear behaviour, nonlinear MPC yields much better and more stable tracking performance than linear MPC.

In order to reduce the mismatch in the linear MPC model, the linearization can be updated once a flight condition further away from the original linearization trim point is reached. Then, the nonlinear model is again linearized but for the new flight condition. Yujia et al. (2010) applied this successive linearization or linear model stitching technique to a 3 DOF simulation in order to improve the model throughout the simulation. They updated the linearization every few steps in the simulation around the new flight conditions [73]. They found that for tracking a doublet of 20 degrees in pitch and in yaw angle, the tracking error was much less when successively linearizing the model compared to linearizing the model once around the initial trim point. However, using successive linearization comes with the drawback of increasing the computation time immensely. Therefore, Frye et al. (2005) used an offline data set of linear models linearized around different flight conditions all over the flight envelope [65]. In this way they could eliminate the computation time needed for online successive linearization, yet still improving the model over the full flight envelope.

Instead of updating the linear model, the mismatch can also be accounted for by implementing a compen-

sation term. Bottasso et al. (2015) and Avanzini et al. (2013) found a way to implement this compensation by including the mismatch of the previous time step into the desired trajectory to track [50], [74]. Hence, the tracking trajectory r_{k+i} is adjusted by proportionally adding the model mismatch compensation term ϵ_k as can be seen in Equation 4.1.

$$
\begin{aligned}
r_{k+i}^* &= r_{k+i} + K \cdot \epsilon_k \quad \text{for} \quad i = 1, 2, ..., N \\
\epsilon_k &= x_k - r_k
\end{aligned}
\tag{4.1}
$$

Here, ϵ_k is computed by subtracting the reference trajectory from the the state computed with the actual nonlinear dynamics for the current time step k. Hence, the mismatch term has a delay of one sample time. The mismatch feedback gain K can then be tuned to a value going from 0 to 1 where Bottasso et al. chose a K of 1, Avanzini et al. picked a K of 0.3. It could be seen from simulations that implementing this compensation term improved the tracking performance of the linear MPC controller.

Table 4.1: Overview and characteristics of papers which apply MPC to helicopters.

Paper	Year	Nonlinear	Linear	UAV	Heli	Flight Tested	Objective
Bogdanov et al. [75]	2001	X			X		TT
Kim et al. [76]	2002	X		X			TT
Dutka et al. [67]	2003	X			X		TT
Frye et al. [65]	2005		X	X			TT
Chung and Sastry [54]	2006		X		X		Formation
Bottasso and Reviello [77]	2006				X		TT
Molenaar [78]	2007		X		X		TT
Witt et al. [79]	2007		X	X		X	TT
Du et al. [80]	2008	X		X		X	TT
Maia and Galvao [70]	2008		X	X		X	TT
Saffarian and Fahimi [81]	2009	X			X		Formation
Yujia et al. [73]	2010		X		X		TT
Liu et al. [64]	2010	X			X		TT
Dalamagkidis et al. [71]	2011	X		X			Autorotation
Liu et al. [82]	2011	X		X		X	TT
Joelianto et al. [83]	2011		X	X			TT
Oktay and Sultan [66]	2012		X		X		TT
Samal et al. [84]	2012		X	X			TT
Shipman [85]	2012	X			X		TT
Guerreiro et al. [86]	2012	X			X		Object avoidance
Liu et al. [63]	2012	X		X		X	TT
Song et al. [87]	2013		X	X		X	TT
Kunz et al. [88]	2013		X	X		X	TT
Avanzini et al. [74]	2013	X			X		TT
Salmah et al. [89]	2013		X	X			Object avoidance
Huck et al. [90]	2014		X	X		X	Formation
Bottasso et al. [50]	2015		X		X		Envelope limit
Greer and Sultan [72]	2016		X		X		Envelope limit
Ramalakshmi et al. [91]	2016		X	X		X	TT
Ngo and Sultan [92]	2016		X		X		TT
Zhong et al. [93]	2016		X	X			TT
Mehndiratta et al. [69]	2018	X			X		TT
Mballo and Prasad [49]	2019				X		Load limit
Gulan et al. [68]	2019		X	X		X	TT

4.2.4. Model Fidelity

The type and fidelity of model used in these papers can go from a 1 DOF model to a 22 DOF model with complex rotor dynamics dynamics to sometimes even using strategies to compensate for model errors. However, all models used in these papers can be classified as level I models according to Padfiel (1988) [94]. More detailed models could become unnecessarily complex for the MPC scheme as they slow down the computation time and do not necessarily improve the control performance. Samal et al. (2012) for example used a 1 DOF simplified heave model to track a stair trajectory and compared the performance of using an online with an offline determined model where the online model performed significantly better when noise and parameter variation are present. Three other papers used 2 DOF models and three more papers used 3 DOF models. Mostly, full 6 DOF models were used with some papers having a higher fidelity model than others. Oktay and Sultan (2012) for instance used a very detailed model that considered fuselage equations of motion, blade flapping and lagging dynamics, blade flexibility and static main rotor downwash to track a banked turn and helical turn [66].

4.2.5. MPC Algorithm

It can be seen that the recent trends in the MPC algorithm, explicit, robust and hybrid MPC, are also being applied to helicopters. Since helicopters are very fast dynamical systems, applying explicit MPC can make real-time application possible as illustrated by Liu et al. (2012) for nonlinear MPC [63]. Liu et al. proved in simulation and experimentally that the explicit optimization scheme for the nonlinear MPC algorithm is 10 times faster than the optimization scheme using a non-convex solver, reaching a control bandwidth of 50 Hz compared to 5 Hz. Furthermore, robust MPC is needed in helicopters when uncertainties and disturbances come into play such as wind gusts, unmodeled phenomena or model parameter variances. For example, Maia and Galvao (2008) applied robust MPC to a 3 DOF helicopter model and showed that in the presence of disturbances to the states the robust MPC algorithm succeeds at meeting the safety and physical constraints whereas the nominal MPC algorithm doesn't [70]. Furthermore, hybrid MPC was used on a helicopter in the paper of Salmah et al. (2013) in order to solve the object avoidance problem by formulating it in a piecewise affine model [89].

Another trend found in the application of MPC to helicopter is the use of neural networks in the MPC algorithm [71], [75] or in the model identification [77], [84]. At least five of the papers investigated in this section made use of neural networks in order to speed up the optimization process and to obtain online and offline models.

4.2.6. Stability Proofs

Out of all the papers investigated only very few papers focused or even included a proof for stability of the closed-loop MPC algorithm. This proves that in practise the artificial end constraints and end penalties are barely implemented. Instead, the controller is tuned by changing the prediction horizon and weights in order to affect the stability of the closed-loop system.

4.2.7. Conclusion

In conclusion it can be said that the previous work applying MPC to helicopters is at an early stage testing the controller mainly in simulation or in flight tests of small-scaled helicopters or limited DOF test set-ups. The previous research mainly focused on tracking reference trajectories for which the tracking performance is very good. Both linear and nonlinear MPC are used for the application of MPC to helicopters where the performance of the linear MPC controller could be improved by means of applying successive linearization, using an offline linear model database or by implementing a model mismatch compensation term. Nonetheless, MPC is showing promising results in terms of optimizing (tracking) performance and robustness for reference tracking and has the capabilities of achieving much more.

5

Conclusion of the Literature Review

In conclusion, this literature review analyzes and summarizes the basic concepts and previous research on the application of Model Predictive Control to helicopters. The topics of helicopter dynamics, stability and handling qualities, MPC theory and MPC applied to helicopters were covered.

Firstly, an 8 DOF longitudinal model was investigated in order to investigate the complex and nonlinear dynamics and stability of the helicopter. It was concluded that the helicopter is a complex, fast and unstable dynamical system with many nonlinearities, cross-coupling effects and time delays. Therefore, controlling a helicopter can be a challenging task. In order to improve the handling qualities of the helicopter, a subjective and objective assessment of handling qualities was established in the ADS-33 document which could be used as a guideline for desired flight behaviour when designing the helicopter and its flight control systems

Secondly, the concept of MPC was explained together with a word on its history and previous research, and an evaluation of its components and their pitfalls and capabilities was conducted. It was found that MPC is an optimal control technique with the powerful capabilities of including input and output constraints and an objective function directly in the control algorithm. Therefore, physical, safety and performance limits and mission objectives can be directly taken into account. This enables the flight control system to simultaneously find the optimal trajectory, based on the defined objective, and control inputs corresponding to the optimal trajectory. Furthermore, it was found that MPC has the advantage of being able to take into account future information of the system and the environment. This allows MPC to deal efficiently with time delays, non-minimum phase behaviour and to anticipate on future events.

On the other hand it was found that the optimization process in MPC brings along a big computational burden. Even though optimization methods and computer power are rapidly improving, the real time application of MPC to fast dynamic systems is still in development. Furthermore, when the theoretical and unpractical Lyapunov stability modifications are not implemented to the MPC problem, the MPC problem has to be stabilized by means of tuning. This can be time consuming and requires expertise as no structured tuning approach exists. Especially for nonlinear MPC, the computational burden and stability matter can become critical. Moreover, a nonlinear prediction model brings with it that the optimization becomes non-convex. A non-convex optimization has multiple local optima which can cause suboptimality to the final control input found, degrading the closed-loop performance.

Next, it was noticed that the research performed in the past 20 years on MPC applied to helicopters is still at an early stage. Mainly tracking tasks are being performed and the algorithm is mainly being tested in simulation and sometimes in flight tests with UAVs. Both linear and nonlinear MPC are being used on helicopters in previous research. Nonetheless, MPC is showing promising results in terms of optimizing (tracking) performance and robustness for reference tracking and has the capabilities of achieving much more.

In short, it was found that helicopters are difficult to control because of nonlinearities and cross-couplings. However, the rather new optimal and model-based control technique of MPC offers great opportunities to improve helicopter flight control and handling qualities.

Part III

Thesis Work

6

Problem Definition

This chapter will introduce the research gap that comes forward from the literature review and explain how this gap will be bridged in the thesis work. Furthermore, the research objective with research questions that will be covered in the thesis work will be presented. Finally, the approach to fulfill this research objective and obtain an answer to the research questions will be discussed.

6.1. Research Gap

The research gap in helicopter and MPC control theory will be made clear in this section in terms of helicopter flight control, model predictive control capabilities and the research on MPC applied to helicopters.

Helicopter   Helicopters have been designed to have extreme maneuverability in low and high speed flight and to have hover and vertical take-off and landing capabilities. However, this comes with the fact that they are very difficult to control as a pilot as the helicopter is an inherently unstable system with fast, nonlinear dynamics with many cross-coupling effects. Even though the first helicopter was produced already in 1936, it is to this date that helicopters are hard to control and are not accessible to the general public. In 1990, a definition and requirements were set up for handling qualities of a helicopter in order to measure the ease for a pilot to fly a helicopter. It was and is still used as a design standard and guidance for helicopter and flight control design.

   With the introduction of flight control systems and fly-by-wire in helicopters in the 90's-00's, the flying characteristics of the helicopter could be adjusted to the pilot's needs and make the helicopter easier to fly. This could be achieved by means of stabilizing the helicopter whilst still having maneuverability e.g. automating hands-free hover or decoupling the controls [95]. Hence, a fly-by-wire flight control system could be used to achieve good handling qualities. Nevertheless, to this day achieving level I handling qualities, which indicates minimal pilot workload and desired aircraft characteristics, remains a major challenge in helicopter and flight control design [35].

MPC   It was found in Section 3 that MPC is a promising optimal control technique with the powerful capabilities of including input and output constraints and an objective function directly in the control algorithm. This enables MPC to directly take into account technical specifications such as physical, safety and performance limits in the control algorithm and to explicitly specify an objective function corresponding to the actual objective of the mission. Furthermore, MPC has the advantage of being able to take into account future information of the system and the environment. This allows MPC to deal efficiently with time delays, non-minimum phase behaviour and to anticipate on future events. Because of these numerous advantages, MPC, which was initially used in industrial processes, is expanding to much broader applications including in the aerospace industry. Still, one of the major disadvantages of MPC is its computational burden in online applications, especially when applied to systems with rapidly varying and/or nonlinear dynamics such as helicopters. However, with rapidly improving optimization methods and computational power MPC is becoming more interesting to be used in flight control systems of helicopters.

MPC for Helicopters   It was shown from previous research in Section 4 that MPC is a suitable control technique for the helicopter with its fast, nonlinear and complex dynamics, offering lots of possibilities. Excellent tracking performance can be achieved when applying MPC to helicopters, tested by numerous papers in simulation and in flight tests with UAV's.   Other objectives such as formation flying, object avoidance, etc. have also been investigated by previous research. However, it was noticed that the research on MPC used for helicopter flight control is still at an early stage with respect to the application in flight tests and real-time application.   With MPC already being used for helicopter flight control in early stage researches, it can now be investigated how MPC can be used to improve helicopter handling qualities.

6.2. Research Objective & Questions

It can be seen that there is a clear need for helicopters to reach level I handling qualities such that they will be easier to fly and maneuver. One of the biggest reasons it is so hard to fly a helicopter is because of the many cross-coupling effects in the dynamics. Therefore, this is also a big aspect in the handling quality requirements specified in the ADS-33. With MPC having numerous advantages and making its way into the aerospace industry, it is being applied to helicopter in multiple researches for tracking trajectories and other tasks such as formation flying, object avoidance, etc. In this research, it will be investigated how MPC can be used for helicopter flight control to reduce cross-coupling effects and achieve better handling qualities. Therefore, the objective of this research is:

> *to investigate whether linear and nonlinear MPC are suitable for online application to helicopters to reduce cross-coupling effects by evaluating its performance on the cross-coupling handling quality requirements of the ADS-33 document.*

From the research objective, research questions have been derived such that when an answer is given to these research questions, the objective is fulfilled. The research questions consist out of a main question with various sub-questions and are presented below.

- Are linear and nonlinear MPC suitable to apply to helicopters to reduce cross-coupling effects?

    1. How well can linear and nonlinear MPC reduce cross-coupling effects in helicopters:
        (a) on the handling qualities rating scale?
        (b) compared to an uncontrolled helicopter?
        (c) compared to a conventional controller?
    2. How sensitive are the linear and nonlinear MPC controllers to disturbances to the helicopter when reducing cross-couplings?
    3. How sensitive are the linear and nonlinear MPC controllers to prediction model errors when reducing cross-couplings?
        (a) Which parts of the prediction model need to be accurate in order to still have level I handling qualities?
        (b) How large can the model error go in order to still have level I handling qualities?
    4. What are the similarities and differences between linear and nonlinear MPC applied to helicopters for reducing cross-couplings:
        (a) in terms of reducing cross-coupling effects?
        (b) in terms of optimization
        (c) in terms of computational speed?
        (d) in terms of model fidelity?

6.3. Research Approach

In this thesis work it will be investigated if linear and nonlinear MPC are suitable to reduce the cross-couplings in helicopters. The effectiveness of MPC to reduce cross-coupling effects in helicopters will be investigated by evaluating its performance in simulation on the cross-coupling requirements of the ADS-33 document for hover and forward flight for a nonlinear helicopter simulation model with and without an uncertainty added

to it. Here, the objective of the MPC will be to minimize the off-axis responses when simulating a step in the on-axis control input. The helicopter without controller and the helicopter with PID controller will be tested as well for the cross-coupling requirements in order to compare the performance of the MPC controllers with them. In addition, the robustness or sensitivity of MPC to prediction model mismatches will be investigated by evaluating the decoupling performance of the MPC controller when an error is added to certain parts in the prediction model. Furthermore, any theoretical differences between the linear and nonlinear MPC controller will be addressed and performance differences in the simulations will be investigated.

7

The Simulation Set-up

This chapter discusses the set-up of the cross-coupling simulations and sensitivity analysis simulations that will be performed for the thesis work in Chapter 8. All the simulations will be performed in Matlab 2020b. First of all, the simulation model configurations will be discussed. Here, the linearization of the nonlinear model presented in Section 2.2 will be explained and verified after which the uncertainty in the nonlinear simulation model will be introduced. Next, the MPC controller set-up will be thoroughly explained in terms of its objective function, constraints, tuning parameters and weights, etc. Finally, the PID controller that is used to compare the MPC controller with will be presented.

7.1. Simulation Model Configurations

First, an overview of the model configurations used in the MPC simulations will be given in this section. After this overview, the linearization of the nonlinear helicopter dynamics will be explained more thoroughly. Thereafter, the linear model will be verified by comparing its response to the response of the nonlinear model. Finally, a word is held on why and how the uncertainty is added to the nonlinear simulation model in the cross-coupling simulations.

7.1.1. Overview

The simulation model is the model that represents the actual helicopter as close as possible whereas the prediction model is the model used by the MPC algorithm to predict the helicopter's future state as good as possible whilst still having a reasonable computation time. Therefore, it is logical to use the 8 DOF nonlinear model from Section 2.2 as simulation model for the cross-coupling simulations as it has the highest fidelity. It is ran at 100 Hz, so the simulation has a sampling time of 0.01 s. In order to evaluate and compare the performance of nonlinear and linear MPC, both the nonlinear and linear model are going to be used as prediction model. However, the nonlinear model is then exactly the same as the simulation model hence the NLMPC will perform 'perfectly'. In order to be able to compare the nonlinear MPC controller with the linear MPC controller without the bias of the nonlinear MPC having a perfect prediction, an uncertainty is added to the simulation model. In this way, not only the comparison can be done unbiased but also the simulation model includes more realistic behaviour of the helicopter. More on this uncertainty that is added to the nonlinear simulation model can be found in Section 7.1.4.

The goal of the sensitivity analysis simulations is to check how robust the MPC controller is to mismatches and errors in the prediction model when trying to reduce cross-couplings. Hence, an error has to be implemented in the prediction model. When it is implemented to the linear model it can be implemented in a very structured manner by applying an error to one of derivatives in the state and input matrix. Therefore, it was chosen to use the linear model as prediction model and to reduce the model mismatch between simulation model and prediction model, the linear model was used as simulation model as well. How the error is implemented in the linear prediction model will be explained in Section 9.1.

An overview of the models used as simulation model and prediction model for the cross-coupling simulations and the sensitivity analysis can be found in Figure 7.1.
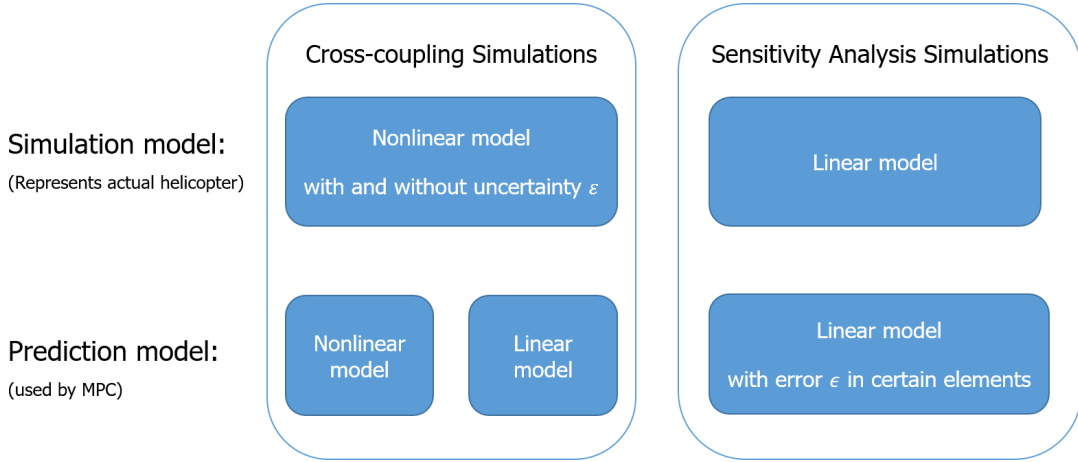
Figure 7.1: Overview of simulation and prediction model set-up for the cross-coupling and sensitivity analysis simulations.

7.1.2. Linearization

The linear model of the system used to predict the future helicopter state in linear MPC (Equation 7.2) can be obtained by linearizing the nonlinear model (Equation 7.1) around a certain trim condition (x_0, u_0). This trim condition is dependant on the flight speed of the helicopter. The trim conditions around which will be linearized in the simulations have a flight speed of V = 0 m/s and V = 41 m/s = 80 knots and can be seen in Equation B.1 and B.2. The linear model then approximates the nonlinear model at and around this trim condition as can be seen in Figure 7.2. The more the helicopter state deviates from the trim condition, the worse the linear approximation will be. Also, the more nonlinear the helicopter behaves at this trim condition, the worse the linear approximation will be.

$$\dot{x} = f(x, u) \tag{7.1}$$

$$\delta\dot{x} = A\delta x + B\delta u$$
with: $\delta x = x - x_0$, $\delta\dot{x} = \dot{x} - \dot{x}_0$ and $\delta u = u - u_0$ $\tag{7.2}$
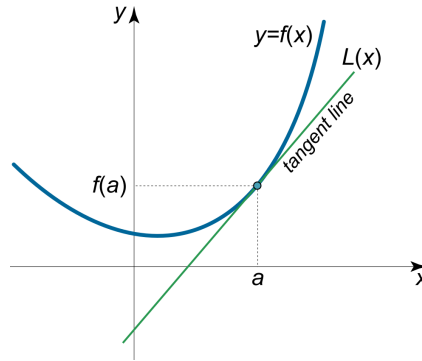

Figure 7.2: Linear approximation $L(x)$ of function $f(x)$ around trim point $x = a$.

Accurate linearization can be obtained by using perturbation linearization [26][p. 563]. Hence, linearization by perturbation was performed by means of numerically perturbing each state and input in trim with a small number δ and calculating the differences in each state after one time step Δt. In this way, the derivatives can be found and the state matrix A and input matrix B can be constructed. For example, the derivative of $\dot{u}$ with respect to w can be found by applying Equation 7.3.

$$\frac{\partial\dot{u}}{\partial w} = \frac{\dot{u}_{k+1} - \dot{u}_k}{\Delta t}$$
with: $w_{k+1} = w_0 + \delta$ $\tag{7.3}$

The simulations of this research are focused on the helicopter in hover and in forward flight. Therefore, a linear model linearized around the trim point at 0 knots and around the trim point at 80 knots with perturbation linearization are used. The state matrix A and control matrix B of the hover and forward flight linear state-space models can be found in Appendix B in Equation B.3 and B.4 (hover) and Equation B.5 and B.6 (forward flight) with state $x = [u\ v\ w\ p\ q\ r\ \psi\ \theta\ \phi\ x\ y\ z\ \lambda_0\ \lambda_{0_{tr}}]'$ and controls $u = [\theta_0\ \theta_{1s}\ \theta_{1c}\ \theta_{0_{tr}}]'$.

7.1.3. Linear Model Verification

In order to verify the linear model, the response of the linear model is compared with the response of the nonlinear model in a 5 second simulation where a doublet input of ± 2 deg is given into one of the controls. In this way, it can be checked if the states of the linear and nonlinear model over time follow a similar trend and how much the state according to the linear model is deviating from the actual nonlinear state.
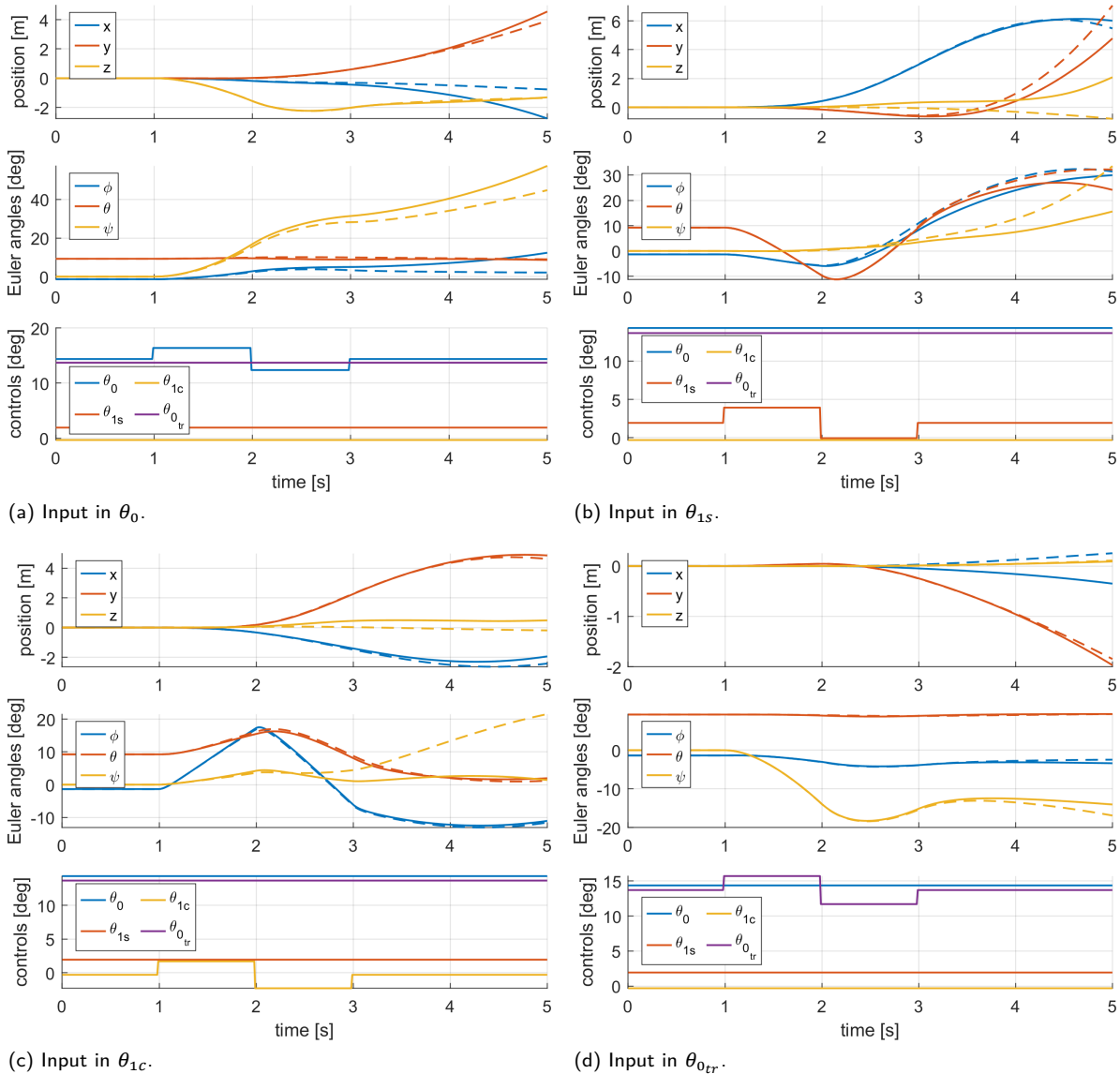

Figure 7.3: Response of the linear model (dashed line) compared to the nonlinear model (solid line) for a doublet input in one of the controls during hover.

In Figure 7.3 the 5 second responses of the linear and nonlinear model during hover can be seen where it is clear that, in general, the linear response follows the nonlinear response concerning position and Euler angles. Especially in the beginning of the simulation, say within 3 seconds, the linear and nonlinear position coordinates and Euler angles are more or less the same. Only after five seconds some differences in the

trends of the linear model can be found. This can be explained by the accumulation of error over time as the models only predict the change in state and build on to the previous state.

For example, the z-position response of the linear model in Figure 7.3 (b) after 5 seconds is deviating about 2 meters from the nonlinear response. Furthermore, the linear model predicts that the helicopter is descending whether the higher fidelity nonlinear model is actually ascending. It can also be seen for all four simulations that there is a deviation in the yaw angle between the linear and nonlinear response of sometimes up to 20 degrees after 5 seconds.

However, this kind of deviations are still not problematic as the linear model will only be used for predictions in the MPC algorithm over the much shorter prediction horizon. Hence, the linear approximation only has to be good over this very small time period. For the simulations in this research a prediction horizon of 0.15 seconds is used. Yet, longer prediction horizons of for example a couple of seconds are also common. In conclusion, it is expected that the linear model is sufficiently accurate in order to have similar performance as the nonlinear MPC controller as long as the state doesn't deviate too much from the trim state and the prediction horizon is small.

7.1.4. Introducing the Uncertainty in the Simulation Model

As explained in the overview of the model configurations in Figure 7.1, an uncertainty was introduced into the nonlinear model used as the simulation model for the cross-coupling simulations. The reason for introducing this uncertainty was twofold. Firstly and most importantly, the error is introduced in order to remove the positive bias of the nonlinear MPC performance. Secondly, the addition of the uncertainty into the helicopter model adds more realistic dynamics as the uncertainty that is added acts as a disturbance to the main rotor thrust. Without the uncertainty, the nonlinear MPC would have a perfect prediction model which is unrealistic and makes it unfair to compare the nonlinear MPC with the linear MPC.

Furthermore, it was decided to introduce the uncertainty in the simulation model instead of in the prediction model in order to keep the uncertainty the same, and hence comparable, for both the linear and nonlinear model. This entails that there is also a disturbance introduced in the actual helicopter dynamics which will be noticeable in the behavior of the helicopter but not unwanted.

$$C_T = C_T \cdot (1 + \varepsilon(\Delta t)) \tag{7.4}$$
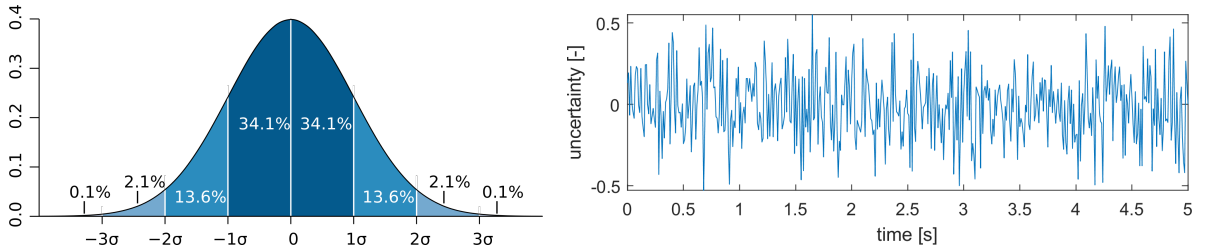
(a) Probability density of a normal distribution with zero mean and standard deviation σ [96].

(b) A 5 second trial of the uncertainty ε with $\sigma = 0.2$ over time.

Figure 7.4: Uncertainty probability density function and trial over time.

The uncertainty ε is introduced as a random variable with normal distribution $\varepsilon \sim \mathcal{N}(\sigma, 0)$ with a standard deviation of σ and zero mean as can be seen in Figure 7.4 (a) [97]. It is applied to the main rotor thrust coefficient as the thrust force is the main aerodynamic force acting on the helicopter affecting the motion in all degrees of freedom and is also very hard to predict so adding an uncertainty to it in the model is realistic. It is applied according to Equation 7.4 so that C_T is being decreased or enlarged with ε times itself. In this equation, the uncertainty varies with time so each simulation time step Δt the uncertainty ε changes. As the uncertainty is randomly generated each time step, every simulation is different. Therefore, a series of 6 simulations, called trials, are ran where the cross-coupling results are averaged.

For the simulations, a standard deviation of $\sigma = 0.2$ is chosen. Then, 68% of the generated uncertainties will be within $[-0.2, 0.2]$ and 95% will be within $[-0.4, 0.4]$. In Figure 7.4 (b), one can see a trial of this randomly generated uncertainty over 5 seconds. Figure 7.5 compares the response of the helicopter to a doublet input in $\theta_{0_{tr}}$ with and without this uncertainty. Here, it can be seen that the response with uncertainty indeed shows jerky behaviour especially in V_z and r. Furthermore, the disturbed response follows

the same trend as the undisturbed helicopter and only deviates slightly from the original response. Hence, no distinct differences between the two models are present while still having a certain variation. No accumulation of error is present as the mean of the uncertainty is 0 and both positive and negative values can be generated.
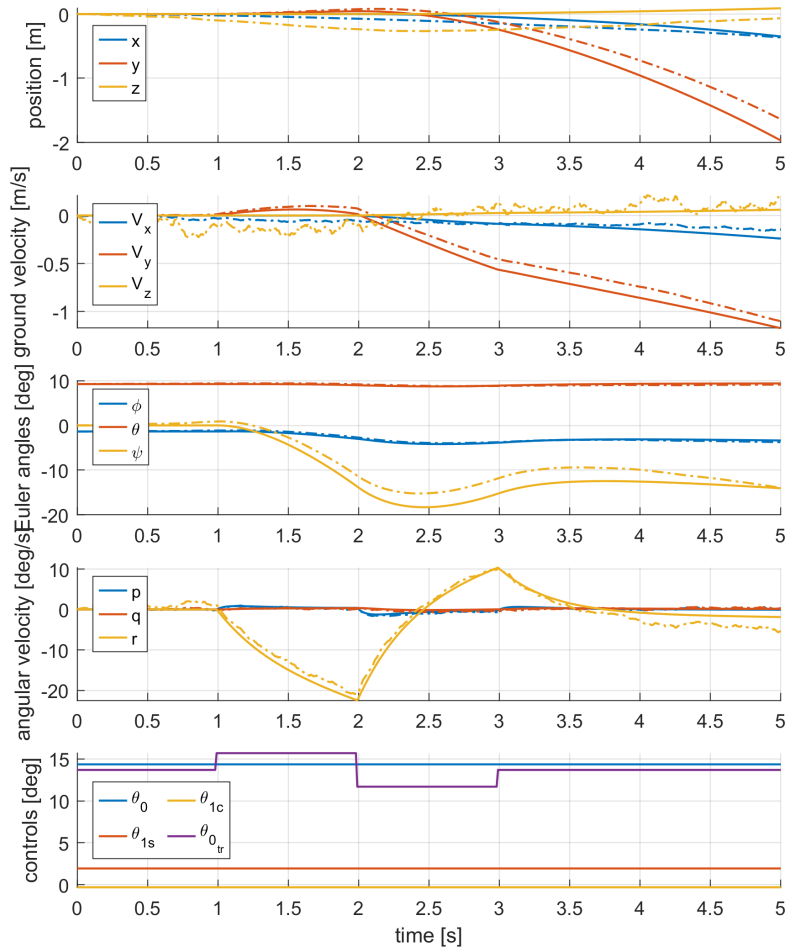

Figure 7.5: Response of the helicopter to a doublet input in $\theta_{0_{tr}}$ without uncertainty (solid line) compared with the response of the helicopter with the uncertainty of Figure 7.4 (b) implemented in the dynamics (dash-dotted line).

7.2. The MPC Controller

This section presents the MPC controller used in the simulations and explains certain MPC design choices that were made. Firstly, the objective function that will be minimized by the MPC controller will be stated. Next, the constraints that are put on the control inputs will be presented. Furthermore, the optimization method and initial value that is used will be explained. Then, the tuning parameters such as sampling time and prediction horizon are defined. Finally, the complete MPC formulation is presented.

7.2.1. Objective

The goal of the controller in the cross-coupling requirement simulations is to reduce the off-axis response when an on-axis input is given. In order to achieve this, the MPC controller is going to track a constant trim reference signal for the off-axis responses only. Then, the objective of the MPC controller in the cross-coupling requirement simulations is to minimize the error between the state and the reference signal for the off-axis states. For example, if the requirement for pitch due to roll cross-coupling is being simulated, an input is given in θ_{1c} in order to excite the roll angle. The pitch and yaw angle will be tracked whereas the roll angle won't be controlled. The reference trajectory of the pitch and yaw angle will be the trim value of the respective angle. It must be noted that only the attitudes (ψ, θ, ϕ) will be controlled and not the angular rates (p, q, r) or angular accelerations ($\dot{p}, \dot{q}, \dot{r}$). This would give steady-state offsets if no integral

term would be added and it is only the attitude that is the direct state that needs to be controlled.

$$\underset{\tilde{u},\,\tilde{x}}{\text{minimize}} \quad \sum_{i=0}^{N} \left\{ \left(x_{k+i} - r_{k+1} \right)' Q \left(x_{k+i} - r_{k+1} \right) \right\} \tag{7.5}$$

A quadratic objective function was chosen to minimize the tracking error with weight Q and reference trajectory r as can be seen in Equation 7.5. On the other hand a quasi-linear objective function could have been used such as $|x_{k+i} - r_{k+i}| Q$. This quasi-linear objective function in an MPC controller would yield deadbeat control meaning that it forces the state to the reference state in the minimum amount of steps possible. Hence, it is most optimal for tracking. However, this comes with the cost of aggressive control inputs and no robustness to disturbances or model mismatches. Furthermore, a quadratic cost function is more commonly used as it is a smooth function which aids in the stability proofs by Lyapunov and enable less complex optimization [98]. Therefore, the quadratic cost function was chosen.

It can also be seen that no input or input rate penalty is added to the objective function. The reason for this is that in this research the tracking performance of the MPC will be measured where the smoothness of the control inputs is not considered. In a real application, this penalty can be beneficial.

7.2.2. Constraints

One of the big advantages of model predictive control is that it can incorporate soft and hard constraints on inputs and states directly in the controller as explained in Section 3.5.3. Hence, some physical boundaries are imposed on the control inputs because of actuator limits. Firstly, the input range is limited for each control input by $u_{min} = [\theta_{0_{min}} \ \theta_{1s_{min}} \ \theta_{1c_{min}} \ \theta_{0tr_{min}}]'$ and $u_{max} = [\theta_{0_{max}} \ \theta_{1s_{max}} \ \theta_{1c_{max}} \ \theta_{0tr_{max}}]'$. The data for these limits of the BO-105 helicopter is retrieved from Prouty (2002) [26]. Secondly, the rate of change in each control input is limited by $\Delta u_{max} = [\Delta\theta_{0_{max}} \ \Delta\theta_{1s_{max}} \ \Delta\theta_{1c_{max}} \ \Delta\theta_{0tr_{max}}]'$. It must be noted that no rate limits were found for the BO-105 so the rate data for the Bell 412 helicopter from Voskuijl et. al. (2010) was used [99]. The values of the limits used in the simulations can be seen in Table 7.1. These limits are implemented according to Equation 7.6 and hold over the entire prediction horizon and for all control inputs. The state variables are not bounded by upper and lower limits but are constraint by the dynamics of the helicopter.

$$
\begin{aligned}
u_{min} < u_{k+i} < u_{max} && \text{for } i = 1, 2, ..., N \\
|u_{k+i} - u_{k+i-1}| < \Delta u_{max} && \text{for } i = 1, 2, 3, ..., N
\end{aligned}
\tag{7.6}
$$

Table 7.1: Input range and rate constraints limits.

Limit	Value [deg]	Limit	Value [deg]	Limit	Value [deg s]
$\theta_{0_{min}}$	-0.2	$\theta_{0_{max}}$	15.0	$\Delta\theta_{0_{max}}$	16.0 $\cdot \Delta t$
$\theta_{1s_{min}}$	-6.0	$\theta_{1s_{max}}$	11.0	$\Delta\theta_{1s_{max}}$	28.8 $\cdot \Delta t$
$\theta_{1c_{min}}$	-5.7	$\theta_{1c_{max}}$	4.2	$\Delta\theta_{1c_{max}}$	16.0 $\cdot \Delta t$
$\theta_{0tr_{min}}$	-8.0	$\theta_{0tr_{max}}$	20.0	$\Delta\theta_{0tr_{max}}$	32.0 $\cdot \Delta t$

7.2.3. Optimization

The optimization problem will be solved by means of the sequential quadratic programming algorithm which is a smooth nonlinear optimization method. It iteratively computes quadratic sub-problems starting with an initial guess of the variable to be optimized: the control input sequence.

As the objective function is nonlinear and for NLMPC the prediction model is also nonlinear, non-convex optimization will take place. This means multiple local optima may exist. In an attempt to find the global optimum, multiple initial values can be tried and compared with each other to then finally use the one with minimal cost. By doing this, the performance of the MPC can be improved to some extent. However, this will go at the cost of a much longer computation time as the same optimization has to take place multiple times now instead of once. Although, this may be prevented by running the optimizations in parallel.

The use of multiple initial values was tested for yaw due to collective coupling where it could be seen that the final tracking error when using 8 different initial values was just slightly less ($<$ 1 degree in total

over 5 seconds) than when one initial value (the trim controls) was used. Hence, the performance gain when using multiple initial values can be considered nonexistent. Therefore, it was chosen to use only one initial value. The initial value used was chosen to be the trim controls for that flight speed as this leans towards the optimal solution in many cases.

7.2.4. Tuning parameters

As explained in Section 3.5.5, the MPC controller contains several design parameters that require tuning specific to each application and task. Those parameters are the control sampling time Δt, the prediction and control horizon, N and N_u, and the weight Q.

Sampling Time   First of all, a simulation sampling time Δt_s was chosen small enough to capture the system dynamics, but large enough to have a reasonable simulation run-time. Therefore, a Δt_s of 0.01 seconds was chosen as mentioned in Section 7.1.1. In order to reduce the run-time even more, a larger control sampling time Δt of 0.03 seconds is set. Hence, every 3 simulation time steps, a new control input is computed. In the remaining steps, the control input is kept the same as the previously calculated input.

Prediction Horizon   A fixed control horizon N_u of 3 control steps, so 0.09 seconds, is taken in order to decrease the computation time. Then, the remaining control inputs in the prediction horizon have the same value as the last control input of the control horizon. For the tuning of the prediction horizon N a trade-off needs to be made between on one hand a large prediction time yielding long computation times, better incorporation of future (predicted) dynamics, trajectories and constraints, and short prediction times yielding shorter computation times but less preview of the future. Furthermore it must be noted that for the MPC to make a good state prediction over the prediction horizon, the prediction model used should approximate the actual helicopter dynamics sufficiently. When a linear model is used and the helicopter state is too far away from the linearization point or the helicopter dynamics is too nonlinear, the closed-loop performance of the linear MPC controller will degrade. Therefore, when the prediction horizon is large, which should normally give better closed-loop performance, now the state will deviate more from the trim point and the linear state prediction will accumulate error. Therefore, larger prediction horizons will degrade the closed-loop performance instead of improving it due to possible model errors. From trial and error it was found that a prediction horizon of 5 time steps, so 0.15 seconds, yields reasonable computation times and good cross-coupling reduction performance. For a tracking task this is a rather small prediction horizon. However, the task of keeping the tracked state constant at its trim value is rather simple which makes it possible to have such a small prediction horizon.

Weight   The only weight that needs to be tuned in this tracking task is the diagonal matrix Q. It was chosen to only track the off-axis attitudes depending on the cross-coupling requirement that is simulated. All attitudes are equally important so they are given equal weights. For example, when a roll due to pitch requirement is simulated, an input is given in θ_{1s} in order to excite the pitch axis. Then, the objective of the MPC controller is to keep both the roll and yaw angle constant at its trim value and leave the pitch axis free. For this example Q will be equal to $\text{diag}(0,0,0,0,0,0,1,0,1,0,0,0,0,0)$.

7.2.5. the Complete MPC Formulation

To summarize the MPC controller used in the cross-coupling simulations and the sensitivity analysis simulations, the complete MPC optimization problem is presented in Equation 7.7 including the objective function that will be minimized, the prediction model of the helicopter and the input constraints. Here, $\bar{u}_k = [u_k, u_{k+1}, ..., u_{k+N-1}]$ is the control input sequence along the prediction horizon and $\bar{x} = [x_{k+1}, ..., x_{k+N}]$ is the predicted state trajectory along the prediction horizon. The optimization problem will be solved in Matlab 2020b with the fmincon-function using the sequential quadratic programming as optimization algorithm which is a smooth nonlinear optimization method. For each simulation individual components can change such as the model when using LMPC or NLMPC or implementing the error from the sensitivity analysis, or the weight Q when a different cross-coupling case is tested.

$$\underset{\bar{u}_k,\, \bar{x}_k}{\text{minimize}} \quad \sum_{i=1}^{N} \left\{ \left(x_{k+i} - r_{k+1}\right)' Q \left(x_{k+i} - r_{k+1}\right) \right\}$$

$$\begin{aligned}
\text{subject to:} \quad & x_{k+i} = f(x_{k+i-1}, u_{k+i-1}) && \text{for } i = 1, 2, \ldots, N \\
& u_{min} < u_{k+i} < u_{max} && \text{for } i = 0, 1, \ldots, N - 1 \\
& |u_{k+i} - u_{k+i-1}| < \Delta u_{max} && \text{for } i = 0, 1, \ldots, N - 1 \\
\text{with:} \quad & x = [u \; v \; w \; p \; q \; r \; \psi \; \theta \; \phi \; x \; y \; z \; \lambda_0 \; \lambda_{0_{tr}}]' \\
& u = [\theta_0 \; \theta_{1s} \; \theta_{1c} \; \theta_{0_{tr}}]'
\end{aligned} \tag{7.7}$$

7.3. The PID Controller

In order to be able to compare the performance of the MPC controller with a controlled helicopter, a simple Proportional–Integral–Derivative (PID) controller is implemented. This PID controller uses control rules based on the error between the reference state and the actual state, the integral of this error and the gradient of this error. For the cross-coupling simulations, only the attitude of the helicopter needs to be controlled. Therefore, the PID rules, which can be seen in Equation 7.8, are only implemented to θ_{1s_0}, θ_{1c} and $\theta_{0_{tr_0}}$ [22]. Here, the $K_{...}$'s are the gains that need to be tuned. Furthermore, the integral term in these PID rules is taken in discrete time over an interval of $t - 5\Delta t$ to t where t is the current time. As can be seen, the inputs are solely dependent on the on-axis tracking error e.g. θ_{1s} depends on $\theta - \theta_{ref}$ only.

Similar to the MPC controller, only the relevant DOFs will be tracked in a simulation. The inputs for the uncontrolled DOFs are then set to the trim value instead of applying the PID rule. Furthermore, in MPC the calculated control input is automatically constraint to their physical boundaries. However, PID doesn't have this ability to implement constraints in the control algorithm. Therefore, whenever the calculated control inputs go outside of their respective physical boundaries, the control input is limited to their maximum or minimum boundary value.

$$\theta_{1s} = \theta_{1s_0} + K_{\theta_1}(\theta - \theta_{ref}) + K_q q + K_{\theta_2} \sum_{t-5\Delta t}^{t} (\theta - \theta_{ref})\Delta t$$

$$\theta_{1c} = \theta_{1c_0} + K_{\phi_1}(\phi_{ref} - \phi) + K_p p + K_{\phi_2} \sum_{t-5\Delta t}^{t} (\phi_{ref} - \phi)\Delta t \tag{7.8}$$

$$\theta_{0tr} = \theta_{0_{tr_0}} + K_{\psi_1}(\psi - \psi_{ref}) + K_r r + K_{\psi_2} \sum_{t-5\Delta t}^{t} (\psi - \psi_{ref})\Delta t$$

In order to tune the gains, each degree of freedom was first tuned separately, with all states in the other degrees of freedom kept constant. The gains were then tuned using the Ziegler-Nichols method [100]. Here, an ultimate gain K_{ult} and ultimate period T_{ult} is determined by increasing the proportional gain until the system becomes unstable - the attitude starts oscillating with no damping. Then, the proportional, derivative and integral gains are set as a fraction of this ultimate gain and the ultimate period namely $0.6K_{ult}$, $1.2K_{ult}/T_{ult}$ and $3K_{ult}T_{ult}/40$ respectively. Some additional fine tuning based on trial and error was performed in order to obtain quasi optimal performance (minimal overshoot, fast rise-time). Once each degree of freedom was tuned separately, the full system with all DOFs enabled was tuned based on trial and error. The final gains obtained after tuning and used for the cross-coupling simulations can be found in Table 7.2 where radians as unit for the angular variables.

Table 7.2: PID gains used in the simulations.

Gain	Value [-]	Gain	Value [-]	Gain	Value [-]
K_{θ_1}	3	K_{ϕ_1}	0.55	K_{ψ_1}	16
K_{θ_2}	11.2	K_{ϕ_2}	40	K_{ψ_2}	170
K_q	0.8	K_p	-0.35	K_r	1.9

8

Cross-coupling Requirement Results

In order to evaluate the effectiveness of MPC to reduce cross-couplings when flying a helicopter, the cross-coupling requirements set out by the ADS-33 document will be tested in simulation on the BO-105 helicopter [36]. The requirements will be evaluated for the helicopter without controller, the helicopter with linear MPC applied to it, with nonlinear MPC applied to it and with a PID controller controlling the helicopter. Furthermore, these 4 control set-ups will be tested in a simulation with and without uncertainty added to the simulation model as explained in Section 7.1.1. The results of these simulations for each cross-coupling case will be presented in this chapter. Here, an elaborate example of how to calculate the cross-coupling parameter will be performed for the pitch due to roll coupling case. In order to analyze and compare the coupling reduction performance of the PID and MPC controller, an off-axis rate response analysis will be performed for pitch due roll coupling as well. Next to this, an overview and comparison of the cross-coupling results will be given. Finally, a word on the differences between the linear and nonlinear model predictive controller will be held in terms of optimization, computation speed, fidelity and performance.

There are 10 cross-coupling requirements that will be tested which are formulated in the ADS-33 in Section 3.3.9 (page 12) on interaxis coupling for hover and low speed flight and 3.4.5 (page 17) on interaxis coupling for forward flight. The hover and low speed flight requirements will be performed for hover only and the forward flight requirements will be simulated for 80 knots or 41 m/s flight speed. For all these requirements, an excitation in one of the on-axis control inputs is given after which the off-axis response will be measured by means of a predefined cross-coupling parameter that scales with the off-axis response as explained in Section 2.1.2. The cross-coupling criteria for hover and low speed flight and for forward flight that will be tested are presented below and will be explained more thoroughly in this chapter.

For hover and low speed flight:

1. Yaw due to collective for aggressive agility

2. Pitch due to roll coupling for aggressive agility

3. Roll due to pitch coupling for aggressive agility

4. Pitch due to roll coupling for target acquisition and tracking

5. Roll due to pitch coupling for target acquisition and tracking

For forward flight:

6. Pitch attitude due to collective control

   (a) Small collective inputs
   (b) Large collective inputs

7. Pitch due to roll coupling for aggressive agility

8. Roll due to pitch coupling for aggressive agility

9. Pitch due to roll coupling for target acquisition and tracking

10. Roll due to pitch coupling for target acquisition and tracking

Both time (for aggressive agility) and frequency (for target acquisition and tracking) requirements are set out in the ADS-33 as coupling handling qualities are not only task dependent but also frequency dependent as will be discussed further in Section 8.5. Therefore, the time domain criteria are valid for aggressive agility with mid- to long-term coupling responses and relatively small amplitude control inputs whereas the frequency domain criteria are valid for high precision maneuvers such as target acquisition and tracking containing short-term coupling responses.

For the time domain requirements, the control input that will be given in order to excite the on-axis response will mostly be a step input of plus or minus 10% of the control input range given one second after the simulation started. This usually leads to a significant and fast change in the on-axis attitude. In some simulation cases, which will be mentioned, the step input is smaller than the 10% change because of helicopter limits. The control input that will be given for the frequency domain requirements will be explained in Section 8.5.

8.1. Pitch due to Roll Coupling for Aggressive Agility

This section will first describe the pitch due to roll requirement for aggressive agility set by the ADS-33-E handling qualities document for hover and for forward flight. Second, an example of how the cross-coupling parameter for pitch due to roll coupling is calculated will be given in order to clarify the calculation method. Then, an off-axis rate response analysis will be performed for pitch due roll coupling as an example in order to analyze and compare the coupling reduction performance of the PID and MPC controller. Finally, the results of the simulations testing this requirement for all control set-ups will be presented.

8.1.1. Requirement

The pitch due to roll and roll due to pitch coupling requirements for aggressive agility are stated in the ADS33 document in Section 3.3.9.2 for hover and low speed flight and in Section 3.4.5.2 (page 12) for forward flight. The ADS33 states that *"The ratio of peak off-axis attitude response from trim within 4 seconds to the desired (on-axis) attitude response from trim at 4 seconds, $\Delta\theta_{pk}/\Delta\phi_4$ ($\Delta\phi_{pk}/\Delta\theta_4$), following an abrupt lateral (longitudinal) cockpit control step input, shall not exceed $\pm$ 0.25 for Level 1 or $\pm$ 0.60 for Level 2. Heading shall be maintained essentially constant."* [36]. The computation of the cross-coupling parameter can be seen in Equation 8.1.

$$
\begin{aligned}
&\text{if a step input is given at } t = 0 \text{ s}\\
&\Delta\theta_{pk} = (\max |\theta| \text{ before } t = 4 \text{ s}) - \theta_0 \\
&\Delta\phi_4 = \phi(t = 4 \text{ s}) - \phi_0
\end{aligned}
\tag{8.1}
$$

This requirement for pitch due to roll will be tested by simulating a step input in the lateral cyclic starting from trim with an increase/decrease of 10% the control input range. Both a negative and positive step input are being simulated for hover and for forward flight. The uncontrolled helicopter simulation has a PID controller applied to the tail rotor collective only in order to maintain a constant heading and eliminate the influence of the yaw rate to the pitch angle. In the controlled simulations the both the pitch and yaw angle will be controlled. The $\Delta\theta_{pk}/\Delta\phi_4$ parameter for each control configuration will be calculated and presented.

8.1.2. Simulation Results

An example of a pitch due to roll coupling simulation for the uncontrolled helicopter can be seen in Figure 8.1. Here, the longitudinal cyclic and collective input are kept constant as to simulate how the uncontrolled helicopter reacts to a step input in the lateral cyclic while maintaining constant heading. As can be seen, the roll rate responds to this input to the right by increasing to about 40 deg/s over 5 seconds. This induces the helicopter to roll to the right. As a secondary response, also the pitch rate increases to about 20 deg/s inducing the helicopter to pitch up. The cross-coupling parameter is then calculated as the ratio of off-axis response to on-axis input using Equation 8.1. With a $\Delta\theta_{pk}$ of 17.7 and a $\Delta\phi_4$ of 39.6, a $\Delta\theta_{pk}/\Delta\phi_4$ of 0.45 was obtained.

In Figures 8.2 and 8.3 one can see the cross-coupling parameter results of the pitch due to roll requirement simulations for hover and forward flight (80 knots) respectively for a positive and a negative lateral cyclic
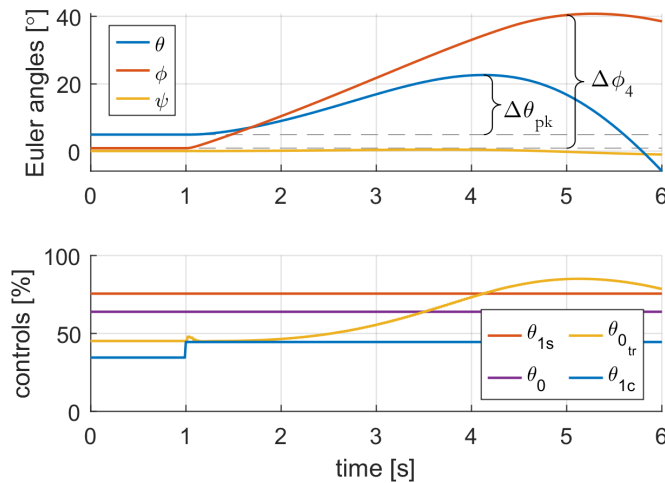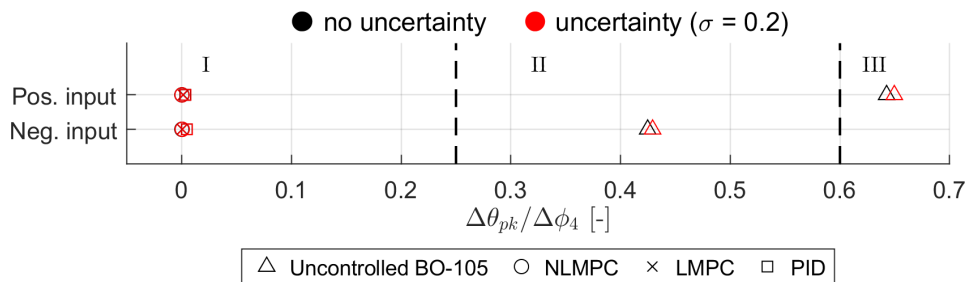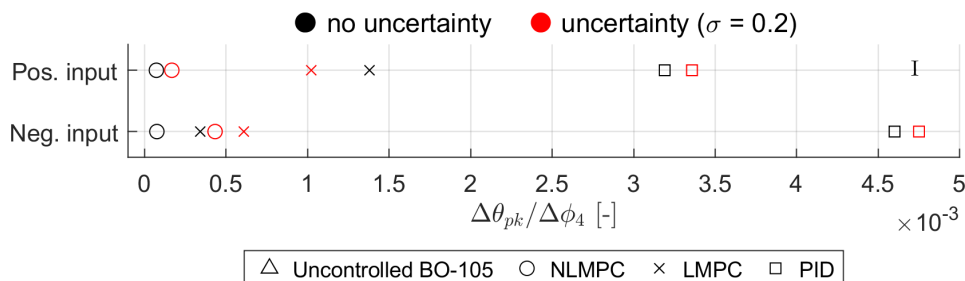
Figure 8.1: Pitch due to roll requirement simulation of the uncontrolled helicopter for 80 knots for a positive (right) lateral cyclic step input.

input. The exact numbers of the cross-coupling parameter can be found in Table 8.1. Some example simulations of the uncontrolled helicopter and LMPC controlled helicopter can be seen in Appendix C in Figure C.3 and C.4. Both for hover and forward flight it can be seen that the cross-coupling parameter is reduced significantly when the helicopter is being controlled, going from level 3/2 to level 1 with plenty of margin. When zooming in to 10^{-3} to see the results of the controlled cases in Figures 8.2 and 8.3 (b), one can see that NLMPC reduces the cross-couplings the most with shortly after that LMPC. The PID controller also performs great but cannot surpass the MPC performance for both hover and forward flight. It can also be seen that the uncertainty doesn't seem to have much of effect to the cross-coupling reduction performance in all set-ups. However, it is remarkable that for the LMPC set-up in hover, the performance with uncertainty is better than the performance without uncertainty. This can be explained by the fact that the disturbance in the model causes a disturbance in the roll rate which in this case induces the roll angle over time to be larger than the roll angle of the simulation without uncertainty. Therefore, the roll angle measured at 4 seconds after the step input will be larger causing the cross-coupling parameter to be lower.

(a) Overview for positive and negative lateral input.

(b) Close-up of Figure 8.2 (a).

Figure 8.2: Pitch due to roll requirement results for hover for a positive (right) and negative (left) lateral input.

(a) Overview for positive and negative lateral input.

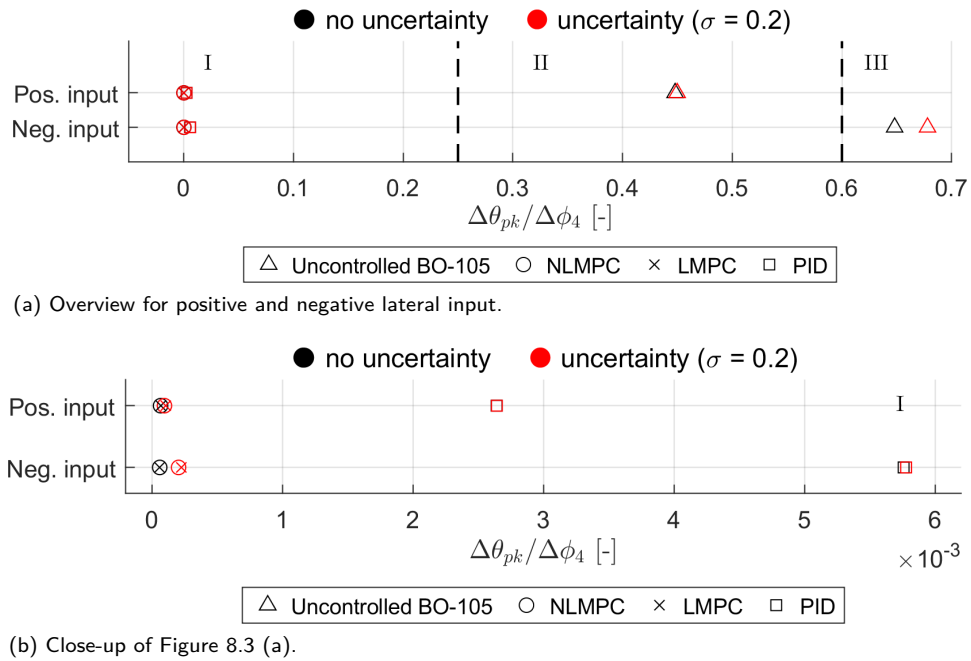(b) Close-up of Figure 8.3 (a).

Figure 8.3: Pitch due to roll requirement results for forward flight (80 knots) for a positive (right) and negative (left) lateral input.

Table 8.1: Pitch due to roll parameter $\Delta\theta_{pk}/\Delta\phi_4$ results for different helicopter flight control configurations for a positive (right) and negative (left) lateral cyclic step input for both hover and forward flight (80 knots).

Hover	BO-105		NLMPC		LMPC		PID	
σ	0	0.2	0	0.2	0	0.2	0	0.2
Pos. lateral input	0.6425	0.6496	7.291e-5	1.675e-4	0.001038	0.001023	0.003190	0.003358
Neg. lateral input	0.4247	0.4247	7.587e-5	4.329e-4	3.420e-4	6.092e-4	0.004605	0.004750

Fwd flight	BO-105		NLMPC		LMPC		PID	
σ	0	0.2	0	0.2	0	0.2	0	0.2
Pos. lateral input	0.4479	0.4498	6.674e-5	9.643e-5	6.896e-5	1.062e-4	0.002641	0.002642
Neg. lateral input	0.6480	0.6780	6.029e-5	2.047e-4	5.911e-5	2.260e-4	0.005758	0.005777

As to investigate the off-axis rate response of the different control set-ups and to indicate the difference between the PID and MPC coupling reduction behaviour, the pitch and roll rate responses for a step input in the lateral cyclic at $t = 1$ s are investigated as well. The different types of off-axis rate responses defined by Blanken et al. (1997) can be seen in Figure 8.4 (a). Here, the ideal off-axis rate response is the response with no coupling so with a rate staying as close to zero as possible. In Figure 8.4 (b) it can be seen that the uncontrolled helicopter shows an off-axis rate response with control coupling. When the controllers are introduced, the off-axis response reduces significantly, eliminating most cross-coupling effects. The PID controller shows a small and quick washed-out coupling response whereas the MPC controller reduces the off-axis rate even more and faster, showing a response with quasi no coupling.

8.2. Roll due to Pitch Coupling for Aggressive Agility

This section will first describe the roll due to pitch requirement for aggressive agility set by the ADS-33-E handling qualities document for hover and forward flight after which the results of the simulations testing this requirement for all control set-ups will be presented.
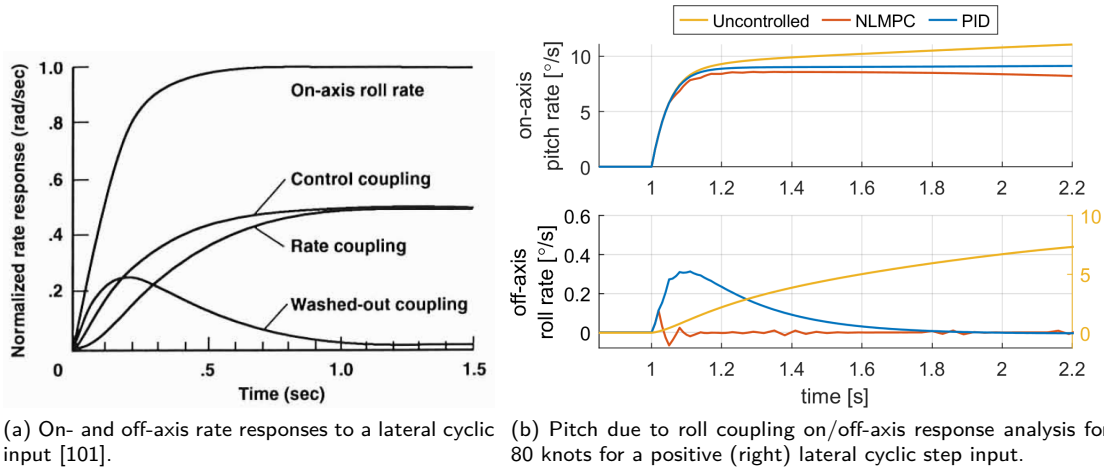
(a) On- and off-axis rate responses to a lateral cyclic input [101].

(b) Pitch due to roll coupling on/off-axis response analysis for 80 knots for a positive (right) lateral cyclic step input.

Figure 8.4: Off-axis rate response analysis.

8.2.1. Requirement

The requirement for roll due to pitch coupling for aggressive agility for both hover and forward flight is similar to the requirement for pitch due to roll and is already described in Section 8.1.1 where it was said that the parameter $\Delta\phi_{pk}/\Delta\theta_4$ should be within certain boundaries to have level 1 or 2 handling qualities. The computation of the cross-coupling parameter can be seen in Equation 8.2.

$$\text{if a step input is given at } t = 0 \text{ s}$$
$$\Delta\phi_{pk} = (\text{max } |\phi| \text{ before } t = 4 \text{ s}) - \phi_{trim} \quad (8.2)$$
$$\Delta\theta_4 = \theta(t = 4 \text{ s}) - \theta_{trim}$$

This requirement will be tested in simulation by giving a step input in the longitudinal cyclic control going from the trim value and increasing/decreasing 10% of the control input range and measuring the off-axis response by means of the handling quality parameter. It must be noted that for a negative input during hover and a positive input during forward flight, the step only decreases/increases to 2% of the control input. This is because when a larger input is given, the helicopter goes unstable. Furthermore, the uncontrolled helicopter has a PID controller in order to keep the yaw angle constant and the controlled simulation control both the yaw and roll angle. The $\Delta\phi_{pk}/\Delta\theta_4$ parameter will be computed after the simulations for each control set-up and will be presented next.

8.2.2. Simulation Results

In Figures 8.5 and 8.6 one can see the results of the roll due to pitch requirement simulations for hover and forward flight (80 knots) respectively for both a positive and negative longitudinal cyclic input. The exact numbers of the cross-coupling parameter can be found in Table 8.2. Some example simulations of the uncontrolled helicopter and LMPC controlled helicopter can be seen in Appendix C in Figures C.5 and C.6.

Again, it can be seen that the uncontrolled helicopter having level 3 (for hover) and level 2 (for forward flight) handling qualities goes to level 1 handling qualities with a large margin once a controller is applied. When zooming in to 10^{-1} and 10^{-3} for hover and forward flight respectively, it can be seen that, again, the nonlinear MPC controller reduces the roll angle response the most. After that the linear MPC controller is the controller that reduces the cross-couplings the most according to the cross-coupling parameter. The PID controller comes in last with one exception in the case with positive input for hover. Here, the PID controller is performing better than LMPC. When looking at the simulations for these cases in Figure C.6 one can see that at around 4.15 seconds in the LMPC case all controls but mainly the collective and hence tail rotor collective make a big change and start fluctuating. The collective input decreases a lot and the lateral cyclic increases whereas in the PID simulation the collective and lateral cyclic stay at more or less the same value or trend.

Multiple attempts where made in order to find the reason for this odd behaviour in the LMPC simulation such as enlarging the step input to see whether it's the constraints that somehow limit the LMPC controller,
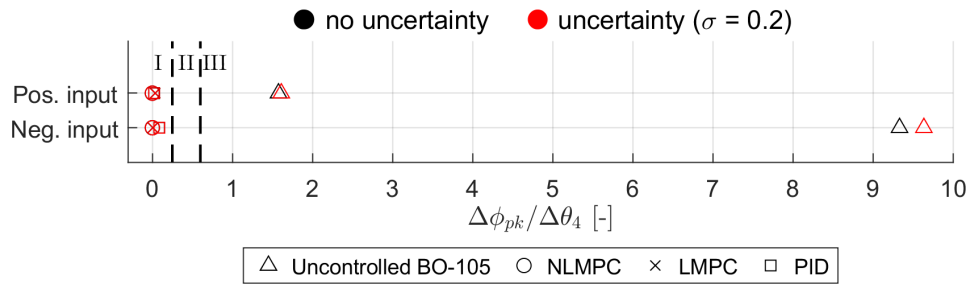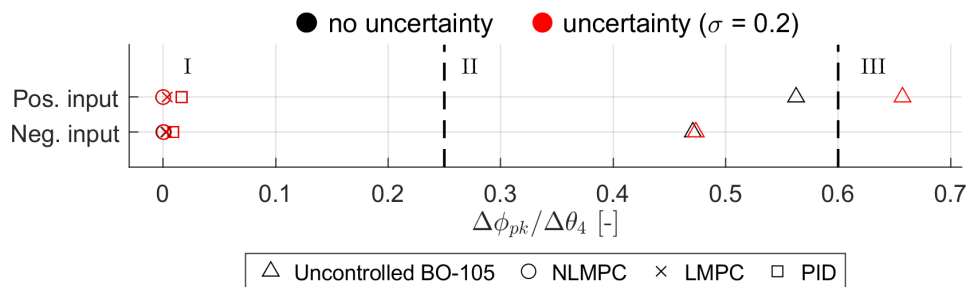
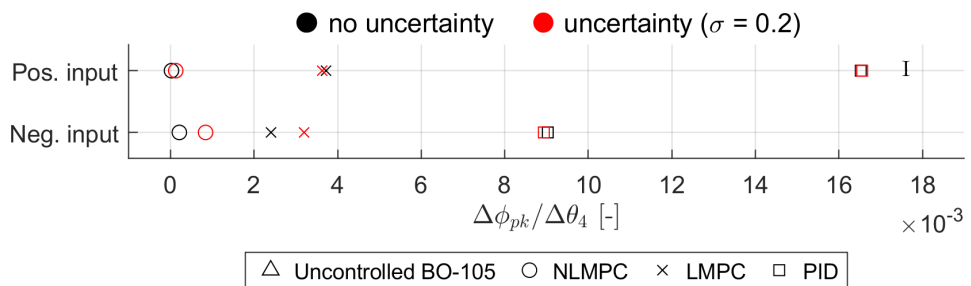(a) Overview for positive and negative longitudinal input.
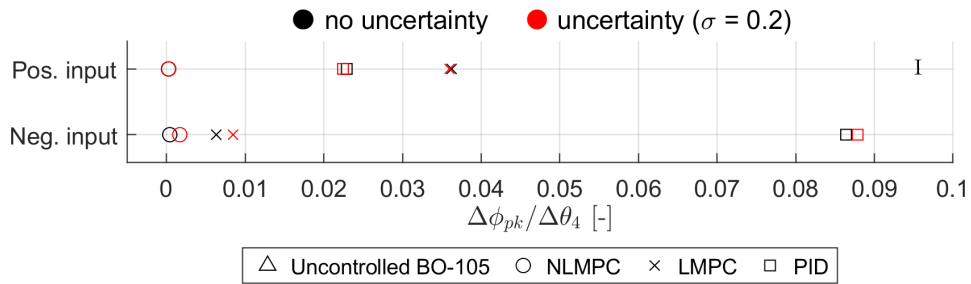
(b) Close-up of Figure 8.5 (a).

Figure 8.5: Roll due to pitch requirement results for hover for a positive (up) and negative (down) longitudinal input.

(a) Overview for positive and negative longitudinal input.

(b) Close-up of Figure 8.6 (a).

Figure 8.6: Roll due to pitch requirement results for forward flight (80 knots) for a positive (up) and negative (down) longitudinal input.

giving more tuning weight to controlling the roll angle with respect to the yaw angle, changing the length of the prediction horizon, etc. It could be seen that changing the step input or weights didn't eliminate the sudden increase/decrease in the controls. However, when shortening the prediction horizon, the cross-coupling reduction performance increased. This could be an indicating that there is a mismatch between the linear model and the nonlinear simulation. After further investigation, it was seen that at 4.15 seconds in the simulation, the linear model predicted that $\dot{p}, \dot{q} > 0$ whereas the nonlinear model states that $\dot{p}, \dot{q} < 0$. This sudden change in roll and pitch rates in the prediction model causes the controller to drastically change the optimal control inputs. This theory is confirmed by the fact that this drastic change in the controls doesn't

happen in the NLMPC simulation in Figure C.5 (b). It can be concluded that in this particular case, the linear model is not accurate enough for the LMPC controller to outperform the PID controller when reducing cross-couplings. However, it still gives level 1 handling qualities.

Table 8.2: Roll due to pitch parameter $\Delta\phi_{pk}/\Delta\theta_4$ results for different helicopter flight control configurations for a positive (up) and negative (down) longitudinal cyclic step input for both hover and forward flight (80 knots).

hover	BO-105		NLMPC		LMPC		PID	
σ	0	0.2	0	0.2	0	0.2	0	0.2
Pos. long. input	0.5626	0.6572	2.264e-5	1.247e-4	0.003722	0.003630	0.01652	0.01655
Neg. long. input	0.4709	0.4735	2.114e-4	8.380e-4	0.002405	0.003197	0.009029	0.008935
Fwd flight	BO-105		NLMPC		LMPC		PID	
σ	0	0.2	0	0.2	0	0.2	0	0.2
Pos. long. input	0.5626	0.6572	2.264e-5	1.247e-4	0.003722	0.003630	0.01652	0.01655
Neg. long. input	0.4709	0.4735	2.114e-4	8.380e-4	0.002405	0.003197	0.009029	0.008935

Lastly, it can be seen that the uncertainty in the simulation model only has a very small deteriorating influence on the cross-coupling handling qualities.

8.3. Yaw due to Collective for Aggressive Agility

This section will first describe the yaw due to collective requirement set by the ADS-33-E document after which the results of the simulations testing this requirement for all control set-ups will be presented.

8.3.1. Requirement

The handling quality requirement for yaw due to collective coupling for hover and low speed is stated in Section 3.3.9.1 (page 12) of the ADS33 document. Here it states that *"The yaw rate response to abrupt step collective control inputs with the directional controller fixed shall not exceed the boundaries specified in Figure 11. The directional controller may be free if the rotorcraft is equipped with a heading hold function. Pitch and roll attitudes shall be maintained essentially constant. ... Oscillations involving yaw rates greater than 5 deg/sec shall be deemed objectionable."* [36]. The yaw rate boundaries that are referred to can be seen in Figure 8.7. Here, r_1 is defined as the largest peak of yaw rate by magnitude between the start of the step input and 3 seconds after the step input. Furthermore, $\dot{h}(3)$ is the value of $\dot{h}$ at 3 seconds after the step input. Finally, r_3 is equal to $r(3) - r_1$ for $r_1 > 0$ and to $r_1 - r(3)$ for $r_1 < 0$ where $r(3)$ is the yaw rate at 3 seconds after the step input. The complete computation of the cross-coupling parameters can be seen in Equation 8.3.
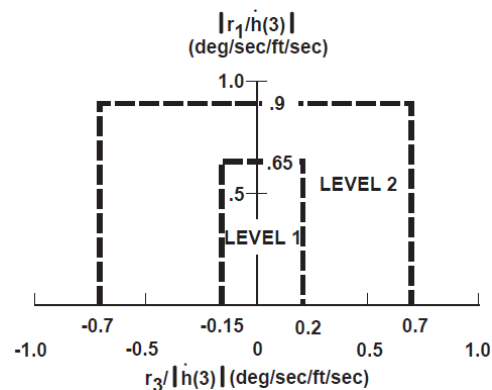

Figure 8.7: Yaw due to collective coupling requirement [36].

if a step input is given at $t = 0$ s

$\dot{h}(3) = \dot{h}(t = 3 \text{ s})$

$r_1 = \max |r|$ before $t = 3$ s   (8.3)

if $r_1 > 0 : r_3 = r(t = 3 \text{ s}) - r_1$

if $r_1 < 0 : r_3 = r_1 - r(t = 3 \text{ s})$

In order to evaluate the yaw due to collective requirement for aggressive agility, simulations are performed for the different control and model configurations. In the simulation the helicopter is trimmed in hover when a step input at t = 1 s is given to the collective. Both a positive and a negative step input are being evaluated. Here, the negative step input starts at the hover trim value of 14.4 deg and goes down 10% of the collective input range namely to 12.8 deg whereas the positive step input goes to 16.0 deg. In the set-ups where the helicopter is being controlled by either the MPC or the PID controller, not only the yaw angle but also the pitch and roll angle are controlled. In the set-up where the helicopter is not controlled, the pitch and roll angle are still controlled with a PID controller in order to only measure the yaw due to collective and not the response of the yaw angle to the varying pitch and roll angles. Once the simulation is finished, the $|r_1/\dot{h}(3)|$ and $r_3/|\dot{h}(3)|$ parameters are calculated.

8.3.2. Simulation Results

Figure 8.8 shows the results of the yaw due to collective requirement simulations for hover for both a positive and negative collective input. The exact numbers of the requirement parameters can be found in Table 8.3. Some example simulations that were performed to get to these results can be seen in Appendix C. It can be seen that the handling qualities of the uncontrolled helicopter can be greatly improved by introducing a controller. For a negative collective step input (Figure 8.8 (b)), both the (N)LMPC and PID controllers can reduce both handling quality parameters drastically to around 0.05 and -0.05 deg/s/ft/s for respectively $|r_1/\dot{h}(3)|$ and $r_3/|\dot{h}(3)|$ for the $\sigma = 0$ case hence without uncertainty. When the uncertainty is introduced to the simulation model, the results of the parameters are slightly larger but still all remain in the level 1 handling quality zone. It must also be noted that the $r_3/|\dot{h}(3)|$ parameters seems to be the limiting parameter as the results are closest to this level 1 boundary.
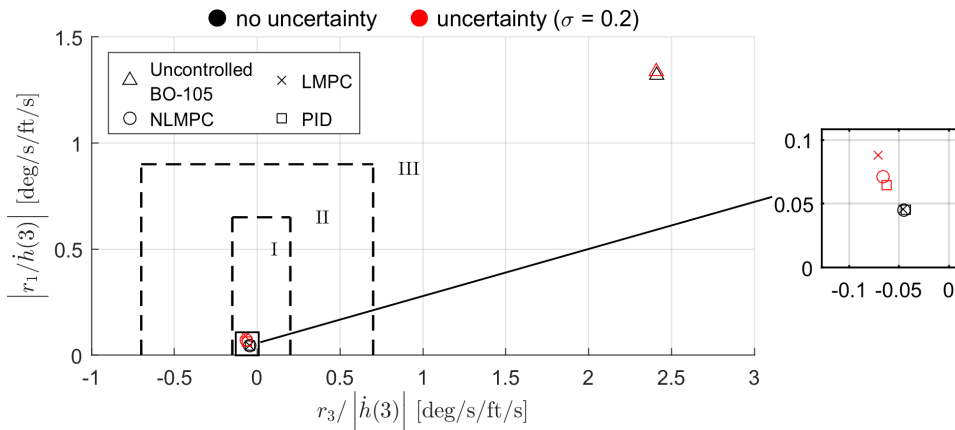
Table 8.3: Yaw due to collective requirement parameters of different helicopter flight control configurations for a positive (up) and negative (down) collective step input (0 knots).

Pos. collective input	BO-105		NLMPC		LMPC		PID	
σ	0	0.2	0	0.2	0	0.2	0	0.2
$\left|r_1/\dot{h}(3)\right|$ [deg/s/ft/s]	1.5677	1.6092	0.0464	0.1372	0.0455	0.1420	0.0490	0.0874
$r_3/\left|\dot{h}(3)\right|$ [deg/s/ft/s]	2.9184	2.9863	-0.0465	-0.1550	-0.0454	-0.1657	-0.0480	-0.0699

Neg. collective input	BO-105		NLMPC		LMPC		PID	
σ	0	0.2	0	0.2	0	0.2	0	0.2
$\left|r_1/\dot{h}(3)\right|$ [deg/s/ft/s]	1.3199	1.3373	0.0450	0.0712	0.0457	0.0881	0.0453	0.0645
$r_3/\left|\dot{h}(3)\right|$ [deg/s/ft/s]	2.4108	2.4087	-0.0451	-0.0661	-0.0459	-0.0710	-0.0432	-0.0624

The positive collective step input simulations show similar results for the case without uncertainty. However, when the uncertain error is introduced, the results of the linear and nonlinear MPC controllers are both located just over the border of the level 1 boundary. Nevertheless, the result of the PID controller for $\sigma = 0.2$ remains in level 1. This rather large performance difference can be explained by the fact that the MPC uses the prediction model of the helicopter which now has a mismatch with the disturbed simulation model whilst the PID controller does not rely on a model. Moreover, the uncertainty is applied to the thrust coefficient which is directly related to the collective input making this cross-coupling most vulnerable to the mismatch. Furthermore, when the positive input is given the thrust of the helicopter is largest making the disturbance in thrust coefficient have more effect explaining why this only happens in the positive input case. This performance difference because of the prediction model mismatch can also be confirmed by the yaw rate response of the PID and LMPC simulations in Figures C.2 (a) and (b) as r in the LMPC simulations is
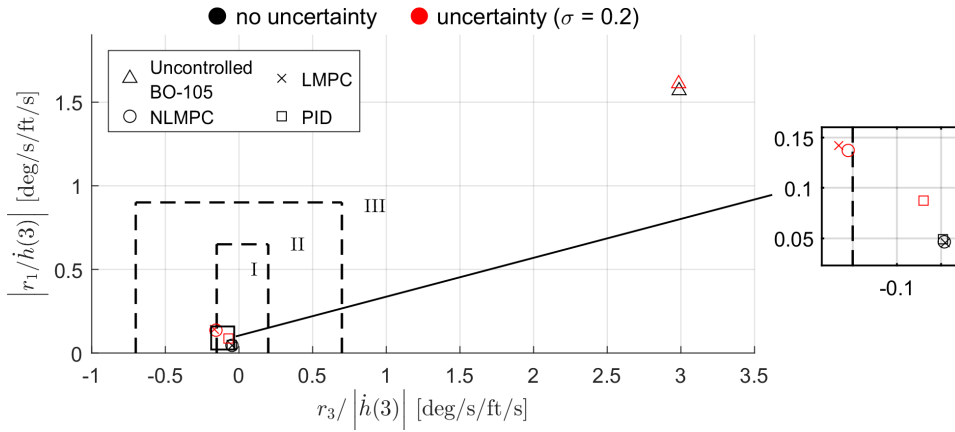
(a) Positive (up) collective step input.

(b) Negative (down) collective step input.

Figure 8.8: Yaw due to collective requirement results for hover.

similar to the response of the PID but with slightly larger values.

8.4. Pitch due to Collective Coupling

This section will first describe the pitch due to collective requirement for forward flight set by the ADS-33-E handling qualities document for both small and large collective inputs after which the results of the simulations testing this requirement for all control set-ups will be presented.

8.4.1. Requirement

The requirement for pitch due to collective coupling holds only for forward flight and is split in a requirement for small collective inputs (<20% rotor torque change) and large collective input (>20% rotor torque change) in Section 3.4.5.1 (page 17) of the ADS-33. For small collective inputs it says that *"the peak change in pitch attitude from trim, $\Delta\theta_{pk}$, occurring within the first 3 seconds following a step change in collective causing less than 20% torque change, shall be such that the ratio $\left|\Delta\theta_{pk}/\Delta n_{z_{pk}}\right|$ is no greater than 1.0 deg/ft/sec^2, where $\Delta n_{z_{pk}}$ is the peak incremental normal acceleration from 1 g flight."* [36]. For large collective inputs, the ratio $\left|\Delta\theta_{pk}/\Delta n_{z_{pk}}\right|$ should be no greater than 0.5 deg/ft/sec^2 for a positive collective input and no greater than 0.25 deg/ft/sec^2 for negative collective inputs. The complete computation of the cross-coupling parameter can be seen in Equation 8.4.

$$\text{if a step input is given at } t = 0 \text{ s}$$
$$\Delta\theta_{pk} = (\max |\theta| \text{ before } t = 3 \text{ s}) - \theta_{trim}$$
$$\Delta n_{z_{pk}} = (\max |\dot{w}| \text{ before } t = 3 \text{ s}) - \dot{w}_{trim} \tag{8.4}$$

This requirement will be tested in simulation by giving a step input of 3% (for small input) and 10% (for large input) increase/decrease in collective input, respectively corresponding to a rotor torque change smaller than 20% the rotor torque and a rotor torque change larger than 20% the rotor torque without exceeding the helicopter limits. Furthermore the uncontrolled helicopter simulation has a PID controller applied to the roll and yaw angle in order to solely measure the pitch due to collective and not the influences of the roll and yaw angle. The controlled simulations control pitch, roll and yaw. The $\left|\Delta\theta_{pk}/\Delta n_{z_{pk}}\right|$ parameter will be computed after the simulations for each control set-up and will be presented next.

8.4.2. Simulation Results

In Figures 8.9 and 8.10 one can see the results of the pitch due to collective requirement simulations for small and large collective inputs respectively and for both positive and negative collective inputs. The exact numbers of the cross-coupling parameter can be found in Table 8.4. Some example simulations of the uncontrolled helicopter and LMPC controlled helicopter can be seen in Appendix C in Figure C.7.

It can be seen that the uncontrolled helicopter has level 3 handling qualities for all cases without uncertainty. Furthermore, when applying a controller to the helicopter the handling qualities go to level 1 with a large margin for both small and large inputs. When zooming in it can be seen that the nonlinear and linear MPC parameters overlap and are lower, hence better at reducing the cross-couplings, than the parameter for the PID controller.

What is remarkable about these simulations is that the disturbed simulation gives, in every case, significantly better cross-coupling reduction performance according to the $\left|\Delta\theta_{pk}/\Delta n_{z_{pk}}\right|$ parameter. This can be explained by the fact that the uncertainty is added to the thrust coefficient which is mainly active in the z-direction and thus majorly influences $\dot{w}$ hence $n_{z_{pk}}$. The random behaviour of the uncertainty that changes each time step also causes the normal acceleration to change every time step yielding a very large $\Delta n_{z_{pk}}$. For example for the nonlinear controlled, small, positive input case, the maximum change in $\dot{w}$ for the undisturbed simulation is ± 1.2 ft/s^2 whereas the maximum change for the disturbed simulation is ± 5 ft/s^2 causing the value of the parameter to be much smaller. Therefore, in this cross-coupling case the cross-coupling parameter does not give a good indication of the off-axis response compared to on-axis input. Or at least, the disturbed cases cannot be compared to the undisturbed cases. Still the same proportions can be seen in the disturbed results between the performance of the uncontrolled, NLMPC, LMPC and PID controlled helicopter compared to the undisturbed results.
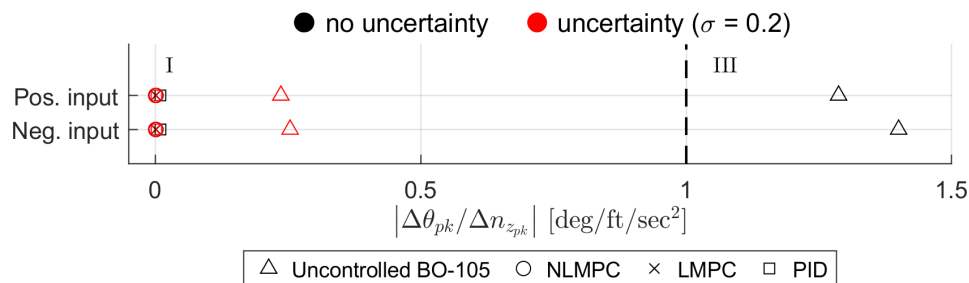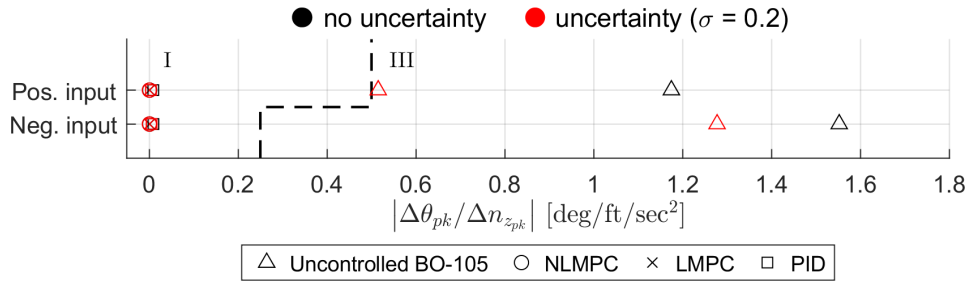

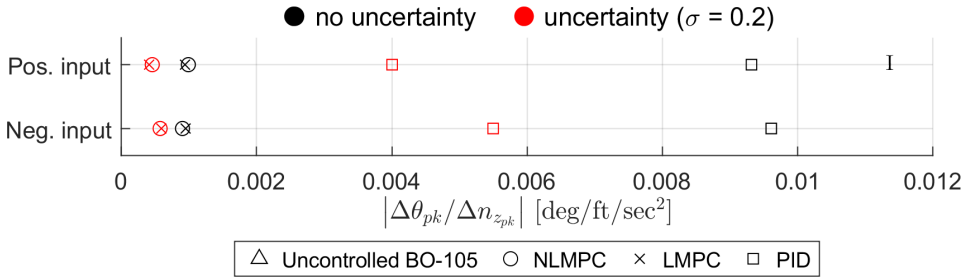(a) Overview for a small positive and negative collective input.
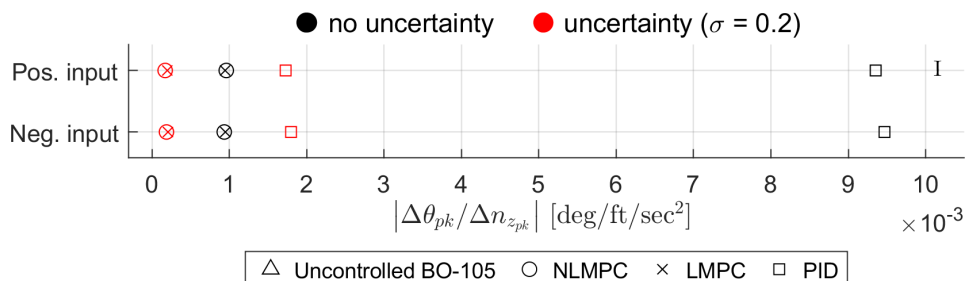
(b) Close-up of Figure 8.9 (a).

Figure 8.9: Pitch due to collective requirement results for forward flight (80 knots) for a small (<20% torque change), positive (up) and negative (down) collective input.

(a) Overview for positive and negative collective input.

(b) Close-up of Figure 8.10 (a).

Figure 8.10: Pitch due to collective requirement results for forward flight (80 knots) for a large (>20% torque change), positive (up) and negative (down) collective input.

Table 8.4: Pitch due to collective requirement $\left|\Delta\theta_{pk}/\Delta n_{z_{pk}}\right|$ results for a small (<20% torque change) and large (>20% torque change), positive (up) and negative (down) collective input.

Small input	BO-105		NLMPC		LMPC		PID	
σ	0	0.2	0	0.2	0	0.2	0	0.2
Pos. coll. input	1.287	0.05030	9.603e-4	2.398e-5	9.457e-4	1.649e-5	0.009354	3.519e-4
Neg. coll. input	1.400	0.06489	9.343e-4	2.346e-5	9.486e-4	2.500e-5	0.009468	3.543e-4

Large input	BO-105		NLMPC		LMPC		PID	
σ	0	0.2	0	0.2	0	0.2	0	0.2
Pos. coll. input	1.174	0.02784	9.904e-4	6.820e-5	9.406e-4	6.989e-5	0.009316	6.244e-4
Neg. coll. input	1.552	0.1696	9.037e-4	9.680e-5	9.500e-4	5.425e-5	0.009609	5.449e-4

8.5. Pitch due to Roll and Roll due to Pitch Coupling for Target Acquisition and Tracking

This section will first describe the frequency domain pitch due to roll and roll due to pitch requirement for target acquisition and tracking set by the ADS-33-E handling qualities document for hover and forward flight after which the results of the simulations testing this requirement for all control set-ups will be presented.

8.5.1. Requirement

First a word will be held on the difference between the frequency and time domain requirement on pitch due to roll and roll due to pitch coupling and the need for both of them. After this, the actual requirement will be explained. Next, the method to find the pitch and roll bandwidth and neutral stability will be presented. Finally, it will be explained how the p/q and q/p cross-coupling parameters are generated.

Need for a Frequency Requirement Both time and frequency requirements are set out in the ADS-33 for pitch and roll coupling as coupling handling qualities are not only task dependent but also frequency

dependent. For example, "A pilot may be less tolerant of large amounts of coupling at high frequency for an aggressive-precision task but may find the same amount acceptable for a non-aggressive low precision task." as discussed by Blanken et. al. (1997) [101]. They also state that the time domain criteria only take into account the mission task and the coupling amplitude which make them only valid for aggressive agility maneuvers. Furthermore, the four-second time window of the pitch due to roll and roll due to pitch requirements for aggressive agility is only applicable to small step inputs as large inputs cannot be safely maintained for this long amount of time. Hence, the time domain criteria can only capture the mid- to long-term responses. Therefore, the frequency domain criteria is needed in order to also capture the short-term coupling response that corresponds to high precision, agile tracking tasks. Furthermore, the nature of the frequency domain criteria enables to easily deal with noisy data, especially since the average p/q and q/p ratios over a certain bandwidth are used.

Requirement on Average p/q and q/p   The frequency domain requirements on pitch due to roll and roll due to pitch coupling are stated in Section 3.3.9.3 (page 12) for hover and 3.4.5.4 (page 18) for forward flight of the ADS-33. The ADS-33 states that the pitch due to roll (q/p) and roll due to pitch (p/q) coupling parameters should not exceed the boundaries of Figure 8.11 where *"the average q/p and average p/q are derived from ratios of pitch and roll frequency responses. Specifically, average q/p is defined as the magnitude of pitch-due-to-roll control input (q/δ_{lat}) divided by roll-due-to-roll control input (p/δ_{lat}) averaged between the bandwidth and neutral-stability (phase = -180 deg) frequencies of the pitch-due-to-pitch control inputs (θ/δ_{lon}). Similarly, average p/q is defined as the magnitude (p/δ_{lon}) divided by (q/δ_{lon}) between the roll-axis (ϕ/δ_{lat}) bandwidth and neutral stability frequencies."* [36]. Here, the bandwidth is defined as the lesser of the phase bandwidth, which is the frequency corresponding to -135° phase, and gain bandwidth, which is the frequency corresponding to the magnitude at neutral stability with a margin of 6 dB added to it. Furthermore, the frequency response data used to calculate the average q/p and average p/q should have minimal off-axis inputs in order to minimize its effects on the to be measured variable. As the limits in Figure 8.11 are not perfectly clear, the limits for q/p will be set to be -21 dB for level 1/2 and -4 dB for level 2/3 and for p/q to -10 dB for level 1/2 and -5 dB for level 2/3.
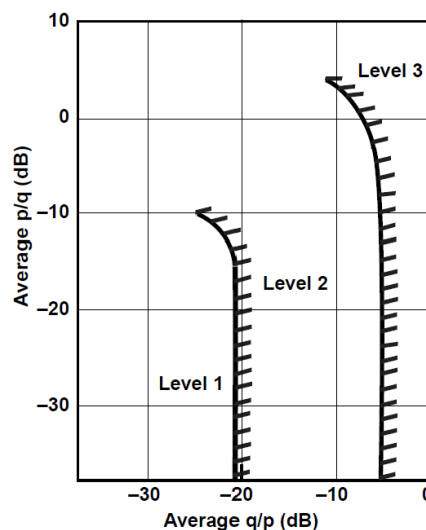

Figure 8.11: Requirement boundaries for pitch due to roll and roll due to pitch coupling for target acquisition and tracking.

Finding Pitch and Roll Bandwidth and Neutral Stability   In order to find the pitch and roll bandwidth and neutral stability frequency, the magnitude and phase of the frequency response of θ/δ_{lon} and ϕ/δ_{lat} respectively needs to be analysed. First of all, it will be assumed that the longitudinal and lateral stick displacement is equivalent to the longitudinal and lateral cyclic pith angle. Then, some best practices to obtain this frequency response were found in Padfield (2007) [31][391-396]. Here, it states that the recommended control input to measure the bandwidth is a sine wave with gradually increasing or decreasing frequency called a frequency sweep. The range of this frequency sweep should then cover the frequencies at which the helicopter is operable which usually goes from ±0.5 rad/s to ±22 rad/s and should cover at least

two times 180° phase lag. The amplitude of the sine wave is recommended to be about 10%-15% of the control range such that the roll and pitch rate stay within $\pm 20°$/s. Furthermore, it is important to maintain stability when performing the frequency sweep as the lower frequencies tend to make the uncontrolled helicopter go unstable. The duration of the sweep in a real flight test is in practice limited by the lowest frequency that needs to be covered and usually takes up 50 to 100 seconds. Since the frequency sweep is being simulated, the duration can be shorter. For the simulations, the duration will be taken as long as possible without going unstable.

So, for finding the pitch bandwidth and neutral stability frequency a simulation with a frequency sweep going from 20 rad/s to 0.5 rad/s in the longitudinal cyclic for 14 seconds for hover and 16 seconds for forward flight (80 knots) was performed with an amplitude of 10% the control range. For finding the roll bandwidth and neutral stability frequency, the sweep was applied in the lateral cyclic and took 21 seconds for hover and 18 seconds for forward flight. When this simulation is performed, the time signals of θ and θ_{1s} for pitch and ϕ and θ_{1c} for roll are being frequency analyzed. First of all, the discrete Fourier transform is taken of these time signals by means of the fast Fourier transform algorithm. Then, the response signal is divided by the input signal and the phase and gain are extracted and plotted in a one-sided frequency plot. From these plots, the gain and phase bandwidths and neutral stability frequencies are determined.

Calculating p/q and q/p   To calculate the pitch due to roll q/p and roll due to pitch p/q coupling parameters another frequency sweep is taken from 20 rad/s tot 0.5 rad/s in respectively the lateral cyclic and longitudinal cyclic input while measuring the pitch and roll response. For the uncontrolled case, the yaw angle will be controlled to be constant by a PID controller in order to reduce the effect of the changing yaw angle to the pitch-roll coupling. The controlled cases will control both the yaw angle and the off-axis angle. After the simulation, the fast Fourier transform is taken of the time signals of p and q and the output signal is divided by the input signal in order to obtain q/p for the pitch due to roll coupling simulation and p/q for the roll due to pitch coupling simulation in a single-sided frequency plot. Finally, the linear average of the magnitude of p/q and q/p between, respectively, the roll and pitch bandwidth and neutral stability frequency is taken in order to arrive at the final p/q and q/p coupling parameters.

8.5.2. Simulation Results

First, the results for finding the pitch and roll bandwidth and neutral stability frequency will be presented. After this, the average p/q and q/p parameters for different configurations will be shown and discussed.

Finding Pitch Bandwidth and Neutral Stability Frequency   Frequency response plots of pitch due to pitch (θ/θ_{1s}) were generated for hover and forward flight of a frequency sweep simulation in the longitudinal cyclic input in order to calculate the bandwidth and neutral stability of the pitch-axis. The simulation for the pitch-axis bandwidth for hover can be found in Appendix C in Figure C.8 (a).

As can be seen in the frequency response plot of θ/θ_{1s} for hover in Figure 8.12 (a), the neutral stability frequency at 180° is 4.78 rad/s. At this frequency, θ/θ_{1s} has a magnitude of 6.4 dB. The gain bandwidth is then defined as the frequency at 12.4 dB which is 4.29 rad/s. Furthermore, the phase bandwidth is defined as the frequency at 135° phase and is equal to 2.16 rad/s. Hence, a pitch-axis bandwidth of 2.16 rad/s is found for hover as this is the smallest of the phase and gain bandwidth.

Furthermore it can be seen in Figure 8.12 (b) for forward flight that the neutral stability frequency at 180° is 3.44 rad/s for pitch. At this frequency, θ/θ_{1s} has a magnitude of 17.3 dB. The gain bandwidth is then defined as the frequency at 23.3 dB which is 2.44 rad/s. Furthermore, the phase bandwidth is defined as the frequency at 135° phase and is equal to 3.07 rad/s. Hence, a pitch-axis bandwidth of 2.44 rad/s is found for forward flight as this is the smallest of the phase and gain bandwidth. The final pitch bandwidth and neutral stability frequency for hover and forward flight can be found in Table 8.5.

Finding Roll Bandwidth and Neutral Stability Frequency   Frequency response plots of roll due to roll (ϕ/θ_{1c}) were generated for hover and forward flight of a frequency sweep simulation in the lateral cyclic input in order to calculate the bandwidth and neutral stability of the roll-axis. The simulation for the roll-axis bandwidth for hover can be found in Appendix C in Figure C.8 (b).

As can be seen in the frequency response plot of ϕ/θ_{1c} for hover in Figure 8.13 (a), the neutral stability frequency at 180° is 4.27 rad/s. At this frequency, ϕ/θ_{1c} has a magnitude of 12.0 dB. The gain bandwidth is then defined as the frequency at 18.0 dB which is 1.72 rad/s. Furthermore, the phase bandwidth is defined
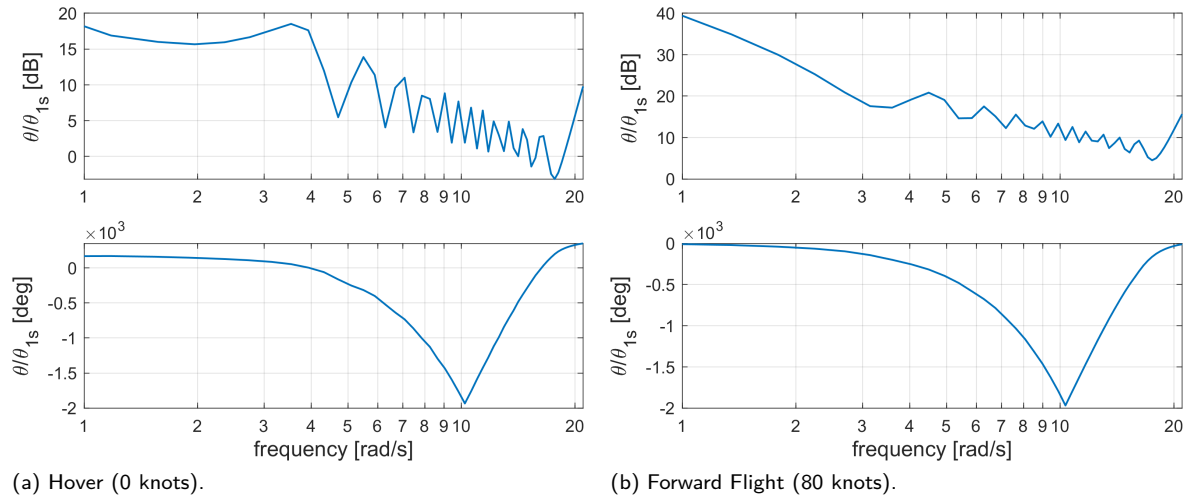
(a) Hover (0 knots).

(b) Forward Flight (80 knots).

Figure 8.12: Magnitude and phase of frequency response of θ/θ_{1s} for hover and forward flight (80 knots).

as the frequency at 135° phase and is equal to 4.00 rad/s. Hence, a roll bandwidth of 1.72 rad/s is found for forward flight as this is the smallest of the phase and gain bandwidth.
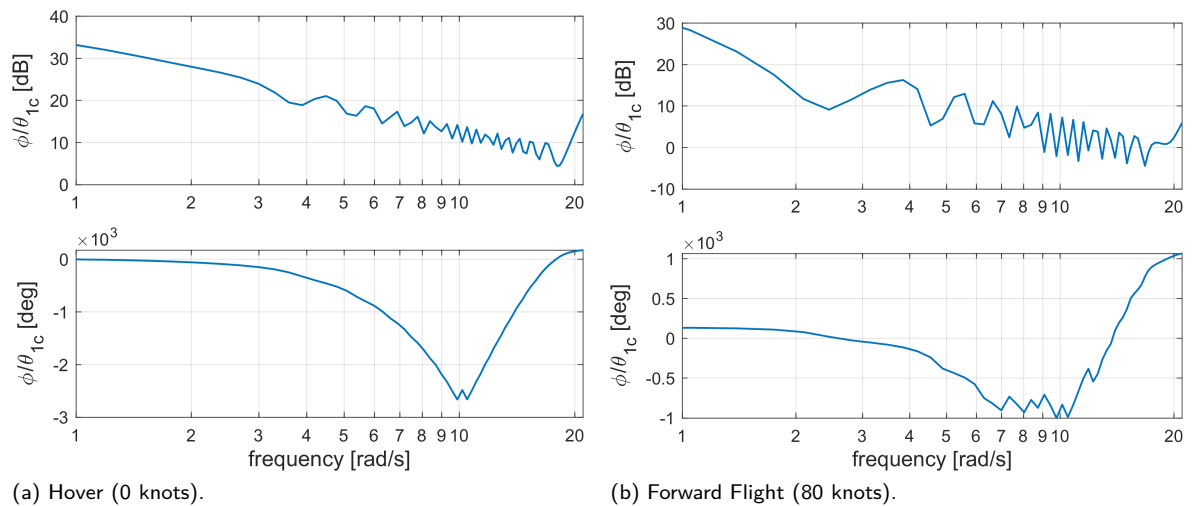

(a) Hover (0 knots).

(b) Forward Flight (80 knots).

Figure 8.13: Magnitude and phase of frequency response of ϕ/θ_{1c} for hover and forward flight (80 knots).

Furthermore it can be seen in Figure 8.13 (b) for forward flight that the neutral stability frequency at 180° is 3.22 rad/s. At this frequency, θ/θ_{1s} has a magnitude of 22.4 dB. The gain bandwidth is then defined as the frequency at 28.4 dB which is 1.91 rad/s. Furthermore, the phase bandwidth is defined as the frequency at 135° phase and is equal to 2.88 rad/s. Hence, a pitch-axis bandwidth of 1.91 rad/s is found for hover as this is the smallest of the phase and gain bandwidth. The final roll bandwidth and neutral stability frequency for hover and forward flight can be found in Table 8.5.

Final Average p/q and q/p Results   In Figure 8.14 one can find the average p/q and q/p parameter results for different controller configurations for both hover and forward flight. The exact numbers of the parameters can be found in Table 8.6. Some example simulations of the uncontrolled helicopter and LMPC controlled helicopter can be seen in Appendix C in Figures C.10 and C.9.

It can be seen that the uncontrolled helicopter has handling qualities of level 2 for hover and level 3, at the border of level 2 for forward flight. When a controller is added to the helicopter the handling qualities go to level 1. The PID controller brings the amount of cross-coupling back to around -30 dB for both pitch due to roll and roll due to pitch coupling. However, for hover the MPC controllers can bring the p/q and

Table 8.5: Pitch and roll bandwidth and neutral stability frequency results compared to reference results.

	BO-105 (0 kn)	BO-105 (80 kn)	Ref. (60 kn) [101]
Pitch bandwidth	2.16	2.44	2.16
Pitch neutral stability	4.78	3.44	3.11
Roll bandwidth	1.91	1.72	3.44
Roll neutral stability	3.22	4.27	/

(a) Hover (0 knots).   (b) Forward flight (80 knots).
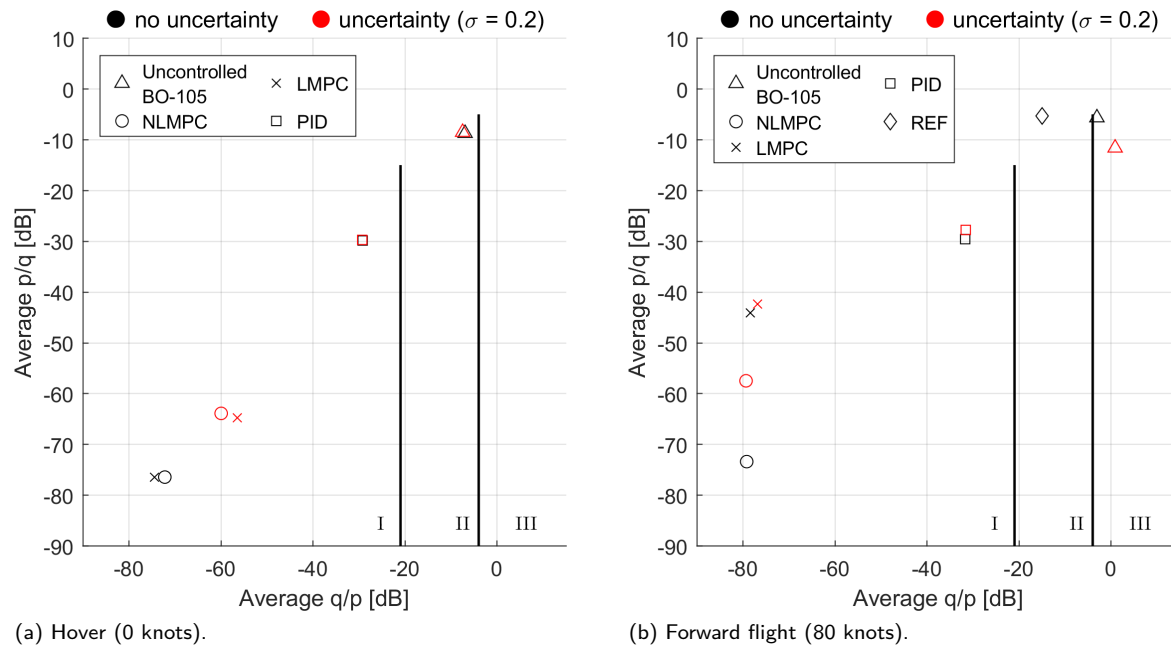
Figure 8.14: Average p/q over average q/p for various control configurations.

q/p coupling to around -75 dB. When the disturbance is introduced the coupling is still in level 1 handling qualities but has a magnitude of around -60 dB for both linear and nonlinear MPC. For forward flight, there is a bigger difference noticeable between p/q of the linear and nonlinear MPC controllers. The nonlinear MPC reduces the cross-coupling to -73 and -79 dB for q/p and q/p whereas the linear MPC only goes to -44 dB and -78 dB. Hence, for roll due to pitch the linear MPC controller performs noticeably worse than the nonlinear MPC controller. It can also be seen that when the uncertainty is introduced the p/q of the nonlinear MPC deteriorates the performance much more than the linear MPC. However, this difference of -44 dB and -73 dB and the difference when the uncertainty is applied is barely noticeable in the time domain as the magnitudes of the off-axis response are so small.

8.6. Overview of Cross-coupling Results

In this section, an overview of the handling quality levels of each control configuration for each cross-coupling case will be given. Furthermore, a comparison of the cross-coupling parameter of NLMPC with the uncontrolled helicopter and of the NLMPC and LMPC with the PID controller will be made for both with and without uncertainty by presenting the percentage increase of the cross-coupling parameter.

Overview of Handling Quality Levels   An overview of the cross-coupling handling quality level results can be seen in Table 8.7. Here, for each cross-coupling case and condition, the level of handling qualities is depicted for the uncontrolled, NLMPC and LMPC controlled and PID controlled helicopter.

It can be seen that the uncontrolled helicopter mostly has level 3 or 2 handling qualities with the exception of the pitch due to collective case with uncertainty. Here, the cross-coupling with disturbance is better than the cross-coupling without due to an incompatibility between the nature of the disturbance and the cross-

Table 8.6: Average p/q and q/p for different control configurations for hover (0 knots) and forward flight (80 knots).

Hover	BO-105		BO-105		NLMPC		LMPC		PID	
σ	0	0.2	0	0.2	0	0.2	0	0.2	0	0.2
Average p/q	/	/	-8.7	-8.5	-76.4	-63.9	-76.5	-64.8	-29.8	-29.7
Average q/p	/	/	-7.0	-7.5	-72.2	-60.0	-74.5	-56.5	-29.2	-29.3

Forward flight	BO-105 [101]		BO-105		NLMPC		LMPC		PID	
σ	0	0.2	0	0.2	0	0.2	0	0.2	0	0.2
Average p/q	-5.3	/	-5.6	-11.6	-73.4	-57.5	-44.1	-42.4	-29.6	-27.7
Average q/p	-15.0	/	-3.1	0.9	-79.2	-79.4	-78.4	-76.9	-31.7	-31.6

coupling parameter ratio. Once a controller is introduced, the handling qualities are improved to level 1. This indicates that all controllers succeed very well at reducing the cross-couplings in order to have good handling qualities. Even with uncertainty added to the simulation model, the controllers are able to obtain level 1 handling qualities. The only exception is the NLMPC controller for the yaw due to collective case for a positive (up) collective input which obtained level 2 handling qualities with the uncertainty. This will be further explained when looking at Table 8.9.

Table 8.7: Overview of the cross-coupling handling quality level results.

Cross-coupling case	Condition	BO-105 $\sigma=0$	BO-105 $\sigma=0.2$	NLMPC $\sigma=0$	NLMPC $\sigma=0.2$	LMPC $\sigma=0$	LMPC $\sigma=0.2$	PID $\sigma=0$	PID $\sigma=0.2$
Pitch d.t. roll	0 kn, +ve input	III	III	I	I	I	I	I	I
	0 kn, -ve input	II	II	I	I	I	I	I	I
	80 kn, +ve input	II	II	I	I	I	I	I	I
	80 kn, -ve input	III	III	I	I	I	I	I	I
Roll d.t. pitch	0 kn, +ve input	III	III	I	I	I	I	I	I
	0 kn, -ve input	III	III	I	I	I	I	I	I
	80 kn, +ve input	II	III	I	I	I	I	I	I
	80 kn, -ve input	II	II	I	I	I	I	I	I
Yaw d.t. collective	+ve input	III	III	I	II	I	II	I	I
	-ve input	III	III	I	I	I	I	I	I
Pitch d.t. collective	small, +ve input	III	I	I	I	I	I	I	I
	small, -ve input	III	I	I	I	I	I	I	I
	large, +ve input	III	III	I	I	I	I	I	I
	large, -ve input	III	III	I	I	I	I	I	I
Pitch d.t. roll for TA & T	0 kn	II	II	I	I	I	I	I	I
	80 kn	III	III	I	I	I	I	I	I
Roll d.t. pitch for TA & T	0 kn	II	II	I	I	I	I	I	I
	80 kn	II	I	I	I	I	I	I	I

Comparison of the Cross-coupling Parameter ($\sigma = 0$) In Table 8.8 a comparison of the cross-coupling parameters in percentage increase can be seen for the simulations without uncertainty. First of all, the NLMPC results are compared to the uncontrolled helicopter results where a negative percentage indicates a reduction of cross-couplings. Next, the NLMPC and LMPC are compared to the PID controller by indicating how much percent the MPC cross-coupling parameter is increased with respect to the PID cross-coupling parameter. Here, the positive values indicate the PID controller is better at reducing cross-couplings than MPC and are indicated in red. Furthermore, it must be noted that for the yaw due to collective case, the $r_3/|\dot{h}(3)|$ parameter is used for the percentages as this was the limiting parameter in most cases.

Table 8.8: Comparison of the cross-coupling parameter results in percentage increase for the simulations without uncertainty.

Cross-coupling case	Condition	NLMPC compared to BO105 [%]	NLMPC compared to PID [%]	LMPC compared to PID [%]
Pitch d.t. roll	0 kn, +ve input	-99.99	-97.71	-56.74
	0 kn, -ve input	-99.98	-98.35	-92.57
	80 kn, +ve input	-99.99	-97.47	-97.39
	80 kn, -ve input	-99.99	-98.95	-98.97
Roll d.t. pitch	0 kn, +ve input	-99.99	-98.99	58.20
	0 kn, -ve input	-100.00	-99.54	-92.70
	80 kn, +ve input	-100.00	-99.86	-77.47
	80 kn, -ve input	-99.96	-97.66	-73.36
Yaw d.t. collective	+ve input	-98.44	-3.13	-5.42
	-ve input	-98.13	4.40	6.25
Pitch d.t. collective	small, +ve input	-99.93	-89.73	-89.89
	small, -ve input	-99.93	-90.13	-89.98
	large, +ve input	-99.92	-89.37	-89.90
	large, -ve input	-99.94	-90.59	-90.11
Pitch d.t. roll for TA & T	0 kn	-99.95	-99.29	-99.45
	80 kn	-99.98	-99.58	-99.54
Roll d.t. pitch for TA & T	0 kn	-99.96	-99.53	-99.53
	80 kn	-99.96	-99.36	-81.21

First of all, it can be seen that the NLMPC reduces the cross-coupling by about 99.9% for almost all cross-coupling cases which is remarkably high. It indicates that the off-axis response can be almost entirely eliminated by introducing the MPC controller. Furthermore, when comparing the MPC to the PID controller almost all cases have much better cross-coupling reduction than the PID controller. Reductions of about 90% and 99% better than the PID controller are achieved for NLMPC whereas the LMPC has slightly lower percentages especially for roll due to pitch.

The roll due to pitch case for hover and a positive (right) input even has the PID controller performing better than LMPC. This degradation of the LMPC performance happens because of the mismatch between the linear prediction model and nonlinear simulation model. It was found that at some point in the simulation the linear model estimates the roll and pitch rate to be of opposite sign as the actual nonlinear model causing the controls to change drastically, decreasing the cross-coupling reduction performance. Nevertheless, the handling qualities still remain far within the level 1 zone.

Next to this, also the yaw due to collective case with a negative input seems to have a better cross-coupling parameter with PID controller. Furthermore, for a positive input the cross-coupling parameter for MPC is only 3 to 5 percent better than the PID controller which is much lower than in other cases. This can be explained by the fact that this parameter relies on the yaw rate response instead of the yaw angle. It is the only cross-coupling parameter depending on the angular rate instead of attitude. Since the MPC controller is focusing solely on minimizing the attitude error, very aggressive yaw rate motions are induced causing the cross-coupling parameter to take up higher values. The PID controller is not that aggressive because of the differential term.

Comparison of the Cross-coupling Parameter ($\sigma = 0.2$) In Table 8.9 one can see the comparison of cross-coupling parameters in percentage increase for the simulations with uncertainty applied to the thrust coefficient. First of all, it can be seen that the percentages are in general only slightly lower to the percentage increase of the simulations without uncertainty. This indicates that the MPC and PID controllers are robust to this disturbance, preserving the cross-coupling reduction performance.

Again, the yaw due to collective case seems to be the case with the least reduction of cross-couplings compared to the uncontrolled helicopter which was also seen for the results without uncertainty (because of measuring the yaw rate instead of angle). With uncertainty, the handling qualities for the positive input are

Table 8.9: Comparison of the cross-coupling parameter results in percentage increase for the simulations with an uncertainty of $\sigma = 0.2$.

Cross-coupling case	Condition	NLMPC compared to BO105 [%]	NLMPC compared to PID [%]	LMPC compared to PID [%]
Pitch d.t. roll	0 kn, +ve input	-99.97	-95.01	-69.54
	0 kn, -ve input	-99.90	-90.89	-87.17
	80 kn, +ve input	-99.98	-96.35	-95.98
	80 kn, -ve input	-99.97	-96.46	-96.09
Roll d.t. pitch	0 kn, +ve input	-99.98	-98.82	60.42
	0 kn, -ve input	-99.98	-98.10	-90.39
	80 kn, +ve input	-99.98	-99.25	-78.07
	80 kn, -ve input	-99.82	-90.62	-64.22
Yaw d.t. collective	+ve input	-94.81	121.77	137.05
	-ve input	-97.26	5.85	13.72
Pitch d.t. collective	small, +ve input	-99.93	-90.12	-88.52
	small, -ve input	-99.93	-89.57	-88.49
	large, +ve input	-99.91	-88.59	-89.74
	large, -ve input	-99.96	-89.57	-89.24
Pitch d.t. roll for TA & T	0 kn	-99.76	-97.07	-95.61
	80 kn	-99.99	-99.59	-99.45
Roll d.t. pitch for TA & T	0 kn	-99.83	-98.04	-98.23
	80 kn	-99.49	-96.73	-81.39

even decreased to level 2. Also when comparing the MPC controllers to the PID controller it can be seen that the PID controller performs much better. As the disturbance is implemented in the thrust coefficient, which greatly influences the rotor torque, the yaw coupling is majorly increased by this especially for a positive collective input which only increases the thrust coefficient. With this poorly estimated main rotor torque in the MPC prediction model, the MPC controller is unable to reduce the cross-couplings in the yaw axis sufficiently. The PID controller however, which does not rely on a prediction model, is able to reduce the cross-coupling to a level 1 handling quality. A solution to this deteriorated performance of the MPC due to a highly influential disturbance is to implement robust model predictive control. This will improve the performance of the MPC to unmeasured disturbances but at the cost of decreased general performance.

8.7. Linear Compared to Nonlinear MPC

The difference between linear and nonlinear MPC in this report lies in the use of the nonlinear or linear prediction model in the MPC algorithm. The nonlinearity in the optimization scheme comes with non-convexity and hence multiple local optima and a heavier computational burden. On the other hand, also the fidelity of the model plays a big roll in the closed-loop performance as the algorithm optimizes the error between the predicted state and the reference state over the prediction horizon. Therefore, a comparison of linear MPC with nonlinear MPC in terms of the optimization, computational speed and model fidelity will be given together with an evaluation of the differences in the cross-coupling simulation results.

8.7.1. Optimization

As said before in Section 3.5.4, an optimization problem is convex if the objective function and inequality constraint functions are convex and the equality constraint functions are affine. Thus, the linear MPC problem in this report with linear prediction model and quadratic objective function with positive definite weight Q is a convex optimization problem [102]. With convex optimization comes the fact that it only has one optimal solution which is automatically the global optimum. Hence, in the open-loop optimization problem, optimality is guaranteed.

When the prediction model is nonlinear, as is the case with the nonlinear MPC in this report, the optimization becomes non-convex. This brings with it that now multiple local optima exist. Therefore, the

nonlinear optimization scheme requires an initial guess to start the optimization from and requires more complex solving algorithms. Depending on the initial value, a different local optimum can be reached. In order to find the global optimum, multiple initial values can be tried. This goes at the cost of the computation time and still does not guarantee to reach the global optimum. The inability to guarantee to reach the global optimum in an optimization scheme is called suboptimality. However, even if the outcome of the optimization is suboptimal, the controller can still be stable provided that a feasible solution exists and the controller is tuned properly (having a sufficiently long prediction horizon) or stabilizing modifications are made [61].

In Section 7.2.3 it was tested how much the optimal solution and the closed-loop performance would increase when trying out multiple initial values in the NLMPC algorithm. Multiple initial values were tried in the same time step and compared to each other to then finally use the solution with the lowest cost for a yaw due to collective coupling simulation. However, this goes at the cost of a much longer computation time as the same optimization has to take place multiple times instead of once. It was seen that indeed a more optimal solution could be found when trying 8 different initial values compared to only trying the trim point as initial value. However, the decrease in tracking error was extremely small (< 1 degree over 5 seconds). Hence, the loss in performance because of suboptimality is negligible for the cross-coupling cases.

8.7.2. Computational Speed

The convexity of the linear MPC optimization problem also comes with the advantage of being able to solve the problem using linear or convex quadratic (in case of the quadratic objective function) programming with algorithms such as dual-simplex and convex interior-point method. When the problem becomes non-convex, so when the nonlinear MPC controller is used, nonlinear programming methods need to be used in order to solve the optimization problem which come with longer computation times [39]. Moreover, convex optimization methods are significantly less complex than nonlinear programming methods: in convex quadratic programming the global optimum can be found within a fixed number of iterations depending on the size of the problem whereas nonlinear programming is considered to be NP-hard according to complexity theory [102]. Furthermore, in convex optimization without constraints an explicit solution can be found by means of dynamic programming such that the optimal control input can be directly computed as a function the the initial state. This severely speeds up the computation process.

As computer power has significantly increased over the years and faster optimization algorithms are found, the computational speed gap between linear and nonlinear MPC is not as large anymore. Furthermore, other algorithms and tuning tricks exist to speed up the optimization process: neural networks can be used that mimic the behaviour of the MPC optimization [57], explicit solutions to the optimization problem can be found even for nonlinear problems [63], [103], the sampling time and prediction horizon can be tuned, the model can be reduced such that there are less variables to compute in the optimization, faster optimization algorithms such as using Pontryagin's Minimum Principle can be implemented [58], etc. However, the computation time can still be limiting as MPC needs to be applied in real-time to helicopters which have very fast dynamics. Yet, in this report the real-time application is not taken into account.

8.7.3. Model Fidelity

It is now clear that linear MPC has the advantage of having convex optimization which brings guaranteed open-loop optimality and faster, less complex optimization with it. However, when dealing with highly nonlinear systems such as helicopters the question if the linear approximation of the system has sufficient fidelity to not only have a stable but also a good performing controller arises.

As explained before in Section 7.1.2, the linearization of the nonlinear system around a trim point approximates the system at and around this trim point. The more the helicopter state deviates from the trim condition, the worse the linear approximation will be. Also, the more nonlinear the helicopter behaves at this trim condition, the worse the linear approximation will be.

For the MPC to make a good state prediction over the prediction horizon, the prediction model should approximate the actual, nonlinear helicopter dynamics sufficiently. Hence, when a linear model is used and the helicopter state is too far away from the linearization point or the helicopter dynamics is too nonlinear, the closed-loop performance of the linear MPC controller deteriorates. This was also seen in Dutka et. al. (2003) where a linear MPC controller for tracking a step in pitch had slower tracking behaviour, more overshoot and a steady-state error compared to the nonlinear MPC controller [67]. Moreover, the tracking point even further away from the trim point resulted in an unstable linear MPC controller. In order to reduce this mismatch between the linear and nonlinear model, the linearization could be updated, either online or

offline, once the current state and the linearization trim state are too far away from each other [65], [73].

Furthermore, the mismatch between linear and nonlinear does not only grow when the linearization point and the helicopter state are far away, the model mismatch error also accumulates over the prediction horizon because of the integration scheme in the dynamics of the helicopter. Therefore, larger prediction horizons will degrade the closed-loop performance instead of improving it for LMPC. However, in this research a very small prediction horizon of 0.15 seconds is used which is small enough to overcome large accumulations of error. This accumulation was also demonstrated in Section 7.1.3.

8.7.4. Reducing Cross-couplings

In the cross-coupling results in this chapter it can be seen that both linear and nonlinear MPC perform very well at reducing cross-couplings, even with an uncertainty applied in the simulation model. It must also be noticed that the performance difference between linear and nonlinear MPC for these simulations is very small. In most cases the nonlinear controller performs slightly better than the linear controller, such as for pitch due to roll and roll due to pitch for aggressive agility and roll due to pitch for tracking, or has almost similar performance as the linear controller, such as for yaw due to collective and pitch due to collective. This is an indication that the fidelity of the linear model is sufficient for the cross-coupling simulations to be used as prediction model. This can be explained by means of two reasons based on properties specific to the cross-coupling simulations. First of all, the model mismatch stays small because of the use of a very short prediction horizon which prevents the accumulation of error along the horizon. Secondly, as the reference trajectory that is tracked is the trim condition around which is linearized, the state stays relatively close to the linearization point which also limits the linear model mismatch.

There is one case, the roll due to pitch coupling case for hover with a positive input, where the linear controller performs worse than the PID controller. This was due to a linear model mismatch where the linear model predicted that $\dot{p}, \dot{q} > 0$ whereas the actual, nonlinear model states that $\dot{p}, \dot{q} < 0$, resulting in a sudden change of controls which is not present in the NLMPC and PID simulations. Nevertheless, the fidelity is still good enough to have level 1 handling qualities.

The few cases where the linear controller is slightly better than the nonlinear MPC controller can be explained by the fact that the cross-coupling parameter is being evaluated and not the actual objective of the MPC, being the tracking error. Also, the suboptimality of the nonlinear MPC controller could be (part of) the reason for the nonlinear controller to have a slightly larger cross-coupling parameter in some cases.

Overall it can be concluded that the differences in cross-coupling reduction performance between LMPC and NLMPC are so small they do not noticeably deteriorate the handling qualities and can be assumed to be non existent.

9

Sensitivity Analysis

This chapter will present a sensitivity analysis to see how sensitive and robust the MPC controller is to errors in the prediction model when reducing cross-couplings. First, the error applied to the prediction model will be introduced after which the results of each cross-coupling case will be presented. Finally, an overview and characteristics of the important derivatives will be given.

On one hand, this sensitivity analysis serves to identify, for each cross-coupling case, the important derivatives in the prediction model that require high accuracy in order to still have level 1 handling qualities. This information is important so that when designing a linear MPC controller, it is known which prediction model derivative needs to be of high accuracy for the controller to work. On the other hand, the important derivatives will be further investigated in order to find out how large the error in these derivatives can go to still have level 1 handling qualities. This information gives understanding to how sensitive these specific derivatives are to errors and to what kind of errors are most performance degrading for example, over/underestimating, changing sign, etc.

This trend of which derivatives are important and how large the errors can go in the linear prediction model can be extended to the nonlinear prediction model by linking the derivatives to its analytical expression. When linearizing the nonlinear dynamics analytically, as was done in Pavel (1996), the derivatives are linked to the helicopter parameters and coefficients which are used in the nonlinear model [1]. In this way, this information can be used for nonlinear MPC as well.

As explained in Section 7.1.1, a linear prediction model is used for the sensitivity analysis such that the error can be implemented in a structured way namely in the elements of the linear state-space model. To reduce the model mismatch between simulation model and prediction model, the linear model was used as simulation model as well. Furthermore, it must be noted that in this research only the influence of one error at a time will be investigated as to pinpoint the important derivatives. The robustness to multiple errors at the same time is beyond the scope of this thesis.

9.1. Introducing the Error in the Prediction Model

First of all, for each cross-coupling case the important derivatives will be identified by means of implementing an error, one at a time, in every derivative relevant to the cross-coupling case in the prediction model of the MPC controller. Then, similar simulations as in Chapter 8 are performed and the cross-coupling parameters are measured. Based on the change in cross-coupling parameter and if the controller still has level 1 handling qualities the derivatives which alter the handling qualities of the MPC controlled helicopter the most can be found. Once the important derivatives have been identified, they will be investigated further by varying the error that is implemented and measuring how this affects the cross-coupling parameter.

The error will be implemented in the prediction model of the MPC controller in the elements of the state matrix A and input matrix B of the linear helicopter model. More specifically, it will be implemented in the relevant elements only e.g. for yaw due to collective coupling the error will be implemented in the derivatives of the yaw acceleration so $\frac{\partial \dot{r}}{\partial u}, \frac{\partial \dot{r}}{\partial v}, \dots$ in the A matrix and $\frac{\partial \dot{r}}{\partial \theta_0}, \frac{\partial \dot{r}}{\partial \theta_{1s}}, \dots$ in the B matrix. Here, a simplified notation will be used such that for example the derivative $\frac{\partial \dot{r}}{\partial u}$ will be noted as $\dot{r}_u$. The values of the derivatives the error will be applied to can be seen in Equation 9.1 for 0 knots and Equation 9.2 for 80

knots. One may wonder how these are related to the force derivatives $X_u, Y_u, ...$ which are more commonly used when speaking of derivatives. An overview of how the elements in the A and B matrix are related to the force derivatives or static stability derivatives can be seen in Equation 2.8.

$$
\begin{bmatrix} \dot{p}_u & \dot{p}_v & \dot{p}_w & \dot{p}_p & \dot{p}_q & \dot{p}_r \\ \dot{q}_u & \dot{q}_v & \dot{q}_w & \dot{q}_p & \dot{q}_q & \dot{q}_r \\ \dot{r}_u & \dot{r}_v & \dot{r}_w & \dot{r}_p & \dot{r}_q & \dot{r}_r \end{bmatrix} = \begin{bmatrix} 1.2 & -0.1 & 0.0 & -16.3 & 3.6 & 0.4 \\ 0.1 & 0.0 & 0.0 & 1.6 & -4.0 & 0.00 \\ 0.2 & 0.2 & 0.0 & -2.3 & 0.6 & -0.9 \end{bmatrix}
$$
$$
\begin{bmatrix} \dot{p}_{\theta_0} & \dot{p}_{\theta_{1s}} & \dot{p}_{\theta_{1c}} & \dot{p}_{\theta_{0tr}} \\ \dot{q}_{\theta_0} & \dot{q}_{\theta_{1s}} & \dot{q}_{\theta_{1c}} & \dot{q}_{\theta_{0tr}} \\ \dot{r}_{\theta_0} & \dot{r}_{\theta_{1s}} & \dot{r}_{\theta_{1c}} & \dot{r}_{\theta_{0tr}} \end{bmatrix} = \begin{bmatrix} 4.1 & -17.9 & 150.3 & 8.6 \\ 0.8 & -46.7 & 4.8 & 0.0 \\ 19.2 & -2.6 & 24.0 & -21.5 \end{bmatrix}
$$

(9.1)

$$
\begin{bmatrix} \dot{p}_u & \dot{p}_v & \dot{p}_w & \dot{p}_p & \dot{p}_q & \dot{p}_r \\ \dot{q}_u & \dot{q}_v & \dot{q}_w & \dot{q}_p & \dot{q}_q & \dot{q}_r \\ \dot{r}_u & \dot{r}_v & \dot{r}_w & \dot{r}_p & \dot{r}_q & \dot{r}_r \end{bmatrix} = \begin{bmatrix} 0.1 & -0.1 & -0.2 & -17.4 & 4.5 & 0.4 \\ 0.1 & 0.0 & 0.2 & 1.5 & -4.0 & 0.0 \\ 0.0 & 0.3 & -0.2 & -2.8 & 1.5 & -1.4 \end{bmatrix}
$$
$$
\begin{bmatrix} \dot{p}_{\theta_0} & \dot{p}_{\theta_{1s}} & \dot{p}_{\theta_{1c}} & \dot{p}_{\theta_{0tr}} \\ \dot{q}_{\theta_0} & \dot{q}_{\theta_{1s}} & \dot{q}_{\theta_{1c}} & \dot{q}_{\theta_{0tr}} \\ \dot{r}_{\theta_0} & \dot{r}_{\theta_{1s}} & \dot{r}_{\theta_{1c}} & \dot{r}_{\theta_{0tr}} \end{bmatrix} = \begin{bmatrix} 4.3 & -8.7 & 159.6 & 9.0 \\ 23.5 & -49.8 & 4.6 & 0.0 \\ 4.6 & 8.4 & 21.8 & -22.5 \end{bmatrix}
$$

(9.2)

The error ϵ will be implemented to the actual derivative in a dimensionless manner as can be seen in Equation 9.3. Here, the estimated derivative D_{MPC}, so the derivative with error, will be equal to the actual derivative D_{actual} plus a fraction ϵ of the actual derivative. Hence, when the error is smaller than -1, the estimated derivative is of opposite sign as the actual derivative. When the error is in between -1 and 0, the estimated derivative is smaller in absolute value as the actual derivative, so underestimated. When the error is larger than 0, the estimated derivative is larger in absolute value than the actual derivative. An overview of how the value of the error influences the proportions between the actual and the MPC derivative can be found in Equation 9.4.

$$
D_{MPC} = D_{actual}(1 + \epsilon)
$$
(9.3)

$$
\begin{aligned}
\epsilon < -1 : & \quad \text{sgn}(D_{MPC}) = -\text{sgn}(D_{actual}) \\
\epsilon = -1 : & \quad D_{MPC} = 0 \\
-1 < \epsilon < 0 : & \quad |D_{MPC}| < |D_{actual}| \\
\epsilon = 0 : & \quad D_{MPC} = D_{actual} \\
\epsilon > 0 : & \quad |D_{MPC}| > |D_{actual}|
\end{aligned}
$$
(9.4)

In order to find out how large such an error realistically could be when modeling a helicopter, data from Pavel (1996), considered as estimated derivatives, was compared to data from the NASA model of Heffley et. al (1979), considered as actual derivatives [1], [2]. Here, it could be seen that most errors are within -1 and 0, hence underestimating the actual derivative in absolute value. It is only for a few cases that a greater positive or negative error occurs but still around an absolute value of 1. Furthermore, some outliers were spotted with errors of ± 30. However, these only occur because the actual derivative is almost zero. As will be clear later from the results of the sensitivity analysis, the accuracy of these derivatives barely influence the MPC performance at all.

Therefore, it was chosen to first find the important derivatives by applying an error of 10 and -10 to all of the relevant derivatives and measuring the cross-coupling parameters. After this a range of errors from -10 to 10, so $\epsilon = -10, -9, -8, -7, -6, -5, -4, -3, -2, -1, 0, 1, 2, 3, 4, 5, 6, 7, 8, 9, 10$, will be applied to the most important derivatives in order to have an individual analysis. The results of the individual analysis can be found in Appendix D.

9.2. Yaw due to Collective for Aggressive Agility

The sensitivity analysis for yaw due to collective coupling for forward flight (80 knots) for both positive and negative collective step inputs and positive and negative derivative error can be seen in Figure 9.1. Here, each dot represents the value of the cross-coupling parameter when the error of 10 or -10 is implemented in the corresponding derivative as can be seen in the legend. It can be seen that the negative error gives significantly

worse cross-couplings than the positive error. The worst cross-couplings are found when a negative error is implemented in the change in yaw acceleration because of tail rotor collective derivative $\dot{r}_{\theta_{0_{tr}}}$ for both positive and negative input, going into level 3 handling qualities with a big margin. Furthermore the yaw due to lateral cyclic derivative $\dot{r}_{\theta_{1c}}$ is also sensitive to negative errors going far into the level 3 zone. Finally, when a positive or negative error is implemented in the yaw due to collective derivative $\dot{r}_{\theta_0}$, the handling qualities almost go to level 3. The other derivatives do not have a big influence on the cross-coupling parameters when a large error is implemented to them, all staying within level 1 handling qualities. These three derivatives were investigated further in order to see how the value of the error influences the cross-coupling handling qualities in Figures D.1, D.2 and D.3 in Appendix D. It is notable that these three derivatives are also the ones with largest absolute value in the A and B matrix as can be seen in the yaw acceleration derivatives in Equation 9.2. This is also highly logical as the elements with the largest absolute value influence the dynamics of that degree of freedom the most.
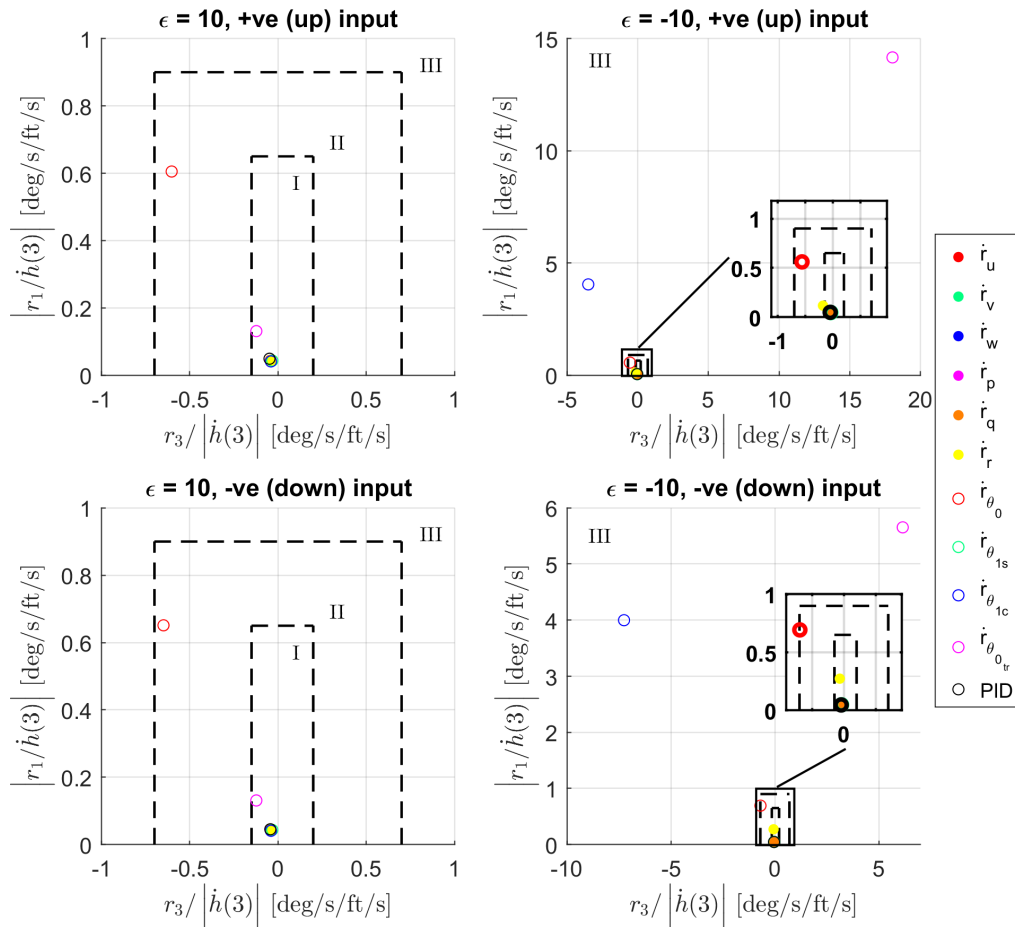
Figure 9.1: Yaw due to collective coupling sensitivity analysis in hover for positive (up) and negative (down) collective step input and for a positive and negative error implemented in one of the derivatives.

It can be seen from the individual analysis that for both $\dot{r}_{\theta_{1c}}$ and $\dot{r}_{\theta_{0_{tr}}}$ the handling qualities stay more or less the same for positive handling qualities. It is only when a negative error is applied that the handling qualities rise high above the level 3 boundary. For $\dot{r}_{\theta_{1c}}$ this happens when the error becomes smaller than -4, gradually degrading more and more, whereas for $\dot{r}_{\theta_{0_{tr}}}$ the handling qualities quickly rise once the error becomes smaller than -1, so when the derivative changes sign. This sudden instability once the $\dot{r}_{\theta_{0_{tr}}}$-derivative changes sign is quite logical as physically the change in sign would mean that the tail rotor force is acting in the opposite direction, totally destabilizing the dynamics.

The $\dot{r}_{\theta_0}$-derivative on the other hand has a gradual increase of cross-coupling when the error increases absolute value for both the positive and negative errors, with the increase in cross-coupling being almost symmetric. Eventually, it is the $r_3/\left|\dot{h}(3)\right|$ parameter that is the limiting factor and degrades the handling qualities the most, going almost into the level 3 zone for the positive collective input and on the border of

the level 3 zone for the negative collective input with an error of 10 or -10. As long as the error remains within -3 and 2, level 1 handling qualities can be obtained.

9.3. Pitch due to Roll Coupling for Aggressive Agility

The sensitivity analysis for pitch due to roll coupling for aggressive agility for both hover and forward flight at 80 knots can be seen in Figures 9.2 and 9.3. It can be seen that the only derivative that get the handling qualities out of the level 1 zone when an error, namely a negative error, is applied is the change in pitch acceleration due to longitudinal cyclic derivative $\dot{q}_{\theta_{1s}}$ for both hover and forward flight. The other derivatives remain in level 1 when the error is implemented. Again, it is remarkable that the $\dot{q}_{\theta_{1s}}$ derivative in the B matrix for both hover and forward flight takes up a very high value compared to the other derivatives of the pitch acceleration.
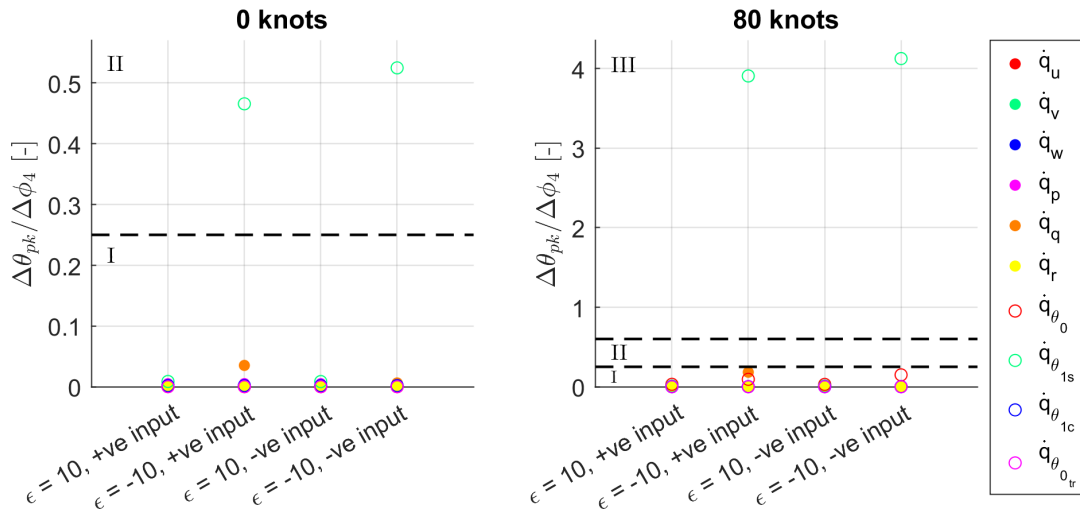
Figure 9.2: Pitch due to roll coupling sensitivity analysis for 0 and 80 knots, positive (right) and negative (left) lateral cyclic and for a positive and negative error implemented in one of the derivatives.
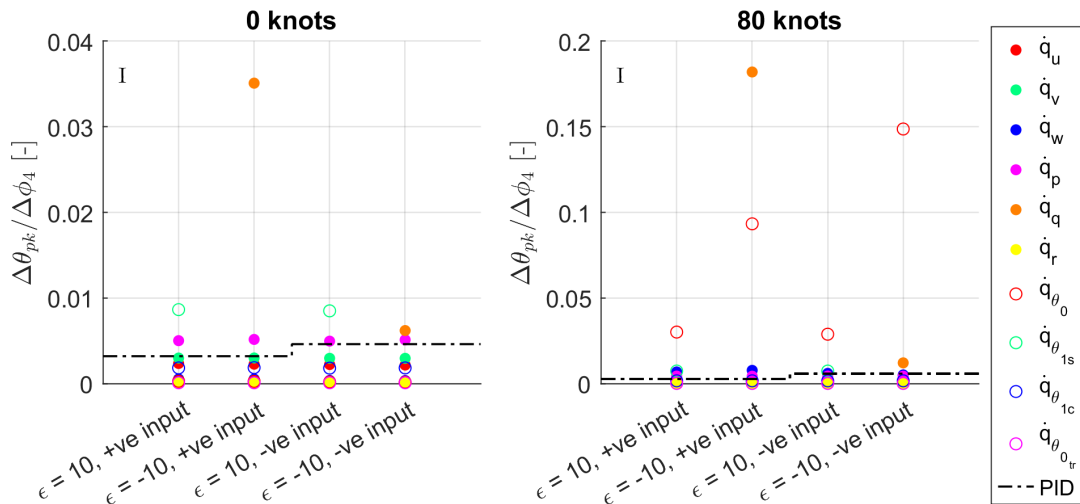
Figure 9.3: Pitch due to roll coupling sensitivity analysis zoomed in to level 1.

It can be seen in these matrices that the $\dot{q}_{\theta_0}$ also takes up a relatively high value for forward flight. However, this derivative does not play an important role in this cross-coupling case. This can be explained by the fact that the dynamics of the pitch rate is not determined by only the value of these derivatives but the product of these derivatives with their corresponding state deviation from trim ($\delta x = x - x_0$). Since the collective input is not deviating much from its trim input, the $\dot{q}_{\theta_0}$ derivative does not degrade the handling

qualities much when an error is implemented to it. When zooming in to level 1 one can see that compared to the PID controller, the $\dot{q}_q$, $\dot{q}_{\theta_0}$ and $\dot{q}_{\theta_{1s}}$ derivatives mainly perform worse than the PID controller which does not rely on a prediction model.

When analyzing the $\dot{q}_{\theta_{1s}}$ derivative individually for varying errors, one can see in Figure D.4 in Appendix D that once the errors gets smaller than -1, so when the estimated derivative changes sign, the handling qualities jump from level 1 to level 3 for forward flight. For hover, the handling qualities only go to level 2 when the error surpasses this boundary. Physically this makes sense because if the change in pitch acceleration due to longitudinal cyclic input is estimated to be of opposite sign, then pulling the cyclic stick up would be making the helicopter pitch down. Hence, when the MPC prediction model has this physically incorrect and highly influential derivative, the resulting optimal control input does not reduce the cross-couplings very well in closed-loop.

9.4. Roll due to Pitch Coupling for Aggressive Agility

The sensitivity analysis for roll due to pitch coupling for aggressive agility for both hover and forward flight at 80 knots can be seen in Figures 9.4 and 9.5. Here it can be seen that for hover and to a lesser extent for forward flight an error of both plus and minus ten in the roll damping derivative $\dot{p}_p$ makes the handling qualities degrade to level 3. A positive error in the $\dot{p}_{\theta_{1c}}$ derivative also degrades the handling qualities for both hover and forward flight to level 3. When looking closely to the level 2/3 handling quality border for hover, one can see that also the $\dot{p}_u$ derivative is sensitive to model errors. Furthermore, the $\dot{p}_{\theta_0}$ and $\dot{p}_w$ derivative go into level 2 when an error is applied to it. Again, the values for $\dot{p}_p$ and $\dot{p}_{\theta_{1c}}$ are very large compared to the other derivatives which makes them influence the dynamics of the helicopter a lot. The $\dot{p}_u$ derivative value is not so large. However, because of the pitching of the helicopter, large deviations of forward velocity from the trim velocity are obtained, coupling the lateral and longitudinal motion. Therefore, this derivative also plays an important role.
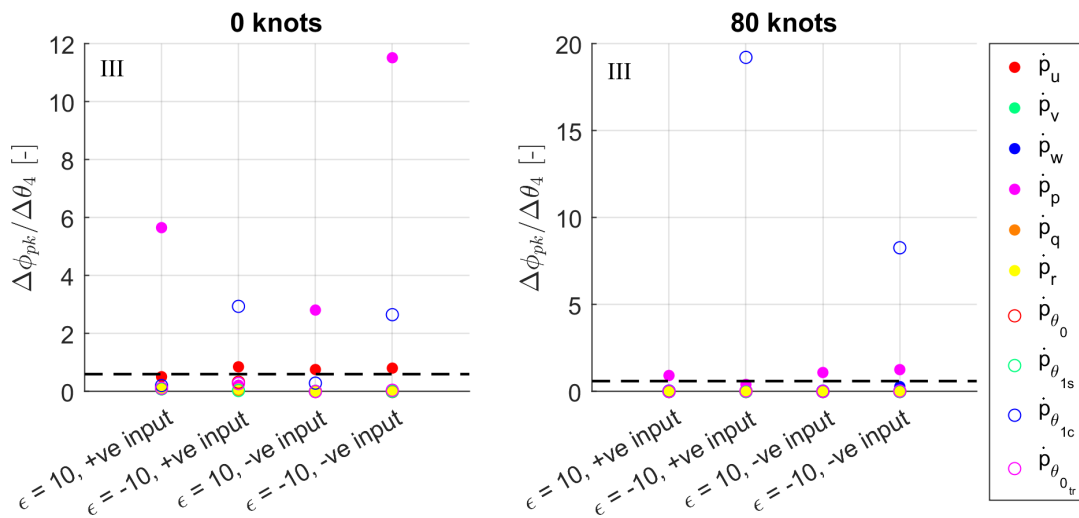
Figure 9.4: Roll due to pitch coupling sensitivity analysis for 0 and 80 knots, positive (up) and negative (down) longitudinal cyclic and for a positive and negative error implemented in one of the derivatives.

When looking at these three derivatives individually in Figures D.5, D.6 and D.7 in Appendix D, one can see how the handling qualities change for an increasingly positive and negative error. For the roll damping derivative $\dot{p}_p$ for example, the handing qualities stay within level 1 for errors from -6 to 3. Here, it is mainly the positive errors that degrade the performance. In the positive input, 0 knots case, the parameter even goes to 92 and 175 for an error of 6 and 7, which is very large indicating that the helicopter went unstable. Also the negative errors, from -6, give level 3 handling qualities for the 0 knots and negative input case and level 2 handling qualities for the 80 knots and positive input case. Furthermore, the $\dot{p}_{\theta_{1c}}$ derivative becomes of importance for errors smaller than or equal to -1, meaning the estimated derivative is either 0 is of opposite sign as the actual derivative. Physically this would mean that the helicopter would roll to the right when giving a lateral cyclic input to the left and vice versa. This is completely contradictory to the actual helicopter dynamics and very decisive for the roll due to pitch maneuver, making the handling
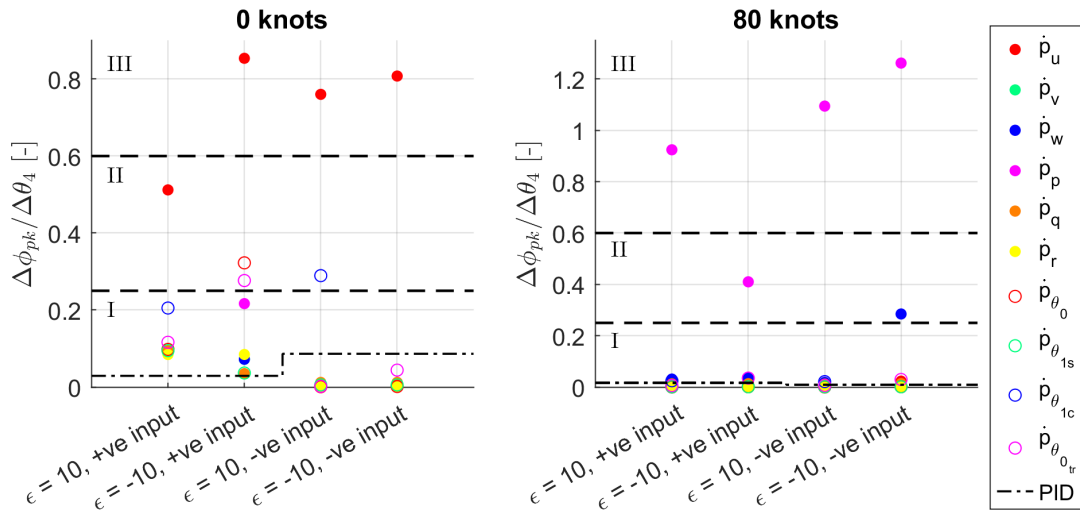
Figure 9.5: Roll due to pitch coupling sensitivity analysis zoomed in to level 1.

qualities degrade to level 3 for all 4 cases. Lastly, the error in the $\dot{p}_u$ derivative seems to influence the handling qualities in a symmetric way: when the absolute value of the error increases the handling qualities decrease, for both positive and negative errors. However, the handling qualities only go into the level 3 zone for hover. In forward flight, the cross-coupling parameter stays within level 1.

9.5. Pitch due to Collective Coupling

The sensitivity analysis for pitch due to collective coupling for small and large collective inputs at 80 knots can be seen in Figures 9.6 and 9.7. It can be seen that only the $\dot{q}_{\theta_{1s}}$ derivative goes into the level 3 zone when negative errors are implemented to it. Again, it is the derivative with a high value in the state-space matrices indicating it greatly influences the dynamics of the helicopter. Besides this, the other derivatives stay well within level 1 handling qualities. When zooming in, it can be seen that some derivatives do perform worse than the PID controller such as the $\dot{q}_w$ derivative.
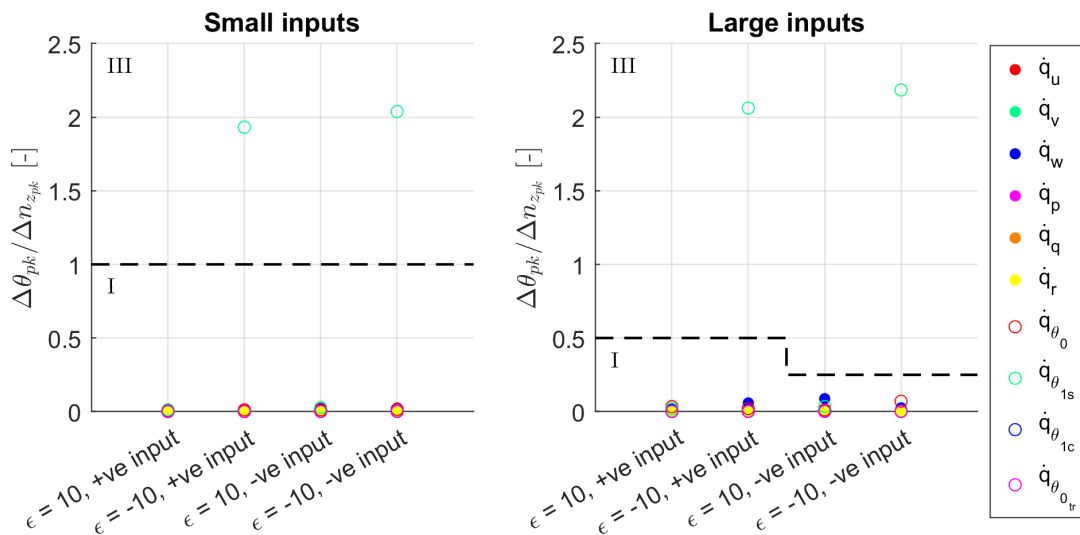
Figure 9.6: Pitch due to collective coupling sensitivity analysis for 80 knots, positive (up) and negative (down) collective step input and for a positive and negative error implemented in one of the derivatives.

When looking at the how the error influences the cross-coupling when implemented in the change pitch acceleration due to longitudinal cyclic input derivative $\dot{q}_{\theta_{1s}}$ in Figure D.8, one can see that the handling qualities only degrade to level 3 once the error goes smaller than or equal to -1. This means that then, the estimated derivative is of opposite sign compared to the actual derivative or zero. Physically this implies
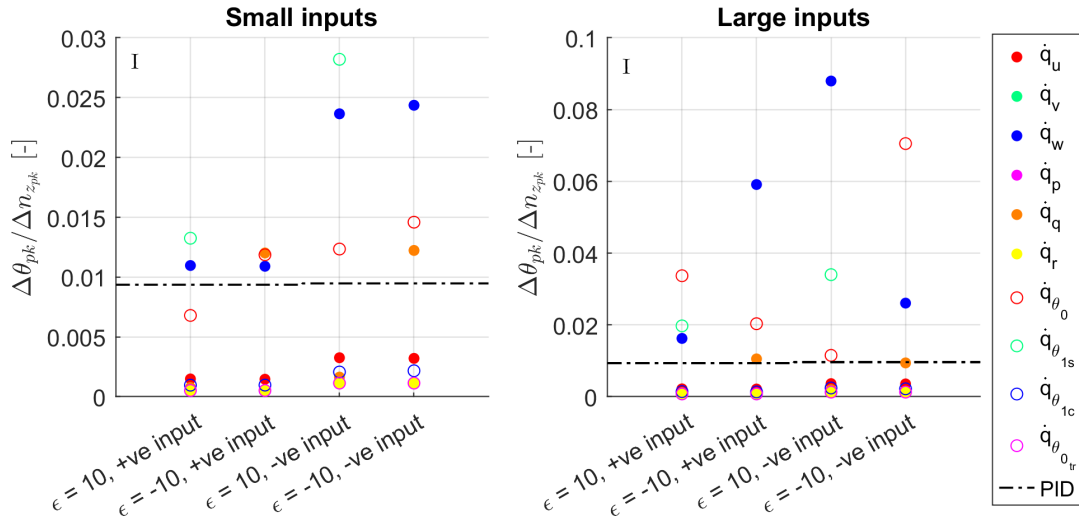
Figure 9.7: Pitch due to collective coupling sensitivity analysis zoomed in to level 1.

that pulling the cyclic stick up makes the helicopter pitch down which is the opposite of how the actual helicopter behaves. This estimation is highly inaccurate and therefore the MPC controller does not succeed at reducing the cross-couplings.

9.6. Pitch due to Roll and Roll due to Pitch Coupling for Target Acquisition and Tracking

The sensitivity analysis for pitch due to roll and roll due to pitch coupling for target acquisition and tracking for both hover and 80 knots flight can be found in Figure 9.8. Here, the boundaries for the p/q coupling are assumed to be at -10 dB and 5 dB, indicated by the grey solid line. For pitch due to roll (q/p) coupling it can be seen that only for a negative error the handling qualities degrade into level 2 or 3 for $\dot{q}_{\theta_{1s}}$, $\dot{q}_{\theta_0}$ and the damping derivative $\dot{q}_q$ which is in line with the values of these derivatives in the state-space matrices. For roll due to pitch (p/q) coupling the important derivatives are roll damping derivative $\dot{p}_p$, going into level 3 for hover and into level 2 for forward flight, $\dot{p}_{\theta_{1c}}$, going into level 1 and 2, and $\dot{p}_{\theta_{0tr}}$ just crossing the border at level 2 for forward flight and a positive input.

The individual sensitivity analysis for the most important derivatives for pitch due to roll coupling can be seen in Figures D.9, D.10 and D.11 and for roll due to pitch coupling in Figures D.12, D.13 and D.14 in Appendix D.

Pitch due to Roll Individual Analysis When looking at the analysis of the error in the pitch damping derivative $\dot{q}_q$ one can see that the only for very small negative numbers ($\epsilon < -8$) the handling qualities degrade to level 2. The degradation is only present for negative errors which can be explained by the fact that $\dot{q}_q$ characterizes the phugoid Eigenmotion and is destabilizing when positive. Hence, when this derivative is estimated to be of opposite sign, the dynamic stability of the helicopter changes degrading the MPC controller closed-loop performance. Furthermore, when the error is implemented in the $\dot{q}_{\theta_0}$ derivative, the handling qualities got to level 3 for negative errors smaller than -4 and for forward flight only. For positive errors, the handling qualities stay in level 1 but do degrade with increasing error. The cross-coupling parameter for hover seems to stay more or less unaffected by the error. Finally, the error in the $\dot{q}_{\theta_{1s}}$ derivative also degrades the handling qualities to level 2 and 3 only for negative errors smaller than 1, but now for both hover and forward flight. The positive errors seem to degrade the handling qualities with increasing error but stay within level 1.

Roll due to Pitch Individual Analysis The analysis of the error in the roll damping derivative $\dot{p}_p$ shows a more or less symmetrical distribution of the cross-coupling parameter across the positive and negative errors. Errors outside of -7 and 3 seem to have handling qualities in level 2 or 3. This derivative characterizes the roll subsidence Eigenmotion and is therefore important for stability. Therefore, majorly overestimating

this derivative ($\epsilon > 3$) or estimating the derivative to be of opposite sign ($\epsilon < -7$) increases the cross-coupling parameter. Furthermore, negative errors in the $\dot{p}_{\theta_{1c}}$ derivative, smaller than or equal to -1 degrade the handling qualities to level 3 for hover and level 2 for 80 knots flight. Positive errors seem to also degrade the handling qualities but it stays in level 1. Finally, when an error is applied to the $\dot{p}_{\theta_{0_{tr}}}$ derivative, the cross-coupling parameter barely changes for hover. However, for forward flight the negative errors ($\epsilon < -5$) degrade the handling qualities to level 2.
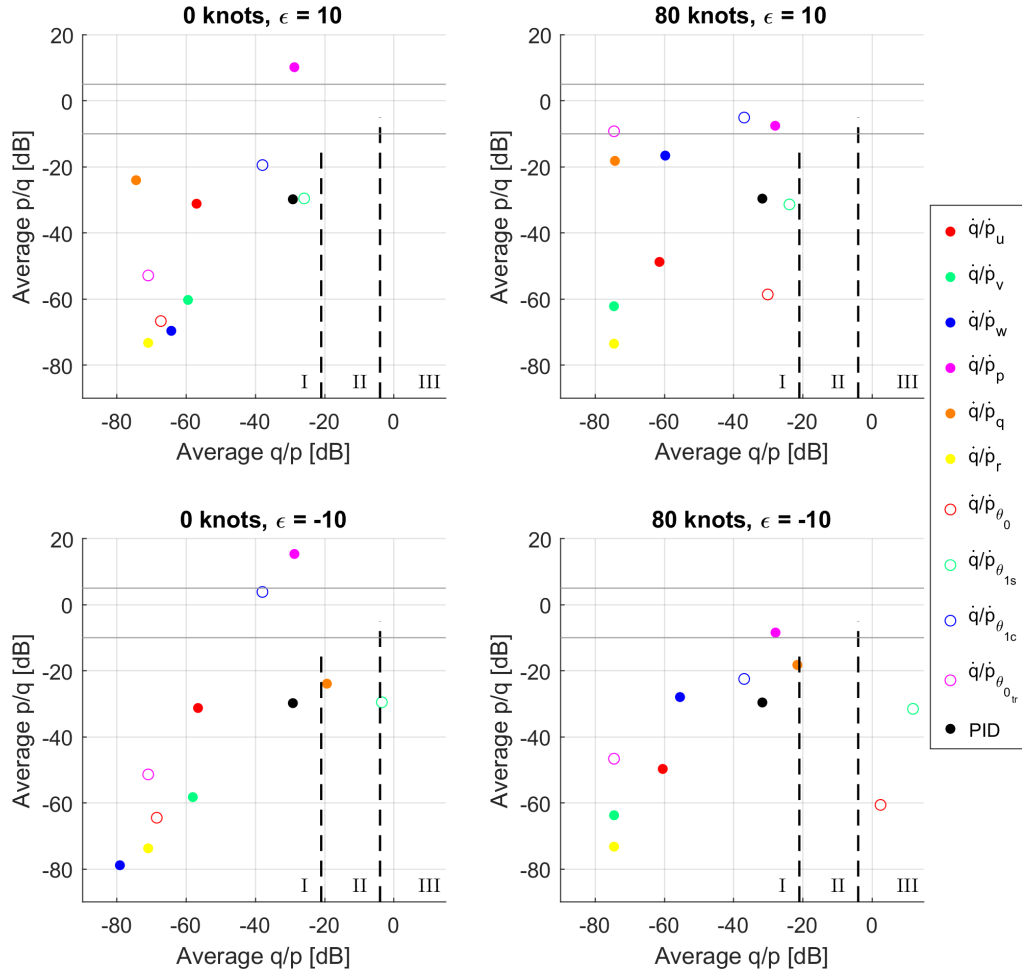
Figure 9.8: Pitch due to roll (q/p) and roll-due-to-pitch (p/q) frequency coupling sensitivity analysis for 0 and 80 knots, positive and negative lateral/longitudinal cyclic and for a positive and negative error implemented in one of the derivatives.

9.7. Overview of Important Derivatives

An overview of the important derivatives for each cross-coupling case can be seen in Table 9.1 together with some characteristics of how the error influences the cross-coupling parameters. For example, when it says $\epsilon < -1$, it means that the handling qualities are degraded to level 2 or 3 only for errors smaller than one. Furthermore, 'symmetrical' means the error in the derivative influences the handling qualities in a symmetric way: when the absolute value of the error increases the cross-coupling parameter increases and hence the handling qualities decrease. When 0 or 80 knots is stated in the characteristics this means the handling qualities are only affected for this flight speed.

As said before, it is noticeable that the important derivatives are the derivatives that either have a relatively large value in the state-space matrix (Equations 9.1 and 9.2) or that experience a large change from trim throughout the cross-coupling simulations. This is also very logical as the product of the derivative and the deviation of the state from trim determines the acceleration of that degree of freedom. Hence, when an error is present in the derivative with a large value the mismatch between the estimated and actual motion increases. Being able to deduct which derivatives are important from the state-space matrices enables to

extend the results of this BO-105 sensitivity analysis to other helicopters as well.

It can also be seen in this overview that the important derivatives are mostly control derivatives from matrix B, so derivatives with respect to a control input. Furthermore, mostly negative errors, at least smaller than -1, degrade the handling qualities to level 2 or 3 whereas the positive errors barely change the cross-couplings. For the control derivatives this is highly logical because the error smaller than -1 indicates the derivative changes sign, meaning that the controls would be working in the opposite direction. For example, if the $\dot{r}_{\theta_{0tr}}$ derivative is of opposite sign, the tail rotor force would be pointing the opposite direction. For the pitch damping $\dot{q}_q$ derivative, the opposite sign is degrading the handling qualities because this is an important stability derivative for the phugoid Eigenmotion. When the sign is estimated incorrectly, the Eigenmotion of the helicopter is majorly affected.

Besides the control derivatives and the pitch damping derivative that degrade when negative errors are implemented, there are the $\dot{p}_p$ and $\dot{p}_u$ derivatives which are important for the roll due to pitch coupling for both positive and negative errors. Here, the roll damping derivative $\dot{p}_p$ is characteristic for the roll subsidence Eigenmotion and is therefore also important to be accurate. The $\dot{p}_u$ derivative is a coupling derivative which couples the lateral and longitudinal motion when the rotor is tilting and a forward velocity change occurs. Hence, the tilting forward during the roll due to pitch maneuver creates this large change in forward velocity u, giving this derivative more importance in the helicopter dynamics.

Table 9.1: Overview and characteristics of the important derivatives for each cross-coupling case.

Cross-coupling case	Important derivatives	Characteristics	Cross-coupling case	Important derivatives	Characteristics
Pitch d.t. roll	$\dot{q}_{\theta_{1s}}$	$\epsilon < -1$	Pitch d.t. roll for TA & T	$\dot{q}_q$ $\dot{q}_{\theta_0}$ $\dot{q}_{\theta_{1s}}$	$\epsilon \leq -8$ $\epsilon \leq -4$, 80 kn $\epsilon \leq -1$
Roll d.t. pitch	$\dot{p}_u$ $\dot{p}_p$ $\dot{p}_{\theta_{1c}}$	symmetrical, 0 kn $\epsilon \leq -1$	Roll d.t. pitch for TA & T	$\dot{p}_p$ $\dot{p}_{\theta_{1c}}$ $\dot{p}_{\theta_{0tr}}$	$\sim$ symmetrical $\epsilon \leq -1$ $\epsilon \leq -6$, 80 kn
Yaw d.t. collective	$\dot{r}_{\theta_0}$ $\dot{r}_{\theta_1c}$ $\dot{r}_{\theta_{0tr}}$	symmetrical $\epsilon \leq -3$ $\epsilon \leq -1$			
Pitch d.t. collective	$\dot{q}_{\theta_{1s}}$	$\epsilon \leq -1$			

10

Conclusion of the Thesis Work

This work investigated whether linear and nonlinear model predictive control are suitable for online application to helicopters to reduce cross-coupling effects by evaluating its performance on the cross-coupling handling quality requirements of the ADS-33 document. The cross-coupling requirements were tested in simulation by implementing a step in one control input and measuring the cross-coupling parameter which represents the amount of off-axis response.

On one hand it was investigated how well the linear and nonlinear MPC can reduce cross-coupling effects when a control input is given based on the rating scale for handling qualities and compared to an uncontrolled and PID controlled helicopter. It was found that both linear and nonlinear MPC are able to reduce the off-axis response of the tested cross-coupling cases by around 99% compared to the uncontrolled helicopter bringing all handling quality levels from level 2 or 3 to level 1. Here, handling qualities of level 1 indicate having minimal pilot workload and desired aircraft characteristics. Also the PID controller is able to bring the handling qualities from level 2 or 3 to level 1. However, when comparing the MPC to the PID controller almost all MPC cases have 90% to 99% better cross-coupling reduction than the PID controller. This can be explained by the optimal and model-based behaviour of the MPC controllers: where the PID controller shows a washed-out coupling off-axis rate response, the MPC controllers almost eliminate all coupling showing a quasi decoupled off-axis rate response.

When a disturbance is introduced in the simulation model, the cross-coupling reduction performance is only slightly less, keeping level 1 handling qualities for most coupling cases. This indicates that MPC is robust to this disturbance. Only the yaw due to collective coupling case with uncertainty for a positive collective input gives level 2 handling qualities for the MPC controllers and not for the PID controller. However, this can be explained by the poorly estimated yaw coupling in the prediction model because of the unknown disturbance in rotor thrust and by the cross-coupling parameter that is based on the yaw rate instead of yaw angle which is optimized for. The PID controller does not have this disadvantage as it purely depends on the error in attitude and not on a prediction model. This lesser performance of the MPC controller could be solved by implementing robust MPC or adapting the objective function to also minimize the yaw rate.

Furthermore, the differences between linear and nonlinear MPC were investigated where it was found that the linear prediction model has lower fidelity and the non-convexity of nonlinear MPC brings a heavier computational burden and the existence of multiple local optima with it. However, the loss in performance because of suboptimality is negligible for the cross-coupling cases. Furthermore, more computer power, faster optimization algorithms and other tricks could possibly enable real-time nonlinear MPC for helicopters. Next to this, the differences in performance between linear and nonlinear MPC for the cross-coupling simulations are so small they do not noticeably degrade the handling qualities and can be assumed to be non-existent. As linear MPC has the advantage of having a shorter computation time and no suboptimal solutions, linear MPC is preferred over nonlinear MPC in order to reduce cross-coupling effects.

On the other hand, it was examined how sensitive MPC is to prediction model errors when reducing cross-coupling effects by implementing a fixed error in the relevant derivatives of the linear prediction model and measuring the performance change. It was found that the derivatives sensitive to errors are the derivatives that either have a relatively large value in the state-space matrix or that experience a large change from trim throughout the simulation. These derivatives were mainly control derivatives. After individual analysis

of the important derivatives it was found that mostly negative errors smaller than -1 degrade the handling qualities to level 2 or 3 whereas the positive errors barely change the cross-coupling effects in most cases. For the control derivatives this is highly logical because the error smaller than -1 indicates the derivative changes sign, meaning that the controls would be working in the opposite direction according to the prediction model. As the error in the derivative was found to mostly stay within -1 and 1, it can be concluded that the MPC controller is robust to these model errors and keeps having level 1 handling qualities. When the absolute error increases and specially when the errors gets smaller than -1, the degradation in performance could be solved by implementing robust MPC which improves the performance when an unmeasured error or disturbance is present.

In short, it can be concluded that both linear and nonlinear MPC are very effective to reduce cross-coupling effects even when a disturbance is applied. Both controllers are able to improve the handling qualities of the helicopter to level 1 indicating a minimal pilot workload and desired aircraft characteristics. However, when large model errors are present in the prediction model, especially negative errors in the control derivatives, a degradation of handling qualities can be seen. Yet, for small errors the handling qualities remain in level 1. As linear MPC has the advantage of having a shorter computation time and no suboptimal solutions, linear MPC is preferred over nonlinear MPC for reducing cross-coupling effects.

11

Recommendations for Future Work

Now that an answer is given to the research questions of this thesis, there are still some recommendations for future work to extend the investigation of MPC applied to helicopters and to test the established MPC controller to reduce cross-couplings even further.

Test the Established Controller More Elaborately The established linear and nonlinear MPC controllers in this research are tested for the cross-coupling requirements in the ADS-33 for both hover and forward flight at 80 knots in simulation. Now, the results for 0 knots are assumed to be valid for all low flight speeds and the results for 80 knots are assumed to be valid for forward flight in general. As the maximum flight speed of the BO-105 is 145 knots, it would be interesting to also test the ability to reduce cross-couplings for this flight speed.

Furthermore, the robustness of the controller to other disturbances in the simulation model should be tested. Now, only an uncertainty in the main rotor thrust coefficient is implemented and tested for. For yaw due to collective coupling, the disturbance degraded the handling qualities to level 2. It should be investigated if uncertainties implemented in other parts of the model or external disturbances such as wind gusts influence the cross-coupling reduction performance of the controller.

Finally, it was seen from the cross-coupling requirement simulations that when the MPC controller is applied to the helicopter to reduce the off-axis response, the on-axis response is influenced as well. It would be interesting to investigate how the on-axis response gets influenced and what kind of effect this has on the handling qualities of the helicopter.

Implement and Evaluate Robust MPC for Reducing Cross-couplings It could be seen from the cross-coupling results with disturbance that the uncertainty degrades the handling qualities significantly in the case for yaw due to collective coupling. Furthermore, large negative errors, mainly in control derivatives, in the prediction model could also bring the handling qualities to level 2 or even level 3. Robust MPC could be implemented in order to improve the robustness to both model errors and disturbances to the actual helicopter. By implementing robust MPC, one increases the robustness going at the cost of the overall performance. Therefore, this trade-off between robustness and performance should be investigated.

Investigate Effectiveness of Linear MPC on Helicopters for Tracking Maneuvers In this research, the differences in optimization such as the (sub)optimality and computation time question and the linear model fidelity were investigated. In practice the cross-coupling cases showed only very small differences between the linear and nonlinear controller. However, it would be interesting to investigate if the linear model is still accurate enough when longer tracking simulation were performed, say to fly a maneuver. It is expected that, as the state moves further away from the trim point, the fidelity of the linear model will degrade. Furthermore, longer prediction horizons would be needed for tracking a maneuver which also increases the accumulation of error along the prediction horizon. Successive linearization or linear model stitching could be used in order to systematically improve the linear prediction model during the maneuver.

Bibliography

[1] M. Pavel, *Six Degrees of Freedom Linear Model for Helicopter Trim and Stability Calculation*, Memorandum (Delft University of Technology, Faculty of Aerospace Engineering, 1996).

[2] R. K. Heffley, W. F. Jewell, J. M. Lehman, and R. A. Vanwinkle, *A compilation and analysis of helicopter handling qualities data. Volume 1: Data compilation*, Tech. Rep. NASA-CR-3144 (NASA, 1979).

[3] H. S. A. T. of IHSTI-CIS, *Helicopter Accidents: Statistics, Trends and Causes*, Tech. Rep. (International Helicopter Safety Team - Commonwealth of Independent States, Louisville, Kentucky, USA, 2016).

[4] H. Huber and P. Hamel, *Helicopter flight control: State of the art and future directions,* in *Nineteenth European Rotorcraft Forum* (European Rotorcraft Forum, Cernobbio (Como), Italy, 1993).

[5] G. Padfield, *Helicopter handling qualities and control: is the helicopter community prepared for change?* in *Royal Aeronautical Society Conference on Helicopter Handling Qualities and Control*, Royal Aerospace Establishment (Controller HMSO London, London, 1988).

[6] D. G. Mitchell, D. B. Doman, D. L. Key, D. H. Klyde, D. B. Leggett, D. J. Moorhouse, D. H. Mason, D. L. Raney, and D. K. Schmidt, *Evolution, revolution, and challenges of handling qualities,* Journal of Guidance, Control, and Dynamics **27**, 12 (2004).

[7] J. Rawlings, D. Mayne, and M. Diehl, *Model Predictive Control: Theory, Computation, and Design*, 2nd ed. (Nob Hill Publishing, Santa Barbara, California, 2017).

[8] Y.-G. Xi, D. Li, and S. Lin, *Model predictive control — status and challenges,* Acta Automatica Sinica **39**, 222–236 (2013).

[9] S. Qin and T. A. Badgwell, *A survey of industrial model predictive control technology,* Control Engineering Practice **11**, 733 (2003).

[10] D. Hrovat, S. Di Cairano, H. E. Tseng, and I. V. Kolmanovsky, *The development of model predictive control in automotive industry: A survey,* in *2012 IEEE International Conference on Control Applications* (2012) pp. 295–302.

[11] S. Vazquez, J. Leon, L. Franquelo, J. Rodriguez, H. Young, A. Marquez, and P. Zanchetta, *Model predictive control: A review of its applications in power electronics,* Industrial Electronics Magazine, IEEE **8**, 16 (2014).

[12] U. Eren, A. Prach, B. B. Koçer, S. V. Rakovic, E. Kayacan, and B. Acikmese, *Model predictive control in aerospace systems: Current state and opportunities,* Journal of Guidance, Control, and Dynamics **40**, 1541 (2017).

[13] T. van Holten and J. A. Melkert, *Helicopter Performance, Stability and Control*, Faculty of Aerospace Engineering, Delft University of Technology (2002).

[14] T. A. H. S. I. S. Committee, *History and overview of rotating wing aircraft,* https://slideplayer.com/slide/14459519/ (2018), accessed: 2020-01.

[15] C. Rotaru and M. Todorov, *Flight physics - models, techniques and technologies,* (IntechOpen, 2017) Chap. Helicopter Flight Physics.

[16] S. Taamalllah, *Small-Scale Helicopter Automatic Autorotation*, Ph.D. thesis, Delft University of Technology (2015).

[17] J. Van Der Vorst, *Advanced pilot model for helicopter manoeuvres*, Master's thesis, Delft University of Technology (1998).

[18] J. Gadewadikar, F. Lewis, K. Subbarao, K. Peng, and B. Chen, *H-infinity static output-feedback control for rotorcraft,* Journal of Intelligent and Robotic Systems **54**, 629 (2009).

[19] M. Insulander, *Development of a Helicopter Simulation for Operator Interface Research*, Ph.D. thesis, KTH Royal Institute of Technology (2008).

[20] P. V. M. Simplicio, *Helicopter Nonlinear Flight Control: An Acceleration Measurements-based Approach using Incremental Nonlinear Dynamic Inversion*, Master's thesis, Delft University of Technology (2011).

[21] N. Moll, *To a bo 105 pilot this thing's pretty: World's first light twin helicopter still going strong,* Flying Magazine **118**, 96–105 (1991).

[22] M. Pavel, *On the Necessary Degrees of Freedom for Helicopter and Wind Turbine Low-Frequency Mode Modelling*, Ph.D. thesis, Delft University of Technology (2001).

[23] M. Pavel and R. V. Aalst, *On the question of adequate modelling of steady-state rotor disc-tilt for helicopter manoeuvring flight,* in *the 28th European Rotorcraft Forum* (European Rotorcraft Forum, Bristol, UK, 2002).

[24] J. R. Majhi and R. Ganguli, *Modeling helicopter rotor blade flapping motion considering nonlinear aerodynamics,* in *16th Congres of the International Council of the Aeronautical Sciences*, Vol. 27 (CMES, 2008) pp. 25–36.

[25] R. Prouty, *Helicopter aerodynamics volume i,* (Eagle Eye Solutions, 2009) Chap. Effects of Rotor Flapping, pp. 71–76.

[26] R. W. Prouty, *Helicopter performance, stability, and control* (Krieger Publishing, 2002) p. 746.

[27] K. Ferguson, D. Anderson, D. Thomson, M. Ireland, Z. Tu, S. Manso, A. Chandran, and G. Ibal, *Comparing the flight dynamics characteristics of tandem and conventional helicopters for the purposes of automatic control,* in *the 41th European Rotorcraft Forum* (Munich, Germany, 2015).

[28] H. Gao, A. He, Z. Gao, Y. Na, and Y. Deng, *Flight dynamics characteristics of canard rotor/wing aircraft in helicopter flight mode,* Chinese Journal of Aeronautics **32**, 1577 (2019).

[29] K. J. Kadhim and A. N. J. shahid, *Simulation of longitudinal stability of helicopter in forward flight,* Journal of Engineering **19**, 357 (2013).

[30] K. Lu, C. Liu, C. Li, and R. Chen, *Flight dynamics modeling and dynamic stability analysis of tilt-rotor aircraft,* International Journal of Aerospace Engineering (2019).

[31] G. D. Padfield, *Helicopter Flight Dynamics*, 2nd ed. (Blackwell Publishing, 2007) p. 641.

[32] A. Faulkner and M. Kloster, *Lateral-directional stability: theoretical analysis and flight test experience,* in *the 9th European Rotorcraft Forum*, 70 (Munich, Germany, 1983).

[33] W. H. Philips, *Appreciation and prediction of flying qualities*, Tech. Rep. 927 (Langley Aeronautical Laboratory, Langley Air Force Base, Va., 1949).

[34] G. E. Cooper and R. P. J. Harper, *The use of pilot rating in the evaluation of aircraft handling qualities*, Tech. Rep. (NASA TN-D5153, 1969).

[35] G. D. Padfield, *Rotorcraft handling qualities engineering: Managing the tension between safety and performance: 32nd alexander a. nikolsky honorary lecture,* Journal of the American Helicopter Society **58** (2013).

[36] M. Höfinger, *Ads-33e-prf - aeronautical design standard, performance specification, handling qualities requirements for military rotorcraft,* (2005).

[37] M. Behrendt, (2020), [CC BY-SA 3.0 (https://creativecommons.org/licenses/by-sa/3.0)].

[38] A. Kassem and A. Hassan, *Performance improvements of a permanent magnet synchronous machine via functional model predictive control,* Journal of Control Science and Engineering (2012).

[39] Y. I. Lee, B. Kouvaritakis, and M. Cannon, *Constrained receding horizon predictive control for nonlinear systems,* in *Proceedings of the 38th IEEE Conference on Decision and Control (Cat. No.99CH36304),* Vol. 4 (IEEE, 1999) pp. 3370–3375 vol.4.

[40] M. Kvasnica, *Implicit vs explicit mpc — similarities, differences, and a path towards a unified method,* in *2016 European Control Conference (ECC)* (2016) pp. 603–603.

[41] A. Bemporad and M. Morari, *Robust model predictive control: A survey,* in *Robustness in Identification and Control*, Lecture Notes in Control and Information Sciences, Vol. 245, edited by A. Garulli, A. Tesi, and A. Vicino (Springer-Verlag, London, 1999) pp. 207–226.

[42] A. Bemporad and M. Morari, *Control of systems integrating logic, dynamics, and constraints,* Automatica **35**, 407 (1999).

[43] C. E. García, D. M. Prett, and M. Morari, *Model predictive control: Theory and practice—a survey,* Automatica **25**, 335 (1989).

[44] D. Clarke, C. Mohtadi, and P. Tuffs, *Generalized predictive control—part i. the basic algorithm,* Automatica **23**, 137 (1987).

[45] K. S. Holkar and L. M. Waghmare, *An overview of model predictive control,* International Journal of Control and Automation **3** (2010).

[46] M. Morari and J. H. Lee, *Model predictive control: past, present and future,* Computers and Chemical Engineering **23**, 667 (1999).

[47] A. Bemporad, *Model predictive control design: New trends and tools,* in *the 45th IEEE Conference on Decision & Control* (IEEE, San Diego, California, 2007) pp. 6678 – 6683.

[48] D. Q. Mayne, *Model predictive control: Recent developments and future promise,* Automatica **50**, 2967 (2014).

[49] C. E. Mballo and J. V. R. Prasad, *Helicopter maneuver performance with active load limiting,* in *the 45th European Rotorcraft Forum* (Warsaw, Poland, 2019).

[50] C. Bottasso Luigi and P. Montinari, *Rotorcraft flight envelope protection by model predictive control,* Journal of the American Helicopter Society **60** (2015).

[51] U.-C. Moon and K. Lee, *Step-response model development for dynamic matrix control of a drum-type boiler–turbine system,* EEE Transactions on Energy Conversion **24**, 423 (2009).

[52] P. Orukpe, *Model predictive control fundamentals,* in *Nigerian Journal of Technology*, Vol. 31 (NIJOTECH, 2012) p. 139–148.

[53] A. Jamshidnejad, *Efficient predictive model-based and fuzzy control for green urban mobility,* Phd dissertation, Delft University of Technology (2017).

[54] H. Chung and S. Sastry, *Autonomous helicopter formation using model predictive control,* in *Collection of Technical Papers - AIAA Guidance, Navigation, and Control Conference*, Vol. 1 (Keystone, CO, USA, 2006) pp. 459–473.

[55] D. Mayne, J. Rawlings, C. Rao, and P. Scokaert, *Constrained model predictive control: Stability and optimality,* Automatica **36**, 789 (2000).

[56] Y. Wang and S. Boyd, *Fast model predictive control using online optimization,* in *IEEE Transactions on Control Systems Technology*, Vol. 18 (2010) pp. 267 – 278.

[57] S. Piche, B. Sayyar-Rodsari, D. Johnson, and M. Gerules, *Nonlinear model predictive control using neural networks,* IEEE Control Systems Magazine **20**, 53 (2000).

[58] M. Cannon, W. Liao, and B. Kouvaritakis, *Efficient mpc optimization using pontryagin's minimum principle,* International Journal of Robust and Nonlinear Control **18**, 831 (2006).

[59] J. B. Rawlings and K. R. Muske, *The stability of constrained receding horizon control,* IEEE Transactions on Automatic Control **38**, 1512 (1993).

[60] W.-H. Kwon and A. Pearson, *A modified quadratic cost problem and feedback stabilization of a linear system,* IEEE Transactions on Automatic Control **22**, 838 (1977).

[61] W.-H. Chen, D. Ballance, and J. O'Reilly, *Model predictive control of nonlinear systems: Computational burden and stability,* in *Control Theory and Applications*, Vol. 147 (IEEE, 2000) pp. 387 – 394.

[62] M. Alamir, *Stability proof for nonlinear mpc design using monotonically increasing weighting profiles without terminal constraints,* Automatica **87**, 455 (2018).

[63] C. Liu, W. Chen, and J. Andrews, *Tracking control of small-scale helicopters using explicit nonlinear mpc augmented with disturbance observers,* Control Engineering Practice **20**, 258 (2012).

[64] C. Liu, W. Chen, and J. Andrews, *Model predictive control for autonomous helicopters with computational delay,* in *UKACC International Conference on Control 2010* (IET, Coventry, UK, 2010) pp. 1–6.

[65] M. T. Frye, Chunjiang Qian, and R. D. Colgren, *Receding horizon control of a 6-dof model of the raptor 50 helicopter: robustness to changing flight conditions,* in *Proceedings of 2005 IEEE Conference on Control Applications, 2005. CCA 2005.* (2005) pp. 185–190.

[66] T. Oktay and C. Sultan, *Model predictive control of maneuvering helicopters,* in *AIAA Guidance, Navigation, and Control Conference* (2012).

[67] A. Dutka, A. Ordys, and M. Grimble, *Non-linear predictive control of 2 dof helicopter model,* in *the 42nd IEEE Conference on Decision and Control*, Vol. 4 (Hawaii, USA, 2003) pp. 3954 – 3959.

[68] M. Gulan, P. Minarcik, and M. Lizuch, *Real-time stabilizing mpc of a 2dof helicopter,* in *Proceedings of the 22nd International Conference on Process Control, PC 2019* (2019) pp. 215–221.

[69] M. Mehndiratta and E. Kayacan, *Receding horizon control of a 3 dof helicopter using online estimation of aerodynamic parameters,* Proceedings of the Institution of Mechanical Engineers, Part G: Journal of Aerospace Engineering **232**, 1442 (2018).

[70] M. H. Maia and R. K. H. Galvao, *Robust constrained predictive control of a 3dof helicopter model with external disturbances,* ABCM Symposium Series in Mechatronics **3**, 19 (2008).

[71] K. Dalamagkidis, K. P. Valavanis, and L. A. Piegl, *Nonlinear model predictive control with neural network optimization for autonomous autorotation of small unmanned helicopters,* IEEE Transactions on Control Systems Technology **19**, 818 (2011).

[72] W. Greer and C. Sultan, *Helicopter ship landing envelope for model predictive control,* in *75th Annual Vertical Flight Society Forum and Technology Display*, Vol. 4 (Pennsylvania, USA, 2019) pp. 2670–2678.

[73] Z. Yujia, M. Nounou, H. Nounou, and Y. Al Hamidi, *Model predictive control of a 3-dof helicopter system using successive linearization,* International Journal of Engineering, Science and Technology **2**, 9 (2010).

[74] G. Avanzini, D. Thomson, and A. Torasso, *Model predictive control architecture for rotorcraft inverse simulation,* Journal of Guidance, Control, and Dynamics **36**, 207 (2013).

[75] A. A. Bogdanov, E. A. Wan, M. Carlsson, Y. Zhang, R. Kieburtz, and A. Baptista, *Model predictive neural control of a high-fidelity helicopter model,* in *AIAA Guidance, Navigation, and Control Conference and Exhibit* (2001).

[76] H. J. Kim, D. H. Shim, and S. Sastry, *Nonlinear model predictive tracking control for rotorcraft-based unmanned aerial vehicles,* in *Proceedings of the American Control Conference*, Vol. 5 (2002) pp. 3576–3581.

[77] C. L. Bottasso and L. Riviello, *Rotor trim by a neural model-predictive auto-pilot,* in *Annual Forum Proceedings - AHS International*, Vol. I (2006) pp. 641–652.

[78] P. J. H. Z. Molenaar, *Model predictive control to autonomous helicopter flight*, Master's thesis, Eindhoven University of Technology, Eindhoven (2007).

[79] J. Witt, S. Boonto, and H. Werner, *Approximate model predictive control of a 3-dof helicopter,* in *Proceedings of the IEEE Conference on Decision and Control* (2007) pp. 4501–4506.

[80] J. Du, Y. Zhang, and T. Lü, *Unmanned helicopter flight controller design by use of model predictive control,* WSEAS Transactions on Systems **7**, 81 (2008).

[81] M. Saffarian and F. Fahimi, *Non-iterative nonlinear model predictive approach applied to the control of helicopters' group formation,* Robotics and Autonomous Systems **57**, 749 (2009).

[82] C. Liu, W. Chen, and J. Andrews, *Piecewise constant model predictive control for autonomous helicopters,* Robotics and Autonomous Systems **59**, 571 (2011).

[83] E. Joelianto, E. M. Sumarjono, A. Budiyono, and D. R. Penggalih, *Model predictive control for autonomous unmanned helicopters,* Aircraft Engineering and Aerospace Technology **83**, 375 (2011).

[84] M. K. Samal, S. Anavatti, and M. Garratt, *Neural network based model predictive controller for simplified heave model of an unmanned helicopter,* in *Swarm, Evolutionary and Memetic Computing*, Vol. 7677 LNCS (Springer-Verlag, Bhubaneswar, India, 2012) pp. 356–363.

[85] W. Shipman, *The Nonlinear Modelling and Model Predictive Control of a Miniature Helicopter UAV*, Ph.D. thesis, University of Johannesburg (2012).

[86] B. J. N. Guerreiro, C. Silvestre, and R. Cunha, *Terrain avoidance nonlinear model predictive control for autonomous rotorcraft,* Journal of Intelligent and Robotic Systems: Theory and Applications **68**, 69 (2012).

[87] D. Song, J. Han, and G. Liu, *Active model-based predictive control and experimental investigation on unmanned helicopters in full flight envelope,* IEEE Transactions on Control Systems Technology **21**, 1502 (2013).

[88] K. Kunz, S. M. Huck, and T. H. Summers, *Fast model predictive control of miniature helicopters,* in *2013 European Control Conference, ECC 2013* (2013) pp. 1377–1382.

[89] S. Salmah, S. Sutrisno, E. Joelianto, A. Budiyono, I. E. Wijayanti, and N. Y. Megawati, *Model predictive control for obstacle avoidance as hybrid systems of small scale helicopter,* in *Proceedings of 2013 3rd International Conference on Instrumentation, Control and Automation, ICA 2013* (2013) pp. 127–132.

[90] S. M. Huck, M. Rueppel, T. H. Summers, and J. Lygeros, *Rcopterx - experimental validation of a distributed leader-follower mpc approach on a miniature helicopter test bed,* in *2014 European Control Conference, ECC 2014* (2014) pp. 802–807.

[91] A. Ramalakshmi, P. Manoharan, K. Harshath, and M. Varatharajan, *Model predictive control of 2 dof helicopter,* International Journal of Innovation and Scientific Research **24**, 337 (2016).

[92] T. D. Ngo and C. Sultan, *Model predictive control for helicopter shipboard operations in the ship airwakes,* Journal of Guidance, Control, and Dynamics **39**, 574 (2016).

[93] Z. Liu, Y. He, L. Yang, and J. Han, *Control techniques of tilt rotor unmanned aerial vehicle systems: A review,* Chinese Journal of Aeronautics **30**, 135 (2017).

[94] G. D. Padfield, *Theoretical modelling for helicopter flight dynamics: development and validation,* in *16th Congres of the International Council of the Aeronautical Sciences*, Vol. 1 (ICAS proceedings, the International Council of the Aeronautical Sciences, 1998) pp. 165–177.

[95] J. Bellera, J. Laffisse, and S. Mezan, *Nh90 control laws simulation and flight validation on the dauphin 6001 fbw demonstrator,* The European Rotorcraft Forum (1997).

[96] J. Kemp, (2005), [CC BY 2.5 (`https://commons.wikimedia.org/w/index.php?curid=1903871`)].

[97] D. P. Loucks and E. van Beek, *Modeling uncertainty,* in *Water Resource Systems Planning and Management: An Introduction to Methods, Models, and Applications* (Springer International Publishing, Cham, 2017) pp. 301–330.

[98] C. V. Rao and J. B. Rawlings, *Optimization strategies for linear model predictive control,* IFAC Proceedings Volumes **31**, 41 (1998), 5th IFAC Symposium on Dynamics and Control of Process Systems 1998 (DYCOPS 5), Corfu, Greece, 8-10 June 1998.

[99] M. Voskuijl, G. Padfield, D. Walker, B. Manimala, and A. Gubbels, *Simulation of automatic helicopter deck landings using nature inspired flight control,* The Aeronautical Journal **114**, 25 (2010).

[100] J. G. Ziegler and N. B. Nichols, *Optimum settings for automatic controllers,* Journal of Dynamic Systems Measurement and Control-transactions of The Asme **115**, 220 (1942).

[101] C. L. Blanken, C. J. Ockier, H.-J. Pausder, and R. C. Simmons, *Rotorcraft pitch-roll decoupling requirements from a roll tracking maneuver,* in *50th American Helicopter Society Annual Forum 1994* (the American Helicopter Society. Inc., Washington, DC, 1997).

[102] S. A. Vavasis, *Complexity theory: quadratic programming,* in *Encyclopedia of Optimization*, edited by C. A. Floudas and P. M. Pardalos (Springer US, Boston, MA, 2001) pp. 304–307.

[103] C. Liu, W.-H. Chen, and J. Andrews, *Explicit non-linear model predictive control for autonomous helicopters,* Proceedings of the Institution of Mechanical Engineers, Part G: Journal of Aerospace Engineering **226**, 1171 (2012).

Part IV

Appendices

A

Non-dimensionalizing and Comparing Stability Derivatives

Stability derivatives are often non-dimensionalized in order to be able to compare them with other models and other helicopters. This is done by dividing the derivative by helicopter parameters of the same units. The non-dimensionalization scheme used for this model is presented in Equation A.1. Here, Λ is used to non-dimensionalize derivatives of force over a velocity e.g. X_u such that $x_u = \frac{X_u}{\Lambda}$. Furthermore, Λ_0 is used to non-dimensionalize derivatives of force over an angle e.g. X_{θ_f}. Next, Λ_1 is used for derivatives of force over angular velocity and moment over velocity e.g. X_q or M_u. Moreover, Λ_2 is used for derivatives of a moment over angular velocity e.g. M_q. Finally, Λ_3 is used for the non-dimensionalization of derivatives of a moment over an angle e.g. M_{θ_f}.

$$\Lambda = \rho A \Omega R$$
$$\Lambda_0 = \rho A \Omega^2 R^2$$
$$\Lambda_1 = \rho A \Omega R^2 \tag{A.1}$$
$$\Lambda_2 = \rho A \Omega R^3$$
$$\Lambda_3 = \rho A \Omega^2 R^3$$

The non-dimensional derivatives of the 6 DOF model of the BO-105 helicopter used in this research can be seen in Table A.1. Furthermore, in Table A.2 the non-dimensional derivatives of the NASA model of Heffley et. al. (1979) can be seen [2]. When comparing the derivatives with each other, it can be noted that the signs of the derivatives are mostly similar, with some exceptions such as z_u, z_w and l_r and some control derivatives. Furthermore, most state derivatives have the same order of magnitude. Moreover it can be seen that the control derivatives of the 6 DOF model are very small in magnitude whereas the NASA model derivatives have much greater magnitude.

Table A.1: Non-dimensional derivatives of the 6 DOF BO-105 model for hover.

Deriv.	Value	Deriv.	Value	Deriv.	Value	Deriv.	Value	Deriv.	Value	Deriv.	Value
x_u	-2.323e-3	x_v	-2.142e-3	x_w	2.094e-3	x_p	-2.521e-2	x_q	3.895e-2	x_r	0.000
y_u	1.862e-2	y_v	-9.303e-3	y_w	-1.738e-3	y_p	-5.330e-2	y_u	4.160e-3	y_r	6.370e-3
z_u	-6.958e-3	z_v	-1.606e-2	z_w	1.004e-1	z_p	2.485e-4	z_q	2.091e-3	z_r	0.000
l_u	1.772e-2	l_v	-1.990e-3	l_w	-4.982e-4	l_p	-4.785e-2	l_q	1.051e-2	l_r	1.038e-3
m_u	5.562e-3	m_v	9.072e-4	m_w	1.005e-3	m_p	1.610e-2	m_q	-4.041e-2	m_r	1.354e-7
n_u	8.897e-3	n_v	6.621e-3	n_w	1.227e-4	n_p	-1.897e-2	n_q	4.593e-3	n_r	-7.410e-3
x_{θ_0}	1.380e-6	$x_{\theta_{1s}}$	3.313e-6	$x_{\theta_{1c}}$	-1.673e-6	$x_{\theta_{0tr}}$	0.000				
y_{θ_0}	-4.715e-7	$y_{\theta_{1s}}$	-1.672e-6	$y_{\theta_{1c}}$	1.069e-6	$y_{\theta_{0tr}}$	1.589e-6				
z_{θ_0}	-3.042e-5	$z_{\theta_{1s}}$	3.459e-7	$z_{\theta_{1c}}$	-2.508e-8	$z_{\theta_{0tr}}$	0.000				
l_{θ_0}	1.909e-7	$l_{\theta_{1s}}$	-8.285e-7	$l_{\theta_{1c}}$	6.944e-6	$l_{\theta_{0tr}}$	3.977e-7				
m_{θ_0}	3.522e-8	$m_{\theta_{1s}}$	-2.155e-6	$m_{\theta_{1c}}$	2.232e-7	$m_{\theta_{0tr}}$	0.000				
n_{θ_0}	8.883e-7	$n_{\theta_{1s}}$	-1.188e-7	$n_{\theta_{1c}}$	1.109e-6	$n_{\theta_{0tr}}$	-9.921e-7				

Table A.2: Non-dimensional derivatives from BO-105 NASA model for hover [2].

Deriv.	Value	Deriv.	Value	Deriv.	Value	Deriv.	Value	Deriv.	Value	Deriv.	Value
x_u	-3.44e-3	x_v	-	x_w	2.569e-3	x_p	-	x_q	2.072e-2	x_r	-
y_u	-	y_v	-6.632e-3	y_w	-	y_p	-2.246e-2	y_u	-	y_r	2.638e-3
z_u	2.073e-3	z_v	-	z_w	-6.875e-2	z_p	-	z_q	4.246e-3	z_r	-
l_u	-	l_v	-1.943	l_w	-	l_p	-1.916	l_q	-	l_r	-4.642e-2
m_u	6.208e-1	m_v	-	m_w	8.147e-2	m_p	-	m_q	-7.041e-1	m_r	-
n_u	-	n_v	3.043e-1	n_w	-	n_p	-1.573e-2	n_q	-	n_r	-6.777e-2
x_{θ_0}	4.767e-3	$x_{\theta_{1s}}$	-1.588e-2	$x_{\theta_{1c}}$	-	$x_{\theta_{0tr}}$	-				
y_{θ_0}	-	$y_{\theta_{1s}}$	-	$y_{\theta_{1c}}$	-4.111e-3	$y_{\theta_{0tr}}$	-7.375e-3				
z_{θ_0}	1.055e-1	$z_{\theta_{1s}}$	8.550e-4	$z_{\theta_{1c}}$	-	$z_{\theta_{0tr}}$	-				
l_{θ_0}	-	$l_{\theta_{1s}}$	-	$l_{\theta_{1c}}$	-2.011	$l_{\theta_{0tr}}$	-1.765				
m_{θ_0}	-1.274e-1	$m_{\theta_{1s}}$	-2.901	$m_{\theta_{1c}}$	-	$m_{\theta_{0tr}}$	-				
n_{θ_0}	-	$n_{\theta_{1s}}$	-	$n_{\theta_{1c}}$	2.588e-2	$n_{\theta_{0tr}}$	9.297e-1				

B

Linear Model of the BO-105 for Hover and Forward Flight

The simulations of this research are focused on the helicopter in hover and in forward flight. Therefore, a linear model linearized around the trim point at 0 knots (Equation B.1) and around the trim point at 80 knots (Equation B.2) with perturbation linearization are used. The state matrix A and control matrix B of the hover and forward flight linear state-space models can be found in Equation B.3 and B.4 (hover) and Equation B.5 and B.6 (forward flight) with state $x = [u\ v\ w\ p\ q\ r\ \psi\ \theta\ \phi\ x\ y\ z\ \lambda_0\ \lambda_{0_{tr}}]'$ and controls $u = [\theta_0\ \theta_{1s}\ \theta_{1c}\ \theta_{0_{tr}}]'$.

$$
\begin{bmatrix} u_0 \\ v_0 \\ w_0 \\ p_0 \\ q_0 \\ r_0 \\ \psi_0 \\ \theta_0 \\ \phi_0 \\ \lambda_{0_0} \\ \lambda_{0_{tr_0}} \end{bmatrix} = \begin{bmatrix} 0.00 & \text{m/s} \\ 0.00 & \text{m/s} \\ 0.00 & \text{m/s} \\ 0.00 & \text{deg/s} \\ 0.00 & \text{deg/s} \\ 0.00 & \text{deg/s} \\ 0.00 & \text{deg} \\ 9.24 & \text{deg} \\ -1.35 & \text{deg} \\ 0.0491 & - \\ 0.0559 & - \end{bmatrix}, \quad u_0 = \begin{bmatrix} \theta_{0_0} \\ \theta_{1s_0} \\ \theta_{1c_0} \\ \theta_{0_{tr_0}} \end{bmatrix} = \begin{bmatrix} 14.36 \\ 1.93 \\ -0.31 \\ 13.69 \end{bmatrix} \text{deg} \tag{B.1}
$$

$$
\begin{bmatrix} u_0 \\ v_0 \\ w_0 \\ p_0 \\ q_0 \\ r_0 \\ \psi_0 \\ \theta_0 \\ \phi_0 \\ \lambda_{0_0} \\ \lambda_{0_{tr_0}} \end{bmatrix} = \begin{bmatrix} 40.85 & \text{m/s} \\ 0.05 & \text{m/s} \\ 3.49 & \text{m/s} \\ 0.00 & \text{deg/s} \\ 0.00 & \text{deg/s} \\ 0.00 & \text{deg/s} \\ 0.00 & \text{deg} \\ 4.88 & \text{deg} \\ 0.85 & \text{deg} \\ 0.0127 & - \\ 0.0136 & - \end{bmatrix}, \quad u_0 = \begin{bmatrix} \theta_{0_0} \\ \theta_{1s_0} \\ \theta_{1c_0} \\ \theta_{0_{tr_0}} \end{bmatrix} = \begin{bmatrix} 9.53 \\ 6.86 \\ -2.28 \\ 4.67 \end{bmatrix} \text{deg} \tag{B.2}
$$

$$A = \begin{bmatrix}
-0.021 & -0.020 & 0.019 & -1.138 & 1.758 & 0.000 & 0.000 & -9.679 & 0.000 & 0.000 & 0.000 & 0.000 & -4.307 & 0.000 \\
0.171 & -0.086 & -0.016 & -2.406 & 0.188 & 0.288 & 0.000 & 0.037 & 9.68 & 0.000 & 0.000 & 0.000 & 3.683 & -20.947 \\
-0.006 & -0.148 & -0.923 & 0.011 & 0.094 & 0.000 & 0.000 & 1.576 & 0.228 & 0.000 & 0.000 & 0.000 & 201.120 & 0.000 \\
1.228 & -0.138 & -0.035 & -16.282 & 3.577 & 0.353 & 0.000 & 0.000 & 0.000 & 0.000 & 0.000 & 0.000 & 7.509 & -25.739 \\
0.111 & 0.018 & 0.020 & 1.579 & -3.962 & 0.000 & 0.000 & 0.000 & 0.000 & 0.000 & 0.000 & 0.000 & -4.298 & 0.000 \\
0.216 & 0.160 & 0.003 & -2.256 & 0.546 & -0.882 & 0.000 & 0.000 & 0.000 & 0.000 & 0.000 & 0.000 & -2.058 & 64.211 \\
0.000 & 0.000 & 0.000 & 0.000 & -0.024 & 1.013 & 0.000 & 0.000 & 0.000 & 0.000 & 0.000 & 0.000 & 0.000 & 0.000 \\
0.000 & 0.000 & 0.000 & 0.000 & 1.000 & 0.024 & 0.000 & 0.000 & 0.000 & 0.000 & 0.000 & 0.000 & 0.000 & 0.000 \\
0.000 & 0.000 & 0.000 & 1.000 & -0.004 & 0.163 & 0.000 & 0.000 & 0.000 & 0.000 & 0.000 & 0.000 & 0.000 & 0.000 \\
0.987 & -0.004 & 0.161 & 0.000 & 0.000 & 0.000 & 0.000 & 0.000 & 0.000 & 0.000 & 0.000 & 0.000 & 0.000 & 0.000 \\
0.000 & 1.000 & 0.024 & 0.000 & 0.000 & 0.000 & 0.000 & 0.000 & 0.000 & 0.000 & 0.000 & 0.000 & 0.000 & 0.000 \\
-0.161 & -0.023 & 0.987 & 0.000 & 0.000 & 0.000 & 0.000 & 0.000 & 0.000 & 0.000 & 0.000 & 0.000 & 0.000 & 0.000 \\
0.000 & 0.001 & 0.009 & 0.000 & 0.000 & 0.000 & 0.000 & 0.000 & 0.000 & 0.000 & 0.000 & 0.000 & -2.967 & 0.000 \\
0.000 & -0.004 & -0.001 & -0.007 & 0.024 & 0.000 & 0.000 & 0.000 & 0.000 & 0.000 & 0.000 & 0.000 & -0.227 & -1.921 \\
0.000 & 0.000 & 0.000 & 0.000 & 0.000 & 0.000 & 0.000 & 0.000 & 0.000 & 0.000 & 0.000 & 0.000 & 0.000 & 0.000
\end{bmatrix} \tag{B.3}$$

$$B = \begin{bmatrix}
6.086 & 14.607 & -7.376 & 0.000 \\
-2.079 & -7.373 & 4.715 & 7.007 \\
-1.34.141 & 1.525 & -0.111 & 0.000 \\
4.134 & -17.936 & 150.335 & 8.610 \\
0.763 & -46.659 & 4.833 & 0.000 \\
19.231 & -2.571 & 24.004 & -21.479 \\
0.000 & 0.000 & 0.000 & 0.000 \\
0.000 & 0.000 & 0.000 & 0.000 \\
0.000 & 0.000 & 0.000 & 0.000 \\
0.000 & 0.000 & 0.000 & 0.000 \\
0.000 & 0.000 & 0.000 & 0.000 \\
0.669 & 0.000 & 0.000 & 0.000 \\
0.000 & 0.000 & 0.000 & 0.383 \\
0.000 & 0.000 & 0.000 & 0.000
\end{bmatrix} \tag{B.4}$$

$$
A = \begin{bmatrix}
-0.035 & 0.000 & -0.062 & -1.025 & -1.868 & 0.052 & 0.000 & -9.771 & 0.000 & 0.000 & 0.000 & 0.000 & 22.518 & 0.000 \\
0.005 & -0.084 & -0.092 & 0.610 & 0.434 & -40.370 & 0.000 & -0.012 & 9.770 & 0.000 & 0.000 & 0.000 & 68.230 & -20.947 \\
-0.041 & -0.000 & -0.966 & -0.457 & 40.827 & 0.000 & 0.000 & -0.836 & -0.146 & 0.000 & 0.000 & -0.000 & 200.712 & 0.000 \\
0.100 & -0.065 & -0.223 & -17.366 & 4.528 & 0.391 & 0.000 & 0.000 & 0.000 & 0.0000 & 0.000 & 0.000 & 346.195 & -25.769 \\
0.078 & 0.000 & 0.146 & 1.505 & -4.019 & 0.000 & 0.000 & 0.000 & 0.000 & 0.000 & 0.000 & 0.000 & -35.490 & 0.000 \\
0.018 & 0.248 & -0.151 & -2.807 & 1.509 & -1.428 & 0.000 & 0.000 & 0.000 & 0.000 & 0.000 & 0.000 & 83.579 & 64.211 \\
0.000 & 0.000 & 0.000 & 0.000 & 0.015 & 1.004 & 0.000 & 0.000 & 0.000 & 0.000 & 0.000 & 0.000 & 0.000 & 0.000 \\
0.000 & 0.000 & 0.000 & 1.000 & 1.000 & -0.015 & 0.000 & -0.002 & 0.000 & 0.000 & 0.000 & 0.000 & 0.000 & 0.000 \\
0.000 & 0.001 & 0.085 & 0.000 & 0.001 & 0.086 & -0.002 & 0.000 & 0.000 & 0.000 & 0.000 & 0.000 & 0.000 & 0.000 \\
0.996 & 01.000 & -0.015 & 0.000 & 0.000 & 0.000 & 41.000 & -41.000 & -3.491 & 0.000 & 0.000 & 0.000 & 0.000 & 0.000 \\
0.000 & 0.015 & 0.996 & 0.000 & 0.000 & 0.000 & 0.000 & 0.000 & 0.000 & 0.000 & 0.000 & 0.000 & 0.000 & 0.000 \\
-0.085 & 0.000 & 0.005 & 0.002 & 0.000 & 0.000 & 0.000 & 0.000 & 0.000 & 0.000 & 0.000 & 0.000 & -4.808 & 0.000 \\
-0.001 & -0.003 & 0.000 & -0.005 & 0.000 & 0.016 & 0.000 & 0.000 & 0.000 & 0.000 & 0.000 & 0.000 & -0.011 & -2.400 \\
-0.000 & 0.000 & 0.000 & 0.000 & 0.000 & 0.000 & 0.000 & 0.000 & 0.000 & 0.000 & 0.000 & 0.000 & 0.000 & 0.000
\end{bmatrix}
\tag{B.5}
$$

$$
B = \begin{bmatrix}
-0.435 & 19.370 & -7.042 & 0.000 \\
-7.581 & -5.529 & 9.227 & 7.347 \\
-141.935 & 1.324 & -0.437 & 0.000 \\
4.326 & -8.702 & 159.581 & 9.028 \\
23.499 & -49.772 & 4.626 & 0.000 \\
4.633 & 8.383 & 21.814 & -22.522 \\
0.000 & 0.000 & 0.000 & 0.000 \\
0.000 & 0.000 & 0.000 & 0.000 \\
0.000 & 0.000 & 0.000 & 0.000 \\
0.000 & 0.000 & 0.000 & 0.000 \\
0.000 & 0.000 & 0.000 & 0.000 \\
0.704 & -0.004 & 0.000 & 0.000 \\
0.000 & 0.000 & 0.000 & 0.402 \\
0.000 & 0.000 & 0.000 & 0.000
\end{bmatrix}
\tag{B.6}
$$

C

Cross-coupling Requirement Simulations

The simulations performed to obtain the cross-coupling requirement results of Chapter 8 can be found in this appendix.
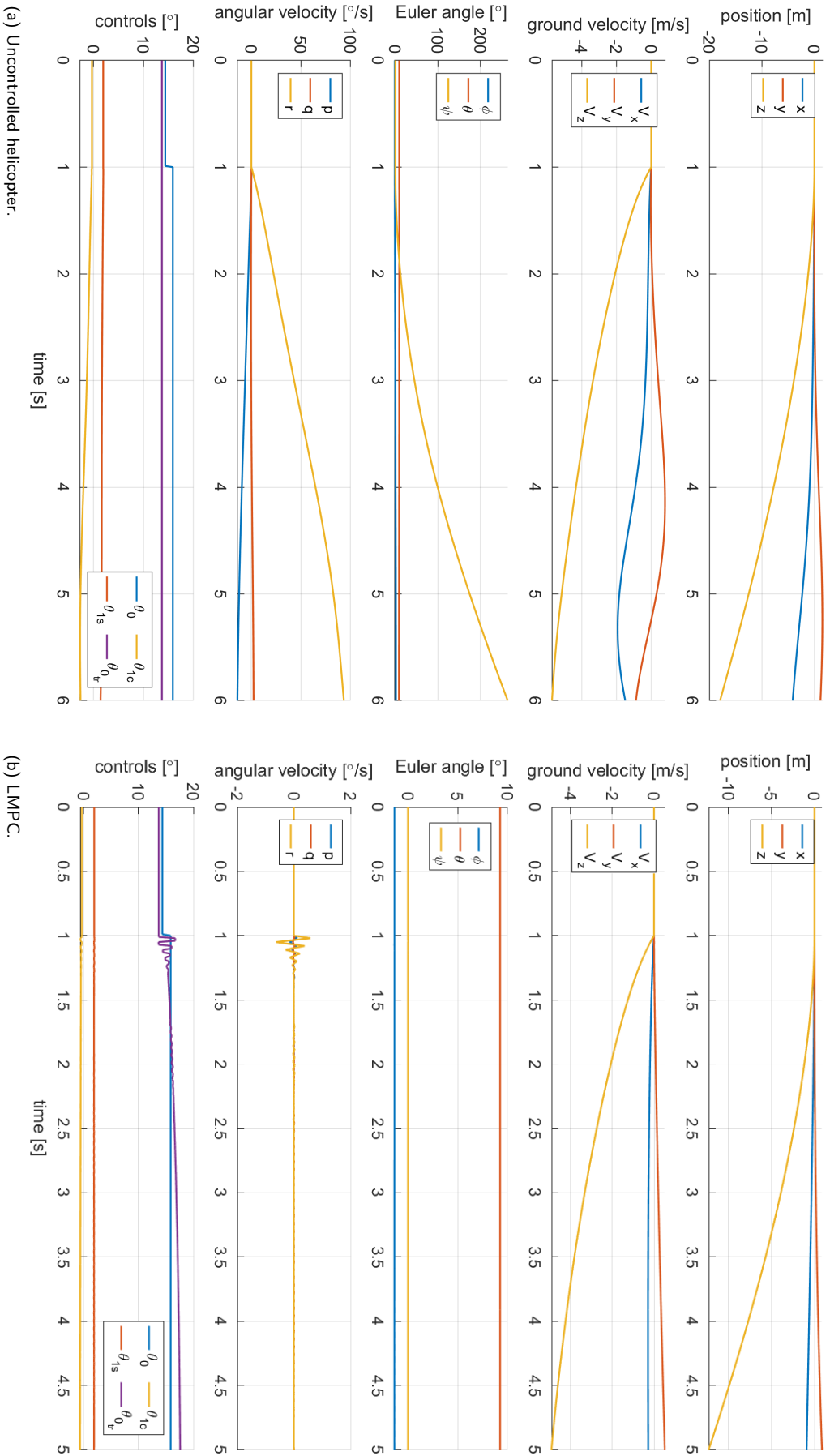
Figure C.1: Yaw due to positive collective step input without uncertainty.
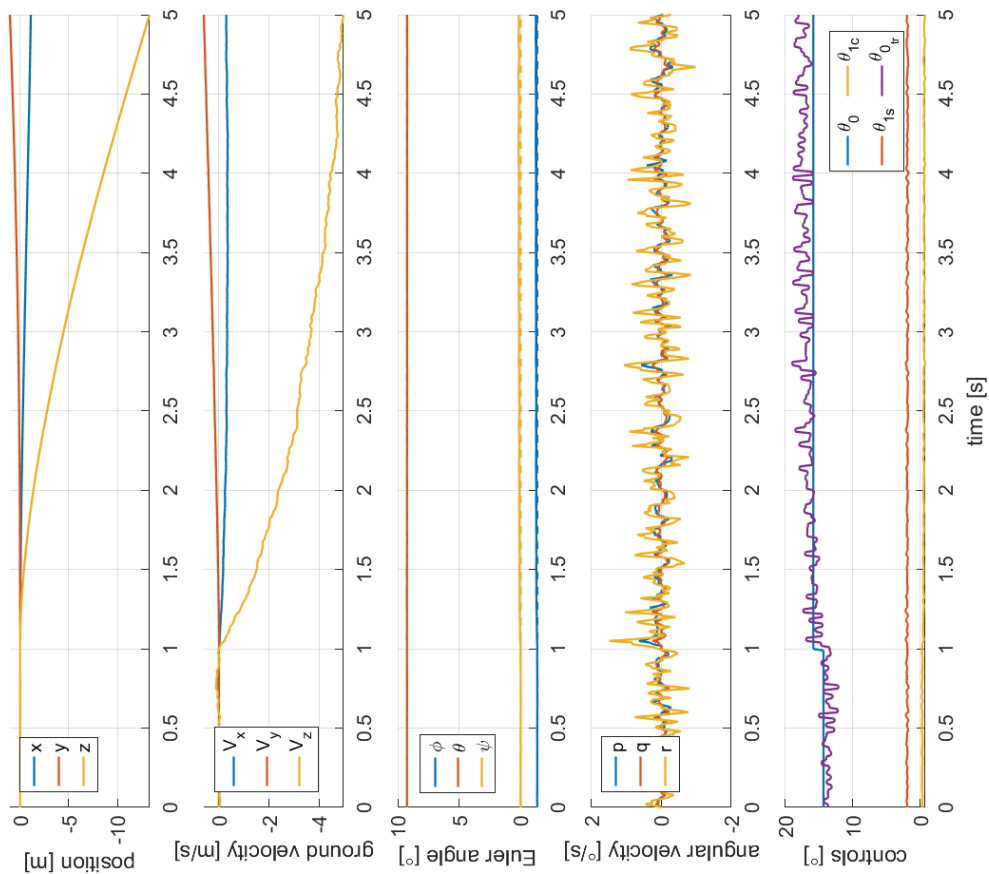
(a) LMPC.

(b) PID.
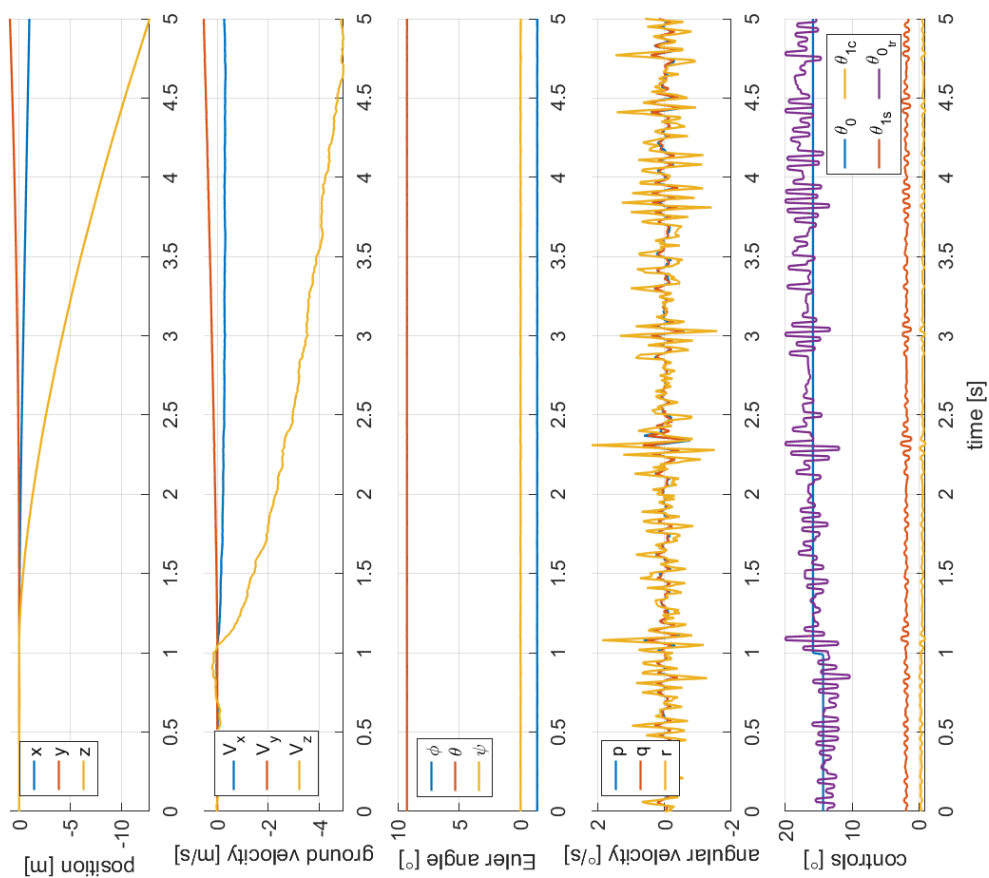
Figure C.2: Yaw due to positive collective step input with uncertainty of 0.2.
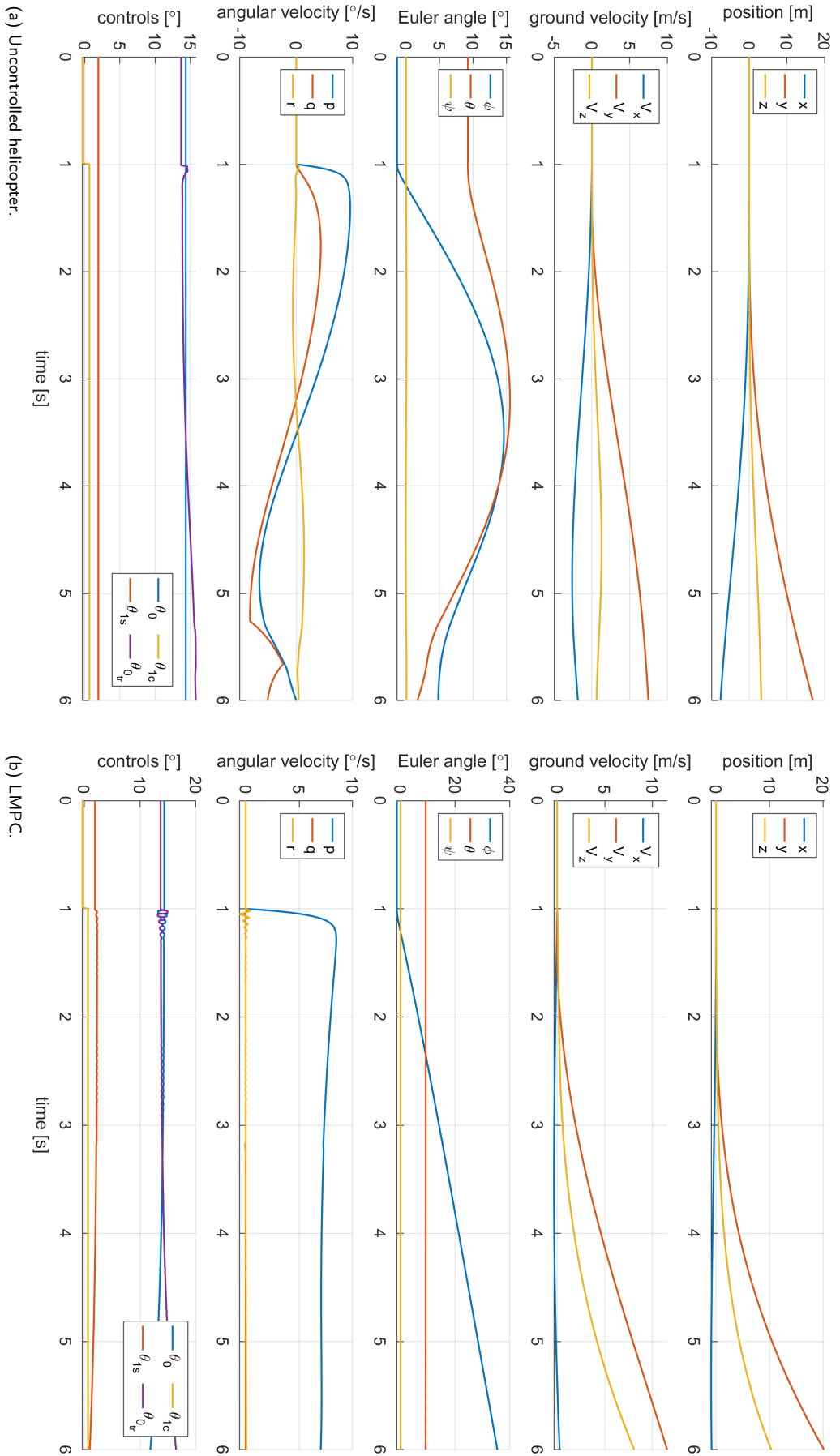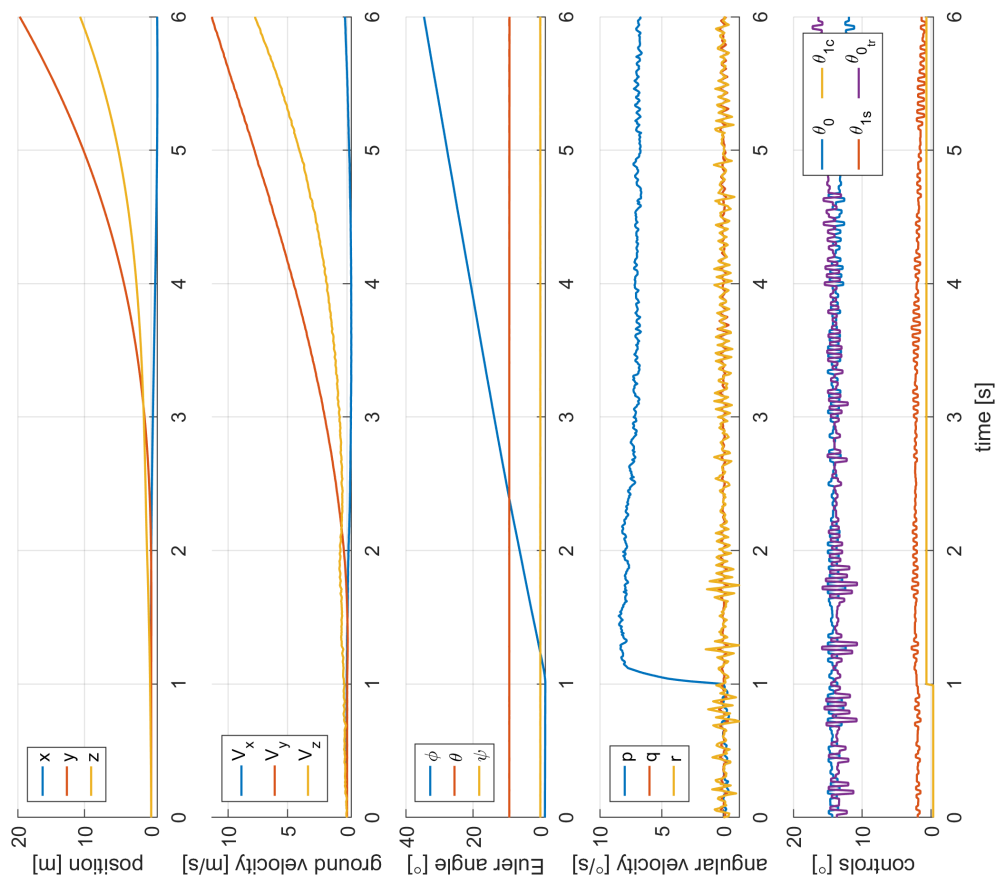
Figure C.4: Pitch due to roll for hover with a positive lateral cyclic input with uncertainty of 0.2 with LMPC applied to it.

(a) Uncontrolled helicopter.

(b) NLMPC.
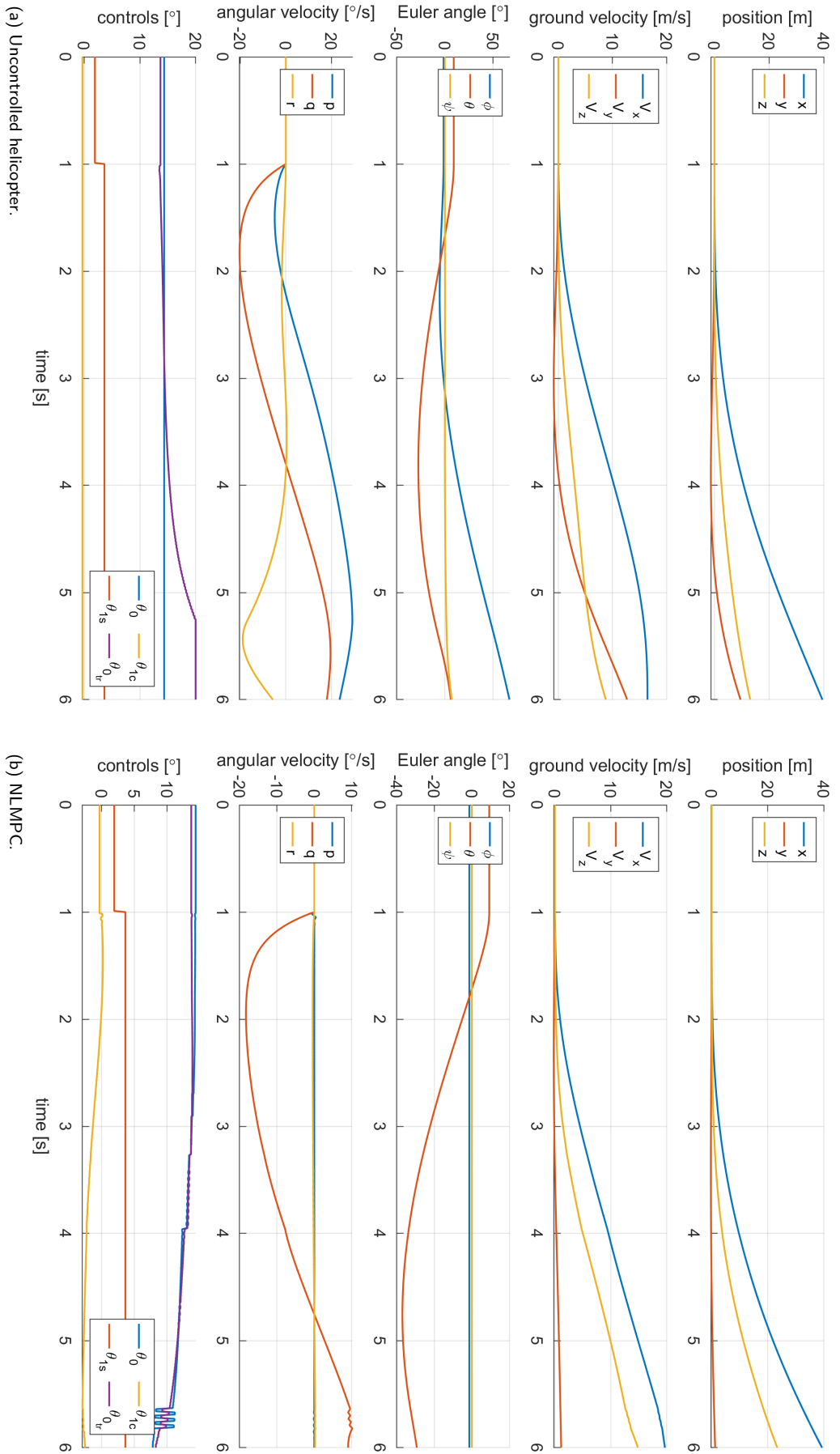
Figure C.5: Pitch due to roll for hover with a positive lateral cyclic input without uncertainty.

(a) LMPC.

(b) PID.
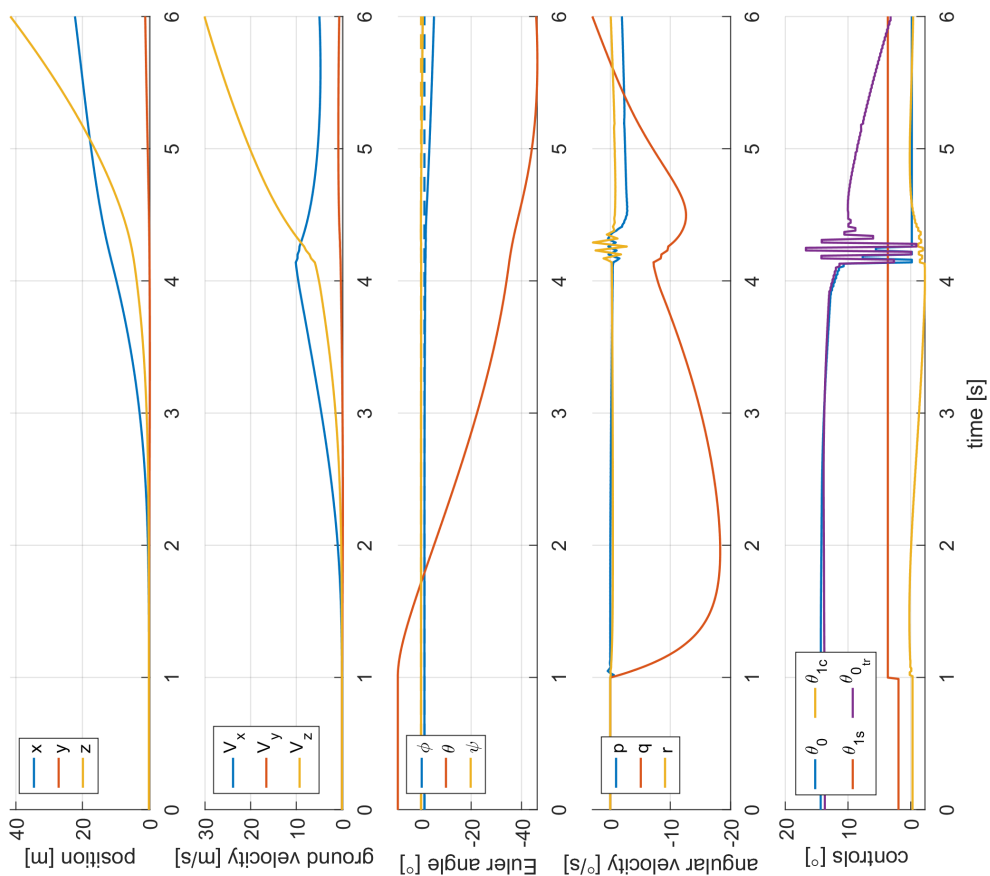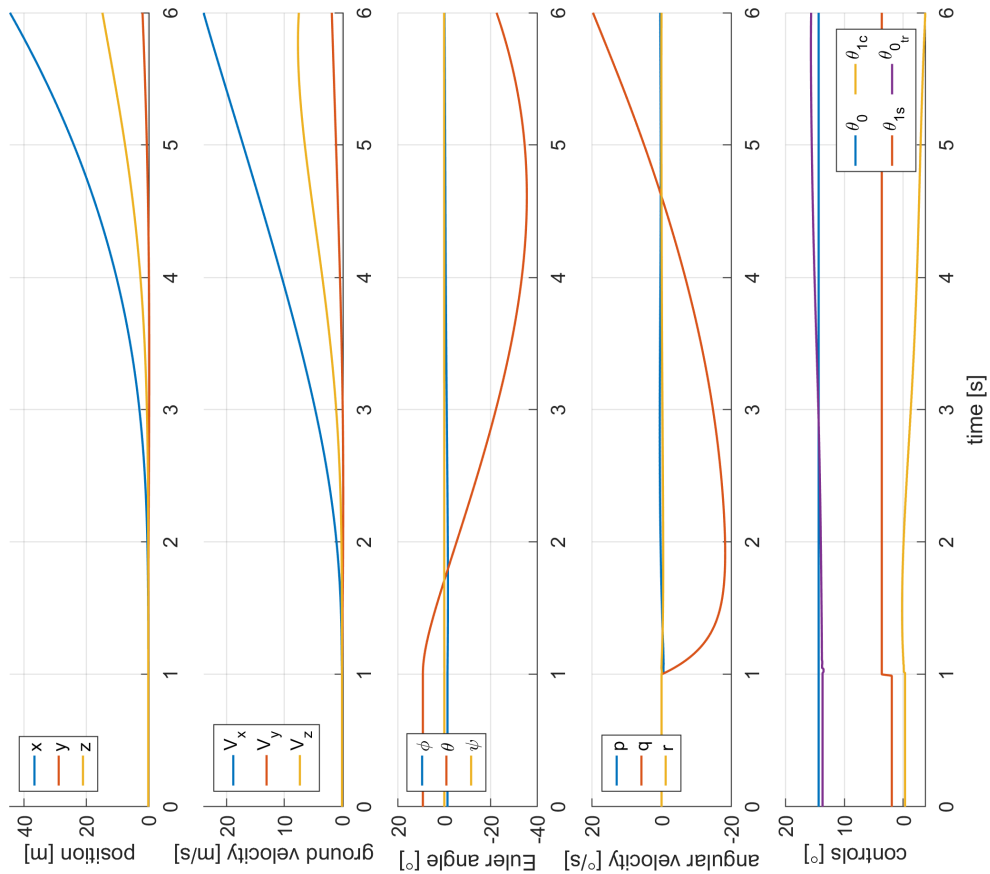
Figure C.6: Pitch due to roll for hover with a positive lateral cyclic input without uncertainty.
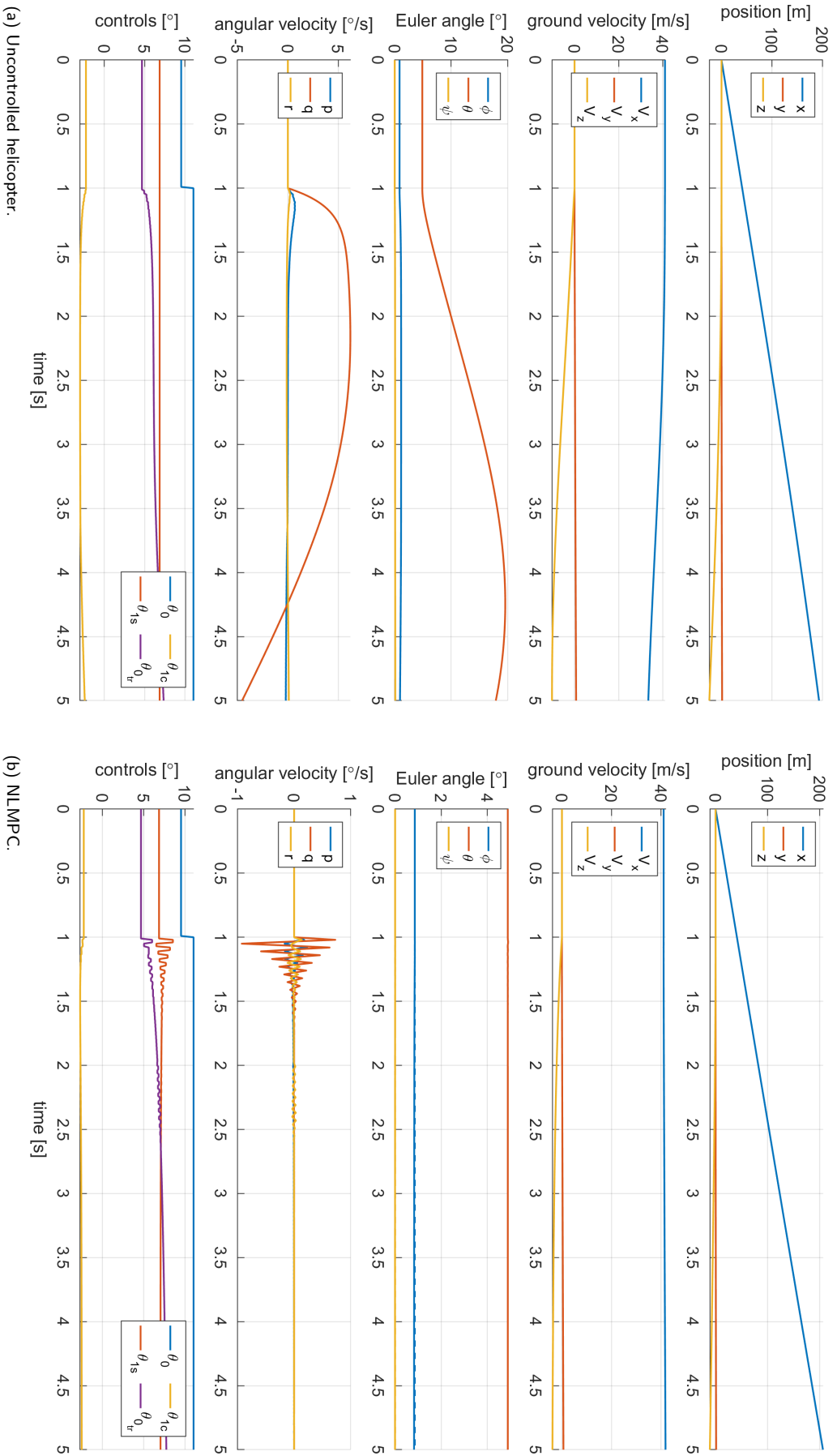
Figure C.7: Pitch due to a large, positive collective input for forward flight without uncertainty.

(a) Pitch-axis.

(b) Roll-axis.
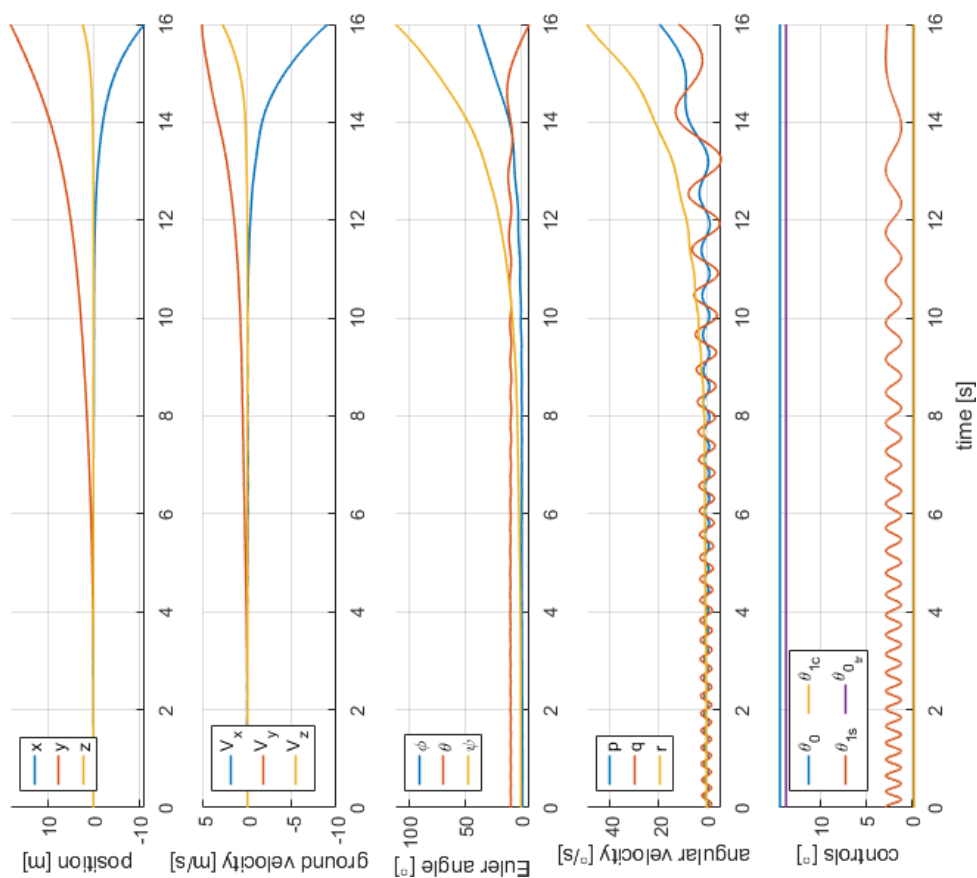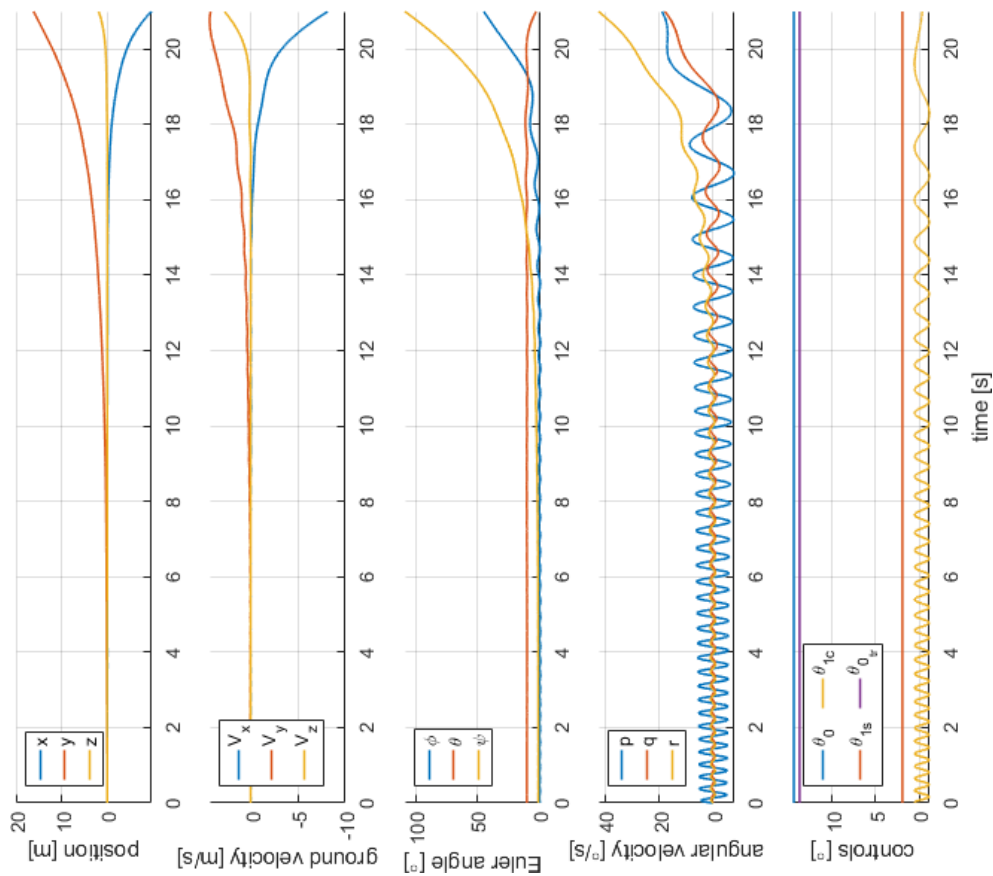
Figure C.8: Pitch and roll bandwidth frequency sweep simulations from 20 rad/s to 0.5 rad/s for hover.

(a) Uncontrolled helicopter.
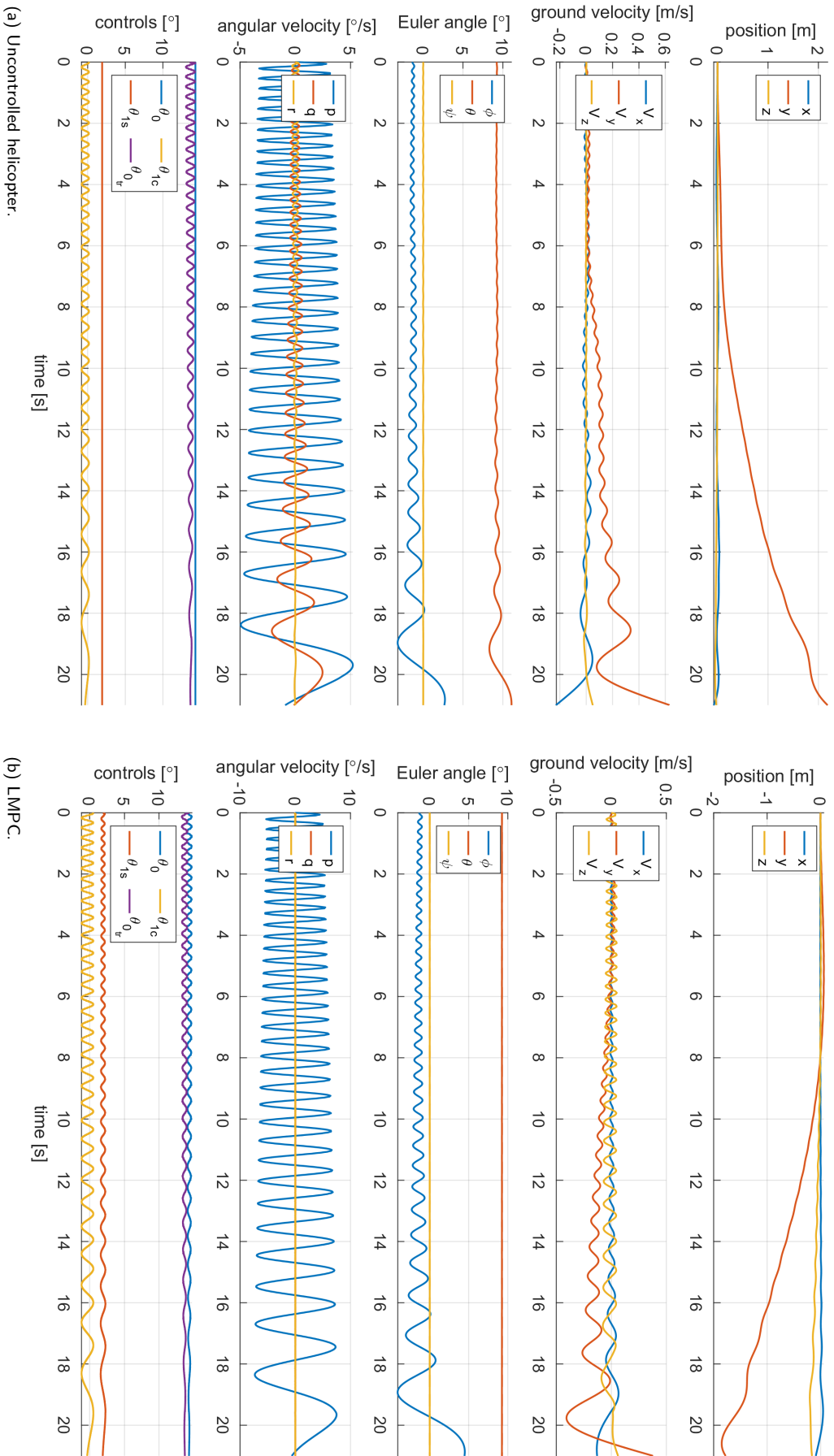
(b) LMPC.

Figure C.9: Pitch due to roll (q/p) frequency sweep simulation from 20 rad/s to 0.5 rad/s.
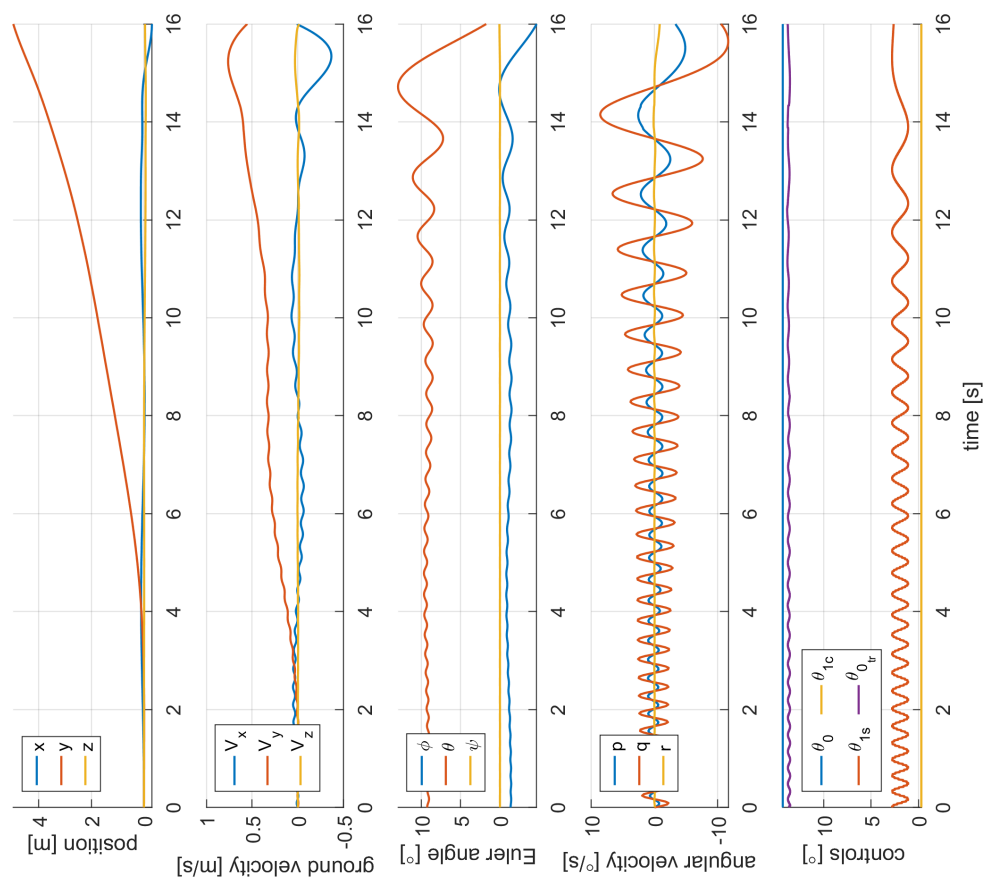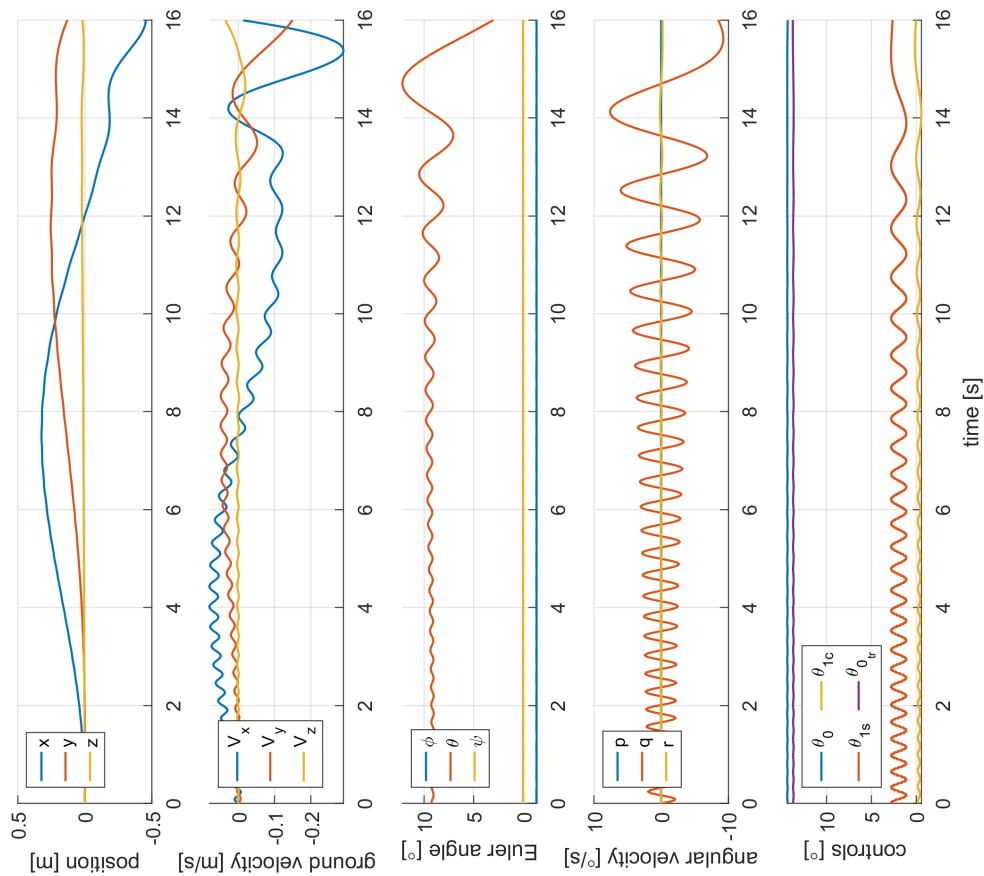
(a) Uncontrolled helicopter.

(b) LMPC.

Figure C.10: Roll due to pitch (p/q) frequency sweep simulation from 20 rad/s to 0.5 rad/s.

D

Individual Sensitivity Analysis

The individual sensitivity analysis of the influence of the prediction model error to the important derivatives for each cross-coupling case of Chapter 9 can be found in this appendix.
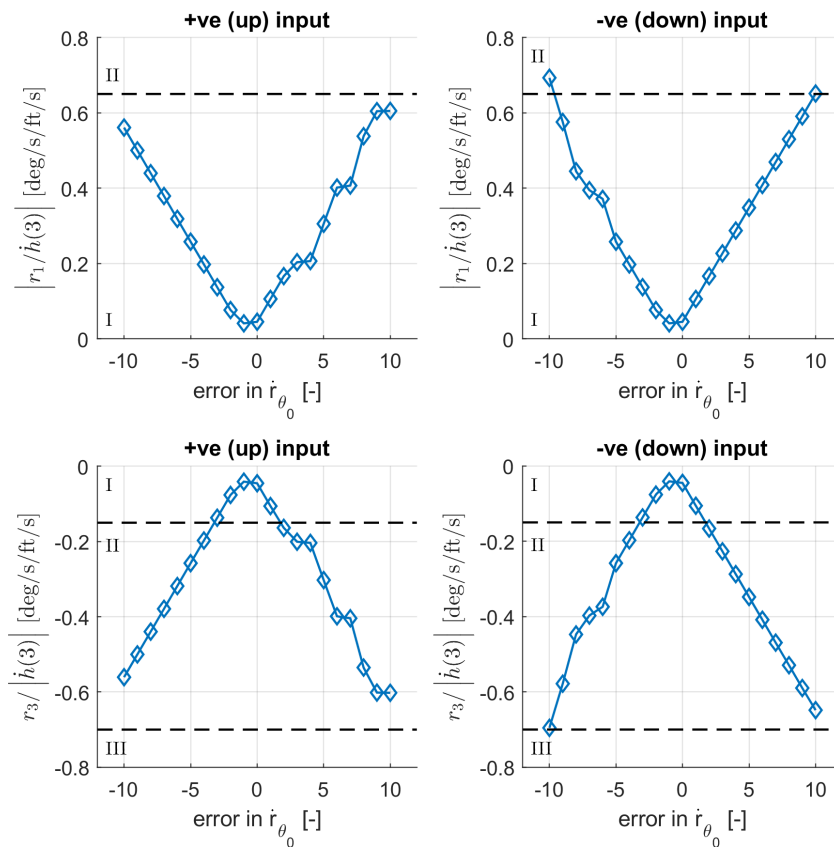
Figure D.1: Analysis of error in $\dot{r}_{\theta_0}$-derivative for yaw due to collective coupling.
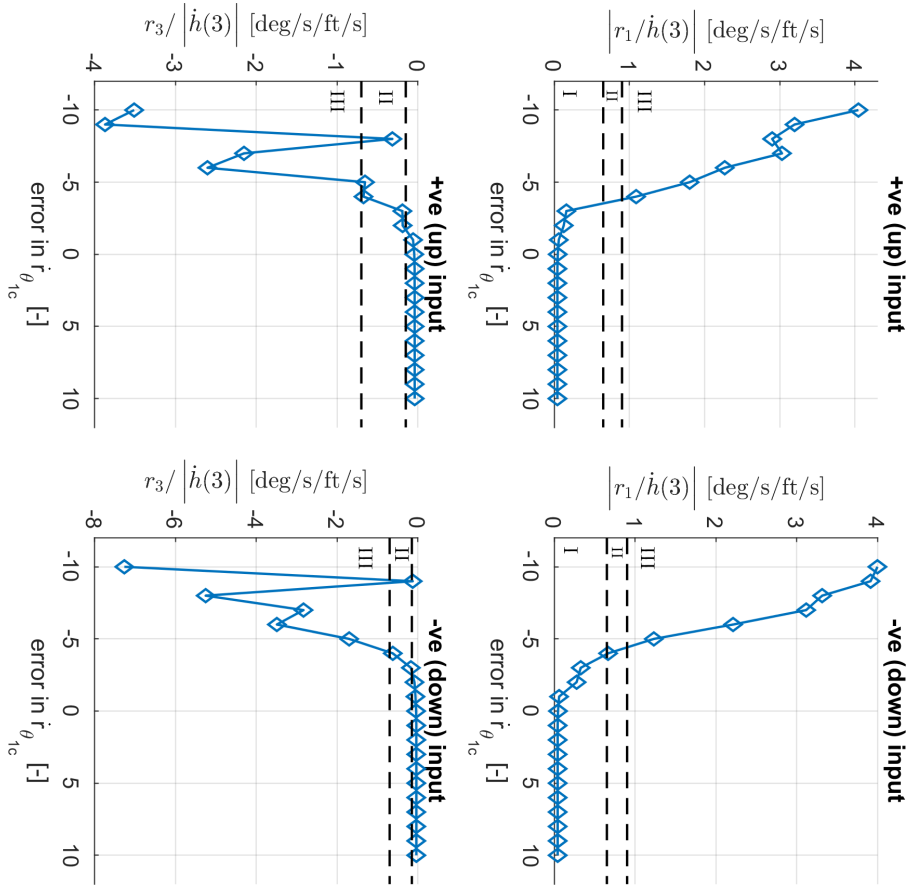
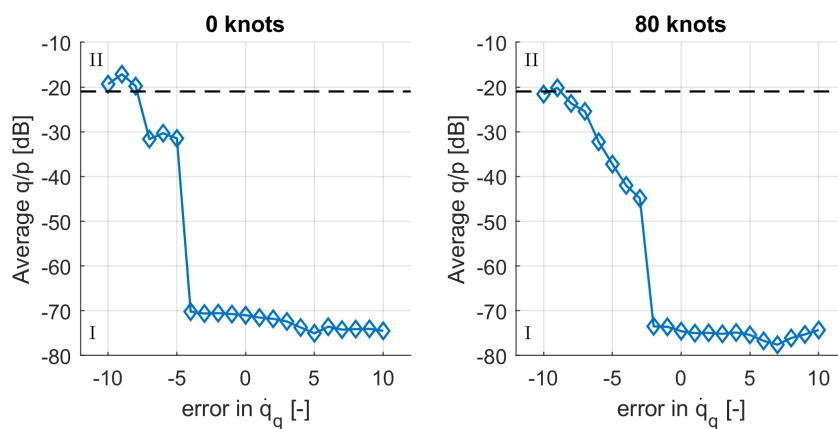Figure D.2: Analysis of error in $\dot{r}_{\theta_{1c}}$-derivative for yaw due to collective coupling.
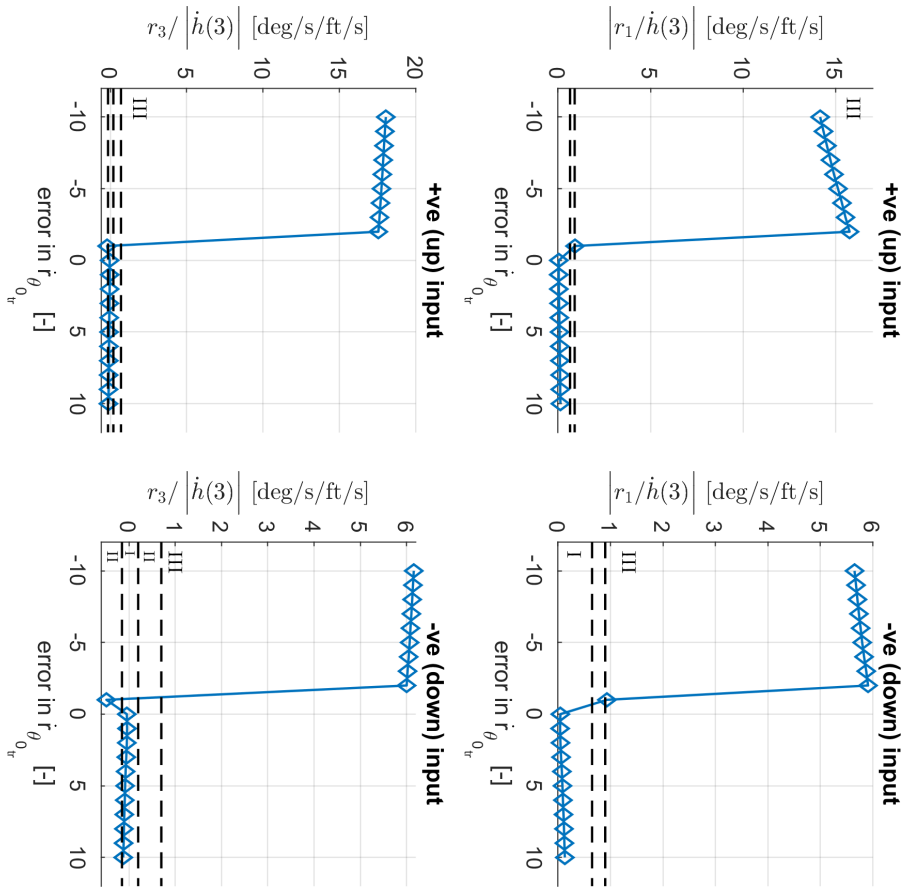
Figure D.3: Analysis of error in $\dot{r}_{\theta_{0_{tr}}}$-derivative for yaw due to collective coupling.
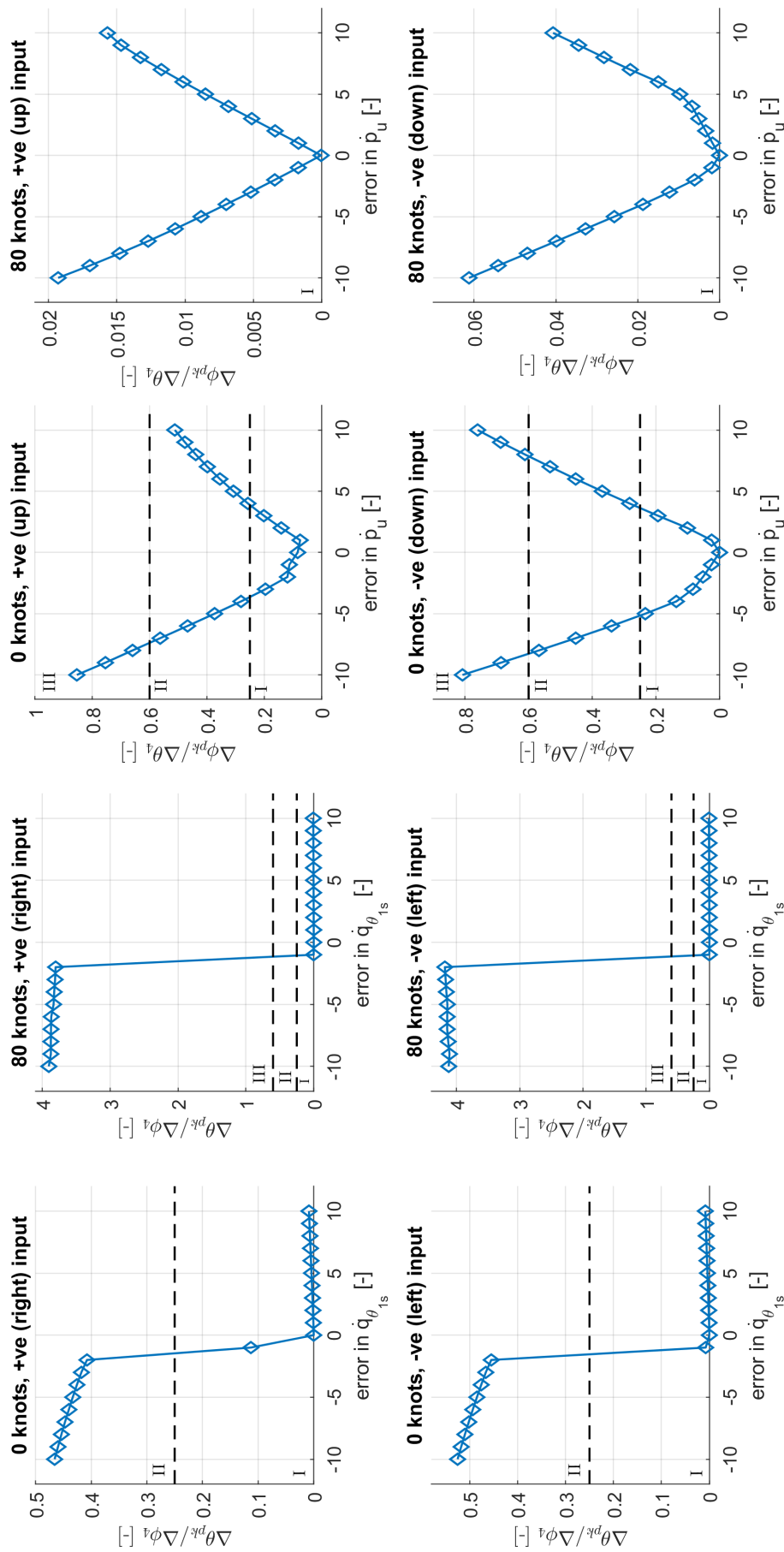
Figure D.4: Analysis of error in $\dot{q}_{\theta_{1s}}$-derivative for pitch due to roll coupling.
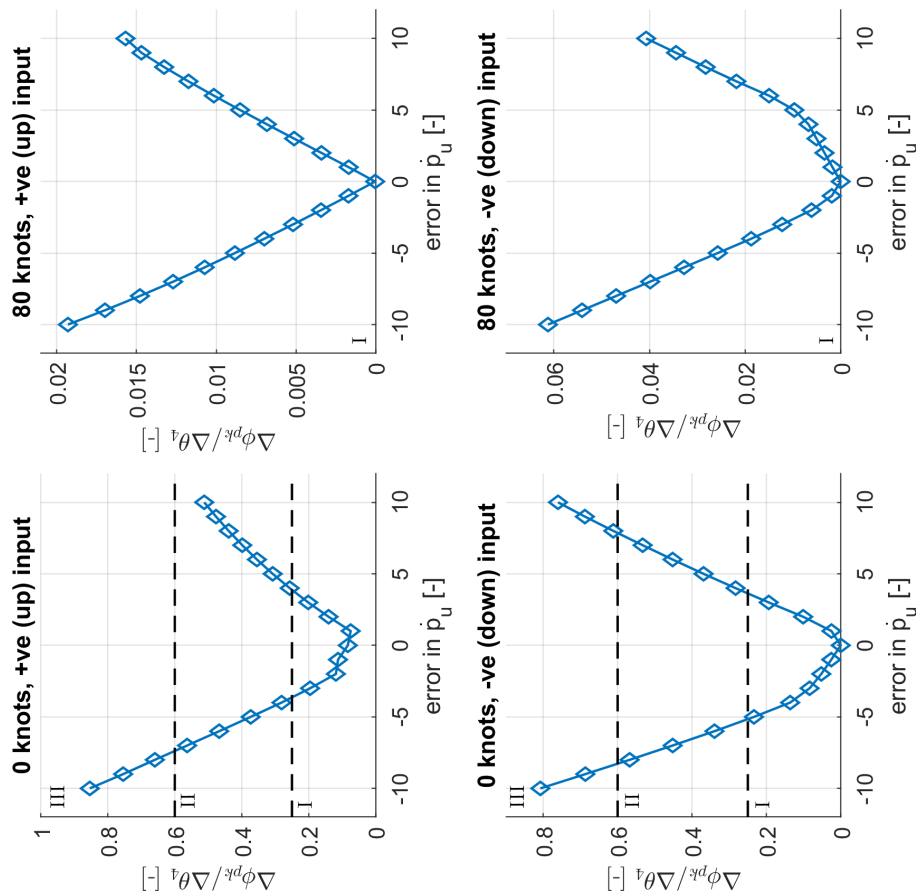
Figure D.5: Analysis of error in $\dot{p}_u$-derivative for roll due to pitch coupling.
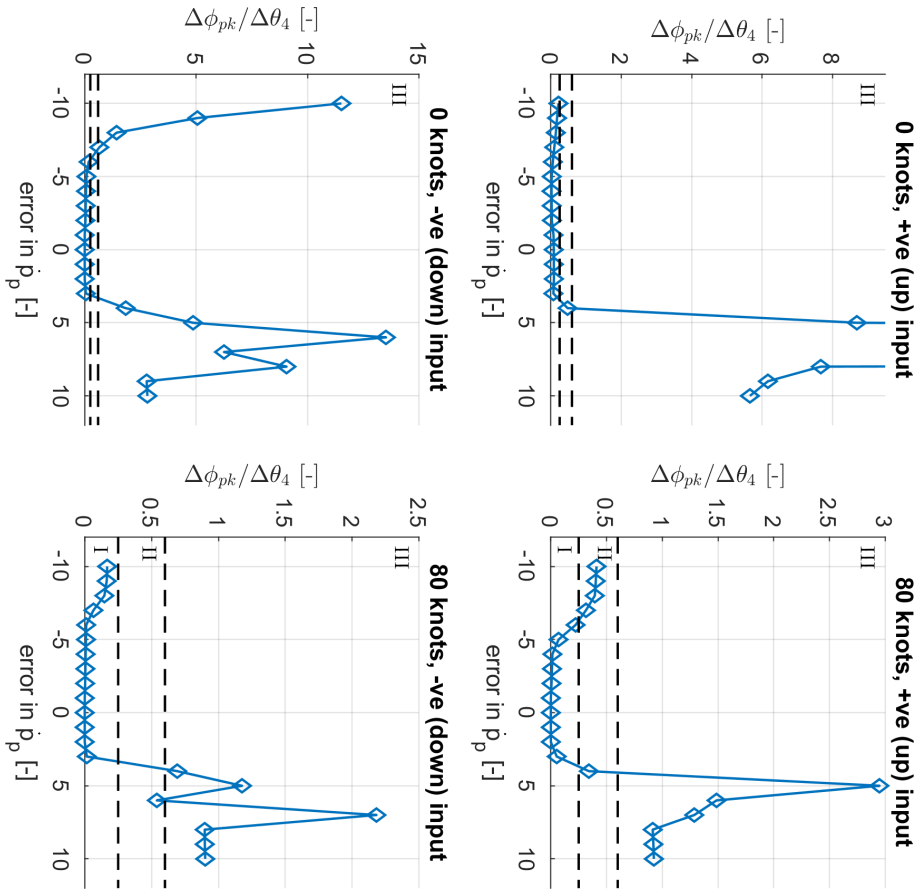
Figure D.6: Analysis of error in $\dot{p}_p$-derivative for roll due to pitch coupling.
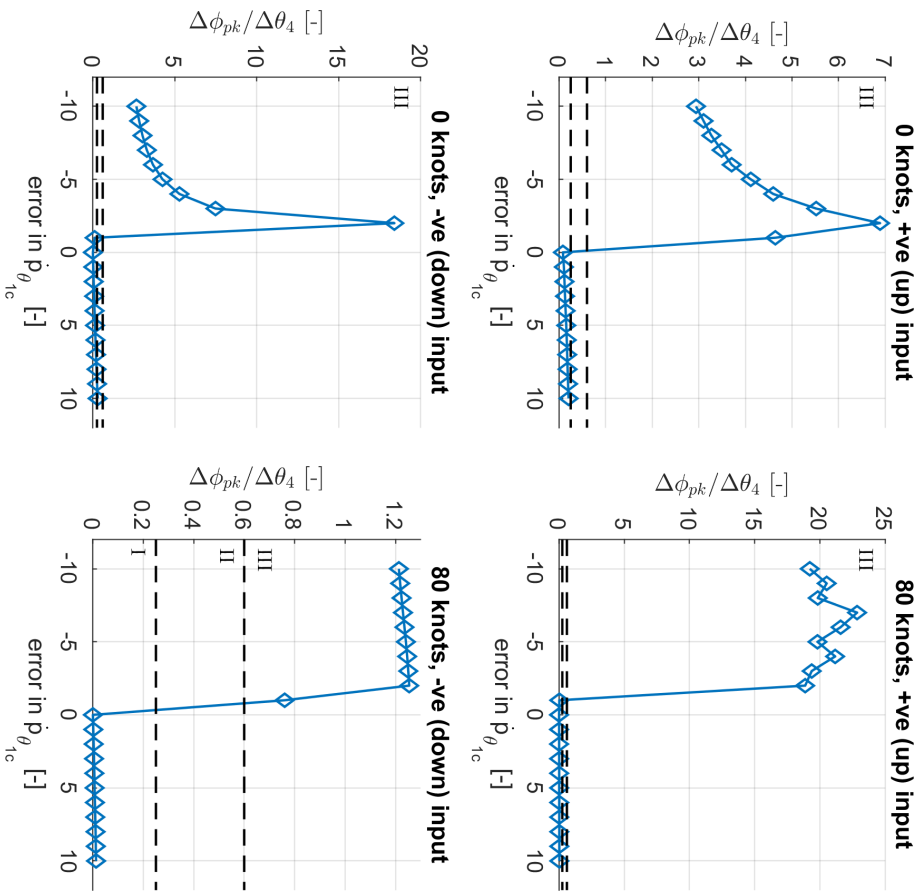
Figure D.7: Analysis of error in $\dot{p}_{\theta_{1c}}$-derivative for roll due to pitch coupling.
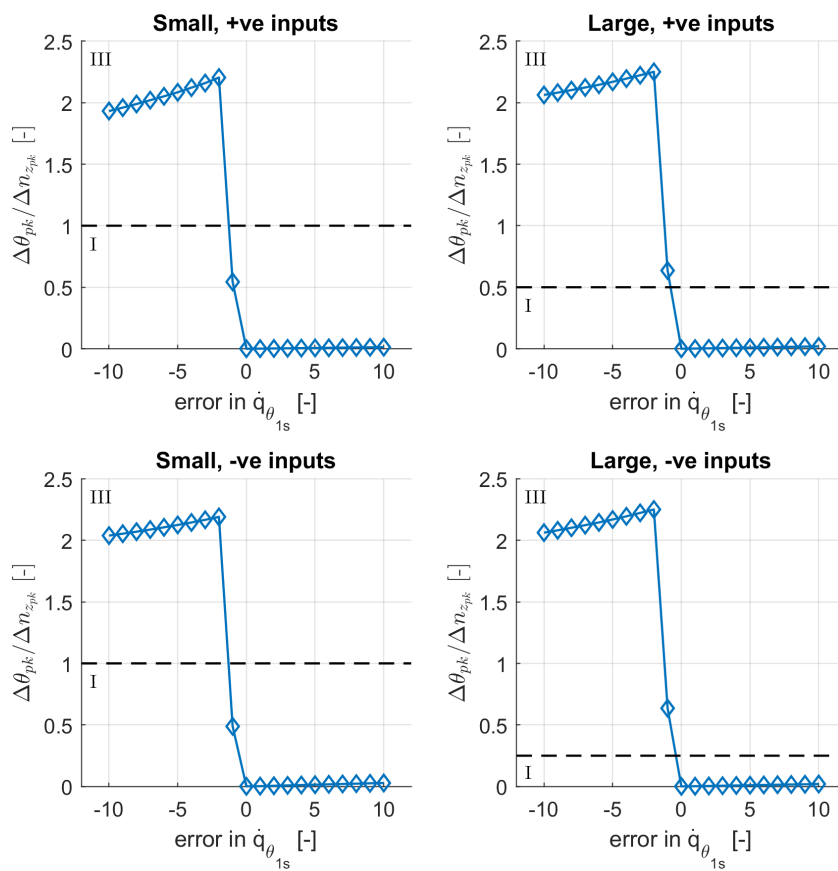
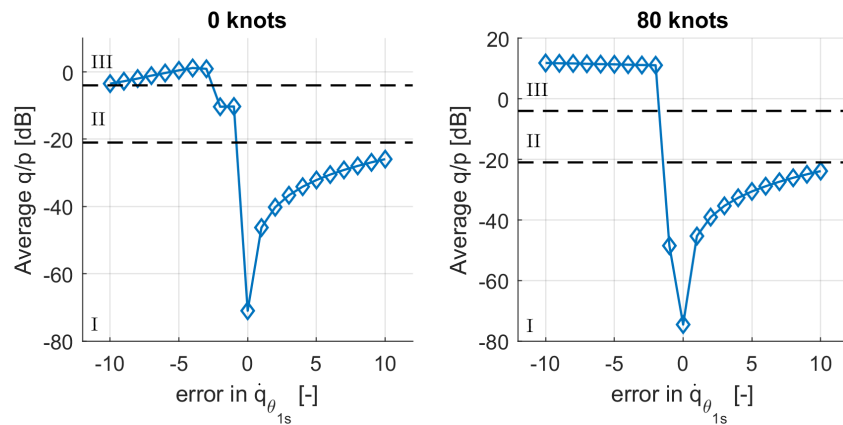Figure D.8: Analysis of error in $\dot{q}_{\theta_{1s}}$-derivative for pitch due to collective coupling.

Figure D.9: Analysis of error in $\dot{q}_q$-derivative for pitch due to roll coupling for target acquisition and tracking.
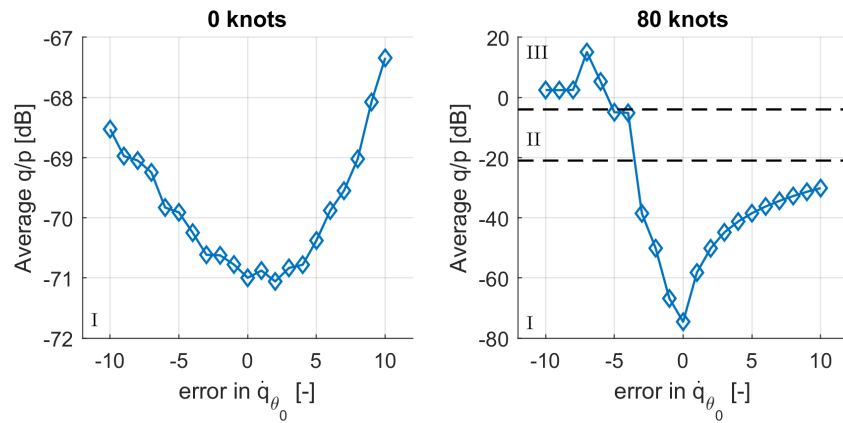
Figure D.10: Analysis of error in $\dot{q}_{\theta_0}$-derivative for pitch due to roll coupling for target acquisition and tracking.

Figure D.11: Analysis of error in $\dot{q}_{\theta_{1s}}$-derivative for pitch due to roll coupling for target acquisition and tracking.
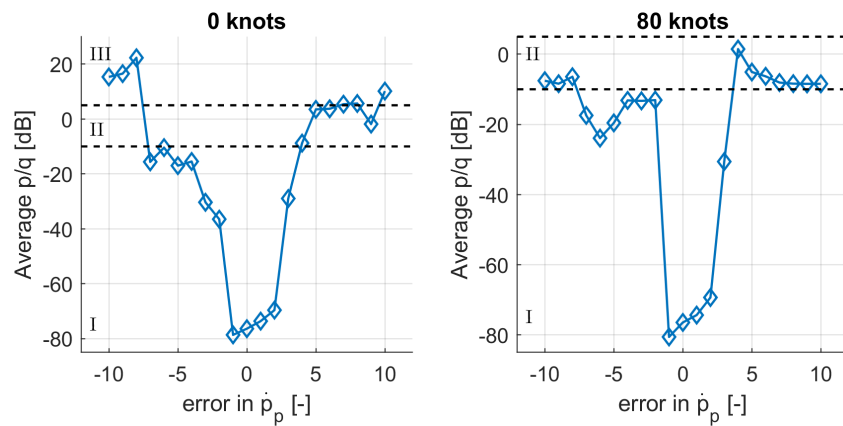

Figure D.12: Analysis of error in $\dot{p}_p$-derivative for roll due to pitch coupling for target acquisition and tracking.
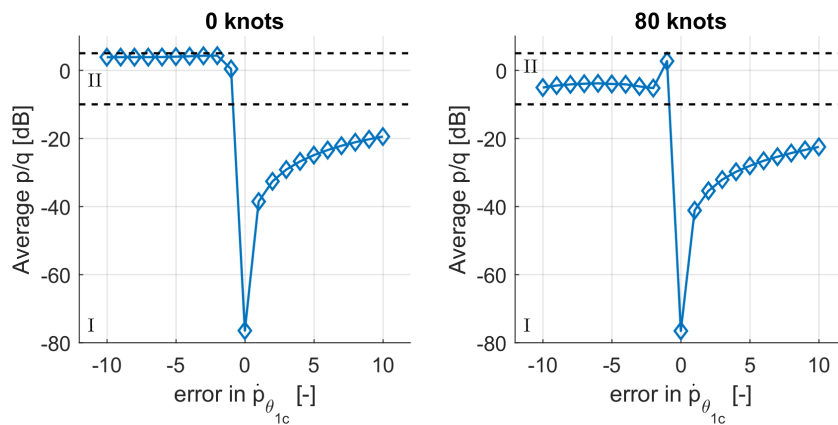
Figure D.13: Analysis of error in $\dot{p}_{\theta_{1c}}$-derivative for roll due to pitch coupling for target acquisition and tracking.
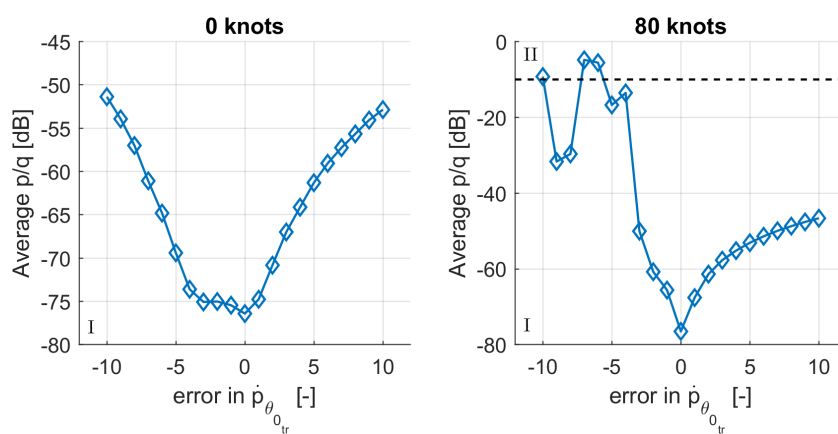

Figure D.14: Analysis of error in $\dot{p}_{\theta_{0_{tr}}}$-derivative for roll due to pitch coupling for target acquisition and tracking.